PB85-175909

Assessment of Fluidized-Bed Combustion Solid Wastes for Land Disposal. Volume 5 Appendix G

Radian Corp., Austin, TX

Prepared for

Environmental Protection Agency
Research Triangle Park, NC

Feb 85

U.S. Department of Commerce
National Technical Information Service
NTIS

PB85-175909

EPA/600/7-85/007e
February 1985

ASSESSMENT OF
FLUIDIZED-BED COMBUSTION
SOLID WASTES FOR LAND DISPOSAL

Volume 5. Appendix G

By:

H. J. Williamson and T. W. Grimshaw

Radian Corporation
P.O. Box 9948, Austin, Texas 78766

and

J.E. Dunn
Department of Mathematics
University of Arkansas
Fayetteville, Arkansas 72701

EPA Project Officer: John Milliken

EPA Contract No. 68-02-3103

Air and Energy Engineering Research Laboratory
Office of Environmental Engineering and Technology
Research Triangle Park, North Carolina 27711

AIR AND ENERGY ENGINEERING RESEARCH LABORATORY
OFFICE OF RESEARCH AND DEVELOPMENT
U.S. ENVIRONMENTAL PROTECTION AGENCY
RESEARCH TRIANGLE PARK, NC 27711

REPRODUCED BY
NATIONAL TECHNICAL
INFORMATION SERVICE
U.S. DEPARTMENT OF COMMERCE
SPRINGFIELD, VA. 22161

TECHNICAL REPORT DATA
(Please read Instructions on the reverse before completing)

1. REPORT NO
EPA/600/7-85/007e

2.

3. RECIPIENT'S ACCESSION NO
PB85 175909/AS

4. TITLE AND SUBTITLE
Assessment of Fluidized-bed Combustion Solid Wastes for Land Disposal, Volume 5. Appendix G

5. REPORT DATE
February 1985

6. PERFORMING ORGANIZATION CODE

7. AUTHOR(S)
H. J. Williamson, J. E. Dunn*, and T. W. Grimshaw

8. PERFORMING ORGANIZATION REPORT NO.

9. PERFORMING ORGANIZATION NAME AND ADDRESS
Radian Corporation
P.O. Box 9948
Austin, Texas 78766

10. PROGRAM ELEMENT NO.

11. CONTRACT/GRANT NO
68-02-3103

12. SPONSORING AGENCY NAME AND ADDRESS
EPA, Office of Research and Development
Air and Energy Engineering Research Laboratory
Research Triangle Park, NC 27711

13. TYPE OF REPORT AND PERIOD COVERED
Final; 6/80 - 6/84

14. SPONSORING AGENCY CODE
EPA/600/13

15. SUPPLEMENTARY NOTES
AEERL project officer John O. Milliken is no longer with the Laboratory; for assistance contact Michael A. Maxwell, Mail Drop 61, 919/541-3091.
(*)Dunn is with the University of Arkansas, Fayetteville, AR 72701

16. ABSTRACT
The report, including 10 appendices, gives results of: (1) an analysis of representative samples of fluidized-bed combustion (FBC) wastes, (2) an assessment of the characteristics of leachates generated from the wastes under laboratory and field (landfill) conditions, (3) a characterization of the attenuation of the leachates by earth materials that are typical of disposal settings, (4) development of a way to predict the leachate generation behavior of FBC wastes under landfill conditions on the basis of laboratory test results by establishing a rigorous statistical relationship between the laboratory and field leaching results, and (5) assessment of the compatibility of commonly used landfill liner materials with FBC waste leachates. FBC is an emerging energy technology that holds promise for both high efficiency of energy conversion and minimization of adverse air quality impacts. A major advantage of FBC is that high-sulfur coal can be burned without the use of flue gas desulfurization equipment to meet air quality standards. The solid residues that are generated in an FBC unit are usually larger in volume and have different properties than the typical bottom ash from a conventional boiler.

17. KEY WORDS AND DOCUMENT ANALYSIS

a. DESCRIPTORS		b. IDENTIFIERS/OPEN ENDED TERMS	c. COSATI Field/Group	
Pollution	Assessments	Pollution Control	13B	14B
Waste Disposal	Desulfurization	Stationary Sources		07A, 07D
Combustion	Earth Fills		21B	13C
Fluidized Bed	Linings			11G
Processing	Sorbents		13H	
Coal			21D	

18. DISTRIBUTION STATEMENT
Release to Public

19. SECURITY CLASS *(This Report)*
Unclassified

20. SECURITY CLASS *(This page)*
Unclassified

21. NO. OF PAGES
260

22. PRICE

EPA Form 2220-1 (9-73)

NOTICE

This document has been reviewed in accordance with U.S. Environmental Protection Agency policy and approved for publication. Mention of trade names or commercial products does not constitute endorsement or recommendation for use.

Abstract

The report, including 10 appendices, gives results of: (1) an analysis of representative samples of fluidized-bed combustion (FBC) wastes, (2) an assessment of the characteristics of leachates generated from the wastes under laboratory and field (landfill) conditions, (3) a characterization of the attenuation of the leachates by earth materials that are typical of disposal settings, (4) development of a way to predict the leachate generation behavior of FBC wastes under landfill conditions on the basis of laboratory test results by establishing a rigorous statistical relationship between the laboratory and field leaching results, and (5) assessment of the compatibility of commonly used landfill liner materials with FBC waste leachates. FBC is an emerging energy technology that holds promise for both high efficiency of energy conversion and minimization of adverse air quality impacts. A major advantage of FBC is that high-sulfur coal can be burned without the use of flue gas desulfurization equipment to meet air quality standards. The solid residues that are generated in an FBC unit are usually larger in volume and have different properties than the typical bottom ash from a conventional boiler.

APPENDICES

Page

Volume 2.

A. Sources of FBC Waste and Disposal Media, Detailed Hydrologic Analysis, and Chemical Analytical Procedures A-1

B. FBC Solid Waste and Disposal Media Physical Properties B-1

C. Solids Composition of FBC Solid Waste and Disposal Media.......... C-1

Volume 3.

D. Laboratory Leaching and Attenuation Behavior of FBC Wastes D-1

E. Behavior of FBC Wastes Under Field Conditions E-1

Volume 4.

F. Compatibility of Landfill Liner Materials with FBC Waste Leachate F-1

Volume 5.

G. Statistical Prediction of Field Leaching and Attenuation Behavior Based on Observed Laboratory Results G-1

Volume 6.

H. Quality Assurance and Control H-1

Volume 7.

I. Interpretation of Chemical Trends and Comparison of Leachate Composition with Water Quality Standards and Criteria I-1

Volume 8.

J. Data List for Leachate Analyses.................................. J-1

Appendix G

STATISTICAL PREDICTION OF FIELD LEACHING AND ATTENUATION BEHAVIOR BASED ON OBSERVED LABORATORY RESULTS

By:

H. J. Williamson, J. E. Dunn, and T. W. Grimshaw

With Contributions By:

R. A. Minear

NOTE: In some cases, lengthy tables and large groups of figures in this appendix are removed from the text and included as attachments to minimize interruption of the flow of the text.

Table of Contents

Page

G.1 Overview G-1

G.2 Leaching and Attenuation Models for FBC Wastes: Predictive Models for Concentrations Developed Directly as Functions of Volume per Mass G-3

G.2.1 Models for Leaching G-5

G.2.1.1 Calculation of Volume per Mass G-7

G.2.1.2 Data Selection G-7

G.2.1.3 Methods Used to Develop Laboratory Leaching Models G-7

G.2.1.4 Laboratory Leaching Models G-9

G.2.1.5 Comparison of Predicted Values from Laboratory Models and Field Concentrations G-12

G.2.1.5.1 Plots Displaying Concentrations from All Field Cells Simultaneously G-13

G.2.1.5.2 Plots Using Chloride Concentrations from Individual Field Cells G-25

G.2.1.5.3 Analytical Comparisons of Field Observed and Predicted Values . G-25

G.2.1.6 Discussion of Data Selection G-44

Table of Contents
(Continued)

Page

G.2.2 Models for Fractional Attenuation G-50
  G.2.2.1 Calculation of Fractional Attenuation and Volume per Mass G-50
  G.2.2.2 Data Selection G-51
  G.2.2.3 Methods Used to Develop Fractional Attenuation Model G-52
  G.2.2.4 Comparison of Predicted Values from Laboratory Models and Field Fractional Attenuations G-53
  G.2.2.5 Models to Predict Field Fractional Attenuations G-58
G.2.3 Discussions of Modeling Results G-71
G.3 Toward a Multi-Species Leaching Model for FBC Wastes: Model for Concentration of a Given Species Developed as a Function of Volume per Mass G-74
G.3.1 Preliminary Modeling Considerations G-76
G.3.2 Theoretical Multi-Species Model G-78
G.3.3 Estimation of G for PFBC Waste G-81
G.3.4 Estimation of the Initial Soluable Fraction y_o . . G-85
G.3.5 Field Cell Rainfall - Percolation Delay Model . . . G-87
G.3.6 Shake-Test Model Validation G-91
G.3.7 Model Validation Assuming Prior Knowledge of Field Cell Results G-101
G.3.8 Possible Extensions G-102
G.4 References G-104

List of Tables

Table		Page
G-1	Contents of Field Cells Used in Modeling Study	G-4
G-2	Models for Laboratory Leaching for Exxon PFBC Waste	G-10
G-3	Models for Laboratory Leaching for Alliance AFBC Waste	G-11
G-4	Comparison of Field Concentrations and Values Predicted by Model Developed from Laboratory Data for Exxon PFBC Waste	G-36
G-5	Comparison of Field Concentrations and Values Predicted by Model Developed from Laboratory Data for Alliance AFBC Waste	G-37
G-6	Significance Tests for Differences Between Laboratory-Predicted and Field-Observed Leaching Trends for Exxon PFBC Waste	G-41
G-7	Significance Tests for Differences Between Laboratory-Predicted and Field-Observed Leaching Trends for Alliance AFBC Waste	G-42
G-8	Comparison of Mean Differences Between Field-Observed and Laboratory-Predicted Values for Different Volumes per Mass for Exxon PFBC Waste	G-45
G-9	Comparison of Mean Differences Between Field-Observed and Laboratory-Predicted Values for Different Volumes per Mass for Alliance AFBC Waste	G-46
G-10	Comparison of Standard Deviations of Field Residuals for Different Volumes per Mass for Exxon PFBC Waste	G-47
G-11	Comparison of Standard Deviations of Field Residuals for Different Values per Mass for Alliance AFBC Waste	G-48
G-12	Models for Laboratory Fractional Attenuation	G-54
G-13	Comparison of Field Fractional Attenuations and Values Predicted by Model Developed from Laboratory Data	G-59

List of Tables
(Continued)

Table | Page
G-14 Significance Tests for Differences Between Lab and Field Fractional Attenuation Trends.......................... G-59
G-15 Models for Field Fractional Attenuation for Exxon PFBC Waste.. G-60
G-16 Models for Field Fractional Attenuation for Alliance AFBC Waste.. G-61
G-17 (See Attachment 2)
G-18 (See Attachment 3)
G-19 (See Attachment 4)
G-20 Estimated Values of Non-Zero Elements and Associated R^2 Values... G-84
G-21 Estimates of the Initial Soluble Fraction y_o for Exxon PFBC Waste Based on Solid Sample Waste Analyses and on Back-Calculation of Lab and Field Data............................ G-86
G-22 (See Attachment 5)
G-23 Mean Squared Errors for the Rainfall-Flow Model with d = 0,1,2, . . ., 15 Days...................................... G-89
G-24 Estimated Regression Coefficients for the Rainfall-Flow Delay Model (In Liters)................................. G-89
G-25 Estimated Cumulative Flow at the Upper Sample Point for Field Cell 1 as a Function of Time................................. G-90
G-26 Model Building Results Based on Shake-Test Extractions of Exxon PFBC Waste: Summary of Estimated Initial Soluble Fraction Obtained by Back-Calculation from Field Cell 1 Data.. G-101

List of Figures

Figure | Page

G-1 Lab (L), Field (F), and Predicted (P) Total Dissolved Solids Concentrations as a Function of Volume per Mass for Exxon PFBC Waste... G-14

G-2 Lab (L), Field (F), and Predicted (P) Total Dissolved Solids Concentrations as a Function of Volume per Mass for Alliance AFBC Waste... G-15

G-3 Lab (L), Field (F), and Predicted (P) Sulfate Concentrations as a Function of Volume per Mass for Exxon PFBC Waste......... G-17

G-4 Lab (L), Field (F), and Predicted (P) Sulfate Concentrations as a Function of Volume per Mass for Alliance AFBC Waste...... G-18

G-5 Lab (L), Field (F), and Predicted (P) Sodium Concentrations as a Function of Volume per Mass for Exxon PFBC Waste......... G-19

G-6 Lab (L), Field (F), and Predicted (P) Sodium Concentrations as a Function of Volume per Mass for Alliance AFBC Waste...... G-20

G-7 Lab (L), Field (F), and Predicted (P) Boron Concentrations as a Function of Volume per Mass for Exxon PFBC Waste............ G-21

G-8 Lab (L), Field (F), and Predicted (P) Boron Concentrations as a Function of Volume per Mass for Alliance AFBC Waste......... G-22

G-9 Lab (L), Field (F), and Predicted (P) Chloride Concentrations as a Function of Volume per Mass for Exxon PFBC Waste......... G-23

G-10 Lab (L), Field (F), and Predicted (P) Chloride Concentrations as a Function of Volume per Mass for Alliance AFBC Waste...... G-24

G-11 Lab (L) and Predicted (P) Chloride Concentrations as a Function of Volume per Mass for Exxon PFBC Waste.............. G-26

List of Figures
(Continued)

Figure | Page

G-12 Field-Observed (F) and Laboratory-Predicted (P) Chloride Concentrations as a Function of Volume per Mass for Exxon PFBC Waste and Limestone.................................... G-27

G-13 Field-Observed (F) and Laboratory-Predicted (P) Chloride Concentrations as a Function of Volume per Mass for Exxon PFBC Waste and Shale.. G-28

G-14 Field-Observed (F) and Laboratory-Predicted (P) Chloride Concentrations as a Function of Volume per Mass for Exxon PFBC Waste and Glacial Till................................. G-29

G-15 Lab (L) and Predicted (P) Chloride Concentrations as a Function of Volume per Mass for Alliance AFBC Waste........... G-30

G-16 Field-Observed (F) and Laboratory-Predicted (P) Chloride Concentrations as a Function of Volume per Mass for Alliance AFBC Waste and Alluvium.................................... G-31

G-17 Field-Observed (F) and Laboratory-Predicted (P) Chloride Concentrations as a Function of Volume per Mass for Alliance AFBC Waste and Interburden................................. G-32

G-18 Field-Observed (F) and Laboratory-Predicted (P) Chloride Concentrations as a Function of Volume per Mass for Alliance AFBC Waste and Limestone................................... G-33

G-19 Field-Observed (F) and Laboratory-Predicted (P) Chloride Concentrations as a Function of Volume per Mass for Alliance AFBC Waste and Shale....................................... G-34

G-20 Lab (L), Field (F), and Predicted (P) Fractional Attenuation of Strontium as a Function of Volume per Mass for Exxon PFBC Waste and Glacial Till..................................... G-55

G-21 Lab (L), Field (F), and Predicted (P) Fractional Attenuation of Sulfate as a Function of Volume per Mass for Alliance AFBC Waste and Alluvium.................................... G-56

List of Figures
(Continued)

Figure | Page

G-22 Lab (L), Field (F), and Predicted (P) Fractional Attenuation of Total Dissolved Solids as a Function of Volume per Mass for Alliance AFBC Waste and Alluvium........................ G-57

G-23 Plots of Field-Observed (F) and Field-Predicted (P) Fractional Attenuations of Boron for Exxon PFBC Waste in Replicate Field Cells 1 and 2.. G-62

G-24 Plots of Field-Observed (F) and Field-Predicted (P) Fractional Attenuations of Calcium for Exxon PFBC Waste in Replicate Field Cells 1 and 2.. G-63

G-25 Plots of Field-Observed (F) and Field-Predicted (P) Fractional Attenuations of Sulfate for Exxon PFBC Waste in Replicate Field Cells 1 and 2.. G-64

G-26 Plots of Field-Observed (F) and Field-Predicted (P) Fractional Attenuations of Strontium for Exxon PFBC Waste in Replicate Field Cells 1 and 2.. G-65

G-27 Plots of Field-Observed (F) and Field-Predicted (P) Fractional Attenuations of Total Dissolved Solids for Exxon PFBC Waste in Replicate Field Cells 1 and 2............................ G-66

G-28 Plots of Field-Observed (F) and Field-Predicted (P) Fractional Attenuations of Boron for Alliance AFBC Waste in Replicate Field Cells 14 and 15...................................... G-67

G-29 Plots of Field-Observed (F) and Field-Predicted (P) Fractional Attenuations of Sulfate for Alliance AFBC Waste in Replicate Field Cells 14 and 15...................................... G-68

G-30 Plots of Field-Observed (F) and Field-Predicted (P) Fractional Attenuations of Strontium for Alliance AFBC Waste in Replicate Field Cells 14 and 15...................................... G-69

G-31 Plots of Field-Observed (F) and Field-Predicted (P) Fractional Attenuations of Total Dissolved Solids for Alliance AFBC Waste in Replicate Field Cells 14 and 15.......................... G-70

List of Figures
(Continued)

Figure | Page

G-32 to G-41 (See Attachment 1)

G-42 to G-50 (See Attachment 6)

G-51 to G-62 (See Attachment 7)

G-63 Model Confirmation Results for Sulfate Based on Shake-Test Extractions of Exxon PFBC Waste: Observed (O) and Predicted (P) Cumulative Field Cell 1 Extractions...................... G-92

G-64 Model Confirmation Results for Silicon Based on Shake-Test Extractions of Exxon PFBC Waste: Observed (O) and Predicted (P) Cumulative Field Cell 1 Extractions...................... G-93

G-65 Model Confirmation Results for Chromium Based on Shake-Test Extractions of Exxon PFBC Waste: Observed (O) and Predicted (P) Cumulative Field Cell 1 Extractions...................... G-94

G-66 Model Confirmation Results for Barium Based on Shake-Test Extractions of Exxon PFBC Waste: Observed (O) and Predicted (P) Cumulative Field Cell 1 Extractions...................... G-95

G-67 Model Confirmation Results for Sodium Based on Shake-Test Extractions of Exxon PFBC Waste: Observed (O) and Predicted (P) Cumulative Field Cell 1 Extractions...................... G-96

G-68 Model Confirmation Results for Iron Based on Shake-Test Extractions of Exxon PFBC Waste: Observed (O) and Predicted (P) Cumulative Field Cell 1 Extractions...................... G-97

G-69 Model Confirmation Results for Calcium Based on Shake-Test Extractions of Exxon PFBC Waste: Observed (O) and Predicted (P) Cumulative Field Cell 1 Extractions...................... G-98

G-70 Model Confirmation Results for Zinc Based on Shake-Test Extractions of Exxon PFBC Waste: Observed (O) and Predicted (P) Cumulative Field Cell 1 Extractions...................... G-99

G-71 Model Confirmation Results for Strontium Based on Shake-Test Extractions of Exxon PFBC Waste: Observed (O) and Predicted (P) Cumulative Field Cell 1 Extractions...................... G-100

G-72 to G-116 (See Attachments 8 to 12)

Attachments

Attachment **Page**

1 Figures G-32 to G-41 .... G-105

G-32 Natural Logarithm of Sulfate Concentration vs. Shake-Test Extraction Step for Exxon PFBC Waste G-107

G-33 Natural Logarithm of Silicon Concentration vs. Shake-Test Extraction Step for Exxon PFBC Waste G-108

G-34 Natural Logarithm of Barium Concentration vs. Shake-Test Extraction Step for Exxon PFBC Waste G-109

G-35 Natural Logarithm of Iron Concentration vs. Shake-Test Extraction Step for Exxon PFBC Waste G-110

G-36 Natural Logarithm of Calcium Concentration vs. Shake-Test Extraction Step for Exxon PFBC Waste G-111

G-37 Natural Logarithm of Strontium Concentration vs. Shake-Test Extraction Step for Exxon PFBC Waste G-112

G-38 Natural Logarithm of Magnesium Concentration vs. Shake-Test Extraction Step for Exxon PFBC Waste G-113

G-39 Natural Logarithm of Boron Concentration vs. Shake-Test Extraction Step for Exxon PFBC Waste G-114

G-40 Natural Logarithm of Fluoride Concentration vs. Shake-Test Extraction Step for Exxon PFBC Waste G-115

G-41 Natural Logarithm of Aluminum Concentration vs. Shake-Test Extraction Step for Exxon PFBC Waste G-116

2 Table G-17 .... G-117

G-17 Model Building Results Based on Shake-Test Extractions of PFBC Waste: Maximum R^2 Models with No Species Leading Value (L) Forced, But pH and Leading pH Available G-119

Attachments
(Continued)

Attachment Page

3 Table G-18 .... G-127
G-18 Model Building Results Based on Shake-Test Extractions of PFBC Waste: Maximum R^2 Models with Each Species' Leading Value (L) Forced and No pH Values Available ... G-129
4 Table G-19 .... G-137
G-19 Model Building Results Based on Shake-Test Extractions of PFBC Waste: Maximum R^2 Models with no Species' Leading Value (L) Forced Into the Model and no pH Values Available G-139
5 Table G-22 .... G-147
G-22 Model Building Results Based on Shake-Test Extractions of Exxon PFBC Waste: Summary of Estimated Initial Soluble Fractions y_o Obtained by Back-Calculation from Shake-Test Results G-149
6 Figures G-42 to G-50 .... G-153
G-42 Model Building Results Based on Shake-Test Extractions of PFBC Waste: Initial Soluble Sulfate Fraction G-155
G-43 Model Building Results Based on Shake-Test Extractions of PFBC Waste: Initial Soluble Silicon Fraction G-156
G-44 Model Building Results Based on Shake-Test Extractions of PFBC Waste: Initial Soluble Chromium Fraction G-157
G-45 Model Building Results Based on Shake-Test Extractions of PFBC Waste: Initial Soluble Barium Fraction G-158
G-46 Model Building Results Based on Shake-Test Extractions of PFBC Waste: Initial Soluble Sodium Fraction G-159
G-47 Model Building Results Based on Shake-Test Extractions of PFBC Waste: Initial Soluble Iron Fraction G-160
G-48 Model Building Results Based on Shake-Test Extractions of PFBC Waste: Initial Soluble Calcium Fraction G-161

Attachments
(Continued)

Attachment **Page**

G-49 Model Building Results Based on Shake-Test Extractions of PFBC Waste: Initial Soluble Zinc Fraction......... G-162

G-50 Model Building Results Based on Shake-Test Extractions of PFBC Waste: Initial Soluble Strontium Fraction.... G-163

7 Figures G-51 to G-62....................................... G-165

G-51 Leading Cumulative Rainfall (R) and Lower Level Field Cell Flow (F): Field Cell 1......................... G-167

G-52 Observed Flow (O) and Flow Predicted from a Rainfall-Flow Delay Model (P), with Rainfall Leading Flow by 12 Days: Field Cell 1............................... G-168

G-53 Leading Cumulative Rainfall (R) and Lower Level Field Cell Flow (F): Field Cell 2......................... G-169

G-54 Observed Flow (O) and Flow Predicted from a Rainfall-Flow Delay Model (P), with Rainfall Leading Flow by 12 Days: Field Cell 2............................... G-170

G-55 Leading Cumulative Rainfall (R) and Lower Level Field Cell Flow (F): Field Cell 3.......................... G-171

G-56 Observed Flow (O) and Flow Predicted from a Rainfall-Flow Delay Model (P), with Rainfall Leading Flow by 12 Days: Field Cell 3............................. G-172

G-57 Leading Cumulative Rainfall (R) and Lower Level Field Cell Flow (F): Field Cell 4......................... G-173

G-58 Observed Flow (O) and Flow Predicted from a Rainfall-Flow Delay Model (P), with Rainfall Leading Flow by 12 Days: Field Cell 4............................... G-174

G-59 Leading Cumulative Rainfall (R) and Lower Level Field Cell Flow (F): Field Cell 5......................... G-175

Attachments
(Continued)

Attachment Page

G-60 Observed Flow (O) and Flow Predicted from a Rainfall-Flow Delay Model (P), with Rainfall Leading Flow by 12 Days: Field Cell 5 .... G-176

G-61 Leading Cumulative Rainfall (R) and Lower Level Field Cell Flow (F): Field Cell 6 .... G-177

G-62 Observed Flow (O) and Flow Predicted from a Rainfall-Flow Delay Model (P), with Rainfall Leading Flow by 12 Days: Field Cell 6 .... G-178

8 Figures G-72 to G-80 .... G-179

G-72 Model Confirmation Results for Sulfate Based on Shake-Test Extraction of PFBC Waste: Observed (O) and Predicted (P) Cumulative Field Cell No. 1 Extractions. G-181

G-73 Model Confirmation Results for Silicon Based on Shake-Test Extraction of PFBC Waste: Observed (O) and Predicted (P) Cumulative Field Cell No. 1 Extractions. G-182

G-74 Model Confirmation Results for Chromium Based on Shake-Test Extraction of PFBC Waste: Observed (O) and Predicted (P) Cumulative Field Cell No. 1 Extractions. G-183

G-75 Model Confirmation Results for Barium Based on Shake-Test Extraction of PFBC Waste: Observed (O) and Predicted (P) Cumulative Field Cell No. 1 Extractions. G-184

G-76 Model Confirmation Results for Sodium Based on Shake-Test Extraction of PFBC Waste: Observed (O) and Predicted (P) Cumulative Field Cell No. 1 Extractions. G-185

G-77 Model Confirmation Results for Iron Based on Shake-Test Extraction of PFBC Waste: Observed (O) and Predicted (P) Cumulative Field Cell No. 1 Extractions. G-186

G-78 Model Confirmation Results for Calcium Based on Shake-Test Extraction of PFBC Waste: Observed (O) and Predicted (P) Cumulative Field Cell No. 1 Extractions. G-187

Attachments
(Continued)

Attachment **Page**

G-79 Model Confirmation Results for Zinc Based on Shake-Test Extraction of PFBC Waste: Observed (O) and Predicted (P) Cumulative Field Cell No. 1 Extractions. G-188

G-80 Model Confirmation Results for Strontium Based on Shake-Test Extraction of PFBC Waste: Observed (O) and Predicted (P) Cumulative Field Cell No. 1 Extractions. G-189

9 Figures G-81 to G-89 .... G-191

G-81 Estimated Initial Soluble Fraction (y_o), of Sulfate in Field Cell 1 Obtained by Back-Calculation from Field Cell 1 Data G-193

G-82 Estimated Initial Soluble Fraction (y_o), of Silicon in Field Cell 1 Obtained by Back-Calculation from Field Cell 1 Data G-194

G-83 Estimated Initial Soluble Fraction (y_o), of Chromium in Field Cell 1 Obtained by Back-Calculation from Field Cell 1 Data G-195

G-84 Estimated Initial Soluble Fraction (y_o), of Barium in Field Cell 1 Obtained by Back-Calculation from Field Cell 1 Data G-196

G-85 Estimated Initial Soluble Fraction (y_o), of Sodium in Field Cell 1 Obtained by Back-Calculation from Field Cell 1 Data G-197

G-86 Estimated Initial Soluble Fraction (y_o), of Iron in Field Cell 1 Obtained by Back-Calculation from Field Cell 1 Data G-198

G-87 Estimated Initial Soluble Fraction (y_o), of Calcium in Field Cell 1 Obtained by Back-Calculation from Field Cell 1 Data G-199

Attachments
(Continued)

Attachment Page

G-88 Estimated Initial Soluble Fraction (y_o), of Zinc in Field Cell 1 Obtained by Back-Calculation from Field Cell 1 Data.. G-200
G-89 Estimated Initial Soluble Fraction (y_o), of Strontium in Field Cell 1 Obtained by Back-Calculation from Field Cell 1 Data.. G-201
10 Figures G-90 to G-98.. G-203
G-90 Observed (O) and Predicted (P) Cumulative Field Cell 1 Extractions for Sulfate.. G-205
G-91 Observed (O) and Predicted (P) Cumulative Field Cell 1 Extractions for Silicon.. G-206
G-92 Observed (O) and Predicted (P) Cumulative Field Cell 1 Extractions for Chromium.. G-207
G-93 Observed (O) and Predicted (P) Cumulative Field Cell 1 Extractions for Barium.. G-208
G-94 Observed (O) and Predicted (P) Cumulative Field Cell 1 Extractions for Sodium.. G-209
G-95 Observed (O) and Predicted (P) Cumulative Field Cell 1 Extractions for Iron.. G-210
G-96 Observed (O) and Predicted (P) Cumulative Field Cell 1 Extractions for Calcium.. G-211
G-97 Observed (O) and Predicted (P) Cumulative Field Cell 1 Extractions for Zinc.. G-212
G-98 Observed (O) and Predicted (P) Cumulative Field Cell 1 Extractions for Strontium.. G-213
11 Figures G-99 to G-107.. G-215
G-99 Observed (O) and Predicted (P) Cumulative Field Cell 1 Extractions for Sulfate.. G-217
G-100 Observed (O) and Predicted (P) Cumulative Field Cell 1 Extractions for Silicon.. G-218

Attachments
(Continued)

Attachment **Page**

G-101 Observed (O) and Predicted (P) Cumulative Field Cell 1 Extractions for Chromium.............................. G-219

G-102 Observed (O) and Predicted (P) Cumulative Field Cell 1 Extractions for Barium................................ G-220

G-103 Observed (O) and Predicted (P) Cumulative Field Cell 1 Extractions for Sodium................................ G-221

G-104 Observed (O) and Predicted (P) Cumulative Field Cell 1 Extractions for Iron.................................. G-222

G-105 Observed (O) and Predicted (P) Cumulative Field Cell 1 Extractions for Calcium............................... G-223

G-106 Observed (O) and Predicted (P) Cumulative Field Cell 1 Extractions for Zinc.................................. G-224

G-107 Observed (O) and Predicted (P) Cumulative Field Cell 1 Extractions for Strontium............................. G-225

12 Figures G-108 to G-116.. G-227

G-108 Observed (O) and Predicted (P) Cumulative Field Cell 1 Extractions of Sulfate............................... G-229

G-109 Observed (O) and Predicted (P) Cumulative Field Cell 1 Extractions of Silicon............................... G-230

G-110 Observed (O) and Predicted (P) Cumulative Field Cell 1 Extractions of Chromium.............................. G-231

G-111 Observed (O) and Predicted (P) Cumulative Field Cell 1 Extractions of Barium................................ G-232

G-112 Observed (O) and Predicted (P) Cumulative Field Cell 1 Extractions of Sodium................................ G-233

G-113 Observed (O) and Predicted (P) Cumulative Field Cell 1 Extractions of Iron.................................. G-234

G-114 Observed (O) and Predicted (P) Cumulative Field Cell 1 Extractions of Calcium............................... G-235

Attachments
(Continued)

Attachment **Page**

G-115 Observed (O) and Predicted (P) Cumulative Field Cell 1 Extractions of Zinc.................................... G-236

G-116 Observed (O) and Predicted (P) Cumulative Field Cell 1 Extractions of Strontium.............................. G-237

G.1 Overview

Two empirical approaches for predicting the environmental effects of the disposal of FBC waste were attempted. Both approaches involved the development of statistical models from laboratory leaching data to predict field leaching behavior. An extensive statistical analysis of leaching and attenuation data for Exxon PFBC and Alliance AFBC waste was performed in the first approach. A feasibility study for the second statistical approach used only leaching data for PFBC waste. The second approach could be extended to analyze attenuation data also.

The two statistical approaches are similar in the following respects:

1. Laboratory data were used to develop models for predicting concentrations (or a function thereof) of the different chemical species. In this step, field data are not used.

2. The model development was accomplished by using regression analysis.

3. A separate model was ultimately produced for each chemical species. In the leaching models, concentration was expressed as a function of volume per mass. In the attenuation models (discussed in the first but not the second approach), fractional attenuation was also expressed as a function of volume per mass. Either approach could be used to develop attenuation models in which concentration is expressed as a function of volume per mass.

4. Thus, the end result of both approaches was the same: a model to predict concentration (or a function thereof) as a function of volume per mass. Since volume per mass is a normalized quantity, the models can be used to predict field conditions.

The methods differed in the steps used to develop the statistical models. In the first approach, a model was developed directly to predict the concentration of a particular species as a function of volumn per mass. The concentrations of other species did not come into play.

In the second approach, a regression model was first developed in which the concentration of a chemical species was predicted in terms of the concentrations of other chemical species at the preceding leaching step and possibly pH at the preceding or current leaching step. Subsequently, transformations were made through a set of mathematical steps to produce models which predict concentration as a function of volume per mass. Thus, for simplicity, the two approaches are referred to as the direct and indirect methods, respectively.

For the sole purpose of developing a model which predicts concentration in terms of volume per mass, the direct method is simpler and less demanding both in terms of labor and computer time. Moreover, the direct method as formulated is guaranteed to predict non-negative, real-value leaching concentrations.

On the other hand, the indirect method produces intermediate results which can be interpreted from the point of view of causal relationships in the leaching process. Suppose, for example, that the concentration of species k is selected as a predictor of species j. This may imply that the presence of species i in the leachate affects the leaching of species j from the waste. It must be remembered, however, that statistical correlations do not automatically imply that a cause and effect relationship exists. A disadvantage of the indirect method is that it is possible for mathematical instabilities to develop.

In each approach, model development to predict leaching behavior was successful. Agreement was achieved between the laboratory-predicted values and the data from which the models were developed. The agreement is described both in terms of large tables presenting statistical measures, such as squared multiple correlation coefficients and standard errors, and plots displaying observed and predicted values.

For the direct method, extensive summary measures of agreement between observed and predicted values are presented. It is shown that field-observed values and predictions from the laboratory models agree within an order of magnitude for most chemical species and waste combinations. For the indirect method, observed and predicted field values are compared through plots of cumulative mass leached.

As noted, models for fractional attenuation were developed using only the direct method. Agreement between field observed and predicted vlaues was achieved only in isolated cases. It is possible that in future work, better agreement will be achieved if concentration, rather than fractional attenuation, is used as the dependent variable.

G.2 Leaching and Attenuation Models for FBC Wastes: Predictive Models for Concentrations Developed Directly as Functions of Volume per Mass

Statistical models were developed to characterize both leaching and attenuation behavior. The primary objective of the models was to determine the feasibility of predicting field leachate concentration values from laboratory data.

The investigation was performed using the following waste and disposal medium combinations:

1. Exxon PFBC waste and shale, sandstone, glacial till, alluvium, and limestone disposal media; and

2. Alliance AFBC waste and shale, interburden, alluvium, and limestone disposal media.

Thus, a resonable variety of waste-medium combinations were represented in the data base. The disposal media affect the leaching results only in that the medium comprises the overburden in the field cells. The contents of the feild cells used in this part of the modeling study are indicated in Table G-1.

TABLE G-1. CONTENTS OF FIELD CELLS USED IN MODELING STUDY

Cell No.	Waste	Disposal Medium
1, 2	Exxon PFBC	Shale
3	Exxon PFBC	Glacial Till
4	Exxon PFBC	Limestone
5	Exxon PFBC	Alluvium
6	Exxon PFBC	Sandstone
13	Alliance AFBC	Interburden
14, 15	Alliance AFBC	Alluvium
16	Alliance AFBC	Limestone
17	Alliance AFBC	Shale

Note: Two control cells (Cells 7 and 12) were also operated, but these were not used in the modeling study. Cell 7 contained shale and Cell 12 contained alluvium.

First, an analysis of leaching behavior was performed. Models were developed from laboratory data to predict leachate concentrations. When these models were developed, certain chemical species whose concentrations were predominantly near or below detection limits were excluded. Subsequently, an analysis was performed to quantify the agreement between observed field concentration and corresponding values predicted from the laboratory models. It was found that for Exxon PFBC waste and for the 13 species investigated, the mean agreement between the observed feild values and the laboratory-predicted field values was within a factor of 10 in 11 cases, a factor of five in eight cases, and a factor of two in three cases. For Alliance AFBC waste and for the 19 species investigated, the mean agreement was within a factor of 10 in 17 cases, a factor of five in 16 cases, and a factor of two in 10 cases. Thus, laboratory models are capable of predicting field trends within an order of magnitude in most cases. The difference between the observed and laboratory-predicted field observed and predicted field values were statistically significant for most species, however. It has been verified through plots of observed and predicted values that the models fit the laboratory data.

The prediction of field data involved an extrapolation, since the laboratory volumes of leachate per unit mass of waste leached were larger than for the field cells. Further investigation showed, however, that the differences between field-observed and laboratory-predicted values are not attributable wholly or predominantly to the extrapolation. Actual differences between the behavior of the laboratory and field systems are believed to explain a significant part of the discrepancies between observed and predicted values.

An analysis was also performed of fractional attenuation, which is the fractional reduction (or increase) in leachate concentration due to contact with the disposal medium. It was observed from raw data plots that prediction of field fractional attenuations from laboratory models is infeasible for the majority of cases. This is due to the dissimilarity of the lab and field trends and random scatter in the fractional attenuation data. Successful predictions of field behavior from laboratory data for a few species were accomplished, however.

As a result of the observations discussed above, an alternative analysis was performed. A set of models was developed from field data to describe fractional attenuation behavior. The models were shown through data plots and statistical measures to be capable of following the field trends, although random scatter about the predictive function existed.

G.2.1 Models for Leaching

Laboratory data from protocol Step 1, 2, and 3 and field data from the upper sampling point were used to develop models for leaching behavior. As noted, the investigation was performed using the following waste and disposal medium combinations: 1) Exxon PFBC waste and shale, sandstone, glacial till, alluvium, and limestone disposal medial; and 2) Alliance AFBC waste and shale, interburden, alluvium, and limestone disposal media.

For the leaching studies the following were the primary questions addressed:

1. Is it possible to develop models to fit the laboratory data?

2. Is it possible to use the laboratory models to predict field leaching concentrations? This question was divided into the following two elements:

    2a. How do the values predicted by the laboratory models compare on the average to the field values?

    2b. How much scatter is there in the observed field minus laboratory-predicted values?

The methods used to develop the laboratory models are discussed first below, and then the models themselves and associated statistical measures are presented. Next, a comparison is made between the field-observed concentrations and the corresponding predicted values from the laboratory models. This comparison is made in two steps. First, observed and predicted values are plotted on the same graph so that they can be compared visually. These plots demonstrate the agreement between laboratory-predicted values and the values from which they were developed as well as the agreement between the field-observed and laboratory-predicted values. Subsequently, a variety of statistical measures is presented to compare field observed and predicted values.

A statistical analysis was performed on the observed laboratory and field leaching behavior of FBC wates. Models developed from laboratory data to predict concentration as a function of volume of leachate per unit mass of waste are presented. Subsequently, the agreement between field observed concentrations and values predicted from the laboratory models is explored through plots and statistical measures. The statistical significance of the differences between field-observed and laboratory-predicted values is also discussed. The laboratory and field data used are for Exxon PFBC and Alliance AFBC waste.

G.2.1.1 Calculation of Volume per Mass

The volume per unit mass (referred to here as "volume per mass") is the volume of liquid which has contacted the waste per unit mass of waste contacted. Normalizing the leachate volume by the mass of waste provides an idependent variable which has a consistent meaning for the laboratory and field data and also facilitates comparisons. The field volume per mass is simply the flow-through volume divided by the mass of waste in the cell. For the laboratory, the volume per mass for protocol Step 1 is 10 mL/g. For Step 2, iteration i, the volume per mass is 10(i+1); the same mass is retained, but Step 1 leachate is added each iteration. For Step 3, iteration i, the volume per mass is 10/(i+1); fresh waste is added each iteration, but the same leachate is retained.

G.2.1.2 Data Selection

Models were not developed for the chemical species for which all or virtually all leachate concentrations were near or below the detection limits for the analytical instrument used. There was no basis for developing meaningful models for these cases. Models were developed for Al, B, Ba, Ca, Cl, Cr, F, Fe, Na, Si, Sr, SO_4, TDS, and Zn for Exxon PFBC waste and for Al, B, Ba, Be, Ca, Cd, Cl, Cr, Cu, F, Fe, Li, Mn, Mo, Na, Ni, Si, SO_4, Sr, Ti, TDS, V, and Zn for Alliance AFBC waste. Additional discussion pertaining to data selection for leaching model development is presented in Section G.2.1.6.

G.2.1.3 Methods Used to Develop Laboratry Leaching Models

The functional form used in developing the models from the laboratory data is as follows:

$$C = 10^{b_0} + b_1V + b_2V^2 + b_3V^3$$

where:

C is concentration (mg/L),

b_0, b_1, b_2, and b_3 are regression coefficients, and

V is volume per mass of waste (mL/g).

It should be noted that if $b_2 = b_3 = 0$, the model has the form:

$$C = 10^{b_0}\, 10^{b_1V} = (B)\, 10^{b_1V}$$

where $B = 10^{b_0}$.

Thus, the model can take the form of a decaying exponential (when $b_1 < 0$ in the expression above) or it can have a variety of other shapes, depending on the values of the b_1. The versatility of the functional form used is one reason for its selection. In any case, the model can be expressed as:

$$C = (10^{b_0})\,(10^{b_1V + b_2V^2 + B_3V^3})$$

Thus, b_0 determines a constant multiplier for the predicted concentrations, and b_1, b_2, and b_3 determine the shape of the curve as a function of volume per mass.

As written above, the model is nonlinear in the coefficients to be determined. Taking the logarithm of both sides of the equation, however, produces an equation which is linear in the coefficients:

$$\log_{10}(C) = b_0 + b_1V + b_2V^2 + b_3V^3$$

Expressing the model in this form allows linear regression techniques to be used; thus, a closed-form expression exists for the regression coefficients. If nonlinear regressions were used, an iterative solution would ordinarily be required, which would increase the computer time needed. Additionally, lack of convergence would be a possibility.

A variable selection method was used to select the best subset of the candidate predictor terms, V, V^2, and V^3. The method used first selects the one-variable model with the highest R^2. The quantity R is the multiple correlation coefficient, and R^2 can be interpreted as the fraction of the variance in the dependent variable which can be explained or predicted in terms of the predictor variables. Subsequently, another term, the one that produces the greatest increase in R^2, is added to the model. Then a series of comparisons are made to determine whether replacing one of the variables with another would increase R^2. The process is continued until no additional replacements can increase R^2. The result is a two-variable model. Subsequently, a three-variable model is developed in a similar manner (in this application, the three-variable model contains all three predictors, V, V^2, and V^3).

The variable selection method used is discussed in the SAS User's Guide (Reference G-1). The method is considered to be better than conventional step-wise regression analysis (Reference G-2), in that more combinations of predictor variables are considered.

The next question to be answered, then, is how many of the terms are needed in the model? Should the three-term model be used or does it differ from the two-term model only by random noise? All terms which model true or repeatable trends should be retained, and those which only follow the noise should be excluded. To choose among the one-, two-, and three-term models, several standard statistical measures were used, including R^2 (discussed above), the standard error, and t-statistics. These measures are discussed in Reference G-2 and in other textbooks on multiple regression analysis.

G.2.1.4 Laboratory Leaching Models

Tables G-2 and G-3 present the models developed for leaching concentrations for Exxon PFBC and Alliance AFBC wastes, respectively. In the tables, the following statistical terms are used to describe the models.

N - sample size (i.e., the number of points used),

R^2 - square of the multiple correlation coefficient, discussed below,

TABLE G-2. MODELS FOR LABORATORY LEACHING FOR EXXON PFBC WASTE

Element/ Species	N	R^2	Standard Error	b_0	b_1	Standard Error of b_1	b_2	Standard Error of b_2	b_3	Standard Error of b_3
Al	14	0.11	0.17	−0.48	0.028	0.024	−0.00077	0.00069	—[1]	—
B	14	0.91	0.058	1.7	−0.082	0.0082	0.0022	0.00024	—	—
Ba	14	0.82	0.086	−0.33	−0.057	0.012	0.0012	0.00035	—	—
Ca	14	0.50	0.053	3.2	0.022	0.021	−0.0026	0.0015	0.000063	0.000031
Cl	13	0.91	0.16	2.1	−0.25	0.064	0.0097	0.0046	−0.00011	0.000095
Cr	13	0.49	0.32	0.25	−0.28	0.13	0.017	0.0094	−0.00030	0.00019
F	13	0.59	0.21	−0.18	0.089	0.083	−0.010	0.0061	0.00024	0.00013
Fe	14	0.0053	0.17	−0.73	0.0014	0.0054	—	—	—	—
Na	14	0.61	0.20	2.6	−0.26	0.077	0.016	0.0056	−0.00028	0.00012
Si	14	0.29	0.15	−0.47	0.037	0.021	−0.00089	0.00062	—	—
Sr	14	0.56	0.16	1.0	−0.12	0.065	0.0060	0.0047	−0.00098	0.000097
SO_4	14	0.44	0.018	3.1	−0.0036	0.0025	0.00014	0.000072	—	—
TDS	14	0.49	0.077	3.6	−0.0082	0.0024	—	—	—	—
Zn	14	0.38	0.17	−1.7	0.86	0.067	−0.0081	0.0049	0.00019	0.00010

Note: Volume per Mass $\leq$30 mL/g

[1] Since variable selection techniques were used in the model development, not all terms were included in all models. Dashes indicate excluded terms.

TABLE G-3. MODELS FOR LABORATORY LEACHING FOR ALLIANCE AFBC WASTE

Species	N	R^2	Standard Error	b_0	b_1	Standard Error of b_1	b_2	Standard Error of b_2	b_3	Standard Error of b_3
Al	23	0.77	0.16	0.15	−0.094	0.034	0.0052	0.0031	−0.00011	0.000069
B	24	0.60	0.24	0.85	−0.17	0.052	0.012	0.0046	−0.00024	0.00010
Ba	23	0.19	0.30	−0.83	—[1]	—	−0.0069	0.00031	—	—
Be	21	0.67	0.19	−1.6	−0.34	0.13	0.033	0.017	−0.00090	0.00052
Ca	22	0.047	0.061	3.2	−0.0015	0.0015	—	—	—	—
Cd	20	0.85	0.095	−1.1	−0.095	0.012	0.0033	0.00059	—	—
Cl	24	0.99	0.053	2.6	−0.11	0.0045	0.0016	0.00015	—	—
Cr	24	0.94	0.087	−0.31	−0.20	0.019	0.013	0.0017	−0.00025	0.000039
Cu	24	0.68	0.19	−0.61	−0.17	0.042	0.012	0.0037	−0.00023	0.000085
F	24	0.45	0.15	−0.86	−0.084	0.033	−0.0051	0.0030	0.000080	0.000067
Fe	22	0.83	0.092	−0.77	−0.21	0.060	0.019	0.0074	−0.00052	0.00024
Li	24	0.99	0.033	0.46	−0.19	0.0073	0.010	0.00065	−0.00019	0.00015
Mn	24	0.67	0.14	−1.5	−0.13	0.032	0.0093	0.0028	−0.00019	0.000064
Mo	24	0.99	0.020	−0.11	−0.044	0.0045	0.0017	0.00040	−0.000033	0.0000090
Na	24	0.99	0.040	2.1	−0.20	0.0089	0.011	0.00079	−0.00020	0.000018
Ni	20	0.91	0.057	−0.68	−0.12	0.042	0.0086	0.0052	−0.00019	0.00017
Si	24	0.66	0.097	−0.26	−0.016	0.0024	—	—	—	—
SO_4	24	0.77	0.014	3.1	−0.019	0.0031	0.0012	0.00028	−0.000021	0.0000063
Sr	22	0.90	0.086	1.6	−0.029	0.0021	—	—	—	—
Ti	24	0.71	0.15	−0.28	−0.15	0.033	0.0097	0.0029	−0.00019	0.000066
TDS	24	0.92	0.0073	3.6	−0.0065	0.00061	0.00013	0.000020	—	—
V	24	0.63	0.16	−0.35	−0.14	0.036	0.0089	0.0032	−0.00017	0.000072
Zn	22	0.81	0.091	−1.0	−0.15	0.060	0.011	0.0074	−0.00025	0.00023

Note: Volume per Mass $\leq$30 mL/g

[1] Since variable selection techniques were used in the model development, not all terms were included in all models. Dashes indicate excluded terms.

standard error - standard deviation of the fluctuations of logarithms of concentrations (mg/L) about the regression line (i.e., the standard deviation of the observed minus predicted values),

b_0, b_1, b_2, and b_3 - regression coefficients, discussed above, and

standard errors of b_1, b_2, and b_3 - standard errors of the regression slopes of b_1, b_2, and b_3; the standard error of a quantity is the standard deviation of its error.

As is discussed above, the regression analysis was performed after a logarithmic transformation to linearize the model in terms of the coefficients. Thus, R^2 and the standard error are both measures of the agreement between logarithms of concentrations and the corresponding predicted values.

The quantity R^2 is the fraction of the variance in the logarithms of the concentrations which is explained by the model. The standard error is the standard deviation of the differences between the observed and predicted values in log-space.

In a few instances, the R^2 value is very low, but the standard error is also low. In these instances, the original variance of the lab concentrations is low; hence, a model which explains a small fraction of the original variance (low R^2) can still be in good agreement with the observed values (low standard error). Thus, a low R^2 value does not necessarily imply that the model is not good. The models are discussed further in the following section.

G.2.1.5 Comparison of Predicted Values From Laboratory Models and Field Concentrations

The agreement betewen values predicted from the laboratory models and the corresponding field concentrations was analyzed through plots and various tabulated statistical measures. A comparison of field observed and predicted values was also made by use of statistical measures.

G.2.1.5.1 Plots Displaying Concentrations From All Field Cells Simultaneously

Several plots showing lab and field observed values and predicted values with different symbols are presented below. The plots that were used are as follows:

1. Laboratory-observed leachate concentrations and corresponding predicted values; and

2 Field-observed and laboratory-predicted values for all field cells. The original observed data points from the field cells are shown separately, i.e., no averaging was performed. Thus, for a given waste and volume per mass, there could be one observed concentration for each field cell.

These plots, which are typical examples, display the agreement between (1) the laboratory-observed values used to develop the models and the corresponding predictions and (2) the field-observed and predicted concentrations. Due to the large range of values of volume per mass (four orders of magnitude), this quantity is shown on a logarithmic axis; if a linear axis were used, the field trends would not be seen at all.

Figures G-1 and G-2 display the results for total dissolved solids for Exxon PFBC and Alliance AFBC wastes, respectively. The plots for PFBC waste include the data for field cells 1-6, while the plots for AFBC waste include the data for field cells 13-17. It is seen in these plots that the predicted values follow the laboratory trends from which they were derived very well. This point is worth mentioning since selection of the wrong functional form for the model or excessive data scatter could prevent agreement between predictions and values used to develop the model. The predicted TDS values also agree with the field values for the AFBC field cells, although some scatter about the regression line exists.

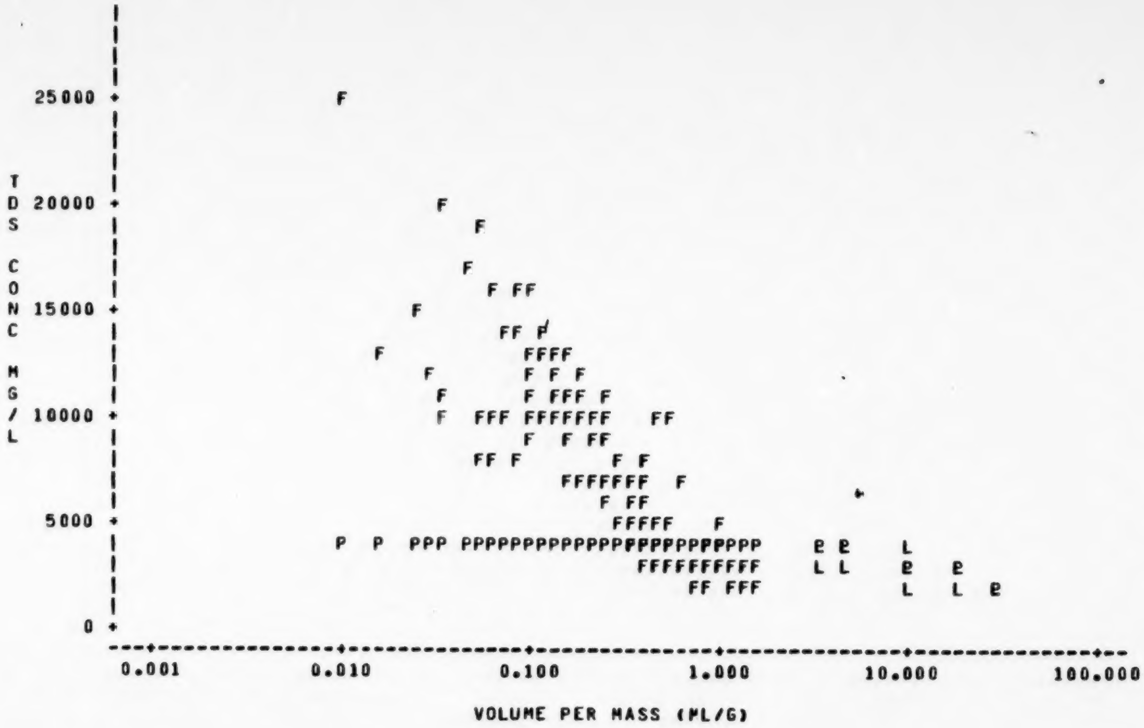

Figure G-1. Lab (L), Field (F), and Predicted (P) Total Dissolved Solids Concentrations as a Function of Volume per Mass for Exxon PFBC Waste.

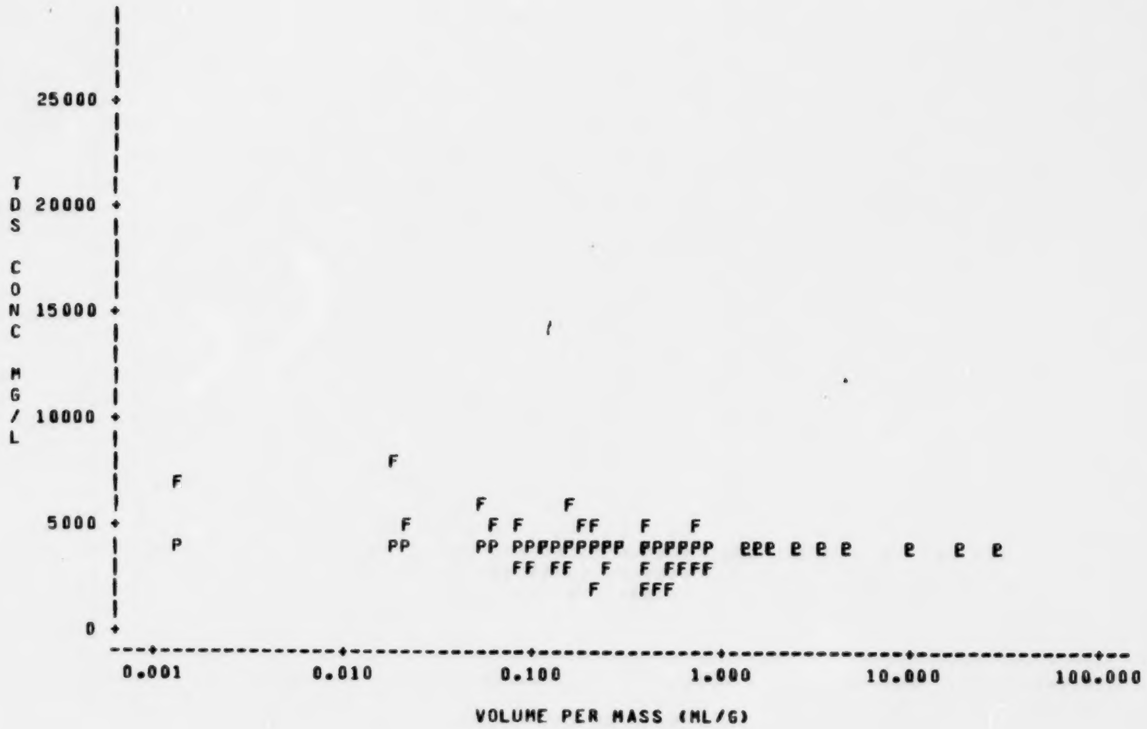

Figure G-2. Lab (L), Field (F), and Predicted (P) Total Dissolved Solids Concentrations as a Function of Volume per Mass for Alliance AFBC Waste.

The predicted TDS values fall predominantly below the field values for the Exxon PFBC cells for smaller values of volume per mass; reasonable agreement exists for the larger field volumes per mass (around 1 mL/g). The lack of agreement here may be due to the large difference in the values of volume per mass in the laboratory as opposed to the field values. Extrapolation is difficult to do accurately in general, and, in this case, the separation between field observed and predicted values increases as the predictive curve moves farther from the range of data used to develop the curve.

It may appear that the predictive function "levels off" (i.e., experiences a sharp reduction in slope) at the left of the plot. This is actually because of the logarithmic transformation, which expands the scale at the left of the plot.

The plots in Figures G-3 and G-4 present the results for sulfate, which constitutes a large part of the TDS concentrations (roughly half). As expected, the sulfate results are very similar to the TDS results discussed above. Figures G-5 and G-6 show the results for sodium for Exxon PFBC and Alliance AFBC, respectively. The predicted values in this case are seen to pass roughly through the centers of the clusters of field points. A considerable amount of scatter exists in this instance, however, especially for PFBC.

Figures G-7 and G-8 present the results for boron. In both cases, the predicted values lie above the field values, although the discrepancy is not large for AFBC. In the case of PFBC, however, the slope of the lab points causes the prediction to fall above the field values by about a factor of nine on the average.

Figures G-9 and G-10 present the results for chloride. In this example, agreement between field observed and predicted values exists for Exxon PFBC. For Alliance AFBC, however, a subset of the points diverge from the predicted values as volume per mass decreases.

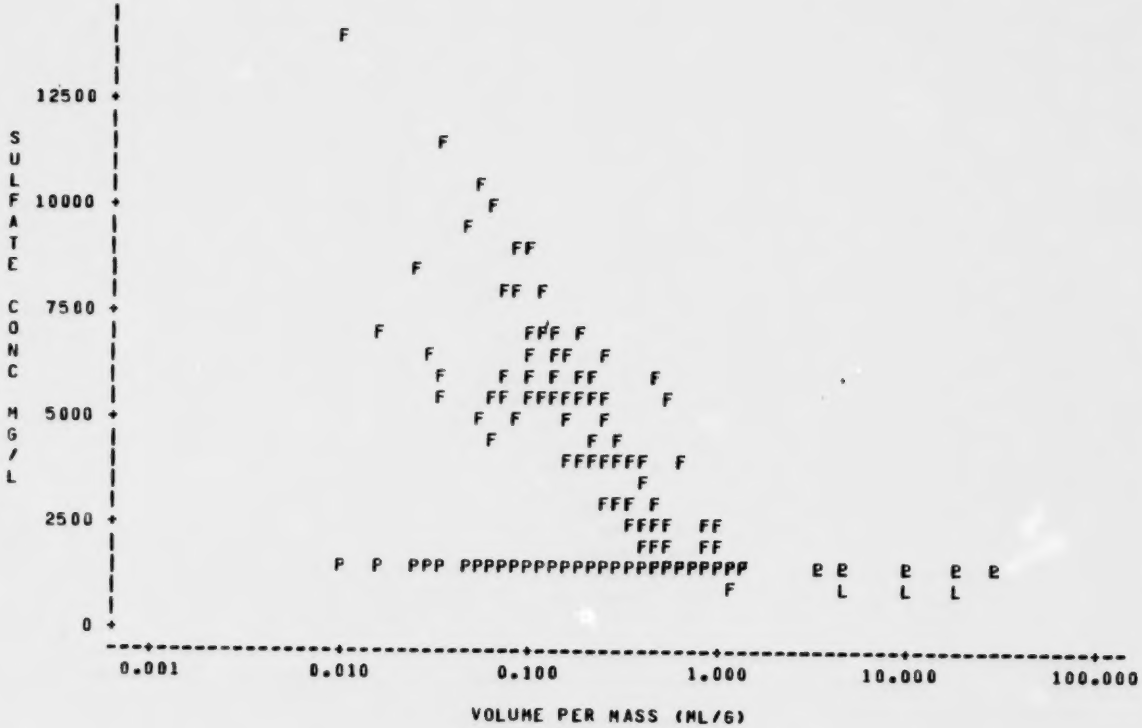

Figure G-3. Lab (L), Field (F), and Predicted (P) Sulfate Concentrations as a Function of Volume per Mass for Exxon PFBC Waste.

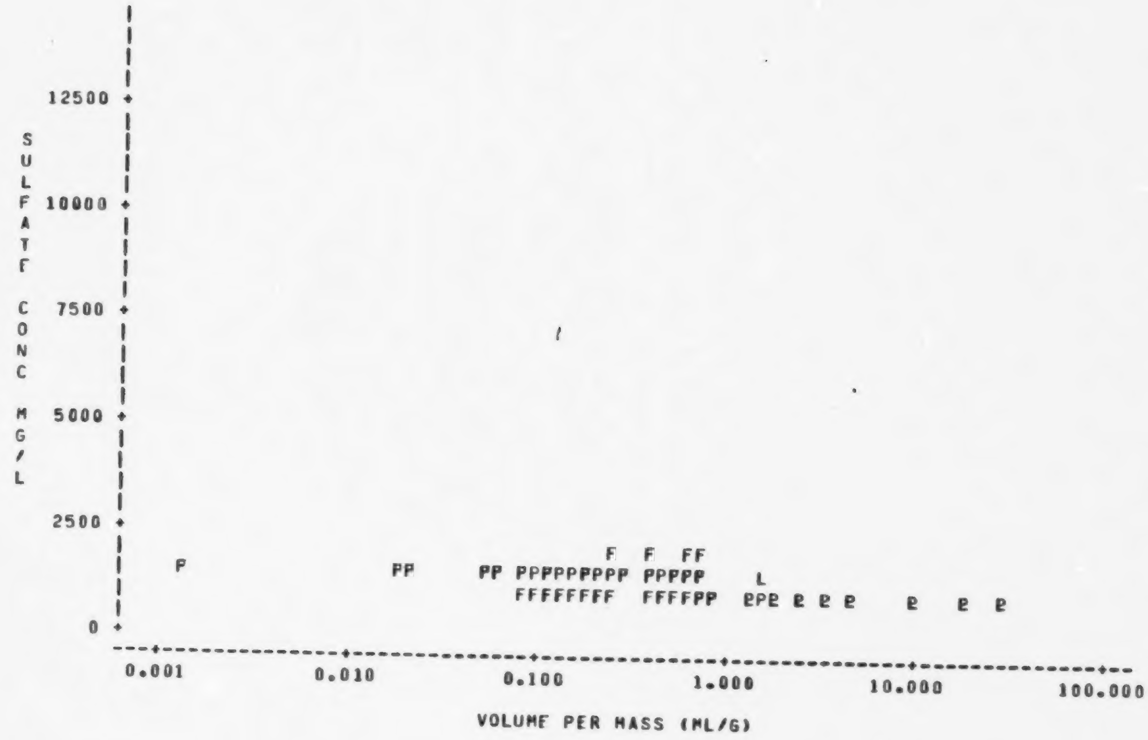

Figure G-4. Lab (L), Field (F), and Predicted (P) Sulfate Concentrations as a Function of Volume per Mass for Alliance AFBC Waste.

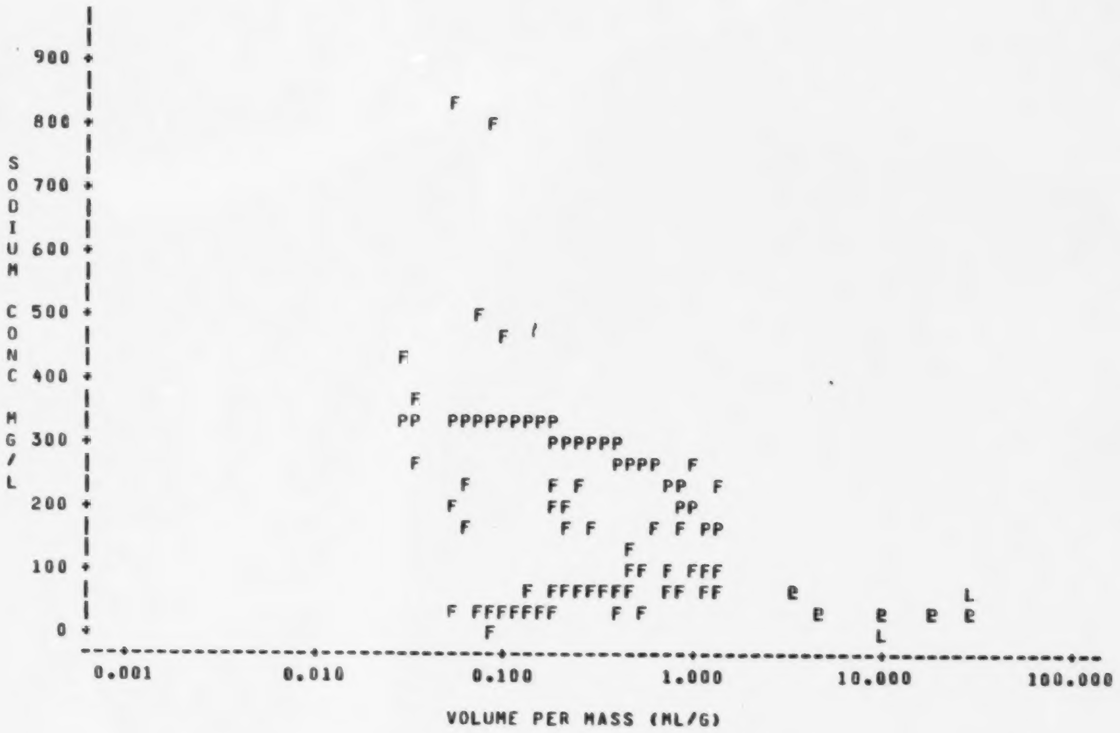

Figure G-5. Lab (L), Field (F), and Predicted (P) Sodium Concentrations as a Function of Volume per Mass for Exxon PFBC Waste.

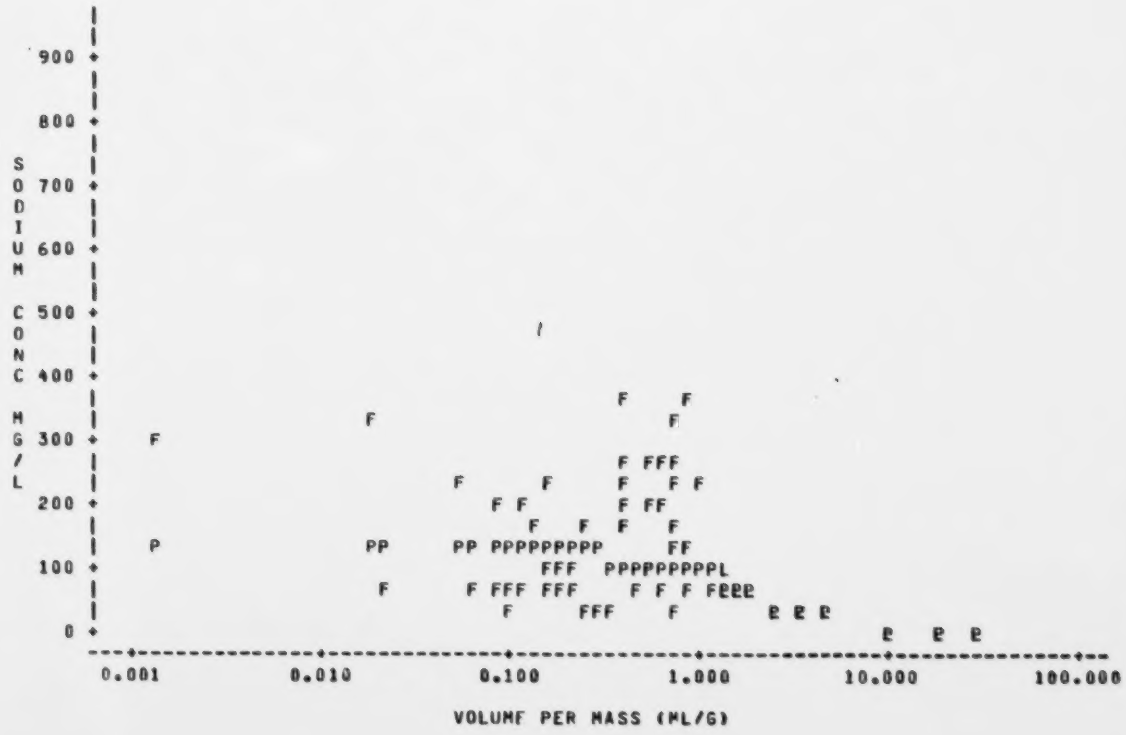

Figure G-6. Lab (L), Field (F), and Predicted (P) Sodium Concentrations as a Function of Volume per Mass for Alliance AFBC Waste.

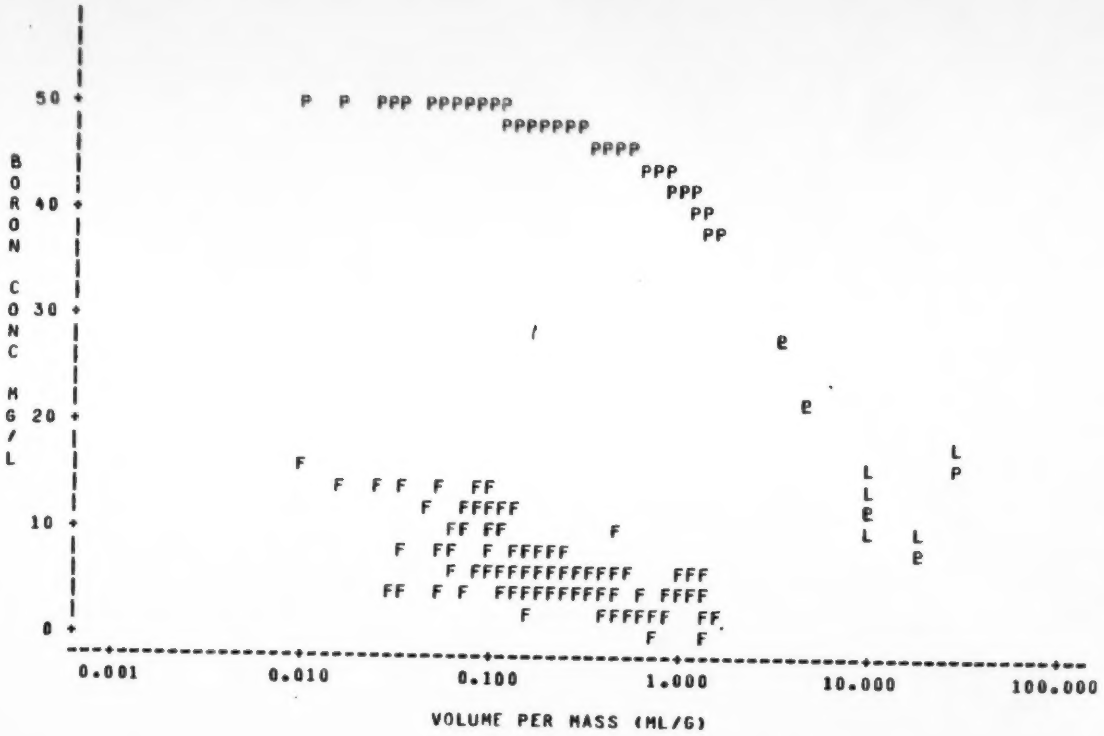

Figure G-7. Lab (L), Field (F), and Predicted (P) Boron Concentrations as a Function of Volume per Mass for Exxon PFBC Waste.

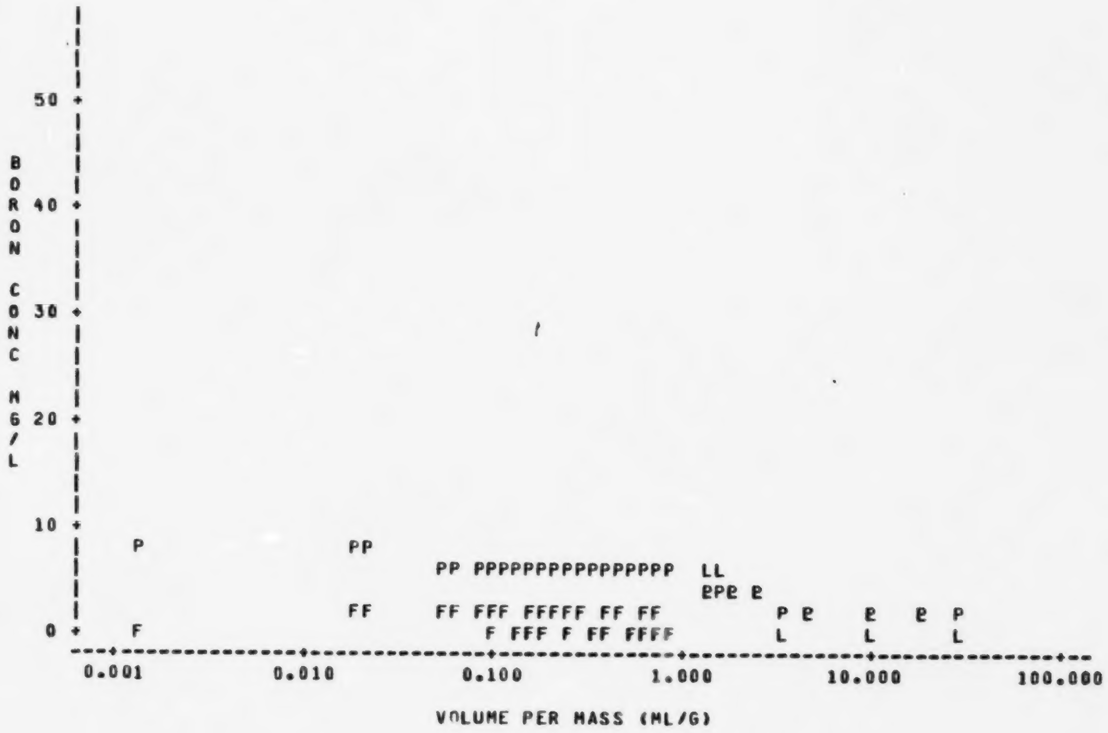

Figure G-8. Lab (L), Field (F), and Predicted (P) Boron Concentrations as a Function of Volume per Mass for Alliance AFBC Waste.

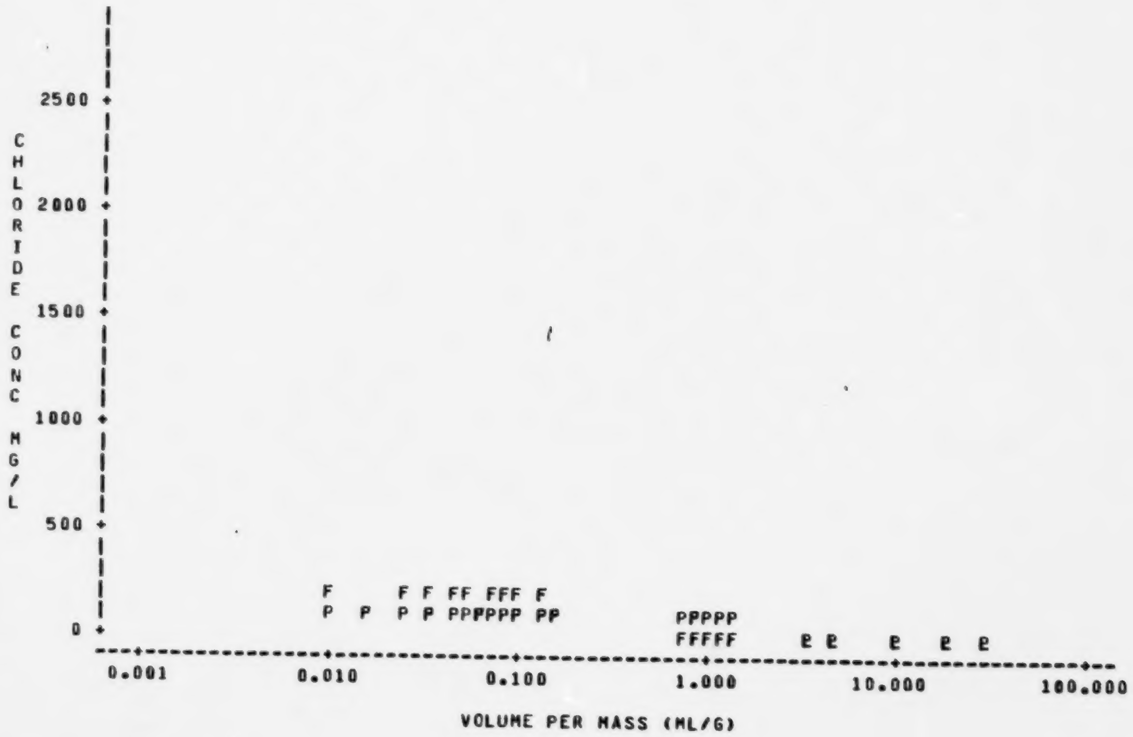

Figure G-9. Lab (L), Field (F), and Predicted (P) Chloride Concentrations as a Function of Volume per Mass for Exxon PFBC Waste.

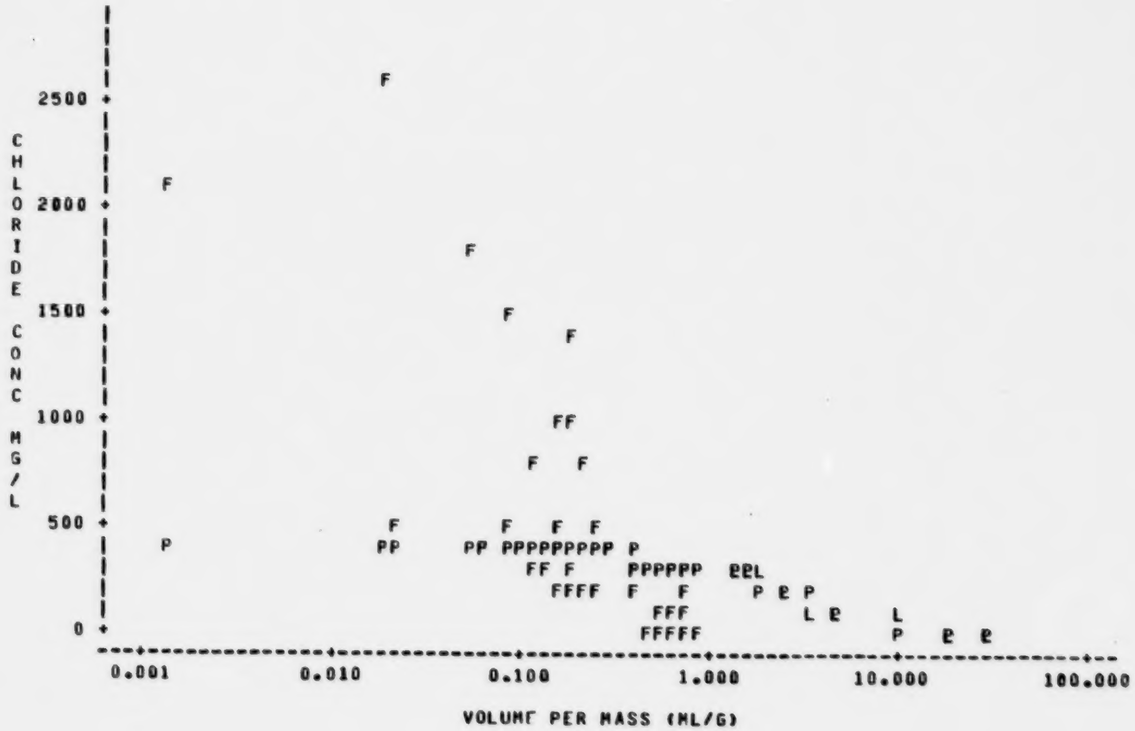

Figure G-10. Lab (L), Field (F), and Predicted (P) Chloride Concentrations as a Function of Volume per Mass for Alliance AFBC Waste.

G.2.1.5.2 Plots Using Chloride Concentrations From Individual Field Cells

Plots were prepared for the observed and predicted chloride concentrations separately for the laboratory and the individual field cells. Chloride was selected as a typical example. While Cells 1-6 all had Exxon PFBC waste and Cells 13-17 all had Alliance AFBC waste, the disposal medium comprising the upper disposal medium layer varied. Data from the replicate Cells 1 and 2 (shale disposal medium) were grouped together in one plot, as were data from Cells 14 and 15 (alluvium disposal medium). To enhance comparisons of the plots, a common scale was used even though the lab values require only the right side of the plot and the field values fall to the left.

Figures G-11 through G-14 present the chloride results for Exxon PFBC waste. Figure G-11 presents the observed and predicted lab data. Figure G-12 through G-14 present the field observed and laboratory-predicted field data for each PFBC field cell. Agreement for all field cells was achieved in this case.

Figures G-15 through G-19 present the chloride results for Alliance AFBC waste. Figures G-15 displays laboratory observed and predicted values. The figure shows that again the model agrees with the data from which it was developed. Figures G-16 through G-19 display observed and predicted field data. The largest discrepancy between observed and predicted values was found for alluvium overburden (Figure G-16), for which the largest range of volume per mass existed. Again, agreement was found for the larger volumes per mass but not for small volumes per mass. Relatively large discrepancies existed between observed and predicted values for shale (Figure G-19), but these differences were due to a large extent to scatter among the field data.

G.2.1.5.3 Analytical Comparisons of Field Observed and Predicted Values

While the plots discussed above are useful for presenting typical examples, statistical measures are necessary for quantifying the differences between field-observed and laboratory-predicted values and for summarizing a

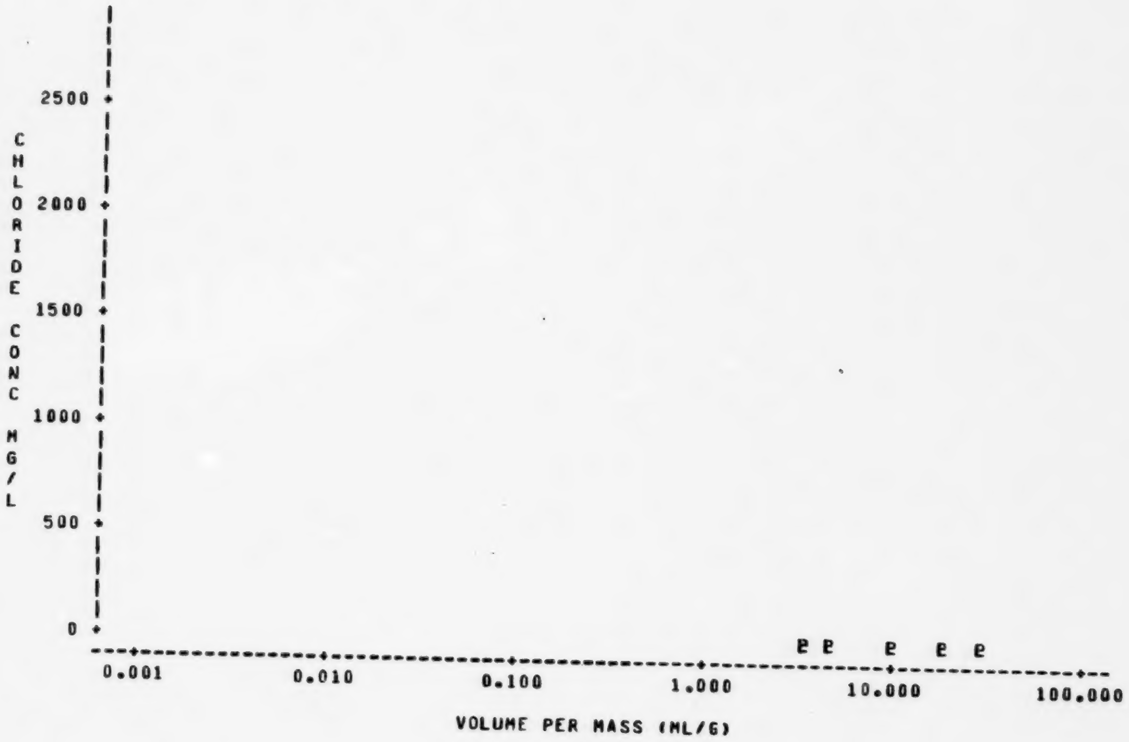

Figure G-11. Lab (L) and Predicted (P) Concentrations as a Function of Volume per Mass for Exxon PFBC Waste.

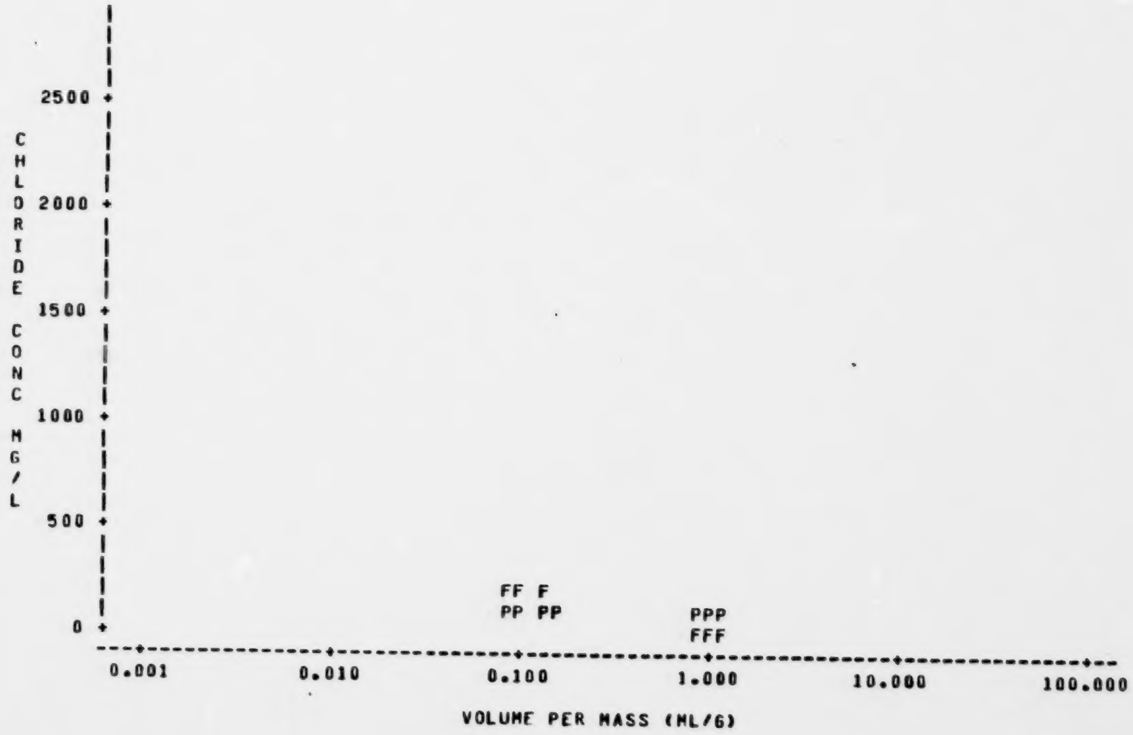

Figure G-12. Field-Observed (F) and Laboratory-Predicted (P) Chloride Concentrations as a Function of Volume per Mass for Exxon PFBC Waste and Limestone.

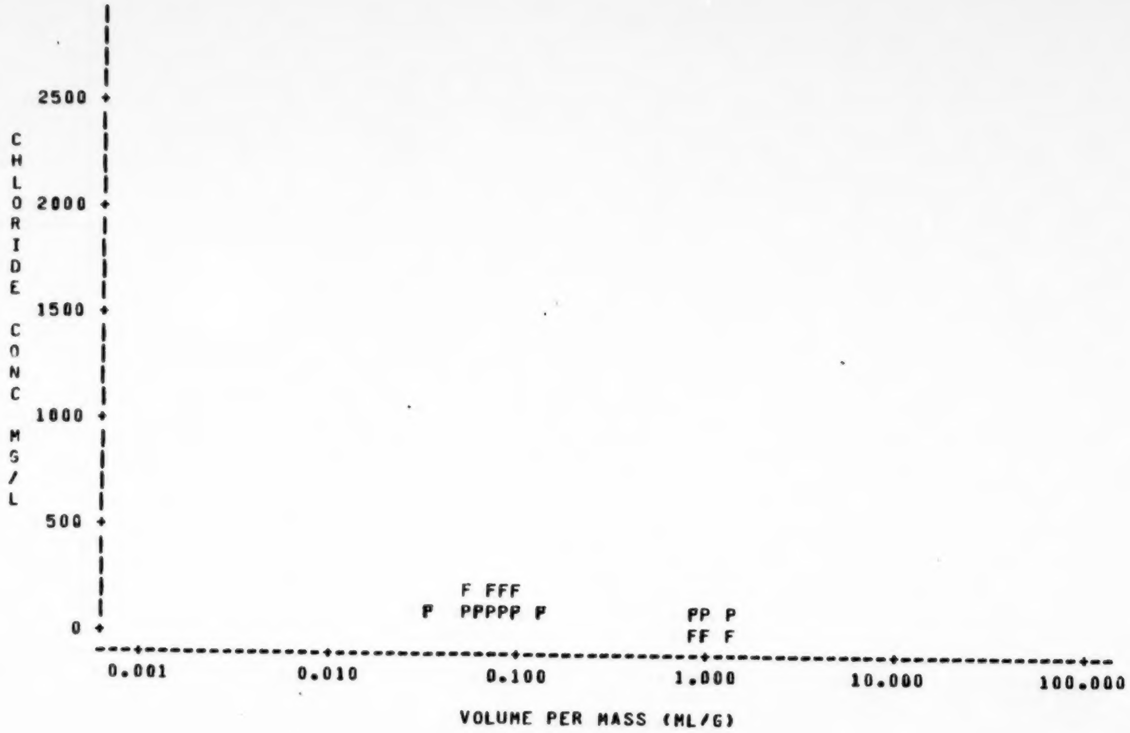

Figure G-13. Field-Observed (F) and Laboratory-Predicted (P) Chloride Concentrations as a Function of Volume per Mass for Exxon PFBC Waste and Shale.

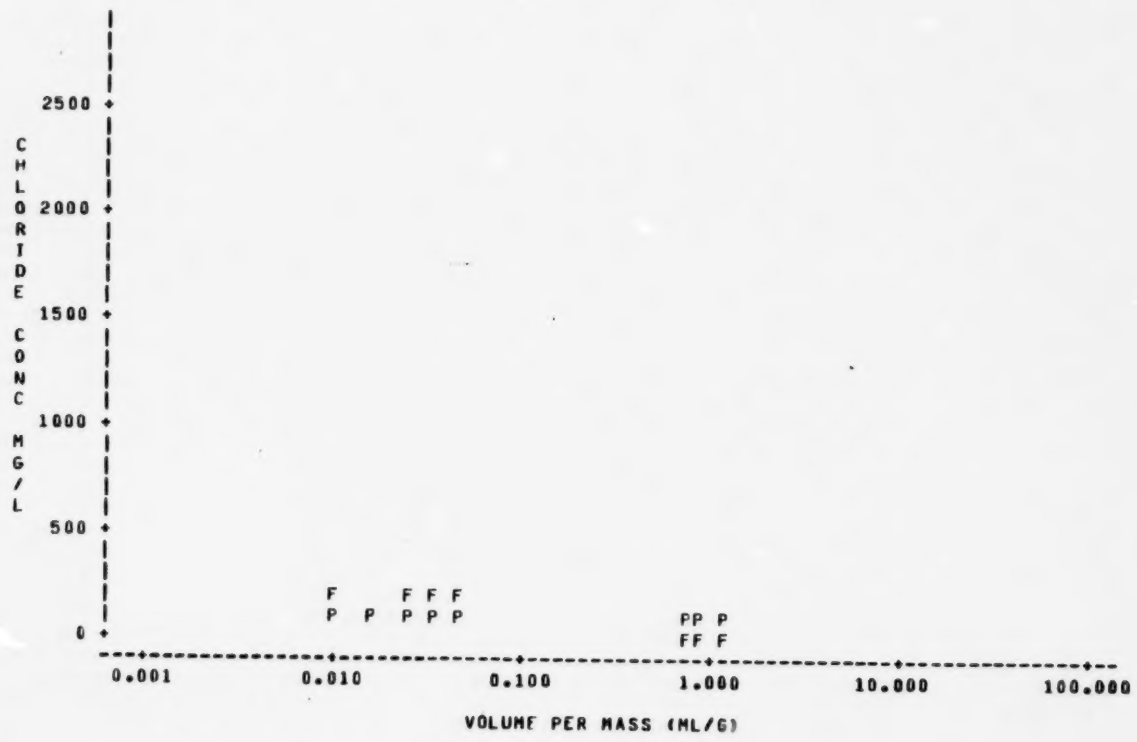

Figure G-14. Field-Observed (F) and Laboratory-Predicted (P) Chloride Concentrations as a Function of Volume per Mass for Exxon PFBC Waste and Glacial Till.

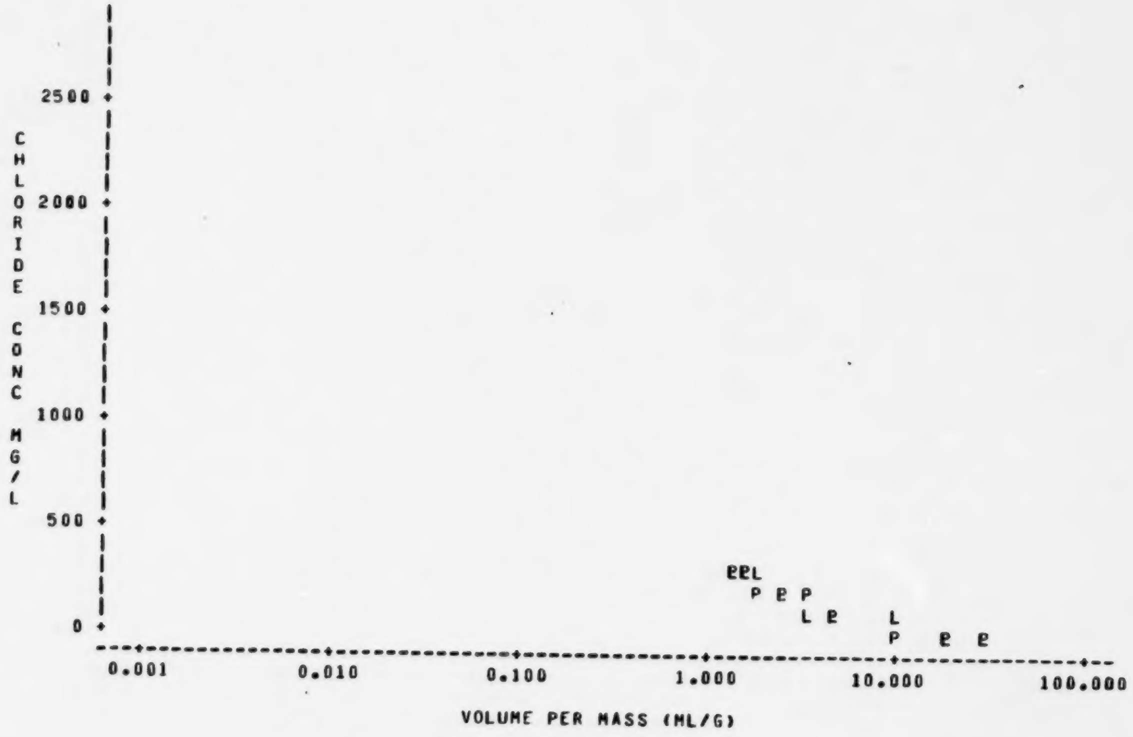

Figure G-15. Lab (L) and Predicted (P) Chloride Concentrations as a Function of Volume per Mass for Alliance AFBC Waste.

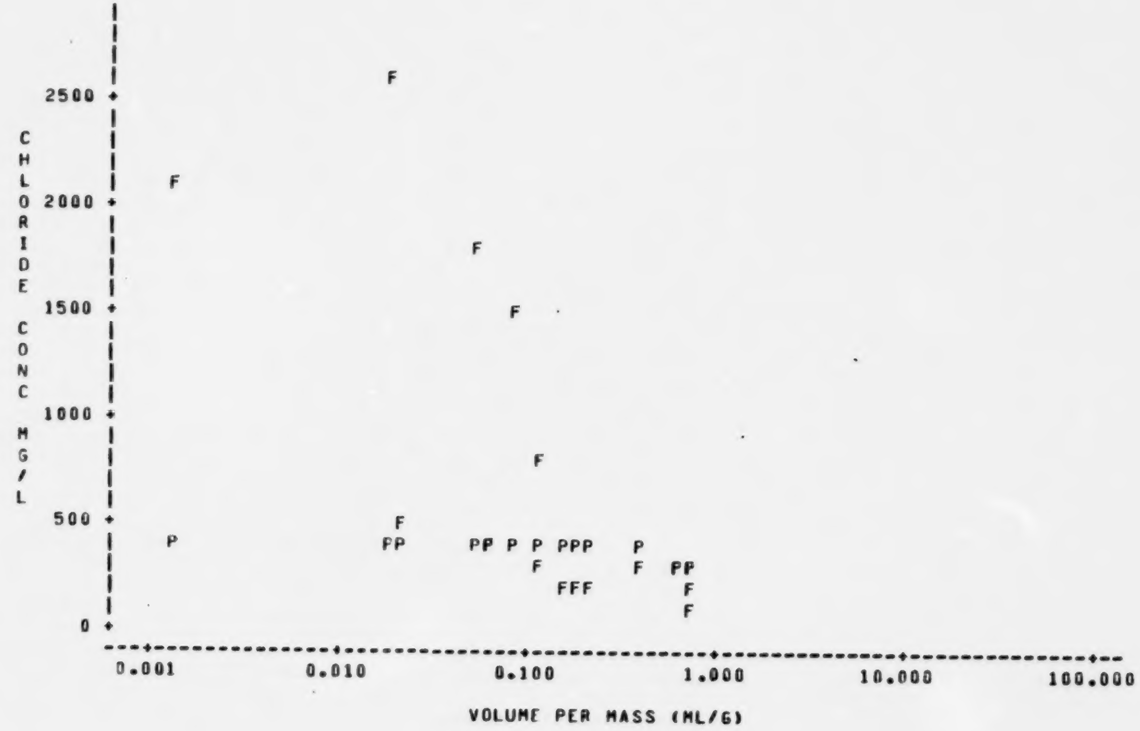

Figure G-16. Field-Observed (F) and Laboratory-Predicted (P) Chloride Concentrations as a Function of Volume per Mass for Alliance AFBC Waste and Alluvium.

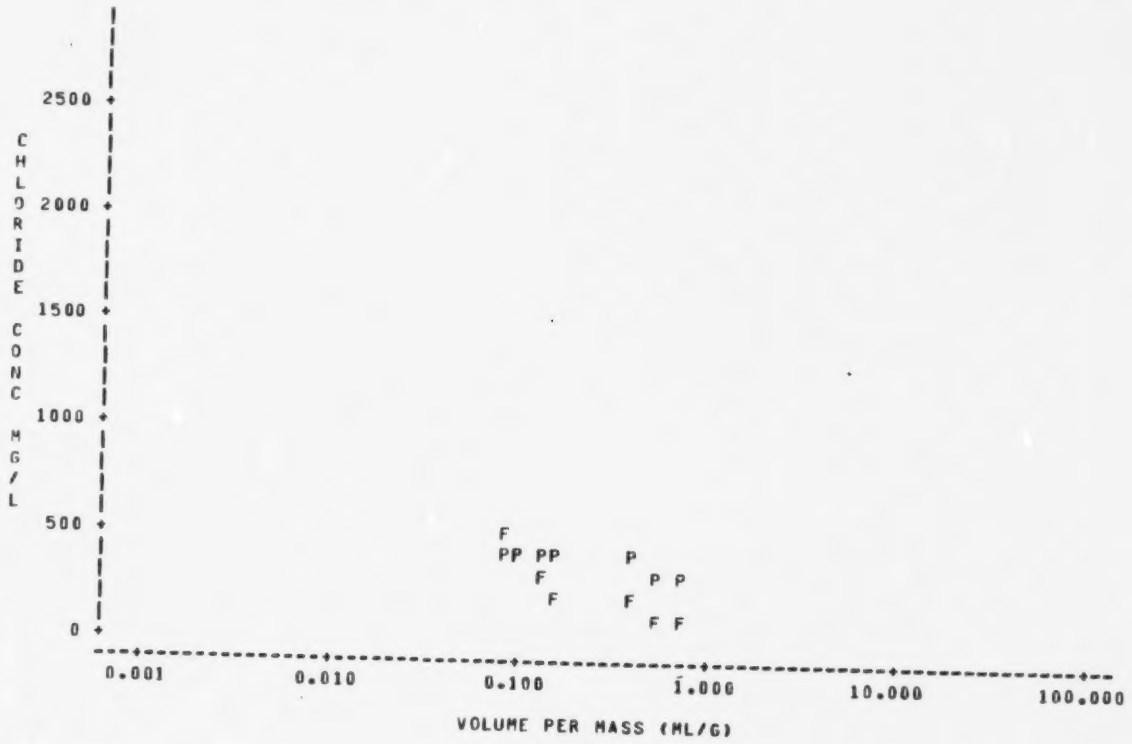

Figure G-17. Field-Observed (F) and Laboratory-Predicted (P) Chloride Concentrations as a Function of Volume per Mass for Alliance AFBC Waste and Interburden.

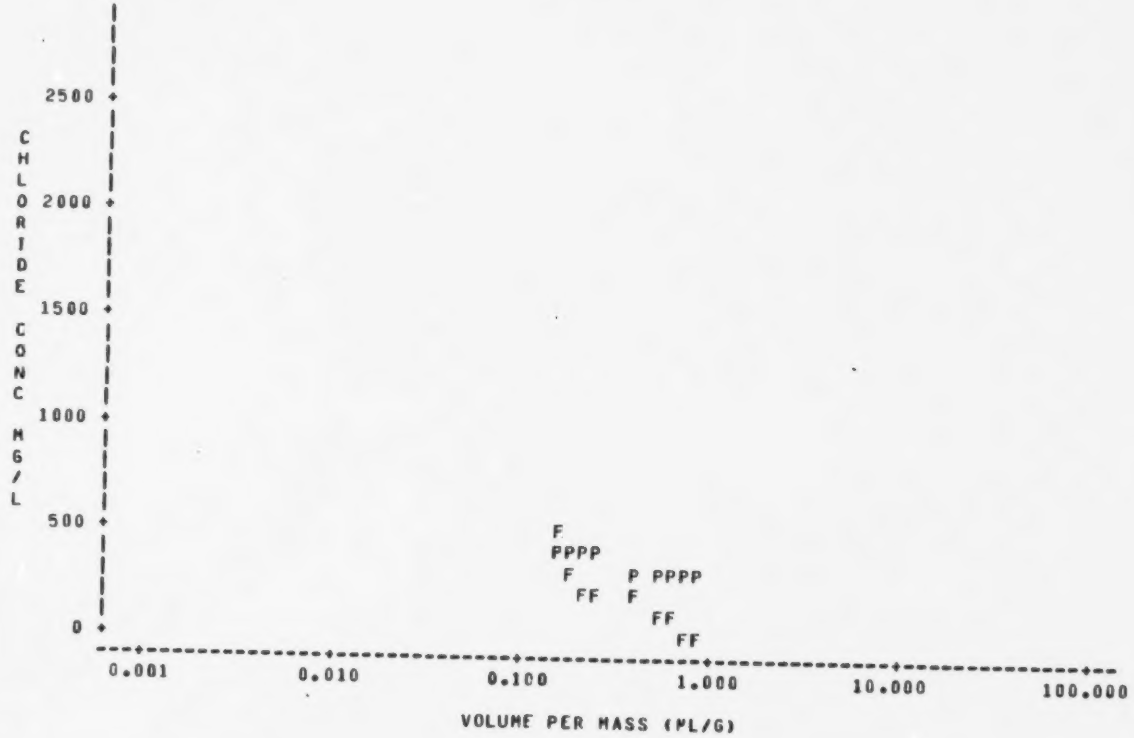

Figure G-18. Field-Observed (F) and Laboratory-Predicted (P) Chloride Concentrations as a Function of Volume per Mass for Alliance AFBC Waste and Limestone.

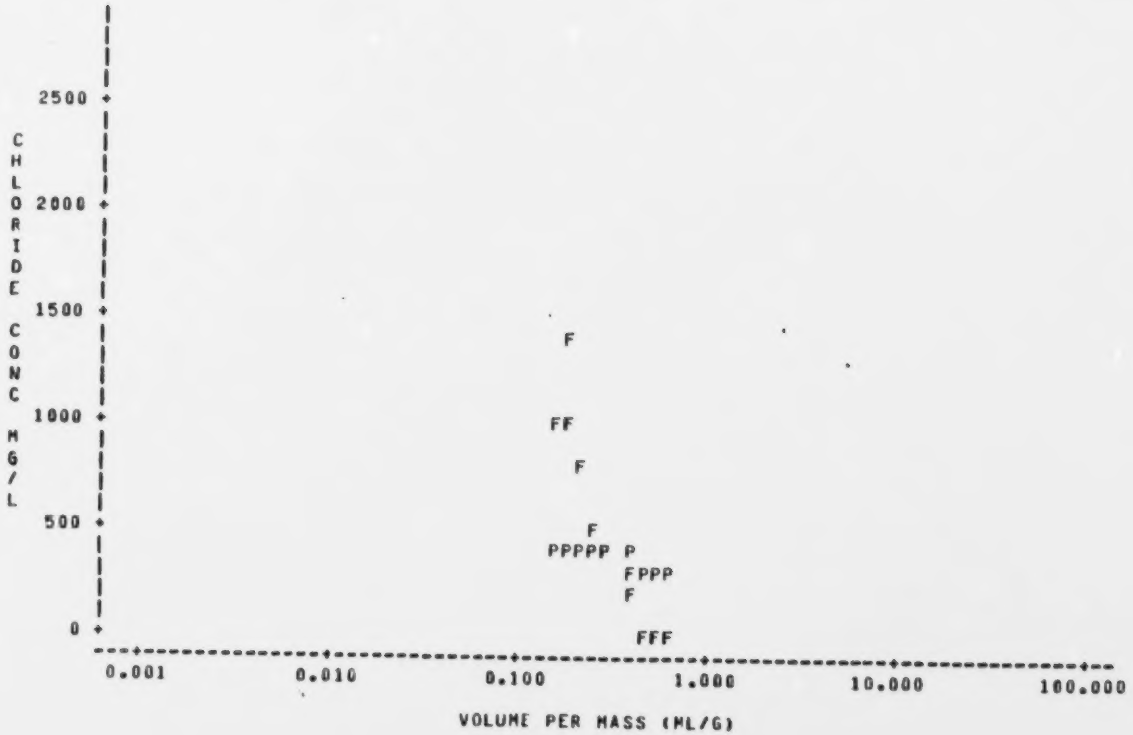

Figure G-19. Field-Observed (F) and Laboratory-Predicted (P) Chloride Concentrations as a Function of Volume per Mass for Alliance AFBC Waste and Shale.

large amount of information in a single table. The tables presented below are designed primarily to address the following basic questions:

(1) How do the observed and predicted values compare on the average (for each waste and chemical species)?

(2) How much scatter is there in the differences between the observed and predicted values?

(3) How does the agreement between field-observed and laboratory-predicted values compare to the agreement between the lab-observed values used to develop the model and the corrsponding predicted values?

(4) Are there statistically significant (i.e., measureable or repeatable) differences between field-observed and laboratory-predicted values? If so, in what respects are the lab models unable to predict field behavior?

Tables G-4 and G-5 present basic statistical measures to compare field-observed and laboratory-predicted values. A residual value is simply the observed minus the predicted value, after taking logarithms to the base 10. The means and standard deviations of the residuals are presented in the tables. The primary reason for calculation of the error measures in log-space is because the regression analysis was done in log-space (see above); comparison of the error measures with statistical measures from the regression analysis is facilitated by performing the calcualtions in a compatible manner. Also, the measures of error in log-space can easily be translated into measures of relative error in linear space, as is discussed below.

To facilitate interpretation of these results, the statistical measures have been converted from logarithms to linear values. Thus, the mean residual is as follow:

TABLE G-4. COMPARISON OF FIELD CONCENTRATIONS AND VALUES PREDICTED BY MODEL DEVELOPED FROM LABORATORY DATA FOR EXXON PFBC WASTE

Species	Standard Error From Regression	Number of Points (Lab)	Std. Deviation of field Residuals	Mean of Field Residuals	Number of Points (Field)
Al	0.17 (1.5)	14	- -	- -	-
B	0.018 (1.1)	14	0.26 (1.8)	-0.97 (0.11)	125
Ba	0.086 (1.2)	14	0.43 (2.7)	-0.79 (0.16)	64
Ca	0.053 (1.1)	14	0.19 (1.6)	-0.50 (0.32)	125
Cl	0.16 (1.4)	13	0.37 (2.3)	-0.17 (0.67)	30
Cr	0.32 (2.1)	13	0.38 (2.4)	-1.3 (0.045)	122
F	0.21 (1.6)	13	0.16 (1.4)	-0.50 (0.32)	123
Fe	0.17 (1.5)	14	0.46 (2.9)	-0.50 (0.32)	82
Na	0.20 (1.6)	14	0.39 (2.4)	-0.51 (0.31)	69
Si	0.15 (1.4)	14	0.33 (2.1)	1.9 (85)	125
SO_4	0.018 (1.0)	14	0.26 (1.8)	0.47 (3.0)	117
Sr	0.16 (1.4)	14	0.18 (1.5)	-0.91 (0.12)	125
TDS	0.077 (1.2)	14	0.26 (1.8)	0.23 (1.7)	123
Zn	0.17 (1.5)	14	0.43 (2.7)	0.011 (1.0)	48

Note: The residual values are $\log_{10}$ (field concentration) - $\log_{10}$ (predicted concentration), where both concentrations are mg/L.

Each value in parentheses is the exponential (base 10) of the number to the left of it.

TABLE G-5. COMPARISON OF FIELD CONCENTRATIONS AND VALUES PREDICTED BY MODEL DEVELOPED FROM LABORATORY DATA FOR ALLIANCE AFBC WASTE

Species	Standard Error From Regression	Number of Points (Lab)	Std. Deviation of field Residuals	Mean of Field Residuals	Number of Points (Field)
Al	0.16 (1.4)	23	0.36 (2.3)	−0.24 (0.58)	37
B	0.24 (1.7)	24	0.41 (2.6)	−0.91 (0.12)	42
Ba	0.30 (2.0)	23	0.59 (3.9)	0.18 (1.5)	49
Be	0.19 (1.5)	21	– –	– –	–
Ca	0.061 (1.2)	22	1.6 (41)	1.9 (0.011)	54
Cd	0.095 (1.2)	20	– –	– –	–
Cl	0.053 (1.1)	24	0.45 (2.8)	−0.15 (0.70)	52
Cr	0.087 (1.2)	24	0.38 (2.4)	−0.69 (0.20)	34
Cu	0.19 (1.5)	24	0.47 (3.0)	−0.62 (0.24)	11
F	0.15 (1.4)	24	0.19 (1.5)	0.10 (1.3)	51
Fe	0.092 (1.2)	22	0.35 (2.3)	0.20 (1.6)	10
Li	0.033 (1.1)	24	0.24 (1.8)	−0.069 (0.85)	40
Mn	0.14 (1.4)	24	0.69 (4.9)	0.26 (1.8)	18
Mo	0.020 (1.1)	24	0.47 (3.0)	−0.33 (0.47)	11
Na	0.040 (1.1)	24	0.33 (2.1)	0.044 (1.1)	54
Ni	0.057 (1.1)	20	– –	– –	–
Si	0.097 (1.3)	24	0.65 (4.5)	1.3 (22)	54
SO_4	0.014 (1.0)	24	0.11 (1.3)	0.0083 (1.0)	52
Sr	0.086 (1.2)	22	0.40 (2.5)	−0.33 (0.47)	53
TDS	0.0073 (1.0)	24	0.12 (1.3)	−0.058 (0.88)	52
Ti	0.15 (1.4)	24	0.78 (6.0)	−0.58 (0.26)	3
V	0.16 (1.4)	24	0.47 (2.9)	−0.66 (0.22)	4
Zn	0.091 (1.2)	22	– –	– –	–

Note: The residual values are $\log_{10}$ (field concentration) − $\log_{10}$ (predicted concentration), where both concentrations are mg/L.

Each value in parentheses is the exponential (base 10) of the number to the left of it.

$\overline{\text{Log c}}$ minus $\overline{\text{Log p}}$

where:

$\overline{\text{Log c}}$ = average of the logarithms of the field concentrations,

$\overline{\text{Log p}}$ = average of the logarithms of the laboratory-predicted concentrations.

Note that it does not mater whether differences are taken before or after averaging.

Conversion of the arithmetic average computed in log-space to linear-space by exponentiation (base 10) produces the geometric mean (Reference G-4). The geometric mean of a set of values X_i , i = 1 to N, is defined as:

$$\sqrt[N]{\prod_{i=1}^{N} X_i}$$

In the present case, X_i is the ratio of the i^{th} field observed value to the corresponding predicted value. Thus, whenever the geometric mean value is between 0.5 and 2, for example, the observed and predicted values agree within a factor of 2 on the average.

Table G-4 shows that for Exxon PFBC waste leachates, of 13 cases, the mean agreement between field observed and predicted values was within a factor of 10 in 11 cases, a factor of 5 in 8 cases, and a factor of 2 in 3 cases. Table G-5 shows that for Alliance AFBC waste leachates, of 19 cases, the mean agreement was within a factor of 10 in 17 cases, a factor of 5 in 16 cases, and a factor of 2 in 10 cases.

The standard deviation of the residuals in log-space and its conversion to linear-space are also presented. The standard deviation quantifies the random scatter of the residuals about their mean value. The conversion of the standard deviation from log-space to linear space by exponentiation (base 10) produces the fractional increase or decrease of the linear residuals corresponding to a one standard deviation perturbation; consider:

$$\mathrm{Log}_{10}(m) + \mathrm{Log}_{10}(s)$$

where:

$\mathrm{Log}_{10}(m)$ = mean residual in log-space, and

$\mathrm{Log}_{10}(s)$ = residual standard deviation in log-space. The quantity s is called the geometric standard deviation (Reference G-4).

Then the inverse transformation to linear space is as follows:

$$10^{\log_{10}(m) + \log_{10}(s)} = (10^{\log_{10}(m)}) \, (10^{\log_{10}(s)})$$
$$= (m) \, (s)$$

Thus, perturbing a value by one standard deviation in log-space corresponds to multiplication by the exponential of the standard deviation in linear space. Thus, if the geometric standard deviation s is 3, this means that the ± one standard deviation limits correspond to a range of ± a factor of 3 in linear concentration. The residuals have limits of ± 3 or less for all models for Exxon PFBC waste and for 14 of 19 cases for Alliance AFBC waste.

The standard error from the regression analysis is also presented. The measures of agreement between the field-observed and lab-predicted values should be compared to this value. Intuitively, one would not expect the field agreement to be better than the agreement between the predicted values and the data from which the model was developed.

Table G-4 and G-5, discussed above, present simple statistical measures that quantify the agreement between field-observed and laboratory-predictd values. The next question to be addressed is whether the differences are statistically significnt. When the differences are not statistically significant, this means that the differences which do exist between the field-observed and laboratory-predicted values can reasonably be explained in terms of random effects alone. When the differences are statistically significant, this means that they are too large to be explained in terms of random errors alone; evidence exists that a true or repeatable difference exists.

Tables G-6 and G-7 present results of a set of hypothesis tests regarding differences between lab and field trends. The tests basically involve the following questions:

(1) For each field cell, is the b_0 term different from the b_0 term for the lab data (recall that the data for replicate field cells are grouped)?

(2) Given the cell-specific values of b_0, can the predictive accuracy be improved significantly by introducing cell-specific b_1 terms?

(3) Given the cell-specific values of b_0 and b_1, can the predictive accuracy be improved significantly by introducing cell-specific b_2 terms?

(4) Given the cell-specific values of b_0, b_1, and b_2, can the predictive accuracy be improved signicantly by introducing cell-specific b_3 terms?

The statistical hypothesis testing was performed using general linear models procedures which are discussed in Reference G-3.

Thus, the terms are tested in the order of increasing complexity (i.e., the coefficient of lower order terms are tested first). Still, it is possible for the higher-order terms only to be significant. The result of this analysis is that for most of the models for both Exxon PFBC and Alliance AFBC wastes, significant differences do exist. It must be remembered, however,

TABLE G-6. SIGNIFICANCE TESTS FOR DIFFERENCES BETWEEN LABORATORY-PREDICTED AND FIELD-OBSERVED LEACHING TRENDS FOR EXXON PFBC WASTE

Species	Number of Points (Field)	Number of Points (Lab)	Significance of[1]				Codes Indicating for Which Cells Observed and Predicted Values are Significantly Different[2]					
			b_0	b_1	b_2	b_3	Shale	Sandstone	Limestone	Alluvium	Till	Signs of Significant Field Terms Consistent?
Al	–	14					–	–	–	–	–	–
B	125	14	x	x	x	x	I,C	C	C	I	I,C	Yes
Ba	64	14	x				–	I	I	I	I	Yes
Ca	125	14	x	x	x	x	I,C	I,C	I,C	I,C	I,C	Yes
Cl	30	13					–	–	–	–	–	–
Cr	122	13	x	x	x	x	I,C	I,C	I,C	I	I	Yes
F	123	13		x	x		–	C	C	C	–	Yes
Fe	82	14	x	x				I,C	I	–	–	No
Na	69	14		x	x	x	C	–	–	C	–	No
Si	125	14	x				I	I	I	I	I	Yes
Sr	125	14	x	x	x	x	I,C	I,C	I,C	I	I,C	Yes
SO	117	14	x	x			I,C	I	I,C	I	I,C	Yes
TDS	123	14	x	x	x		I,C	I	I,C	I,C	I,C	Yes
Zn	48	14			x	x	–	–	–	–	C	Yes

---

[1] At 0.10 level.

[2] I indicates the intercept term b_0 is significant. C indicates that one or more of the coefficients of volume per mass is significant. Cells are identified by medium forming overburden.

TABLE G-7. SIGNIFICANCE TESTS FOR DIFFERENCES BETWEEN LABORATORY-PREDICTED AND FIELD-OBSERVED LEACHING TRENDS FOR ALLIANCE AFBC WASTE

			Significance of[1]				Codes Indicating for Which Cells Observed and Predicted Values are Significantly Different[2]				
Species	Number of Points (Field)	Number of Points (Lab)	b_0	b_1	b_2	b_3	Shale	Interburden	Alluvium	Limestone	Signs of Significant Field Terms Consistent?
Al	37	23	x	x	x	x	I,C	–	–	–	Yes
B	42	24	x				–	–	I	–	Yes
Ba	49	23		x	x	x	–	C	C	C	Yes
Be	–	21					–	–	–	–	–
Ca	54	22	x	x			–	–	I,C	I	Yes
Cd	–	20					–	–	–	–	–
Cl	52	24	x	x	x	x	–	–	I,C	I,C	Yes
Cr	34	24		x	x	x	–	–	C	–	Yes
Cu	11	24	x	x			–	I,C	–	–	Yes
F	51	24					–	–	–	–	–
Fe	10	22	x	x			–	I,C	–	–	Yes
Li	40	24	x	x	x	x	–	I,C	C	I,C	No
Mn	18	14	x	x	x	x	I,C	I,C	–	–	Yes
Mo	11	24	x	x	x	x	I,C	I,C	–	–	No
Na	54	24	x	x	x	x	C	I,C	C	I,C	No
Ni	–	20					–	–	–	–	–
Si	54	24	x				–	I	I	I	No
SO	52	24	x	x	x	x	–	–	I,C	I,C	No
Sr	53	22	x	x	x	x	I,C	–	C	I	Yes
Ti	3	24					–	–	–	–	–
TDS	52	24	x	x	x	x	–	–	I,C	–	Yes
V	4	24	x	x			–	I,C	–	–	Yes
Zn	–	22					–	–	–	–	–

[1] At 0.10 level.

[2] I indicates the intercept term b_0 is significant. C indicates that one or more of the coefficients of volume per mass is significant. Cells are identified by medium forming overburden.

that a difference can be statistically significnt but not practically significant, especially when the sample size is large, as in this analysis. In this regard, the measures presented in Tables G-4 and G-5 of the amount of difference between field and observed and predicted values are useful.

In instances in which significant differences exist in Tables G-6 and G-7, it is indicated for which field cells the lab and field trends are significantly different. Also, it is indicated whether the b_0 term, representing the constant multiplier for predicted concentrations, or the coefficients (b_0, b_1, and b_2) of the different powers of volume per mass are statistically significant. If the lab and field were the same in shape but offset, only the b_0 term would be significant. If the lab and field trends had different shapes one or more of the coefficients b_1, b_2, and b_3 would be significant.

Additionally, it is indicated in the tables whether all significant terms for a given model have consistent signs. The answer is yes if all significant cell-specific values of b_0 have the same sign, and the analogous condition holds for each of the other coefficients. Thus, if the signs are consistent, this means that the trends for all cells either did not differ significantly from the lab trend or differed in a consistent manner (all higher, all steeper, etc.). Consistent signs exist in most cases for the models for both wastes.

The difficulties involved in extrapolation are mentioned above. A further question is whether the differences which were observed between field-observed and laboratory-predicted values are due largely to extrapolation. If the answer is yes, then the implication is that field values could probably be estimated much more accurately if the lab and field data were available for comparable volumes per mass. If the answer is no, the implication is that differences between the lab and field chemical systems account for a significant part of the observed differences.

To address this issue, the mean residuals were computed separately for volumes per mass that are: (1) between 0.01 and 0.1 mL/g; and (2) greater than 0.1 (0.1 to just over 1) mL/g. A third category, less than 0.01, was considered but contained too few points to allow meaningful calculations. Recall that the lab volumes per mass are greater than and disjoint from the field values. Thus, if extrapolation were the primary problem, one would expect the field residuals to be smaller for larger volumes per mass. This would be the case, for example, if lab and field trends agreed for larger volumes per mass but diverged as volume per mass decreased. This occurred for some species (e.g., TDS for Exxon PFBC waste, plotted above) but not all.

Tables G-8 and G-9 present the mean residuals for the two volume-per-mass categories for Exxon PFBC and Alliance AFBC waste, respectively. The agreement between observed and predicted values is not dramatically different in the two categories. The agreement is better for larger volumes per mass for 9 of 13 cases for PFBC waste and for 7 of 19 cases of AFBC waste (agreement is "better" if the mean in log-space is nearer to zero). The mixed results observed suggest that the differences between field-observed and laboratory-predicted values are probably not due primarily to extrapolation. While the mean of the residuals is the most useful measure to test for divergence of observed and predicted trends as volume per mass decreases, the residual standard deviations are presented for completeness in Tables G-10 and G-11.

G.2.1.6 Discussion of Data Selection

The data selection performed for leaching model development was discussed briefly in Section G.2.1.2. This section includes a more detailed discussion of the data selection.

Models were not developed for chemical species for which all or virtually all leachate concentrations were near or below the detection limits of the analytical instrument used. There was no basis for developing meaningful models for these cases. For the species which were used, certain data selections were performed on the basis of examination of raw data tables and plots; the laboratory and field leaching data are presented in Appendix J.

TABLE G-8. COMPARISON OF MEAN DIFFERENCES BETWEEN FIELD-OBSERVED AND LABORATORY-PREDICTED VALUES FOR DIFFERENT VOLUMES PER MASS FOR EXXON PFBC WASTE

	Volume Per mass 0.01 to 0.1 mL/g		Volume Per Mass 0.1 mL/g	
Species	No. Points	Mean of Field Residuals	No. Points	Mean of Field Residual
Al	0	—	0	—
B	23	-0.74 (0.18)	101	-1.0 (0.95)
Ba	15	-1.1 (0.080)	49	-0.70 (0.20)
Ca	23	-0.65 (0.23)	101	-0.46 (0.34)
Cl	11	0.094 (1.2)	18	-0.36 (0.44)
Cr	23	-1.5 (0.034)	98	-1.3 (0.048)
F	23	-0.45 (0.35)	99	-0.51(0.31)
Fe	19	-0.74 (0.18)	62	-0.42 (0.38)
Na	15	-0.37 (0.43)	54	-0.55 (0.28)
Si	23	2.0 (96)	101	1.9 (83)
Sr	23	-1.1 (0.089)	101	-0.87
SO_4	23	0.71 (5.1)	93	0.41 (2.6)
TDS	23	0.48 (3.0)	99	0.17 (1.5)
Zn	14	-0.28 (0.52)	33	0.14 (1.4)

TABLE G-9. COMPARISON OF MEAN DIFFERENCES BETWEEN FIELD-OBSERVED AND LABORATORY-PREDICTED VALUES FOR DIFFERENT VOLUMES PER MASS FOR ALLIANCE AFBC WASTE

	Volume Per mass 0.01 to 0.1 mL/g		Volume Per Mass 0.1 mL/g	
Species	No. Points	Mean of Field Residuals	No. Points	Mean of Field Residual
Al	7	-0.025 (0.94)	29	-0.29 (0.52)
B	7	-0.72 (0.19)	34	-0.95 (0.11)
Ba	7	0.38 (2.4)	41	0.16 (1.4)
Be	0	- -	0	- -
Ca		-2.4 (0.0037)	46	-1.8 (0.015)
Cd	0	- -	0	- -
Cl	7	0.32 (2.1)	44	-0.25 (0.56)
Cr	7	0.40 (0.39)	26	-0.78 (0.16)
Cu	2	0.80 (0.16)	9	-0.57 (0.27)
F	7	0.044 (1.1)	43	0.12 (1.3)
Fe	2	0.093 (0.81)	8	0.28 (1.9)
Li	7	0.21 (0.61)	32	-0.040 (0.91)
Mn	2	0.030 (1.1)	16	0.29 (2.0)
Mo	2	0.21 (0.62)	9	-0.36 (0.44)
Na	7	0.029 (0.93)	46	0.048 (1.1)
Ni	0	- -	0	- -
Si	7	1.1 (14)	46	1.4 (24)
SO_4	7	0.017 (1.0)	44	0.0050 (1.0)
Sr	6	0.10 (0.80)	46	-0.37 (0.43)
TDS	7	0.053 (1.1)	44	-0.081 (0.83)
Ti	2	0.80 (0.16)	1	-0.14 (0.73)
V	2	0.52 (0.30)	2	-0.79 (0.16)
Zn	0	- -	0	- -

TABLE G-10. COMPARISON OF STANDARD DEVIATIONS OF FIELD RESIDUALS FOR DIFFERENT VOLUMES PER MASS EXXON PFBC WASTE

	Volume Per Mass 0.01 to 0.1 mL/g		Volume Per Mass >0.1 mL/g	
Species	No. Points	Standard Deviation of Residuals	No. Points	Standard Deviation of Residuals
Al	0	- -	0	- -
B	23	0.19 (1.5)	101	0.24 (1.7)
Ba	15	0.18 (1.5)	49	0.44 (2.8)
Ca	23	0.097 (1.3)	101	0.19 (1.6)
Cl	11	0.12 (1.3)	18	0.36 (2.3)
Cr	23	0.19 (1.6)	98	0.40 (2.5)
F	23	0.13 (1.3)	99	0.16 (1.4)
Fe	19	0.29 (2.0)	62	0.48 (3.0)
Na	15	0.56 (3.6)	54	0.32 (2.1)
Si	23	0.28 (1.9)	101	0.34 (2.2)
Sr	23	0.19 (1.5)	101	0.16 (1.4)
SO_4	23	0.12 (1.3)	93	0.24 (1.8)
TDS	23	0.12 (1.3)	99	0.28 (1.8)
Zn	14	0.23 (1.7)	33	0.45 (2.8)

TABLE G-11. COMPARISON OF STANDARD DEVIATIONS OF FIELD RESIDUALS FOR DIFFERENT VOLUMES PER MASS FOR ALLIANCE AFBC WASTE

	Volume Per Mass 0.01 to 0.1 mL/g		Volume Per Mass >0.1 mL/g	
Species	No. Points	Standard Deviation of Residuals	No. Points	Standard Deviation of Residuals
Al	7	0.14 (1.4)	29	0.38 (2.4)
B	7	0.13 (1.3)	34	0.44 (2.8)
Ba	7	0.42 (2.7)	41	0.61 (4.1)
Be	0	- -	0	- -
Ca	7	2.0 (100)	46	1.5 (34)
Cd	0	- -	0	- -
Cl	7	0.36 (2.3)	44	0.40 (2.5)
Cr	7	0.19 (1.5)	26	0.37 (2.4)
Cu	2	0.81 (6.5)	9	0.43 (2.7)
F	7	0.060 (1.1)	43	0.20 (1.6)
Fe	2	0.40 (2.5)	8	0.33 (2.1)
Li	7	0.24 (1.7)	32	0.24 (1.7)
Mn	2	0.15 (1.4)	16	0.72 (5.3)
Mo	2	0.059 (1.1)	9	0.52 (3.3)
No	7	0.30 (2.0)	46	0.33 (2.2)
Ni	0	- -	0	- -
Si	7	0.81 (6.4)	46	0.64 (4.4)
SO_4	7	0.072 (1.2)	44	0.11 (1.3)
Sr	6	0.19 (1.6)	46	0.41 (2.5)
TDS	7	0.15 (1.4)	44	0.10 (1.3)
Ti	2	0.95 (9.0)	1	- -
V	2	0.50 (3.1)	2	0.58 (1.3)
Zn	0	- -	0	- -

In a few instances, the concentrations decreased to undetected values and subsequently fluctuated above and below the detection limit or remained undetected. An example is chromium, which is undetected for volume per mass greater than 30 mL/g for Exxon PFBC waste in the laboratory leaching data. In these instances, the data were excluded for values of volume per mass beyond the point at which the undetected values first occurred. Exclusion of these data was advantageous since the model development was done in log-space. The undetected values have small uncertainties but large relative uncertainties. Thus, the logarithms of concentrations below the detection limit have large uncertainties and would have contributed litle or no additional accuracy to the predictive models. In a few rare instances, a single undetected value was observed before the general trend reached the undetected level (e.g., for one of eight replicate measurements for protocol Step 1). In these instances the undetected values were deleted. It is unlikely that these deletions contributed a significant high bias to the trends, since a very small number of values were removed on this basis.

Additionally, it was observed that fluctuations of significant magnitude occurred in several instances in the laboratory leaching data for volumes per mass greater than 20 mL/g. Examples of this behavior were observed for Exxon PFBC waste for aluminum, nickel, silicon, boron, calcium, and TDS and for Alliance AFBC waste for aluminum, beryllium, cadmium, cobalt, chromium, copper, iron manganese, nickel, silicon, titanium, vanadium, zinc, and fluoride (see Appendix D). Thus, the leaching data for volumes per mass grater than 30 mL/g were uniformly excluded in the leaching model development procedure. Inclusion of these data would have required the use of much more complicated polynomial models to fit the observed data fluctuations. Since the excluded volumes per mass are the farthest from those observed in the field, agreement between laboratory models and field data was not sacrificed. The largest volumes per mass observed in the field were slightly over 1 mL/g. Moreover, inclusion of very high-degree polynomial terms in volumes per mass would have caused numerical problems in some of the calculations, due to the large range (over four orders of magnitude) of values of volume per mass. The range of values of, say, a fifth degree term in volume per mass would vary by over 20 orders of magnitude.

Additionally, erratic behavior was exhibited by the field data during the first week of field leaching data. Thus, data for the first week were uniformly eliminated from the field data set in comparing them to predictions from the laboratory models.

G.2.2 Models for Fractional Attenuation

Statistical models were also developed for fractional attenuation. Simply defined, fractional attenuation is the fractional reduction in the concentration of a species as a result of contact with the disposal medium (see Appendix D).

Attempts to predict field fractional attenuation in terms of models developed from laboratory data are first discussed. It was found that, generally, the lab and field data were so dissimilar that such lab-to-field correlation was not possible except for a very few cases. Analysis of these cases is presented. As an alternative analysis, models were developed from field data. These models do not relate to prediction of field results from lab models, but serve to characterize trends observed in the field.

G.2.2.1 Calculations of Fractional Attenuation and Volume Per Mass

As discussed in Appendix E, fractional attenuation for the field data, A_F, is defined as

$$A_F = \frac{C_U - C_L}{C_U}$$

where:

C_U = concentration of leachate from the upper sampling point of the field cells, and

C_L = concentration at the lower sampling point.

For the laboratory data fractional attenuation, A_L, is defined as

$$A_L = \frac{C_a - C_b}{C_a}$$

where:

C_a = leachate concentration before contact with the disposal medium, and

C_b = concentration after contact with the disposal medium.

For protocol Steps 4 and 5, C_a is the concentration in the leachate from Step 1. For Step 6, iteration number 1, C_a is the concentration in the leachate from Step 4. For iteration i (i > 1), C_a is the concentration after iteration i-1. In each instance C_b is the concentration after contact with the disposal medium.

For both the laboratory and field data, negative fractional attenuations indicate contribution (mobilization) rather than attenuation of the chemical species by the disposal medium.

The volume per mass used for fractional attenuation is the total volume of liquid that has contacted the medium divided by the mass of disposal medium. For the field data, the volume per mass was simply the flow-through volume divided by the mass of disposal medium in the cell. For protocol Step 4, the volume per mass was 10 mL/g. For Step 5, iteration i, the volume per mass was 10 (i + 1); volume per mass increased with iteration, since fresh liquid was added each iteration, but the same disposal medium sample was retained. For Step 6, iteration i, the volume per mass was 10/(i + 1); the same leachate was retained, but fresh disposal medium was added each iteration.

G.2.2.2 Data Selection

Exclusion of the leachate concentration values beyond the volume per mass at which the concentrations become undetected was discussed in a previous section. When the amount leached is undetected, the fraction of that amount which is reduced by contact with the disposal medium is not considered to be meaningful. Thus, fractional attenuations were excluded for all cases for which the concentrations were excluded in the analysis discussed above.

It was observed that the protocol Step 6 fractional attenuations frequently were negatve and did not follow the same trend as did the Step 4 and 5 points. In instances in which the latter displayed an exponential decay with volume per mass, such as for SO_4 and TDS for Alliance AFBC waste and strontium for Exxon PFBC waste, the Step 6 points (with smaller volumes per mass) fell sharply and, thus, were inconsistent with the trend. Thus, in the few cases in which it was possible to predict field fractional attenuation in terms of laboratory data, this would not have been possible if the Step 6 points had been used in developing the laboratory models.

Moreover, in Step 6 a fresh disposal medium sample was added at each iteration, but the same leachate was retained. Thus, if high attenuation occurred in Step 4, the concentrations after attenuation were perhaps very low, so that little or no additional attenuation would be expected to occur. In fact, one would expect the fractional attenuations to vary randomly about zero, and this is what was observed. Clearly, the Step 6 fractional attenuation as a function of volume per mass was very different in nature from that in Steps 4 and 5 and in the field.

G.2.2.3 Methods Used to Develop Fractional Attenuation Model

Due to the numerous occurrences of negative fractional attenuations (i.e., mobilization), a non-negative model such as was used for leaching would not be applicable. Thus, a polynomial model of the form

$$A_F = b_0 + b_1V + b_2V^2 + b_3V^3$$

was used, where:

A_F is fractional attenuation,

V is volume per mass of disposal medium, and

b_0, b_1, b_2, and b_3 are regression coefficients.

The same variable selection method discussed above was used in the development of the models from both lab and field data. The objective of variable selection is to choose the best subset of the candidate predictor variables, V, V^2, and V^3 for inclusion in the model.

G.2.2.4 Comparison of Predicted Values from Laboratory Models and Field Fractional Attenuation

As is discussed above, it was clear from observations of raw data plots that prediction of field fractional attenuation through models developed from laboratory data was infeasible in almost all cases. Nevertheless, the three cases (strontium, sulfate, and TDS) in which field prediction appeared to be most promising were investigated. The models and associated statistical measures for the three models are presented in Table G-12. In all three cases, a good fit to the laboratory data was achieved; the R^2 values fell between 0.86 and 0.95, and the standard errors were all below 0.1. Recall that the standard error is the standard deviation of the fluctuations of the observed data about the predicted values.

In Figures G-20, G-21, and G-22, the laboratory- and field-observed values and the predicted fractional attenuations are shown for the three selected cases. It is clear that the laboratory observed and predicted values agreed very well. The field-observed and lab-predicted values were in good agreement for sulfate and TDS. For strontium, however, agreement was not achieved. Due to the steep negative slope of the laboratory points, the predictions went off scale (above 1) when extrapolation to lower volumes per mass was made. It would be possible to employ a functional form that was constrained to be less than one. In this manner, reasonable agreement for the larger volumes per mass could be achieved. The fact remains, however, that the lab and field strontium fractional attenuations have opposite slopes, and

TABLE G-12. MODELS FOR LABORATORY FRACTIONAL ATTENUATION

Waste	Disposal Medium	Field Cell	Species	N	R^2	Standard Error	b_0	b_1	Standard Error of b_1	b_2	Standard Error of b_2	b_3	Standard Error of b_3
PFBC	Till	3	SR	16	0.86	0.097	1.3	−0.080	0.018	0.0017	0.00053	−0.000011	0.0000045
AFBC	Alluvium	14, 15	SO_4	22	0.95	0.044	0.86	−0.036	0.0040	0.00058	0.000085	−0.0000031	0.00000052
AFBC	Alluvium	14, 15	TDS	22	0.91	0.052	0.76	−0.029	0.0047	0.00040	0.00010	−0.0000018	0.00000062

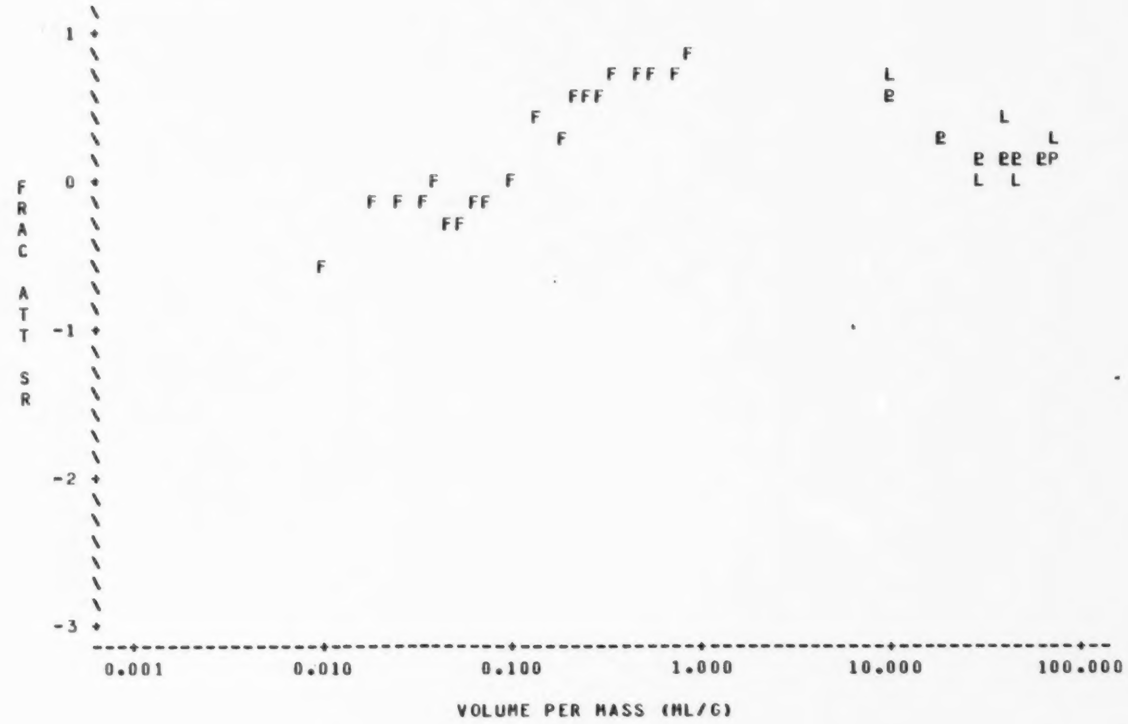

Figure G-20. Lab (L), Field (F), and Predicted (P) Fractional Attenuation of Strontium as a Function of Volume per Mass for Exxon PFBC Waste and Glacial Till.

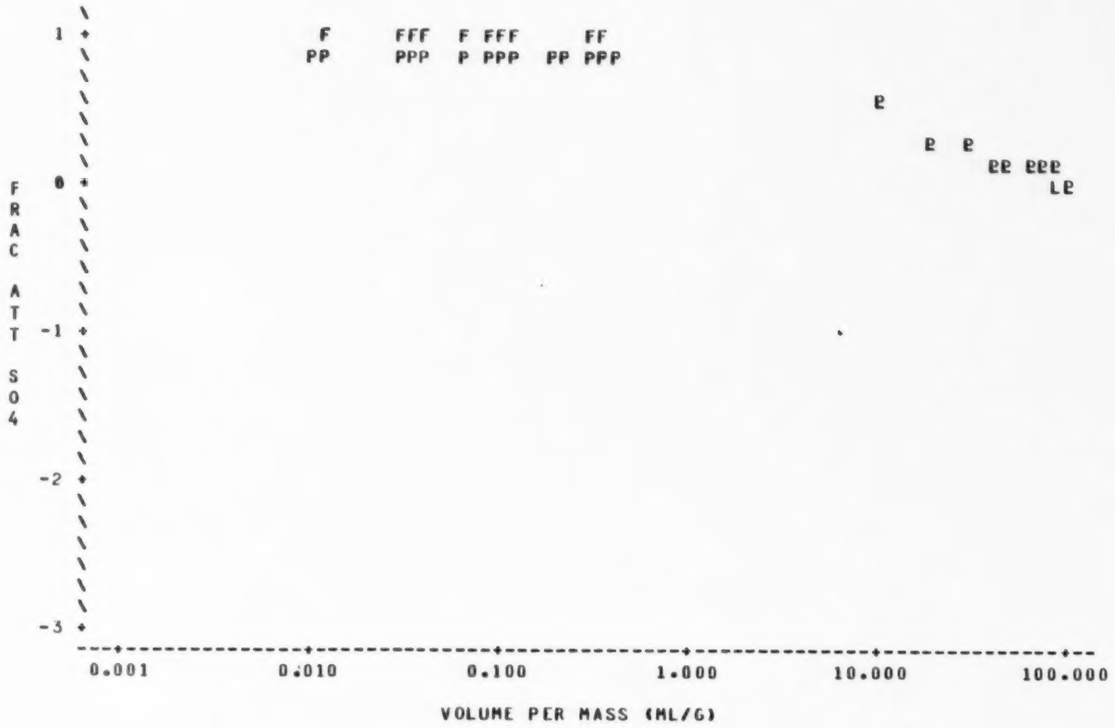

Figure G-21. Lab (F), Field (F), and Predicted (P) Fractional Attenuation of Sulfate as a Function of Volume per Mass for Alliance AFBC Waste and Alluvium.

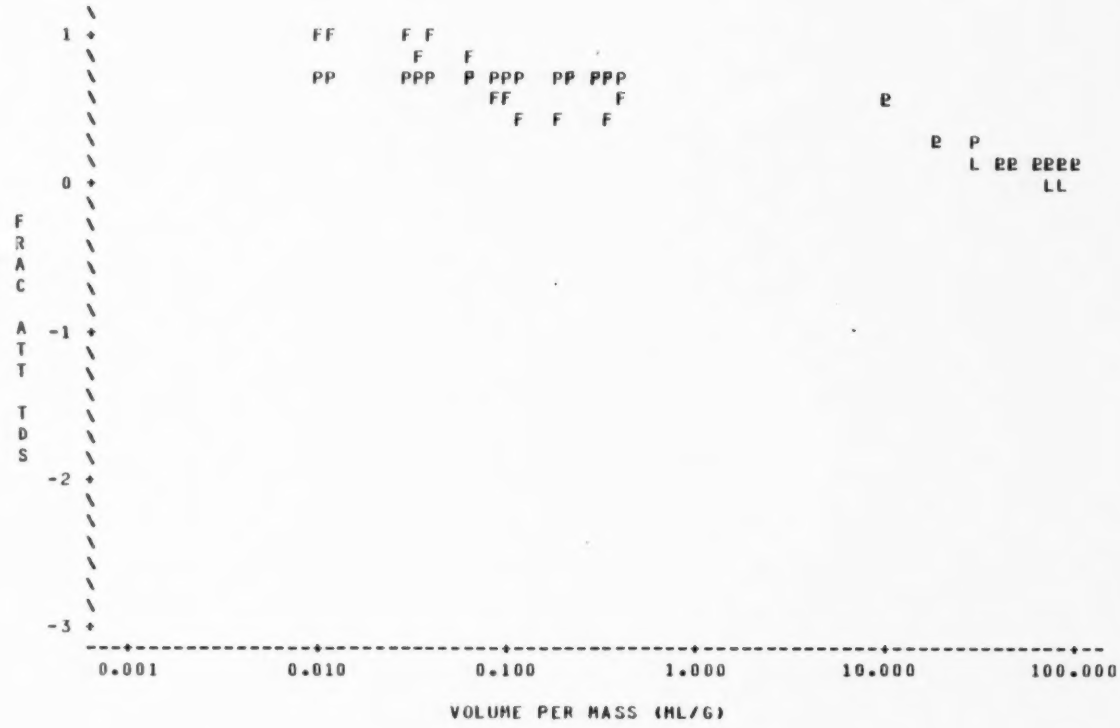

Figure G-22. Lab (L), Field (F), and Predicted (P) Fractional Attenuation of Total Dissolved Solids as a Function of Volume per Mass for Alliance AFBC Waste and Alluvium.

accurate prediction of the field values from a laboratory model was not feasible in this case.

Table G-13 presents measures of agreement between field-observed and lab-predicted values. These are similar to the measures presented for the leaching models, but all calculations for fractional attenuation were performed in linear space. Table G-14 presents the results of hypothesis tests regarding the differences between field-observed and lab-predicted values. These tests are analogous to those performed for the leaching models explained in detail above. The tests are simpler here, however, since each case involves a single waste and disposal medium combination. Field and laboratory trends had significant differences in all three cases considered. As is discussed above, however, differences can be statistically significant but not practically significant; the agreement for sulfate and TDS for AFBC waste is considered to be good.

G.2.2.5 Models to Predict Field Fractional Attenuations

Models were also developed from field data to predict field fractional attenuations. The regression coefficients and associated statistics are presented for Exxon PFBC and Alliance AFBC wastes and for selected chemical species in Tables G-15 and G-16, respectively. Table G-1 shows the contents (waste and disposal medium) of each field cell numbered in Tables G-15 and G-16.

Figures G-23 through G-27 present field-observed and field-predicted fractional attenuations for the replicate field cells 1 and 2 for selected chemical species (B, Ca, SO_4, Sr, TDS). Figures G-28 through G-31 present selected plots (for B, SO_4, Sr, and TD) for replicate Cells 14 and 15. Plots for replicate cells are presented to provide an indication of the amount of scatter in the data. To facilitate comparisons, a consistent scale was used for all fractional attenuation plots presented in this section. Consequently, some plots cover only a small part of the scale provided.

TABLE G-13. COMPARISON OF FIELD FRACTIONAL ATTENUATIONS AND VALUES PREDICTED BY MODEL DEVELOPED FROM LABORATORY DATA

Waste	Disposal Medium	Field Cell	Species	Standard Error from Regression	Number Points (Lab)	Standard Deviation of Field Residuals	Mean of Field Residuals	Number Points (Field)
Exxon PFBC	Till	3	Sr	0.097	16	0.94	-1.2	21
Alliance AFBC	Alluvium	14, 15	SO_4	0.044	22	0.041	0.080	17
Alliance AFBC	Alluvium	14, 15	TDS	0.052	22	0.20	-0.046	17

NOTE: A residual value is the field fractional attenuation minus the corresponding predicted value.

TABLE G-14. SIGNIFICANCE TESTS FOR DIFFERENCES BETWEEN LAB AND FIELD FRACTIONAL ATTENUATION TRENDS

Waste	Disposal Medium	Field Cell	Species	No. Points (Field)	No. Points (Lab)	Significance* of			
						b_0	b_1	b_2	b_3
Exxon PFBC	Till	3	Sr	21	16	x	x	x	x
Alliance AFBC	Alluvium	14, 15	SO_4	17	22	x			
Alliance AFBC	Alluvium	14, 15	TDS	17	22	x	x	x	x

* At 0.10 level.

TABLE G-15. MODELS FOR FIELD FRACTIONAL ATTENUATION FOR EXXON PFBC WASTE

Field Cell	Species	N	R^2	Standard Error	b_0	b_1	Standard of b_1	b_2	Standard Error of b_2	b_3	Standard Error of b_3
1	B	21	0.76	0.17	0.97	–	–	-9.4	1.4	12	1.9
1	Ca	21	0.67	0.20	-0.85	3.1	0.76	-2.7	1.0	–	–
1	SO_4	19	0.91	0.15	0.98	-8.5	1.7	21	6.6	-19	6.8
1	Sr	21	0.72	0.23	-1.2	4.7	0.87	-4.7	1.2	–	–
1	TDS	20	0.93	0.13	0.87	-6.6	1.2	13	4.1	-9.9	3.6
2	B	20	0.29	0.21	0.73	–	–	-4.8	2.0	5.9	2.6
2	Ca	20	0.26	0.088	-0.15	0.24	0.094	–	–	–	–
2	SO_4	18	0.63	0.16	0.22	–	–	3.2	1.7	-7.1	2.7
2	Sr	20	0.33	0.21	-0.38	1.26	0.86	-2.7	1.1	–	–
2	TDS	19	0.58	0.16	0.27	–	–	–	–	-1.5	0.30
1 & 2[1]	B	41	0.52	0.20	0.86	–	–	-7.3	1.2	9.0	1.7
1 & 2	Ca	41	0.32	0.25	-0.62	3.5	1.6	-8.0	5.5	5.8	4.9
1 & 2	SO_4	37	0.55	0.25	0.48	1.5	0.23	–	–	–	–
1 & 2	Sr	41	0.31	0.32	-0.80	3.4	0.88	-4.0	1.2	–	–
1 & 2	TDS	39	0.61	0.23	0.45	-1.3	0.17	–	–	–	–
3	B	21	0.71	0.30	1.1	-2.7	0.59	–	–	1.8	0.86
3	Ca	21	0.41	0.25	-0.094	-4.3	1.7	16	5.3	-13	4.2
3	SO_4	20	0.86	0.27	1.0	-5.6	0.61	–	–	6.9	1.3
3	Sr	20	0.92	0.14	-0.45	6.5	0.98	-11	3.0	6.4	2.4
3	TDS	21	0.91	0.18	1.0	-7.3	1.2	12	3.9	-6.1	3.1
4	B	21	0.49	0.20	0.057	3.6	2.5	-20	8.6	22	8.2
4	Ca	21	0.63	0.13	-0.60	5.6	1.5	-15	5.4	12	5.1
4	SO_4	20	0.75	0.24	0.41	-6.0	0.84	–	–	16	2.6
4	Sr	21	0.71	1.7	-11	24	4.9	–	–	-29	11
4	TDS	21	0.64	0.28	0.42	-7.3	1.3	10	1.9	–	–
5	B	21	0.69	0.50	1.0	–	–	-28	4.5	39	6.7
5	Ca	21	0.76	0.17	1.0	-7.8	1.6	20	5.7	-15	5.4
5	SO_4	20	0.84	0.32	1.4	-8.8	0.96	–	–	21	3.0
5	Sr	21	0.52	0.23	0.94	-8.1	2.1	25	7.6	-20	7.3
5	TDS	21	0.77	0.33	1.4	-9.5	1.3	12	1.9	–	–
6	B	21	0.84	0.14	0.61	2.5	1.7	-26	6.6	35	6.9
6	Ca	21	0.71	0.075	-0.26	4.4	0.88	-13	3.5	11	3.6
6	SO_4	20	0.79	0.23	0.15	–	–	-19	3.7	28	7.0
6	Sr	21	0.48	0.36	-1.0	–	–	13	4.3	-18	7.0
6	TDS	21	0.76	0.21	0.32	-3.6	0.65	–	–	5.1	1.7

---

[1] Cells 1 and 2 are replicates; i.e., they contain the same type of waste (PFBC) and disposal medium (shale).

TABLE G-16. MODELS FOR FIELD FRACTIONAL ATTENUATION FOR ALLIANCE AFBC WASTE

Cell	Species	N	R^2	Standard Error	b_0	b_1	Standard error of b_1	b_2	Standard error of b_2	b_3	Standard error of b_3
13	SO_4	9	0.07	2.8	-12	–	–	–	–	-23	33
13	Sr	7	0.96	0.14	-1.0	4.1	0.74	–	–	-2.2	1.8
13	TDS	9	0.05	1.5	-5.4	-2.0	3.3	–	–	–	–
14	B	6	0.99	0.066	-0.18	14	3.6	-50	18	56	26
14	SO_4	7	0.94	0.013	0.92	0.54	0.18	–	–	-4.3	1.1
14	Sr	8	0.97	0.014	0.95	0.80	0.12	-2.0	0.23	–	–
14	TDS	7	0.97	0.050	0.96	–	–	-17	3.7	37	9.3
15	B	10	0.96	0.12	-0.14	-4.2	3.0	60	17	-111	26
15	SO_4	10	0.58	0.030	0.98	–	–	-4.7	1.5	13	4.3
15	Sr	9	0.98	0.014	1.0	-1.5	0.49	7.3	2.5	-13	3.7
15	TDS	10	0.85	0.087	1.1	-10	2.4	49	16	-66	29
14 & 15[1]	B	16	0.86	0.21	0.034	-4.6	4.1	53	24	-91	37
14 & 15	SO_4	17	0.34	0.037	0.96	-0.17	0.062	–	–	–	–
14 & 15	Sr	17	0.55	0.046	0.98	–	–	-0.56	0.13	–	–
14 & 15	TDS	17	0.73	0.11	1.1	-8.3	2.1	35	12	-45	20
16	SO_4	12	0.76	0.15	-0.86	4.7	1.6	–	–	-45	11
16	Sr	10	0.92	0.22	4.7	-81	14	349	64	-429	89
16	TDS	12	0.34	0.20	-0.16	–	–	-3.2	1.4	–	–
17	SO_4	12	0.73	0.27	-0.90	7.9	4.1	–	–	-131	41
17	TDS	11	0.77	0.17	3.3	-65	26	395	166	-766	323

[1] Cells 14 and 15 are replicates; i.e., they have the same type of waste (AFBC) and disposal medium (alluvium).

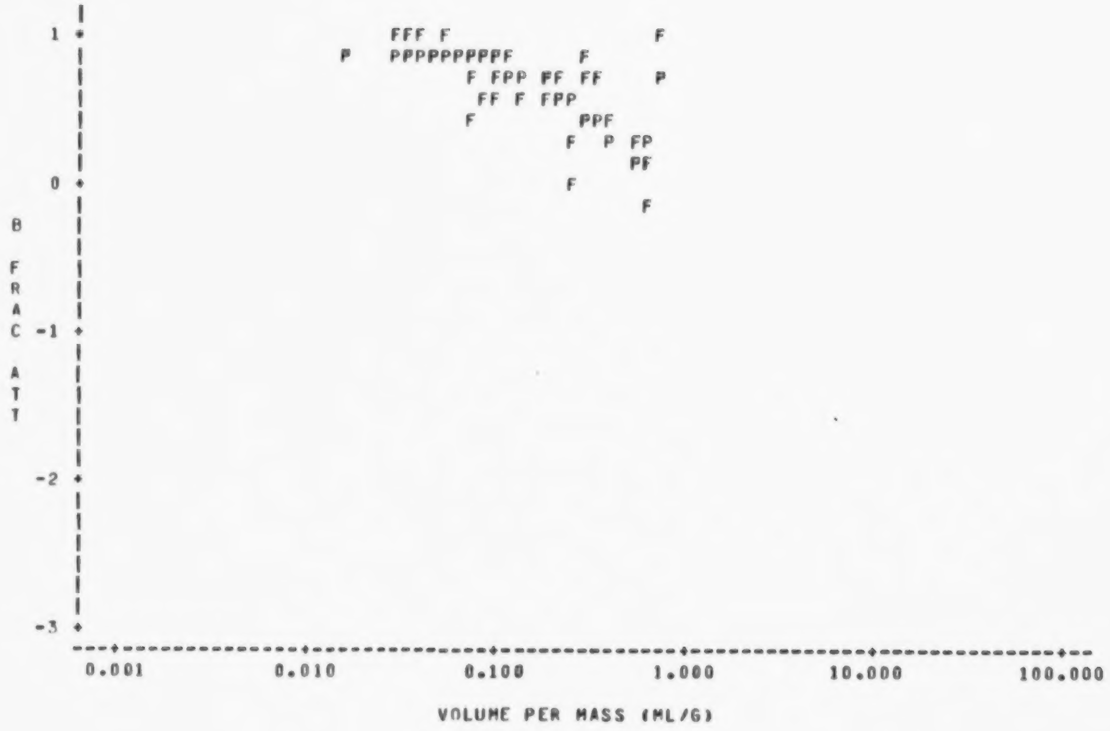

Figure G-23. Plots of Field-Observed (F) and Field-Predicted (P) Fractional Attenuations of Boron for Exxon PFBC Waste in Replicate Field Cells 1 and 2.

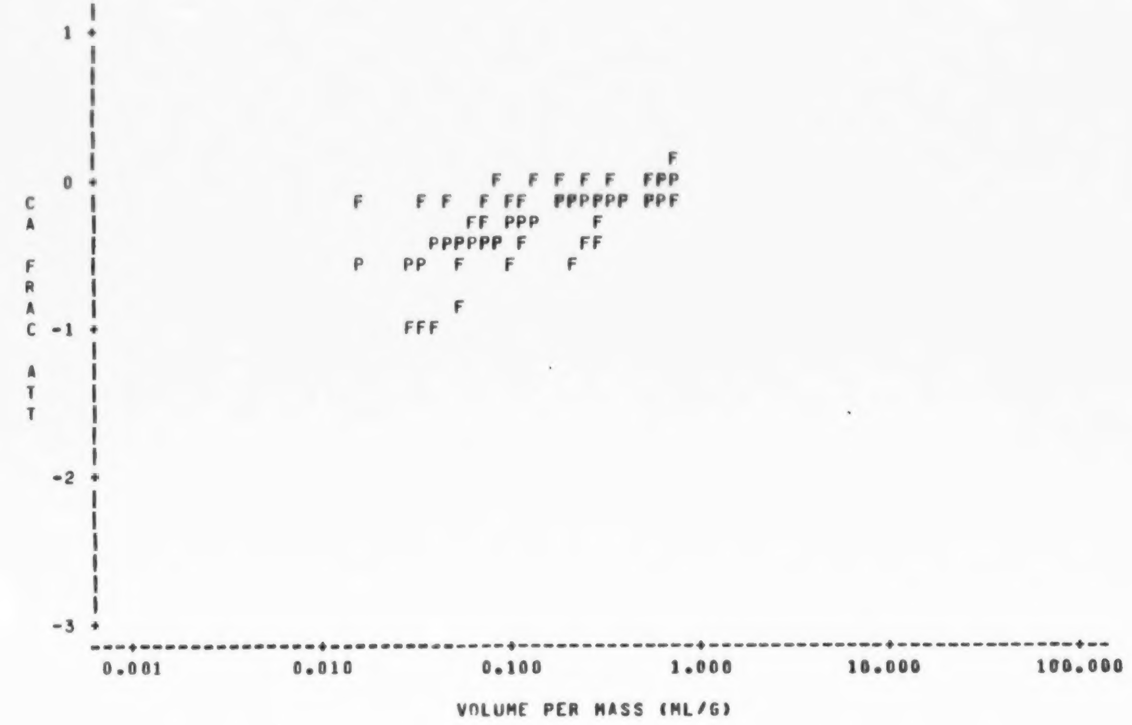

Figure G-24. Plots of Field-Observed (F) and Field-Predicted (P) Fractional Attenuations of Calcim for Exxon PFBC Waste in Replicate Field Cells 1 and 2.

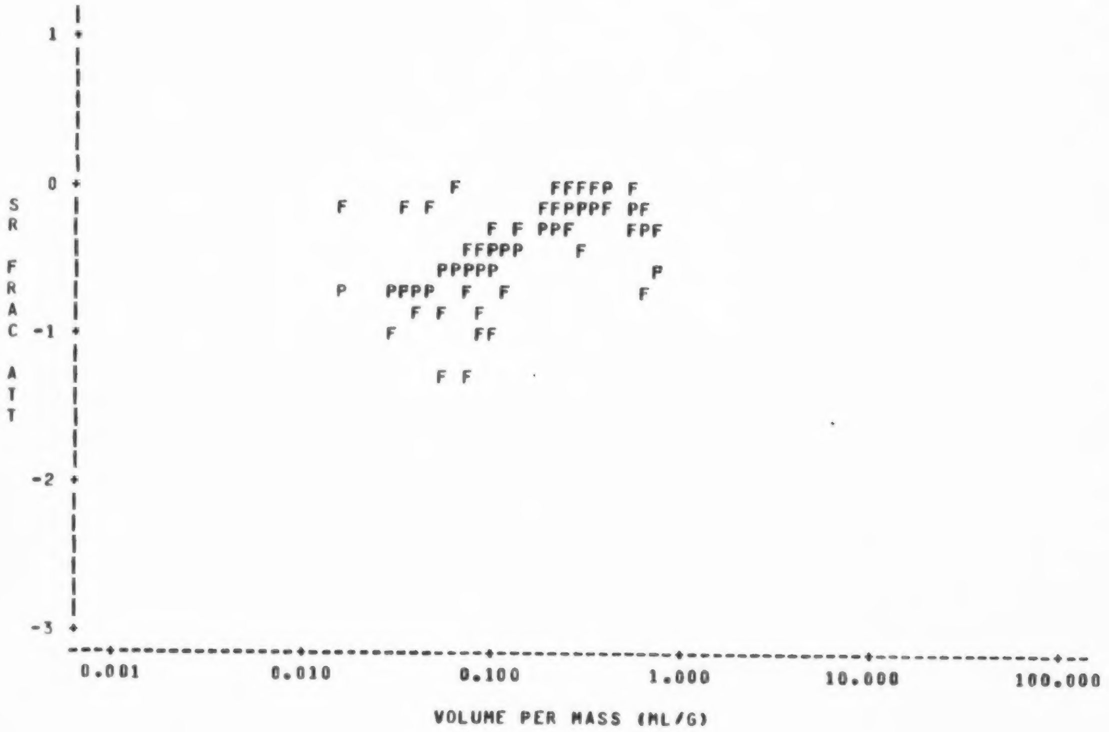

Figure G-25. Plots of Field-Observed (F) and Field-Predicted (P) Fractional Attenuations of Sulfate for Exxon PFBC Waste in Replicate Field Cells 1 and 2.

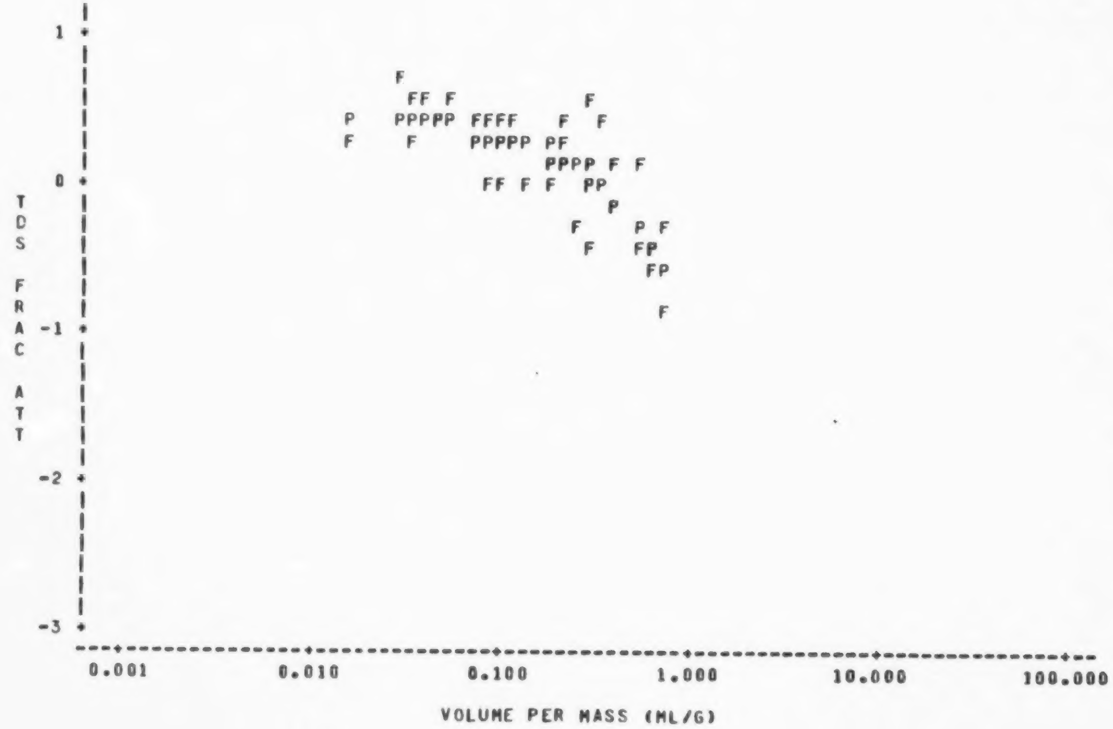

Figure G-26. Plots of Field-Observed (F) and Field-Predicted (P) Fractional Attenuations of Strontium for Exxon PFBC Waste in Replicate Field Cells 1 and 2.

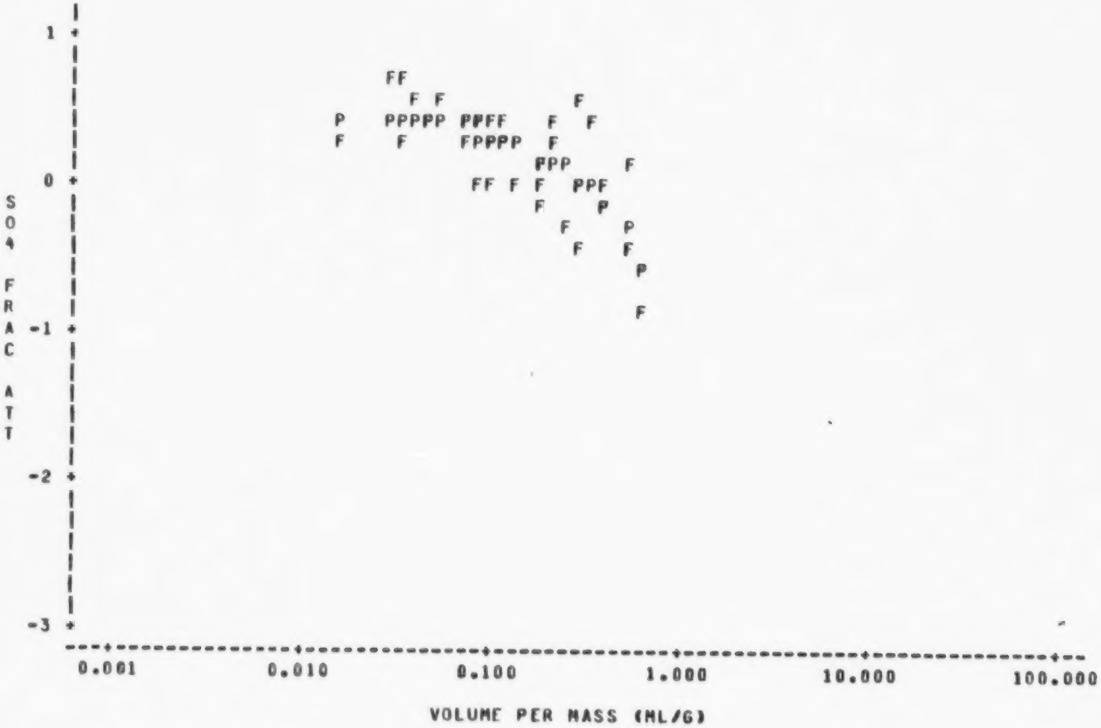

Figure G-27. Plots of Field-Observed (F) and Field-Predicted (P) Fractional Attenuations of Total Dissolved Solids for Exxon PFBC Waste in Replicate Field Cells 1 and 2.

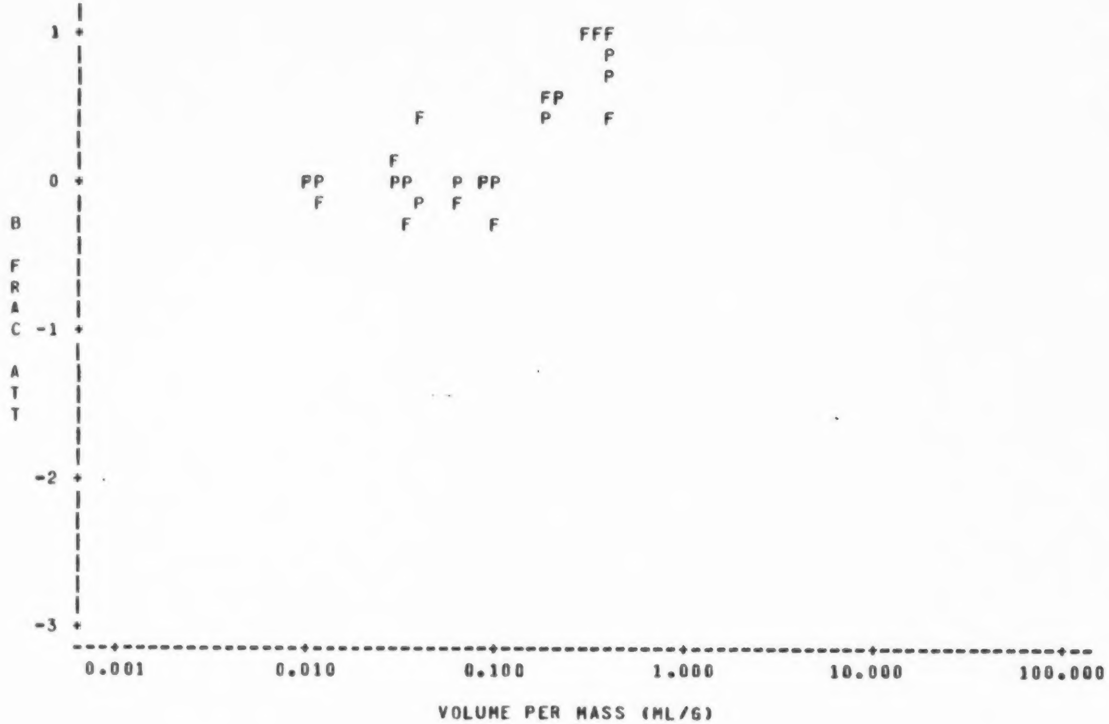

Figure G-28. Plots of Field-Observed (F) and Field-Predicted (P) Fractional Attenuations of Boron for Alliance AFBC Waste in Replicate Field Cells 14 and 15.

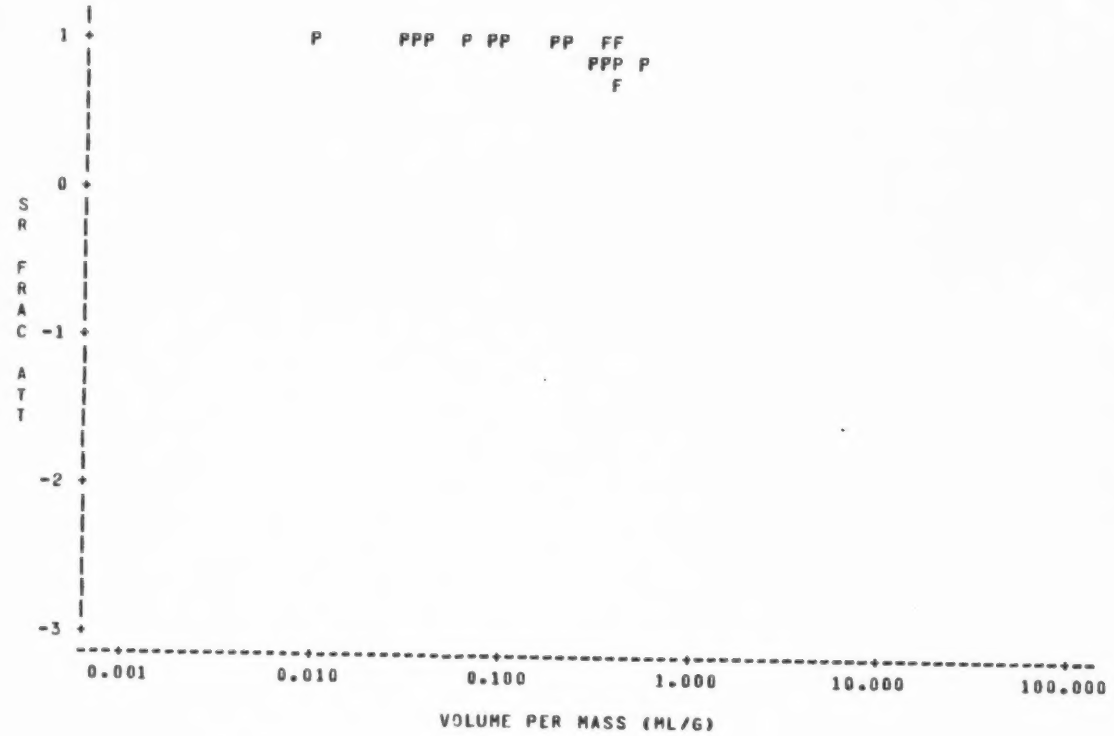

Figure G-29. Plots of Field-Observed (F) and Field-Predicted (P) Fractional Attenuations of Sulfate for Alliance AFBC Waste in Replicate Field Cells 14 and 15.

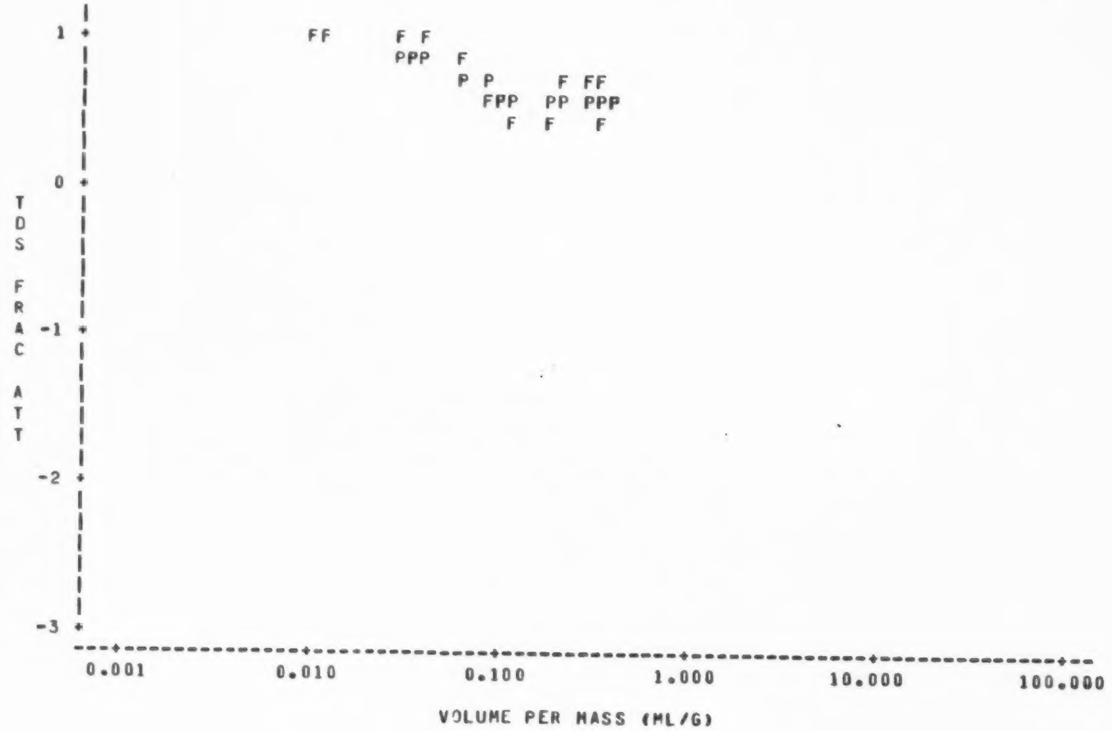

Figure G-30. Plots of Field-Observed (F) and Field-Predicted (P) Fractional Attenuations of Strontium for Alliance AFBC Waste in Replicate Field Cells 14 and 15.

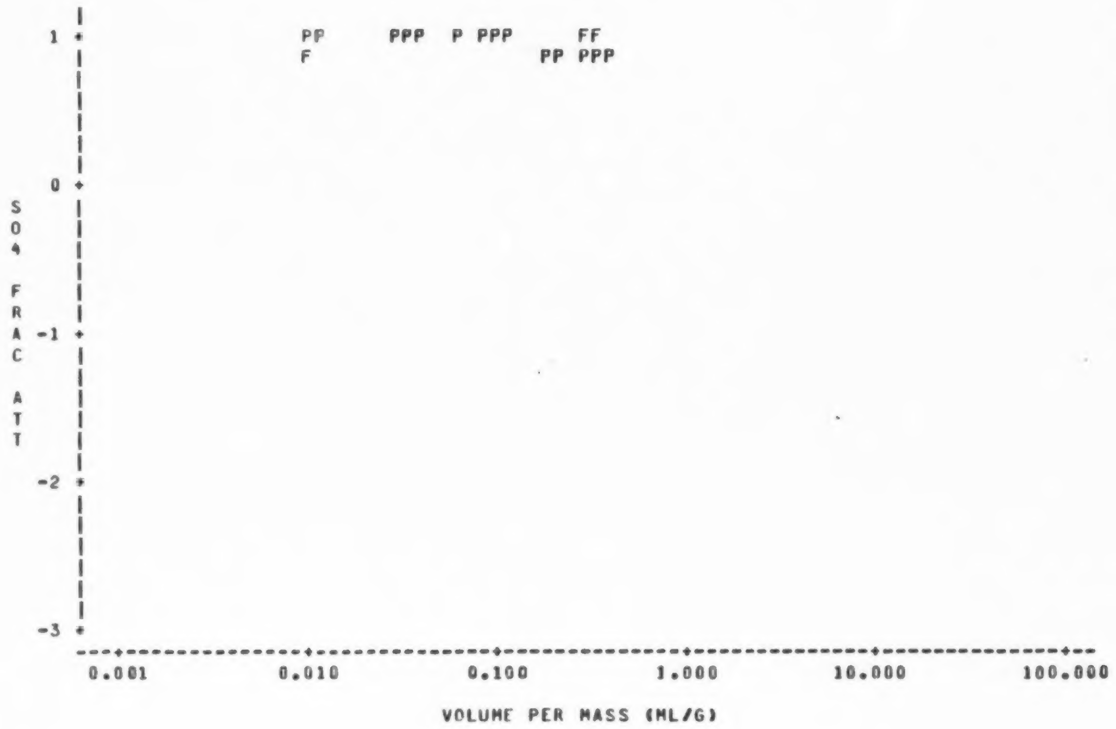

Figure G-31. Plots of Field-Observed (F) and Field-Predicted (P) Fractional Attenuations of Total Dissolved Solids for Alliance AFBC Waste in Replicate Field Cells 14 and 15.

It is clear from the plots that, although data scatter exists, the predicted values followed the trends of the observed values. The large amount of scatter displayed by the fractional attenuations, together with dissimilar lab and field trends, are the major reasons why attempts to predict field fractional attenuations from lab models were not considered fruitful for most cases.

G.2.3 Discusson of Modeling Results

Statistical models were developed from laboratory data to predict field leaching and attenuation behavior. The purpose was to investigate the feasibility of using models developed from batch leaching tests in place of field columns in order to predict field behavior. The laboratory models in the present study are not needed to predict field behavior, since field data were collected; the laboratory models developed, however, serve the purposes of the feasibility study.

The investigation was performed using the following waste and disposal medium combinations: 1) Exxon PFBC waste and shale, sandstone, glacial till, alluvium, and limestone disposal media; and 2) Alliance AFBC waste and shale, interburden, alluvium, and limestone disposal media. Thus, a reasonable variety of waste-medium combinations were represented in the data base. The disposal media affect the leaching results only in that the medium comprises the overburden in the field cells.

For the leaching studies, the following are the primary questions addressed:

1) Is it possible to develop models to fit the laboratory data?

   The answer to this question is yes. A set of typical plots of observed and predicted concentrations from laboratory studies were presented, and the models developed were seen to follow the laboratory trends. The plots of observed and predicted concentration trends of the other species were also examined, and the models followed the observed concentration trends in these cases as well.

These qualitative statements are supported by the statistical measures presented in Tables G-2 and G-3. From the 14 Exxon PFBC models, the R^2 values were above 0.3 in 11 cases, above 0.5 in 6 cases, abve 0.8 in 3 cases, and above 0.9 in 2 cases. For the 23 Alliance AFBC models, the R^2 values were above 0.3 in 20 cases, above 0.5 in 20 cases, above 0.8 in 11 cases, and above 0.9 in 7 cases.

In only 5 of 27 models was the R^2 value less than 0.3. In these cases, the scatter about the regression line ranged from ±20% for Ca for AFBC to ±100% for Ba for AFBC. Except for the latter, the scatter about the regression line is ±50% or less among these 5 cases. There is no indication that changing the functional form of the model would improve the agreement between the field-observed and laboratory-predicted values in these cases.

2) How do the values predicted by the laboratory models compare on the average to the field values?

Comparison between field-observed and laboratory-predicted values were possible for 13 species for Exxon PFBC waste leachates and for 19 species for Alliance AFBC waste leachates (see Tables G-4 and G-5). For PFBC, the mean agreement was within a factor of 10 in 11 of 13 cases, a factor of 5 in 8 cases, and a factor of 2 in 3 cases. For AFBC, the mean agreement was within a factor of 10 in 7 of 19 cases, a factor of 5 in 16 cases, and a factor of 2 in 10 cases.

Failure to achieve mean agreement within a factor of 10 was obseved only for Cr and Si for Exxon PFBC and for Ca and Si for Alliance AFBC waste. Thus, mean agreement within a factor of 10 was achieved in 28 of 32 cases, or for 88% of the species.

3) How much scatter is there in the field observed minus predicted values?

To address this question, the standard deviation of the field residual (observed minus predicted) values was computed for each element or species. The scatter was found to be less than or equal to a factor of 3 in all of the 13 cases for Exxon PFBC and in 14 of 19 cases for Alliance AFBC. The scatter is extreme (± a factor of 41) only for calcium for AFBC.

Thus, random scatter of ± a factor of three or less was achieved in 27 of 32 cases, or for 84 percent of the species.

Thus, in the majority of the cases, the mean agreement between field-observed and laboratory-predicted values was less than a factor of 10, and the random scatter of the residuals was less than a factor of 3.

It was found that prediction of field fractional attenuation values by models developed from laboratory data was not possible in most cases. The reasons were scatter in the fractional attenuation data and dissimilarity in the trends observed in the field and the lab. It should be mentioned that fractional attenuation is a derived quantity, involving concentrations before (C_b) and after (C_a) contact with the disposal medium:

$$\frac{C_b - C_a}{C_b}$$

If C_b and C_a are small (say, near the detection limit), the ratio can have a large uncertainty. Due to division by the small value C_b, the ratio can be large in magnitude even when the concentrations are small. This problem was solved in part by not developing models for species with predominantly undetected C_b values; this exclusion was no sacrifice, since the fractional attenuation is not of practical imporatnce if the concentration before contact with the medium is very low or undetected.

It should be noted that a scatter of a factor of two or three in concentration data, while not small, still allows an evaluation of the magnitude of the values. A scatter over a range of 1 (i.e., 100%) in fractional attenuation, however, constitutes major obscuration of the quantity. A scatter from 0 to 1 indicates that reduction in concentration due to contact with the medium could be anywhere from 0 to 100%. A range from -0.5 to 0.5 in fractional attenuation indicates that the effect of the medium could range from a decrease of 50% to an increase of 50% in the concentration. Thus, the meaningfulness of the fractional attenuation parameter is sensitive to moderate scatter in the concentration data.

In view of the comments above, it is clear that further research would be beneficial to determine whether field values of C_a itself, or some derived measure of field attenuation other than fractional attenuation, could be predicted by laboratory models.

G.3 Toward a Multi-Species Leaching Model for FBC Wastes: Model for Concentration of a Given Species Developed as a Function of Lagged Concentration and Transformed to be a Function of Volume Per Mass

A second approach for predicting field behavior in terms of models developed from laboratory data was also attempted. Models for Exxon PFBC waste leaching results only are presented. However, the same approach could also be applied to the data for other wastes and could also be extended to develop attenuation models. As formulated, the model development requires points equally spaced in volume per mass. Thus, protocol Step 1 and 2 data, which satisfy this criterion, were used. Subsequent prediction of concentration as a continuous function of volume per mass is possible, however. A model is presented for (normalized) concentration as a function of volume per mass for each species considered. High R^2 values, above 0.9 in most cases, were achieved, indicating very good agreement between the predicted values and the laboratory data from which the models were developed. The quantity R^2, the square of the multiple correlation coefficient, can be interpreted as the fraction of the variation in the dependent variable which can be explained by the model.

Predictions made with the models are compared to the corresponding observed leaching values for field cell 1 to test the modeling results. For this comparison, the concentrations were transformed to cumulative mass leached per mass of original waste. The comparison was made by presenting a plot of observed and predicted values for each model developed.

At an intermediate step, models were obtained such that the concentration for a given species in the i^{th} laboratory leaching extraction (a repetition of Step 2) could be predicted in terms of the concentrations of a selected subset of the chemical species at the preceding (i.e., (i-1)st) extraction and possibly pH at the preceding or current extraction. Selection of the predictor variables included in each model was made by statistical model development techniques.

These models, then, can be used as a means for chemical interpretation of the causal relationships in the leaching process. For example, if the concentration of species k is selected as a predictor of the concentration of species j, this may imply that the presence of species k in the leachate affects the leaching of species j from the waste. As always, however, it must be remembered that statistical correlations do not automatically imply that a cause-and-effect relationship exists. Chemical reasoning must supplement the statistical results in each case to identify the most likely causal relationships. A possible extension of the work presented here would include the formulation of theorized sets of causal relationships and subsequent use of statistical relationships to verify or refine the theory.

With the above mentioned points in mind, the following chemical deductions were made from the modeling results. The species were classed into two groups. In the first group, consisting of SO_4, Si, Cr, Ba, Na, Fe, Ca, Zn, and Sr, the species were self-controlled; that is, the concentration at the i^{th} extraction of one of these species is related to leading concentrations of species within the group. Sulfate and silicon were individually self-contained. Concentrations for the second group, consisting of Mg, B, F, Cl, and Al, were largely controlled by the first group.

It was observed that pH did not play a crucial role as a predictor variable. This is not surprising, since pH varied only between 11.0 and 12.0 during the sequence of laboratory extractions for Exxon PFBC waste.

While significant progress in development of the mathematical approach is presented here, extensions of the work are possible. The last section presents suggestions for future work.

The multi-species modeling approach presented in this section was developed by an independent consultant, Dr. James Dunn, Professor of Statistics at the University of Arkansas and formerly a statistician at the Environmental Protection Agency.

G.3.1 Preliminary Modeling Considerations

When the shake-test extraction data from protocol Steps 1 and 2 are examined from the standpoint of suggesting a tentative leaching model, one finds that the logarithm of concentration is linear with respect to step number for many species. This is illustrated by Figures G-32 to G-41 (see Attachment 1) using PFBC results for those species whose concentrations never fell below detection limits SO_4, Si, Ba, Fe, Ca, Sr, Mg, B, F, and Al). In these plots, the dependent variable, "STEP", is an index indicating the number of leachings which have been performed. A single quantity was needed as the independent variable for plotting purposes. The correspondence between the "STEP" variable and protocol step and iteration within protocol is as follows:

Protocol Step	Iteration	STEP
1	1	0
2	1	1
2	2	2
2	3	3
2	4	4
2	5	5
2	6	6
2	7	7

In Figures G-32 to G-41, Ba, Si, Sr, and to a lesser extent, Al and Ca demonstrate this linear tendency. The implied model then must be:

$$y(n) = y_o e^{bn} , \qquad (1)$$

where $y(n)$ = concentration at the n^{th} step,

b = coefficient defining the slope of the line

n = STEP number,

so that:

$$\ln y(n) = \ln(y_o) + bn , \qquad (2)$$

which is a linear regression of log concentration on STEP number.

In actual fact, the STEP number, n, is a surrogate value for a more meaningful quantity, namely the accumulated volume of water, say v_n, which has been applied to the solid in n successive steps. Hence, an entirely equivalent model is:

$$y(v_n) = y_o e^{bv_n} . \quad (3)$$

But since the volumes added at each step are identical, say v_o, then:

$$\begin{aligned} y(v_n) &= y_o e^{b(nv_o)} = e^{bv_o} \{y_o e^{b[(n-1)v_o]}\} \\ &= e^{bv_o} y(v_{n-1}) , \end{aligned} \quad (4)$$

which suggests that b might be estimable in terms of a first order autoregressive model:

$$y(v_n) = g\, y(v_{n-1}) + \varepsilon_n , \quad (5)$$

where $b = (\ln(g))/v_o$.

Unfortunately, not all of the species exhibit this trend. Even though they might do so in isolation in a pure system, surely strong species interactions, e.g., salt effects, must occur in the complex solution chemistry environment of FBC waste. Hence, the next section is concerned with the development of a multi-species model which has the capability of admitting at least certain types of species interaction, while at the same time exhibiting the characteristic behavior of the univariate model given by equation (4) in the absence of interaction.

G.3.2 Theoretical Multi-Species Model

In order to express all quantities in standard measure, let $\underline{y}(v)$ denote an mx1 column vector representing the concentrations of m species, expressed as mg of species per mL of water per gram of original solid waste, after extraction with 10 mL per gram of solvent. It is then postulated that $\underline{y}(v)$ is related to a vector $\underline{y}_o$, representing unknown initial soluble fractions of the m species in the solid waste (expressed as mg per gram), through the model:

$$\underline{y}(v) = e^{Bv}\underline{y}_o \quad , \tag{6}$$

where B is an mxm unknown matrix. Again if v has accumulated in n uniform increments of v_o mL per gram, as in the shake-tests, then $\underline{y}(v)$ becomes

$$\begin{aligned} \underline{y}(v)_n &= e^{Bnv_o}\,\underline{y}_o = e^{Bv_o}\,[e^{B(n-1)v_o}]\,\underline{y}_o \\ &= e^{Bv_o}\,\underline{y}(v_{n-1}) \quad , \end{aligned} \tag{7}$$

again suggesting that B may be estimated from an MAR(1) multivariate first order autoregressive model:

$$\underline{y}(v_n) = G\,\underline{y}(v_{n-1}) + \underline{\varepsilon}_n \quad , \tag{8}$$

where G is an mxm unknown matrix and:

$$B = v_o^{-1}\ln(G) \quad . \tag{9}$$

A convenient means of evaluating either the matrix logarithm $B = v_o^{-1}\ln(g)$ or fractional powers G^{v/v_o} of G is in terms of the eigenvalues $(g_1, \ldots, g_m)$ of G. Suppose these eigenvalues are distinct, and let diag(g) = diag $(g_1, \ldots, g_m)$ denote a diagonal matrix which displays these eigenvalues. Let Z be an mxm matrix whose columns are the corresponding right eigenvectors of G, i.e., which satisfies:

$$GZ = Z\,\mathrm{diag}(g) \quad .$$

Using the series expansion definition of the matrix logarithm, then it may be verified that:

$$B = v_o^{-1}\,Z\,\mathrm{diag}\,[\ln(g)]\,Z^{-1} \tag{10}$$

and

$$G^{v/v_o} = Z\,\mathrm{diag}\,(g^{v/v_o})\,Z^{-1} \tag{11}$$

as convenient computational devices using only scalar (possibly complex) functions of the eigenvalues.

Since for model validation purposes it will be more convenient to compare accumulated amounts removed by leaching rather than concentrations, an expression representing the integral of equation (6) will be required. Let $\underline{t}(v)$ represent an mx1 vector of accumulated amounts by species in mg per gram which have been leached by vmL per gram of solvent.

Thus:

$$\underline{t}(v) = \int_0^v e^{Bv} \underline{y}_0 \, dv$$

$$= \int_0^v \sum_{j=o}^{\infty} [v_0^{-1} \ln(G)] \, v^j/j! \; dv \, \underline{y}_0$$

$$= \sum_{j=o}^{\infty} [v_0^{-1} \ln(G)]j \; v^{j+1}/(j+1)! \; \underline{y}_0$$

$$= [v_0^{-1} \ln(G)]^{-1} \sum_{j=o}^{\infty} [v_0^{-1} \ln(G)]^{j+1} \, v^{j+1}/(j+1)! \; \underline{y}_0$$

$$= B^{-1} (e^{Bv} - I)\underline{y}_0 \quad , \qquad (12)$$

or in the terms of the eigenvalues of G:

$$\underline{t}(v) = v_0 \, Z \, \mathrm{diag}\, [1/\ln(g)]Z^{-1}[Z \, \mathrm{diag}(g^{v/v_0})Z^{-1} - ZZ^{-1}]\underline{y}_0$$

$$= v_0 \, Z \, \mathrm{diag}[(g^{v/v_0} - 1)/\ln(g)]Z^{-1}\underline{y}_0 \qquad (13)$$

using equations (10) and (11) to obtain B^{-1} and e^{Bv}. Equation (12), or its algorithmic implementation in equation (13), will be referred to as the forward solution for $\underline{t}(v)$, given $\underline{y}_0$. Clearly if no eigenvalues are either zero or one, then both of these expressions are invertible so that:

$$\underline{y}_0 = v_0^{-1} Z \text{ diag } [\ln g/(g^{v/v_0-1}) Z^{-1} \underline{t}(v) \qquad (14)$$

will be referred to as the backward solution for $\underline{y}_0$, given $\underline{t}(\ )$. The existence of equation (14) suggests the exciting possibility of estimating the initial soluable fractions of the species from the accumulated amount extracted. This idea is pursued extensively in later sections.

In order for any of the above expressions to be useful in the physical situation visualized, all defining equations must result in real-valued functions, in spite of the fact that at least some of the eigenvalues of G are likely to be imaginary. At this stage of analysis, it is conjectured that a sufficient condition is simply that no eigenvalue be both real and negative. Since imaginary eigenvalues appear only as complex conjugate pairs, as do their associated eigenvectors, the imaginary parts always appear to cancel in pairs as an expression of the form Z diag (.) Z^{-1} is evaluated.

G.3.3 Estimation of G for Exxon PFBC Waste

In order to estimate the G matrix from shake-test data, the following, rather strong, assumptions were made:

(1) That G in theory should have a relatively simple structure whose few non-zero elements reflect the chemical relations among the species.

(2) That the $\underline{\varepsilon}_n$ of the MAR(1) model defined by equation (8) are independent $N(0,\Sigma)$, so that sequential estimation of the rows of G yields the maximum likelihood estimator of G.

(3) That any physically acceptable estimate of G must have no real negative eigenvalues.

Variable selection was accomplished using the principle of maximizing R^2, subject to restricting the number of terms in the model (as implemented by SAS procedure RSQUARE). The available predictor set for the concentration of each species always consisted of the concentrations of all species at the previous extraction steps (here designated by a prefix L). Estimation was hampered by the presence of values listed as being below instrumental detection limits. These values were arbitrarily set to zero, provided the series contained at least some measured values. Two open questions remained, namely whether or not pH should be made available as a potential controlling variable, and whether or not each species should be forced to be a predictor of itself at the next step. Table G-17 (see Attachment 2) gives the results of variable selection when both pH and pH leading by one step (designated LPH) are made available. Even though variables PH and LPH were selected upon occasion, their role did not seem crucial. This is not surprising since pH only varied between 11.0 and 12.0 during the sequence of extractions. From a logical standpoint, it seemed likely that pH was acting only as a surrogate variable from certain species, particularly calcium, so that pH was omitted from all subsequent analyses.

Table G-18 (see Attachment 3) gives the results of variable selection when each species leading value (L) was forced to act as its own predictor. Clearly in the case of sulfate and silicon, this is an entirely tenable model, while for chromium and chloride it is not. If a working rule is adopted whereby one selects the best K term model such that $R^2 \geq 0.9$ when $R^2 < 0.9$ for all K-1 term models, then non-zero elements of the resulting G matrix are indicated by (x) in the array shown at the end of Table G-18. However, if actual estimates of the indicated regression coefficients are substituted, then 7 of the 14 eigenvalues are real and negative, thus indicating a physically untenable model. Hence, forcing non-zero elements to appear on the principal diagonal of B appeared to be inconsistent with the actual chemistry observed.

By dropping the assumption that each species must serve as its own control, variable selection then proceeded as indicated in Table G-19 (see

Attachment 4). Again indicating the non-zero elements of the resulting G by (x), the array shown at the end of Table G-19 was obtained.

Actual estimated values of these non-zero elements are given in Table G-20 along with each model's associated R^2. The eigenvalues $\{g_i\}$ of this G matrix are respectively, 0.9805, 1.3485, 0.7086, − 1.2948 + 0.6268i, − 1.2948 − 0.627i, 0.308 + 0.431i, 0.308 = 0.431i, 1.089, 0.0209; that is, none are both real and negative. The first two are, of course, simply the diagonal elements of G corresponding to the autoregressive parameters for sulfate and silicon.

Even though an ultimate physical requirement is that max $\{g_1\} < 1$ so that $\lim_{v \to \infty} e^{Bv} \underline{y}_0 = \underline{0}$, a decision was made to accept a model with g_2 and $g > 1$, particularly since the silicon concentration continues to increase through the entire sequence of laboratory extractions. The chemistry of chromium seems particularly complex. However, this may be due to data uncertainty, since replications A and B differ markedly in their reported concentrations. The chemistry of iron also seems complicated.

Some of the implied chemistry seems reasonable. Certainly a relationship between silicon and aluminum seems to follow from considerations of concrete chemistry. The apparent key role of chromium with respect to several cations is consistent with respect to the solubility of various chromates.

In effect, this last analysis has divided the species into two distinct groups. Group 1 consists of SO_4, Si, Cr, Ba, Na, Fe, Cu, Zn, and Sr. These species are self-controlled as a group (sulfate and silicon are individually self-controlled). Group 2 consisting of Mg, B, F, Cl, and Al, which are concomitant in the sense that their fates are determined by the Group 1 species. Hence, in all subsequent analyses, only the behavior of the Group 1 species will be considered.

TABLE G-20. ESTIMATED VALUES OF NON-ZERO ELEMENTS AND ASSOCIATED R^2 VALUES

Element/ Species	Predictor	Coefficient	R^2
SO_4	SO_4	0.9805	0.990
Si	Si	1.3485	0.963
Cr	SO_4	-0.00011	0.942
	Na	0.01274	
	Fe	0.42481	
	Zn	2.31065	
	Sr	0.17787	
Ba	Cr	0.246	0.969
	Ba	0.681	
Na	Cr	134.140	0.931
	Sr	11.892	
Fe	SO_4	-0.000103	0.911
	Na	-0.00535	
	Ba	3.363	
	Fe	0.509	
Ca	Cr	3232.632	0.941
	Ca	0.709	
Zn	Na	0.00687	0.926
	Zn	-2.055	
	Sr	0.0746	
Sr	Cr	5.739	0.983
	Ba	8.041	
Mg	Fe	2.058	0.924
	Ca	0.000160	
B	Cr	35.575	0.911
	Sr	4.27	
F	SO_4	0.000302	0.907
Cl	Na	-0.180	0.977
	Fe	5.657	
	Ca	0.0063	
	Mg	2.803	
	F	9.678	
Al	Si	0.875	0.946

G.3.4 Estimation of the Initial Soluable Fraction $\underline{y}_0$ From Shake-Tests

As a first approximation for the $\underline{y}_0$ vector of the model defined by equation (6), one might use the bulk analyses of the raw waste as given in the second column of Table G-21. As an alternative, one may apply the back-calculation formula defined by equation (14) to the cumulative amounts extracted by shake-tests using the G matrix as estimated in the previous section. The results are summarized in Table G-22 (see Attachment 5) and plotted in Figures G-42 to G-50 (see Attachment 6).

In Table G-21, a 'mean' estimator of $\underline{y}_0$ was obtained by taking the mean of the back-calculated values for each species. With the exception of sodium and iron, this $\underline{y}_0$ estimator yielded non-negative values which are less by several orders of magnitude than that predicted by the raw waste analysis. However, an examination of Figures G-42 to G-50 indicated a continuous decreasing trend in back-calculated values for Si, Cr, Na, Fe, and Zn, often becoming quite negative at a high volume-per-mass ratio. Hence, a mixed rule of estimation was formulated, namely:

(1) Choose the mean of all back-calculated values if it is positive and three is no trend.

(2) Choose the mean of back-calculated values for the initial shake-test (o'th step), provided it is positive and there is an obvious trend.

(3) Choose the mean of back-calculated values for the first step shake-test, provided it is positive and rules (1) and (2) fail to produce an estimate.

(4) Choose the maximum of the back-calculated values for the initial shake-test, provided it is positive and rules (1) through (3) fail to produce an estimate.

TABLE G-21. ESTIMATES OF THE INITIAL SOLUBLE FRACTION y_o FOR EXXON PFBC WASTE BASED ON SOLID SAMPLE WASTE ANALYSES AND ON BACK-CALCULATION OF LAB AND FIELD DATA

Element/ Species	Raw Waste[1]	Shake-Test		Field Cell	
		Mean[1]	Mixed Rule[1]	Mean[1]	Asymptotic[1]
SO_4	225	1.29	1.29[2]	7.48	2.8
Si	52	0.000421	0.000572[3]	0.0333	0.033[2]
Cr	0.128	0.0000158	0.0000738[4]	0.000299	0.00022
Ba	0.087	0.000156	0.000156[2]	0.0000808	0.0000808[2]
Na	5.2	(0.0283	0.0283[3]	0.626	0.23
Fe	30	(0.000242)	0.000242[5]	0.00111	0.00061
Ca	220	1.571	1.571[2]	0.334	0.334[2]
Zn	0.290	0.0000182	0.000163[3]	0.00102	0.00034
Sr	0.160	0.00167	0.00167[2]	0.000987	0.000987[2]
Mg	117				
B	0.725				
F	0.182				
Cl	0.280				
Al	24				

[1] mg/g

[2] mean

[3] first

[4] second

[5] maximum first

Use of this 'mixed rule' is summarized in Table G-21. Note that 'mixed rule' estimates are indicated for sodium and iron as well under the 'mean' rule.

G.3.5 Field Cell Rainfall-Perculation Delay Model

In order to provide a basis for validation of the tentative extraction model, a quantitative assessment of the amounts actually leached from the FBC wastes in the field cells was required. The problem was complicated by the fact that even though species concentrations were determined at the upper sampling level, no time-related measure of water flow was available for this point. Only a record of water accumulated at the lower level was available. If a suitable delay model could be obtained which related bottom flow to rainfall, then water flow at the upper sampling point could be approximated by interpolation. A satisfactory model appears to be as follows:

Let t = day number since the beginning of the experiment,

$v_L(t)$ = accumulated volume (liters) at the lower sampling level on day t,

r_i = rainfall (liters) on the i^{th} day,

d = days delay in order for a rainfall event to influence bottom flow.

Then the proposed model is:

$$E[v_L(t)] = \beta_0 + \beta_1 \sum_{i=1}^{t-d} r_i + \beta_2 \sin(2\pi t/365) + \beta_3 \cos(2\pi t/365) \quad ,$$

where β_0, β_1, β_2, and β_3 are coefficients to be estimated from the data. The trigonometric terms were introduced when subsequent analysis indicated the need for a seasonal effect of the form sin $(2\pi t/365 + K)$ in terms of some unknown translation parameter K.

Using rainfall-flow data beginning at t=15 and ending at t=513 (the last volume measurement before the cells were capped), the above model was fitted for field cells 1 to 6 using respectively d=0,1,2,....,15. The best choice of delay d was chosen to correspond to the minimum mean squared error. Table G-23, which gives the mean squared errors for successive values of d, clearly indicates a universal delay of at least 9 days.

The best empirical delay models as specified by their estimated regression coefficients are indicated in Table G-24. Figures G-51 to G-62 (see Attachment 7) demonstrate the adequacy of these fitted models. For each cell, the first figure shows $\sum_{i=1}^{t-d} r_i$ and $v_L(t)$ plotted on t as R and F respectively, while the second figure shows observed (O) and predicted (P) $v_L(t)$ plotted on t.

To interpolate any of these models in order to estimate the volume of water which has passed through the FBC layer only, an assumption was made that the percolation rate is constant through all media. In this case, with the upper disposal medium layer and FBC layer comprising the upper 2 1/2 feet of the 7 feet of fill in a field cell, the linear approximation yielded

$$d_v = 2\tfrac{1}{2} \times \tfrac{1}{7} \times 12$$

$$\sim 4 \text{ days delay when } d = 12, \text{ and}$$

$$d_v = 2\tfrac{1}{2} \times \tfrac{1}{7} \times 15$$

$$\sim 5 \text{ days delay when } d = 15$$

An estimated rainfall-flow delay model at the upper sampling point thus became:

TABLE G-23. MEAN SQUARED ERRORS FOR THE RAINFALL-FLOW MODEL WITH d = 0,1,2, ..., 15 DAYS

d	Field Cell 1	2	3	4	5	6
0	591	408	505	667	541	470
1	615	426	508	693	538	476
2	556	386	479	655	500	473
3	668	466	536	759	575	522
4	680	472	538	768	582	534
5	688	479	529	758	570	524
6	709	497	544	749	553	539
7	697	498	565	740	542	597
8	660	466	497	700	495	546
9	449	298	362	465	353	349
10	448	307	371	446	340	360
11	412	277	318	419	314	348
12	364	250	227	367	261	284
13	408	295	301	369	254	351
14	459	370	381	364	239	480
15	357	285	299	270	179	376

TABLE G-24. ESTIMATED REGRESSION COEFFICIENTS FOR THE RAINFALL-FLOW DELAY MODEL (IN LITERS)

Cell No.	d	R^2	β_0	β_1	β_2	β_3
1	12	0.998	-62.982	0.6353	-46.048	-25.242
2	12	0.999	-58.216	0.646	-36.784	-13.802
3	12	0.998	-108.612	0.558	-36.830	-25.136
4	15	0.998	41.506	0.557	-66.944	-29.102
5	15	0.998	-5.757	0.501	-39.437	-26.862
6	12	0.998	-85.127	0.599	-41.651	-4.466

$$v_U(t) = \beta_0 + \beta_1 \sum_{i=1}^{t-d_v} r_i + \beta_2 \sin(2\pi r/365) + \beta_3 \text{ cost } (2\pi t/365).$$

Since the data for field cell 1 were used extensively for model validation studies in the following sections, $v_o(t)$ (in liters) is given below corresponding to the actual sampling times of the study (see Table G-25).

TABLE G-25. ESTIMATED CUMULATIVE FLOW AT THE UPPER SAMPLE POINT FOR FIELD CELL 1 AS A FUNCTION OF TIME

t (days)	$v_U(t)$ (liters)	t (days)	v(t) (liters)
5	20.904	74	297.40
6	57.818	92	319.41
10	94.434	115	345.51
11	100.21	135	390.32
13	113.87	169	479.18
15	133.13	218	550.13
18	132.71	271	699.27
23	142.36	333	863.00
27	149.91	407	1,100.1
32	171.23	513	1,287.1
39	174.37	552	1,428.9
50	192.90	581	1,539.1
59	229.65	612	1,623.9
		643	1,647.4

As a final remark, it is apparent from Figures G-51, G-53, G-55, G-57, G-59, and G-61 that the cumulative rainfall (R) and bottom flow (F) curves never become parallel. In fact, the estimates β_1 of Table G-24 indicate that only about 60% of the rainfall completed its percolation through the field cells. The most plausible explanation is that evaporation proceeded at an essentially constant rate. The hydrologic balance asesssment for Field Cells 1 to 6 presented in Appendix E indicates an average loss of 44% of precipitation input for the Exxon PFBC field cells.

If the peak positive seasonal excursion from the trigonometric terms is estimated using the formula:

$$\overset{\circ}{t} = [1 - \tan^{-1} (\beta_3/\beta_2] \; 365/2\pi,$$

estimates ranging from 23 to 52 days for the six field cells, (i.e., August 24 through September 22) are obtained. Quite likely, this corresponds to a period of maximum evaporation rate. These empirical rainfall-flow delay models provided, a reasonable means of adjustment for the discrepancy between rainfall and percolated flow.

G.3.6 Shake-Test Model Validation

For comparison purposes, an attempt was made to estimate the cumulative species leached from the Exxon PFBC waste in field cell 1. Although this problem was complicated by lack of volume measurements at the upper sampling level and the apparently sizeable increments of flow between sampling dates late in the experiment, the water volume increments were estimated by the methodology described in the previous section and the computed values given there.

Values predicted by the estimated shake-test model were computed using equation (13) with $\underline{y}_0$ estimated by the 'mixed rule' as given in Table G-21. Figures G-63 to G-71 illustrate the results over the range of water percolation actually experienced in the field. Barium and strontium are predicted very well, and zinc almost as well. Sulfate was predicted within a factor of two, and calcium and chromium within a factor of three. In most cases, predicted values were higher than observed with the exceptions being sulfate, silicon, and sodium. In retrospect, since silicon and sulfate are self-controlled, their prediction curves could be raised to the level of that observed simply by increasing their respective values in the $\underline{y}_0$ vector. However, since this presumes prior knowledge of the field cell results, this was not done and the result of applying the "mixed rule" is displayed.

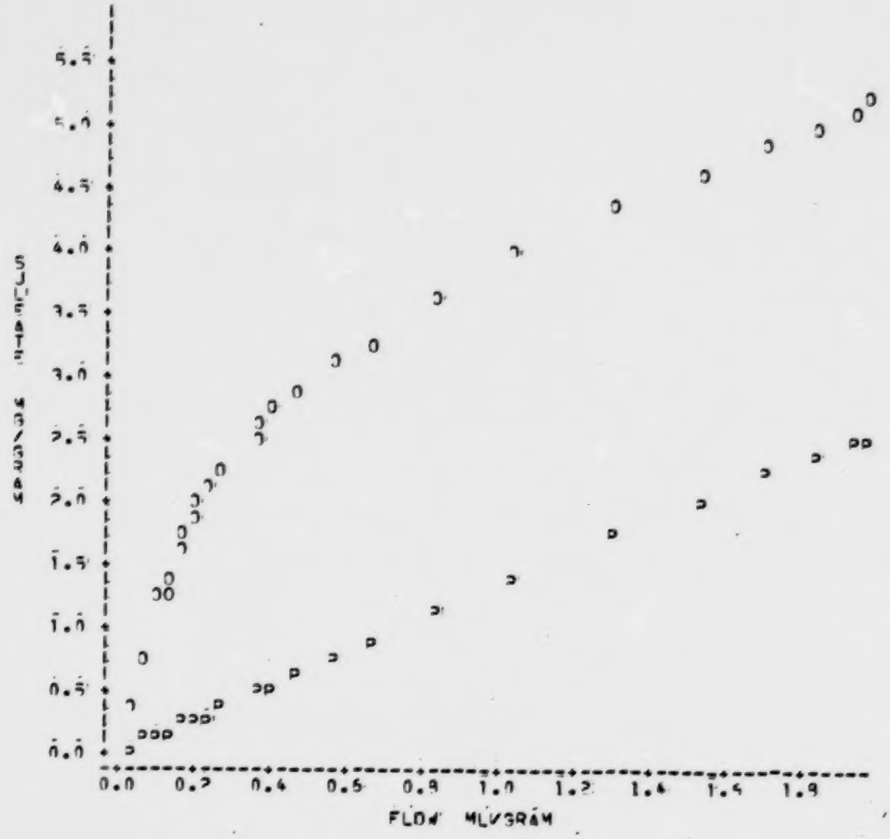

NOTE: The initial soluble fraction ($\underline{y}_o$) was estimated by a "mixed-rule" applied to back-calculated shake-test results. Flow is over the range experienced in the field.

Figure G-63. Model Confirmation Results for Sulfate Based on Shake-Test Extractions of Exxon PFBC Waste: Observed (O) and Predicted (P) Cumulative Field Cell 1 Extractions.

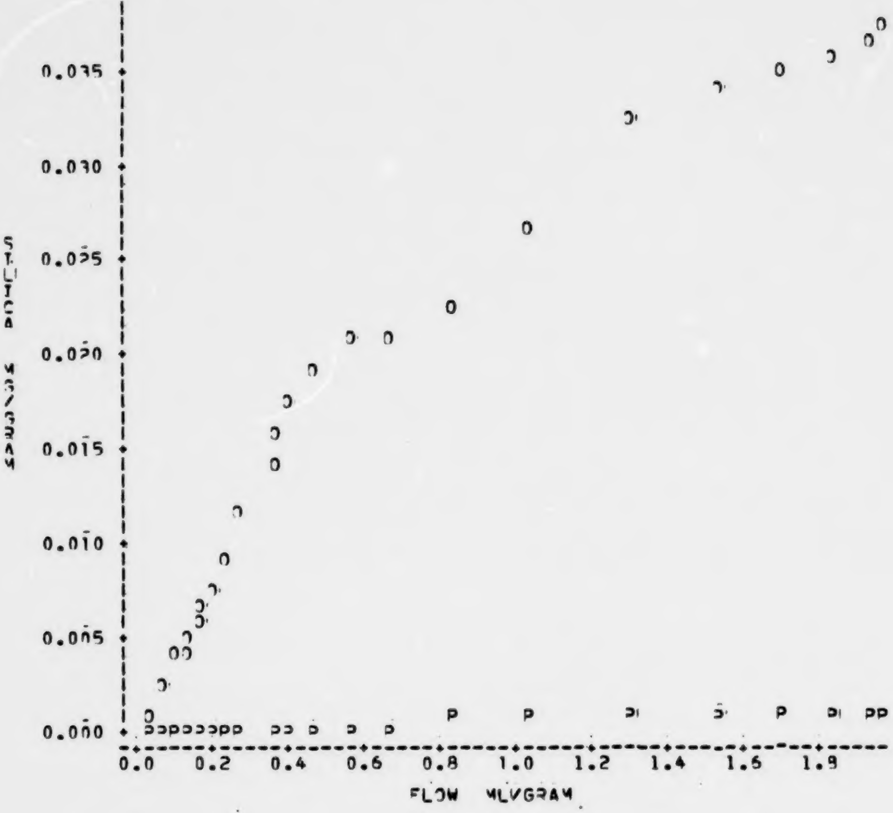

NOTE: The initial soluble fraction (y_o) was estimated by a "mixed-rule" applied to back-calculated shake-test results. Flow is over the range experienced in the field.

Figure G-64. Model Confirmation Results for Silicon Based on Shake-Test Extractions of Exxon PFBC Waste: Observed (O) and Predicted (P) Cumulative Field Cell 1 Extractions.

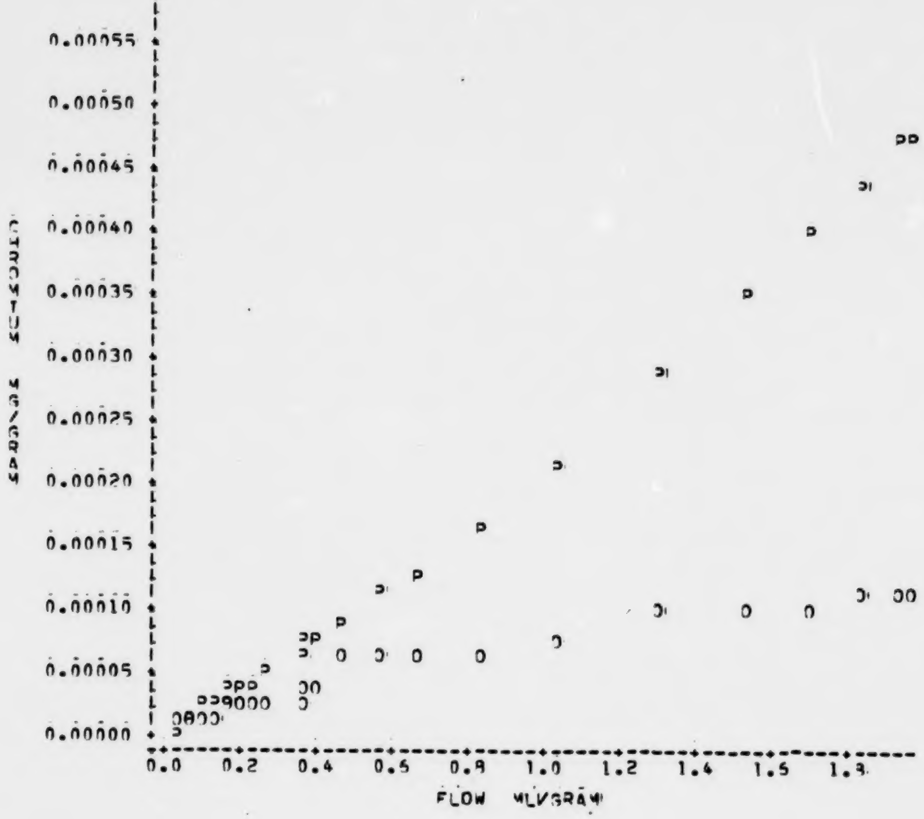

NOTE: The initial soluble fraction (y_0) was estimated by a "mixed-rule" applied to back-calculated shake-test results. Flow is over the range experienced in the field.

Figure G-65. Model Confirmation Results for Chromium Based on Shake-Test Extractions of Exxon PFBC Waste: Observed (O) and Predicted (P) Cumulative Field Cell 1 Extractions.

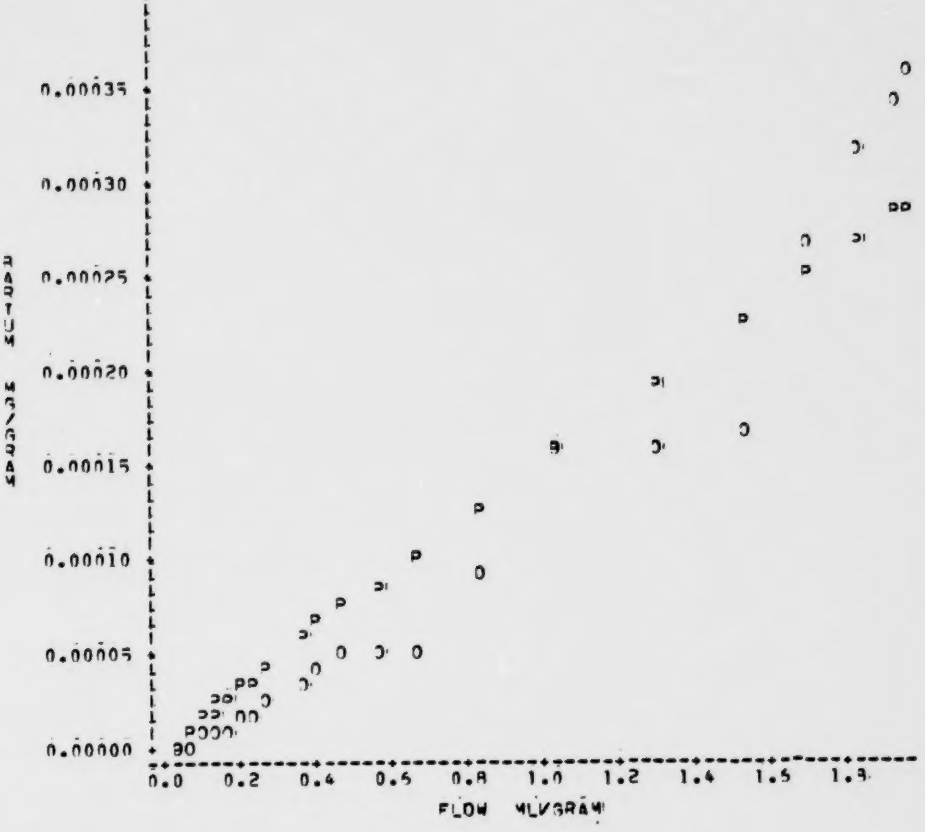

NOTE: The initial soluble fraction ($\underline{y}_o$) was estimated by a "mixed-rule" applied to back-calculated shake-test results. Flow is over the range experienced in the field.

Figure G-66. Model Confirmation Results for Barium Based on Shake-Test Extractions of Exxon PFBC Waste: Observed (O) and Predicted (P) Cumulative Field Cell 1 Extractions.

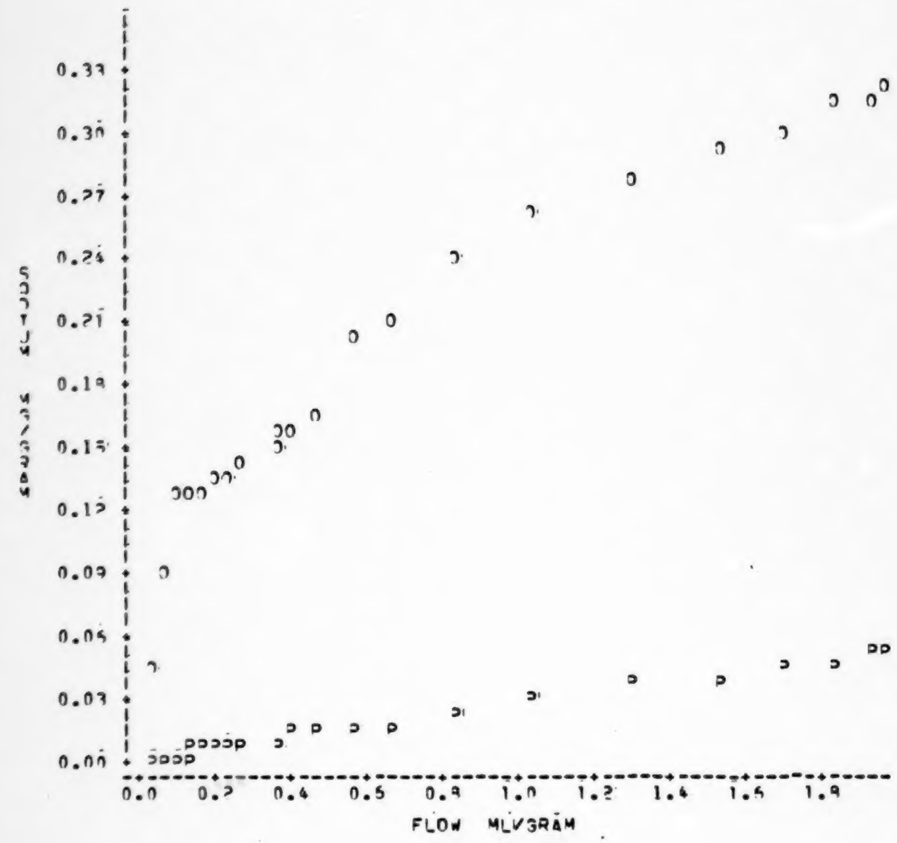

NOTE: The initial soluble fraction ($\underline{y}_o$) was estimated by a "mixed-rule" applied to back-calculated shake-test results. Flow is over the range experienced in the field.

Figure G-67. Model Confirmation Results for Sodium Based on Shake-Test Extractions of Exxon PFBC Waste: Observed (O) and Predicted (P) Cumulative Field Cell 1 Extractions.

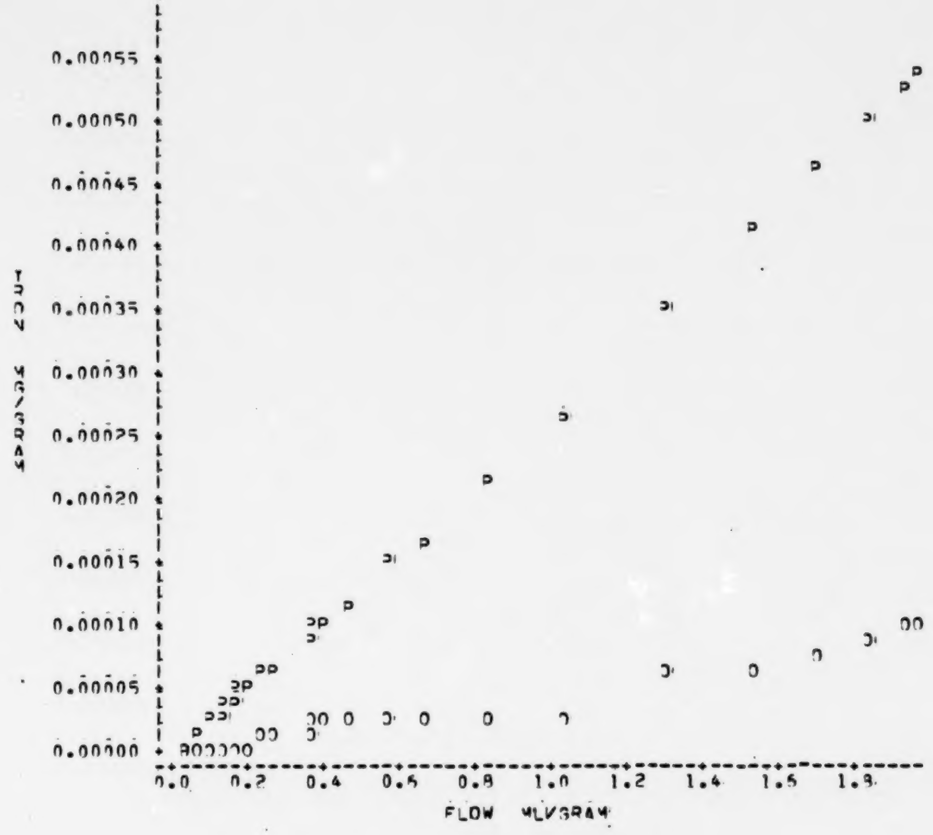

NOTE: The initial soluble fraction ($\underline{y}_0$) was estimated by a "mixed-rule" applied to back-calculated shake-test results. Flow is over the range experienced in the field.

Figure G-68. Model Confirmation Results for Iron Based on Shake-Test Extractions of Exxon PFBC Waste: Observed (O) and Predicted (P) Cumulative Field Cell 1 Extractions.

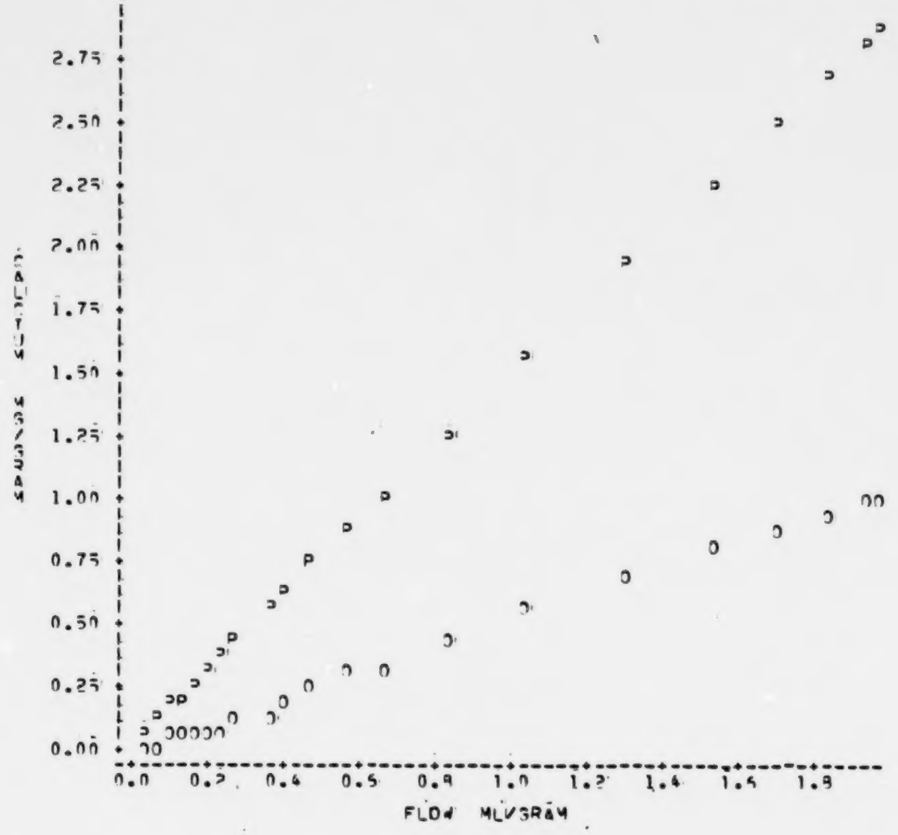

NOTE: The initial soluble fraction ($\underline{y}_0$) was estimated by a "mixed-rule" applied to back-calculated shake-test results. Flow is over the range experienced in the field.

Figure G-69. Model Confirmation Results for Calcium Based on Shake-Test Extractions of Exxon PFBC Waste: Observed (O) and Predicted (P) Cumulative Field Cell 1 Extractions.

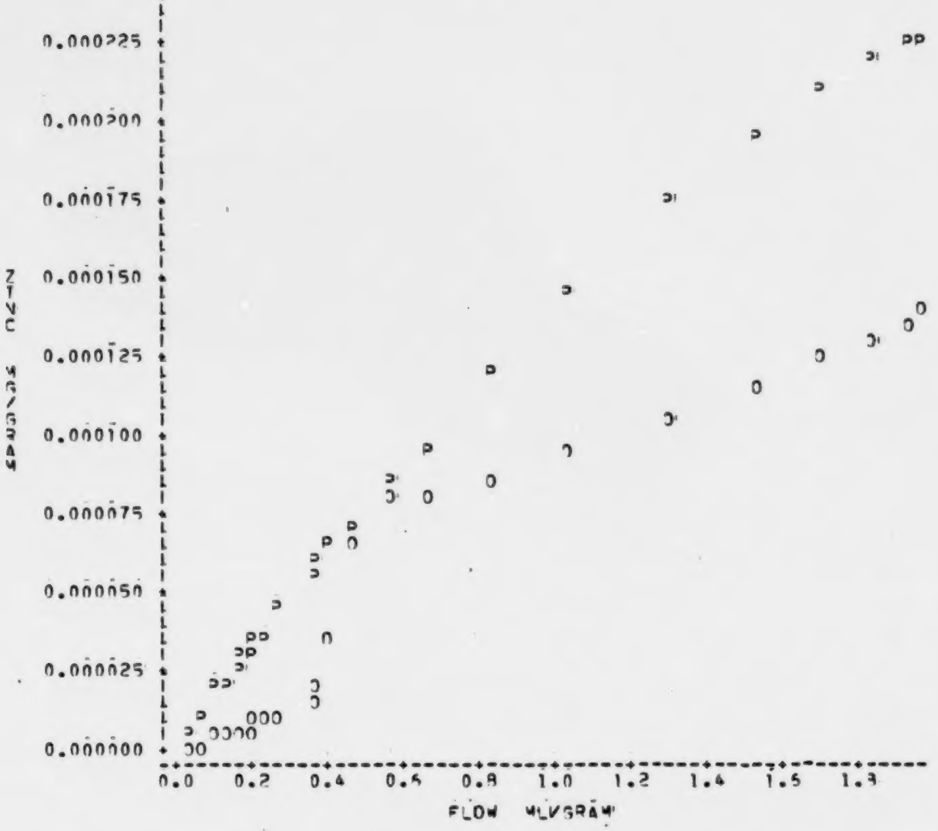

NOTE: The initial soluble fraction ($\underline{y}_o$) was estimated by a "mixed-rule" applied to back-calculated shake-test results. Flow is over the range experienced in the field.

Figure G-70. Model Confirmation Results for Zinc Based on Shake-Test Extractions of Exxon PFBC Waste: Observed (O) and Predicted (P) Cumulative Field Cell 1 Extractions.

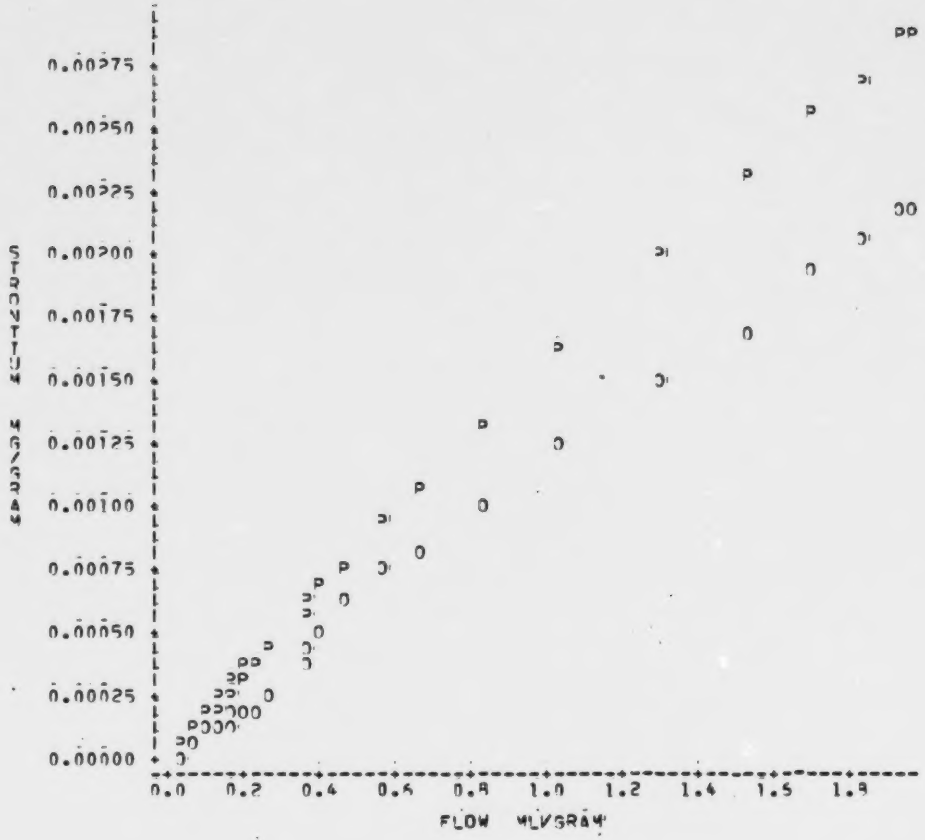

NOTE: The initial soluble fraction (y_0) was estimated by a "mixed-rule" applied to back-calculated shake-test results. Flow is over the range experienced in the field.

Figure G-71. Model Confirmation Results for Strontium Based on Shake-Test Extractions of Exxon PFBC Waste: Observed (O) and Predicted (P) Cumulative Field Cell 1 Extractions.

Figures G-72 to G-80 (see Attachment 8) extend these identical prediction curves to the water/solid rates experienced at the zero'th laboratory step.

G.3.7 Model Validation Assuming Prior Knowledge of Field Cell Results

In the process of evolving the "mixed rule", it became apparent that the prediction equations were quite sensitive to the choice of $\underline{Y}_o$. Not only the predicted amounts but the rate at which they changed could be adjusted by small variations in $\underline{Y}_o$. In an attempt to isolate the separate effects of uncertainty in choice of G and $\underline{Y}_o$, equation (14) was used to back-calculate estimates of $\underline{Y}_o$ from field cell 1 data, using G estimated from the shake-tests and flow increments estimated from the rainfall-flow delay model. The results are plotted in Figures G-81 to G-89 (see Attachment 9) and summarized in Table G-26.

TABLE G-26. MODEL BUILDING RESULTS BASED ON SHAKE-TEST EXTRACTIONS OF EXXON PFBC WASTE: SUMMARY OF ESTIMATED INITIAL SOLUBLE FRACTION OBTAINED BY BACK-CALCULATION FROM FIELD CELL 1 DATA

Variable	N	Minimum Value	Maximum Value	Mean	Standard Deviation	Std. Error of Mean
SO_4	26	2.669	13.904	7.480	3.278	0.643
Si	26	0.0186	0.0420	0.0333	0.00746	0.00146
Cr	26	0.000211	0.00103	0.000299	0.000163	0.0000320
Ba	26	0.0000332	0.000178	0.0000808	0.0000433	0.00000843
Na	26	0.221	1.889	0.626	0.404	0.0793
Fe	26	0.000584	0.00594	0.0011	0.00106	0.000209
Ca	26	0.213	0.486	0.333	0.0867	0.0170
Zn	26	0.000322	0.00654	0.00102	0.00123	0.000241
Sr	26	0.000818	0.00127	0.000986	0.000126	0.0000246

Note: Values are in mg/g

Using means of these back-calculated values to estimate $\underline{Y}_o$, equation (13) was used to predict the accumulated species as shown in Figures G-90 to G-98 (see Attachment 10). Even though these were noticeable improvements with respect to sulfate, silicon, and sodium prediction, instability was introduced with respect to chromium and iron prediction, probably due to the drastic increase in $\underline{y}_o$ values for sodium or sulfate or both as compared to the "mixed rule" estimates. However, comparison of Figures G-90 to G-98 with Figures G-42 to G-50 indicates quite striking differences. The former are much smoother, and in the case of SO_4, Cr, Na, Fe, and Zn, appear to approach asymptotic values which were estimated visually and listed in Table G-26. Using the mixture of mean and asymptotic values to estimate $\underline{y}_o$ and applying equation (13) resulted in yet another set of predictions shown as Figures G-99 to G-107 (see Attachment 11). Now observed and predicted curves correspond very well, except for serious instability with respect to iron and to a lesser extent chromium. Unfortunately, this instability does not damp out with increased flow, as illustrated by Figures G-108 to G-116 (see Attachment 12).

The main conclusions which seem to follow from this exercise are that the G matrix, which was estimated from shake-test data, provided a reasonably accurate representation of species interaction, and was fairly inaccurate in estimating $\underline{y}_o$. On the other hand, precise estimation of $\underline{y}_o$ is absolutely essential for precise prediction of species leaching, even if G is accurately known.

The analysis which was performed here with respect to field cell 1 could be extended to the remainder of the field cells. Clearly, this could be accomplished with respect to field cells 2 to 6 with minimal effort, since they involve Exxon PFBC waste. Application to Alliance AFBC waste would require additional effort to estimate a new G matrix.

The proposed rainfall-percolation delay model seems to work quite well in the sense that the resulting cumulative species extraction curves look fairly smooth.

G.3.8 Possible Extensions

The parameters of the proposed concentration model $\underline{y}(v) = e^{BV}\underline{y}_o$ physically more meaningful than in the polynomials of Section G.2 The matrix B summarizes species interactions, including the past history of the species itself; the vector $\underline{y}_o$ reflects the initial soluble fraction which exists before leaching begins. In integral form, $\underline{t}(v) = \int_o^v \underline{y}(v)dv$ provides an expression for the physical amounts of all species which would be leached by v units of solvent. This seems exactly the type of information which policy makers require. Clearly, $\underline{t}(o) = \int_o^o \underline{y}(v)dv = \underline{0}$ as it should.

The asymptotic nature of estimates of $\underline{y}_o$ from field cell 1 data (as illustrated by Figures G-81 to G-89) suggests an augmented integral form

$$\underline{t}(v) = B^{-1}\,[e^{Bv}-I]\,\underline{y}_o(v),$$

where $\underline{y}_o(v)$ expresses the fact that the initial solvable fraction for field cell 1 seemed to change for some species as leaching proceeded.

In general, G estimated from shake-test data has seemed relatively applicable to field cell data. The crucial step seems to be to obtain an accurate estimate of $\underline{y}_o$. If this sort of model is adopted in practice, then special attention should be given to the problem of optimal experimental design to estimate $\underline{y}_o$ from shake-test data.

Adding an estimation constraint that all elements of G be non-negative would guarantee that all elements of e^{Bv} and hence $\underline{y}(v)$ would be non-negative for all v. This, of course, would be in addition to the existing constraint of no negative real eigenvalues for G.

On the horizon, the problem of modeling attenuation and mixed attenuation-leaching still remains. Since in some sense, attenuation is the inverse of leaching, perhaps it could be modeled similarly as:

$$\underline{x}(v) = e^{Av}\,\underline{x}_o \quad ,$$

where A could be estimated from an inverse recursion of the form:

$$\underline{x}\,(v_{n-1}) = H\,\underline{x}\,(v_n) + \underline{\varepsilon}_{n-1} \quad ,$$

where $H = e^{-Av_1}$. If this were so, then possibly the mixed system consisting of layers of waste and disposal media could be modeled as:

$$\underline{y}(t) = e^{Av} e^{Bv} \underline{y}_o = e^{(A+B)v} \underline{y}_o ,$$

provided AB = BA (an additional constraint).

G.4 References

G-1. Barr, Anthony J., 1979, SAS Users Guide, 1979 Edition, SAS Institute, Inc., Raleigh, North Carolina.

G-2. Wine, R. Lowell, 1964, Statistics for Scientists and Engineers, Prentice-Hall, Inc., Englewood Cliffs, New Jersey.

Appendix G

Attachment 1

Figures G-32 to G-41

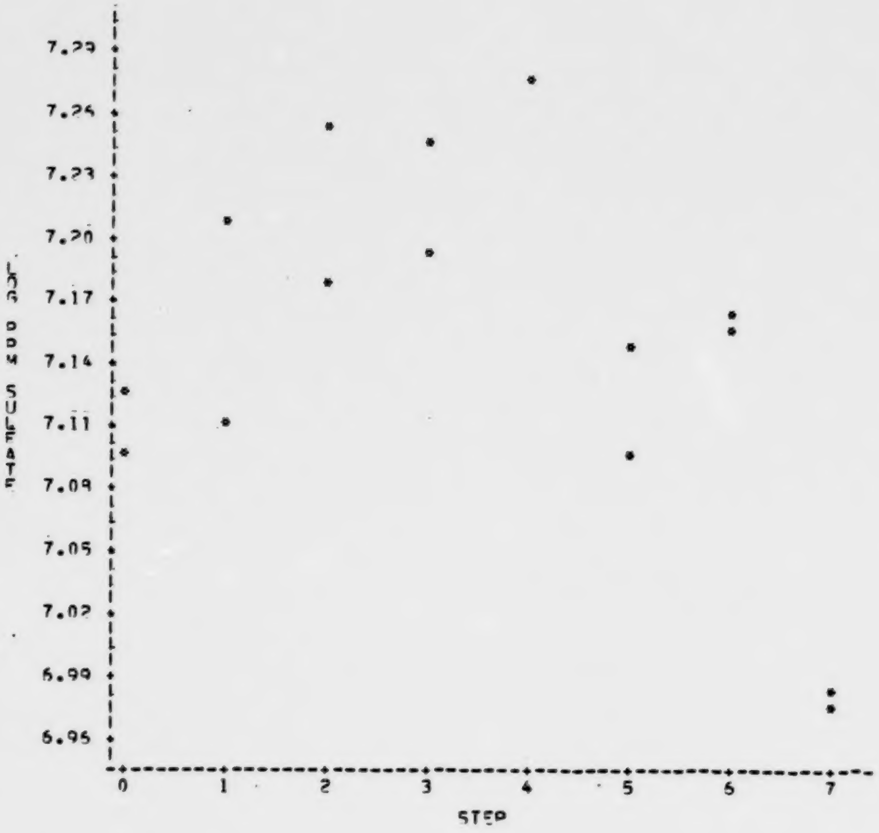

Figure G-32. Natural Logarithm of Sulfate Concentration vs. Shake-Test Extraction STEP for Exxon PFBC Waste.

Preceding page blank

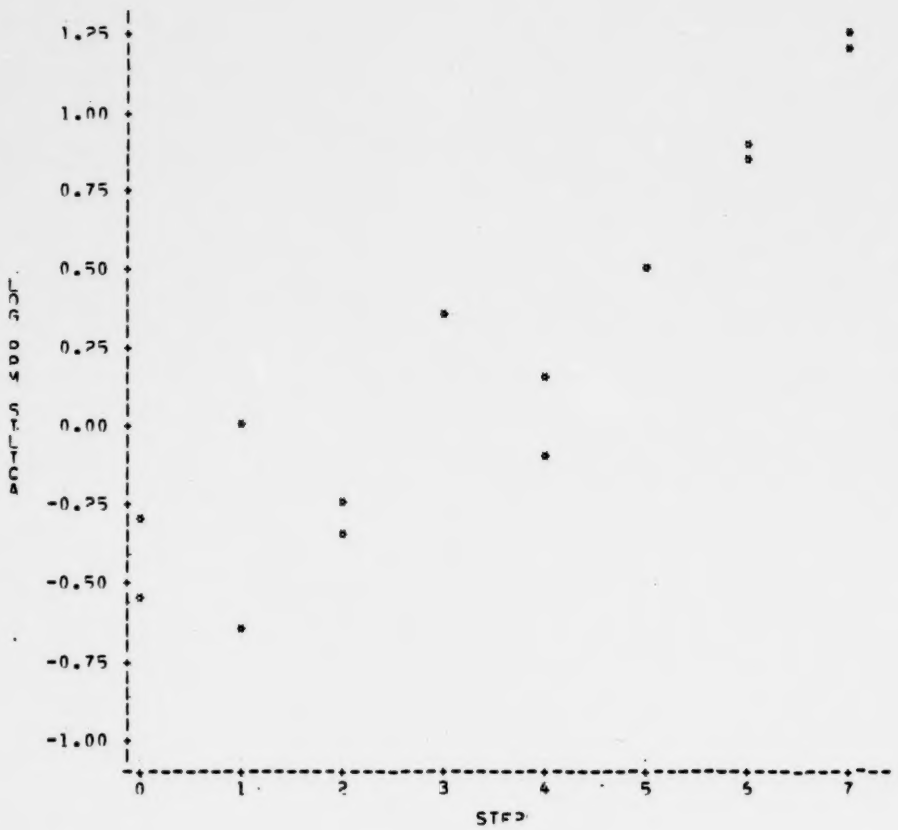

Figure G-33. Natural Logarithm of Silicate Concentration vs. Shake-Test Extraction STEP for Exxon PFBC Waste.

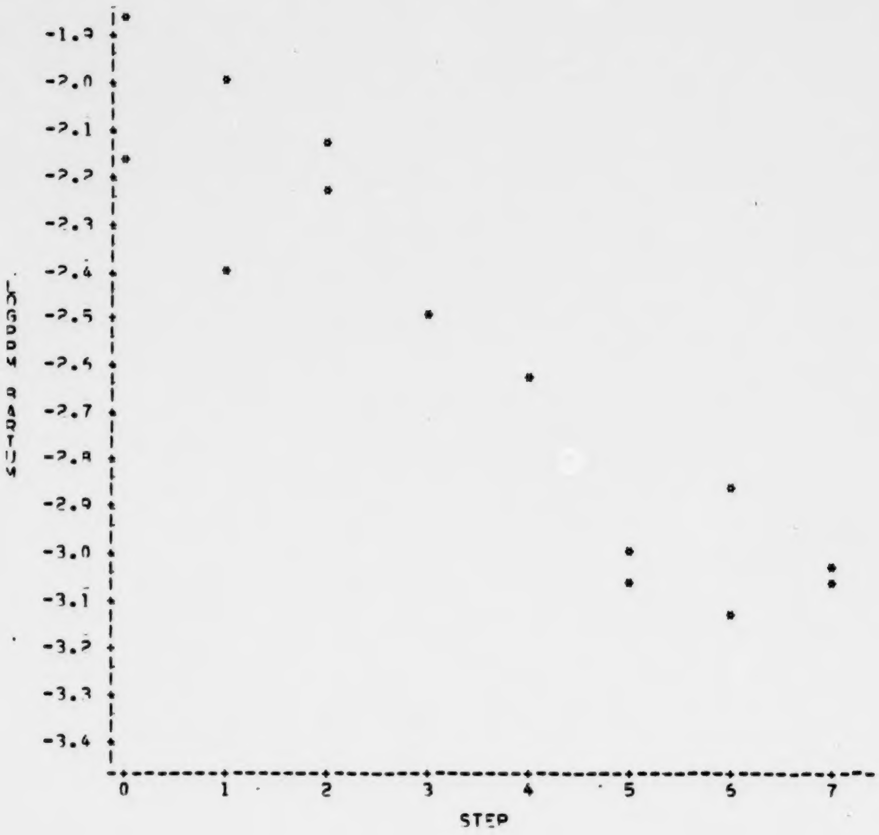

Figure G-34. Natural Logarithm of Barium Concentration vs. Shake Test Extraction STEP for Exxon PFBC Waste.

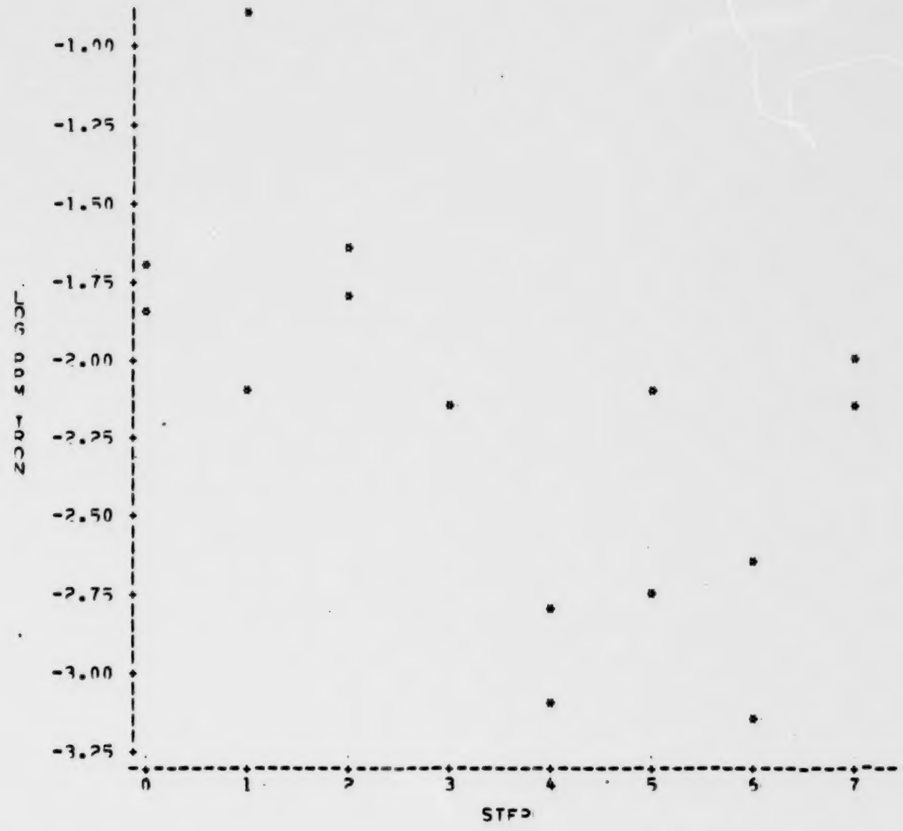

Figure G-35. Natural Logarithm of Iron Concentration vs. Shake-Test Extraction STEP for Exxon PFBC Waste.

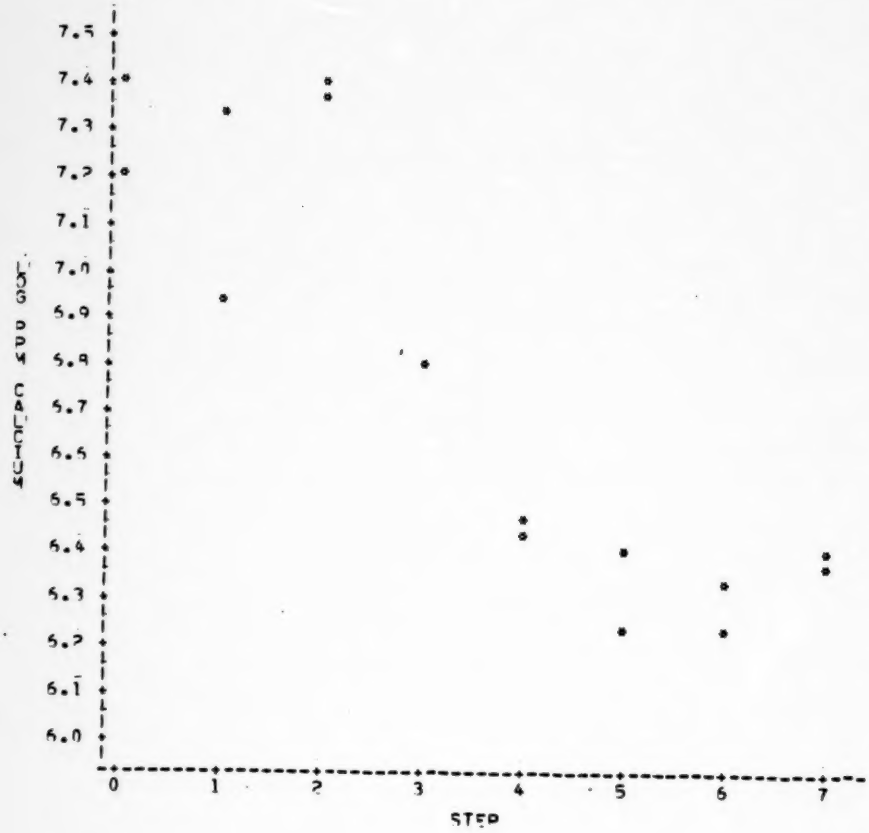

Figure G-36. Natural Logarithm of Calcium Concentration vs. Shake-Test Extraction STEP for Exxon PFBC Waste.

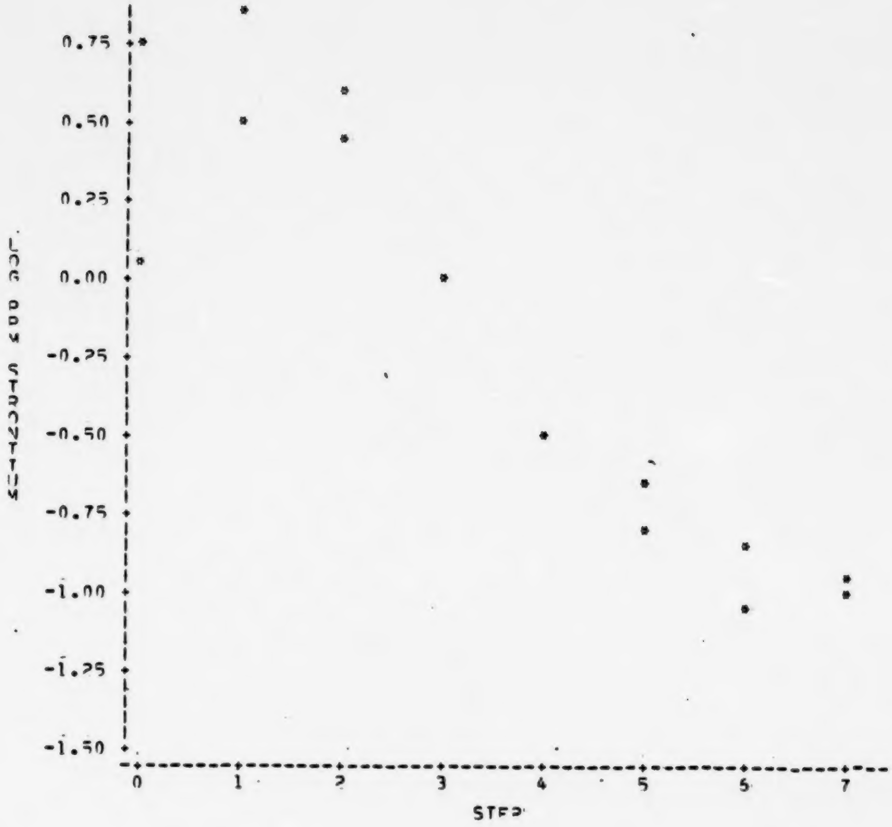

Figure G-37. Natural Logarithm of Strontium Concentration vs. Shake-Test Extraction STEP for Exxon PFBC Waste.

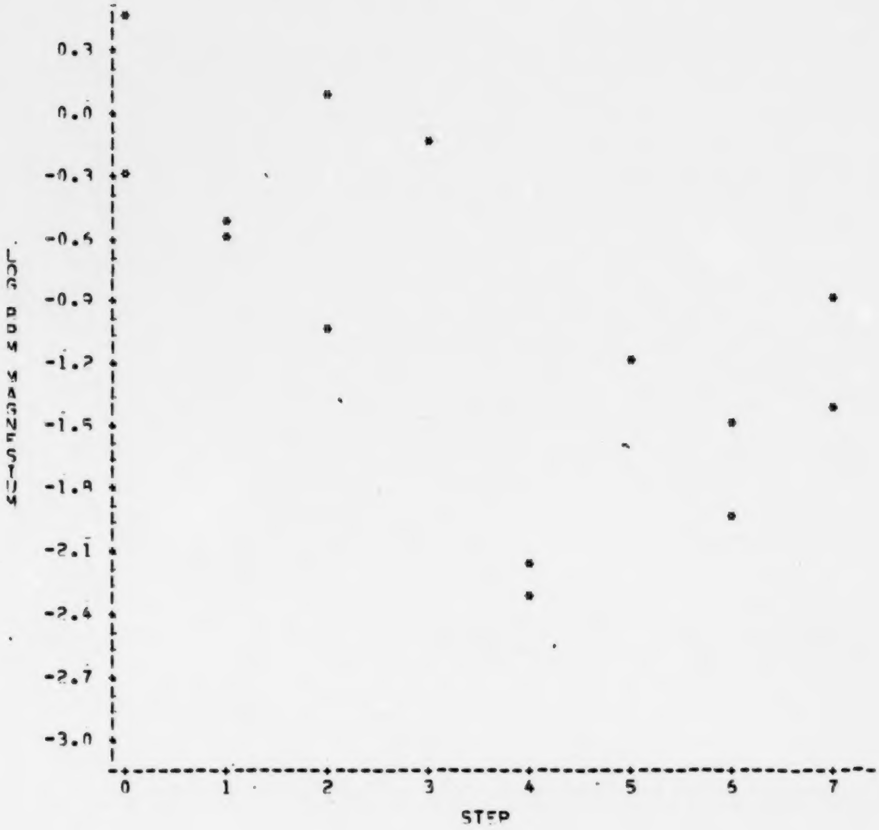

Figure G-38. **Natural Logarithm of Magnesium Concentration vs. Shake-Test Extraction STEP for Exxon PFBC Waste.**

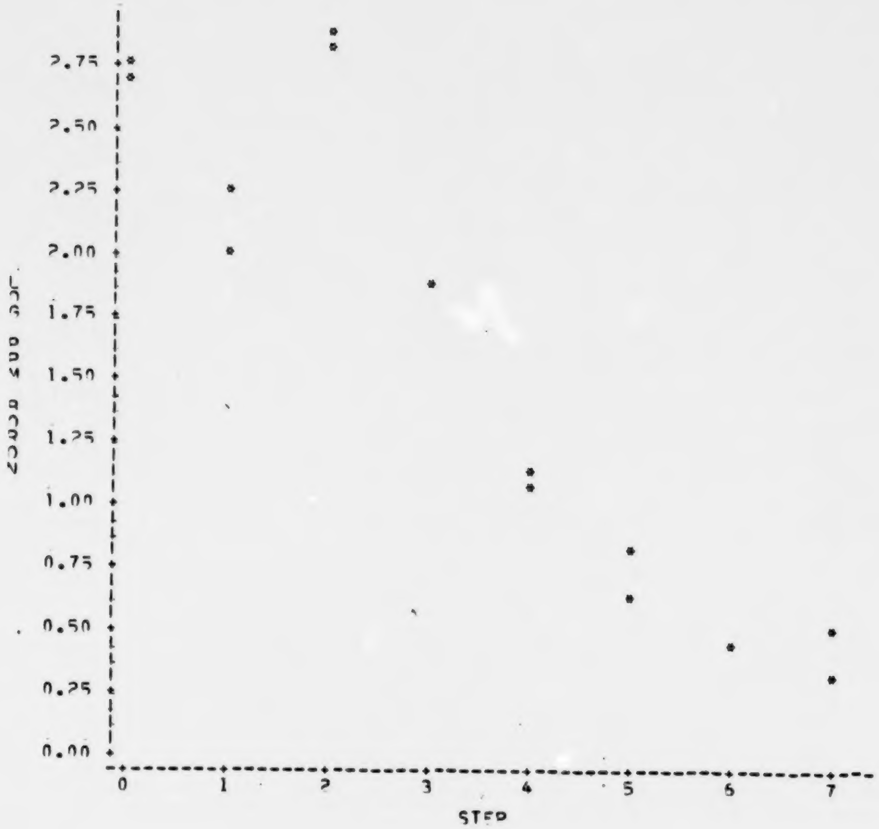

Figure G-39. Natural Logarithm of Boron Concentration vs. Shake-Test Extraction STEP for Exxon PFBC Waste.

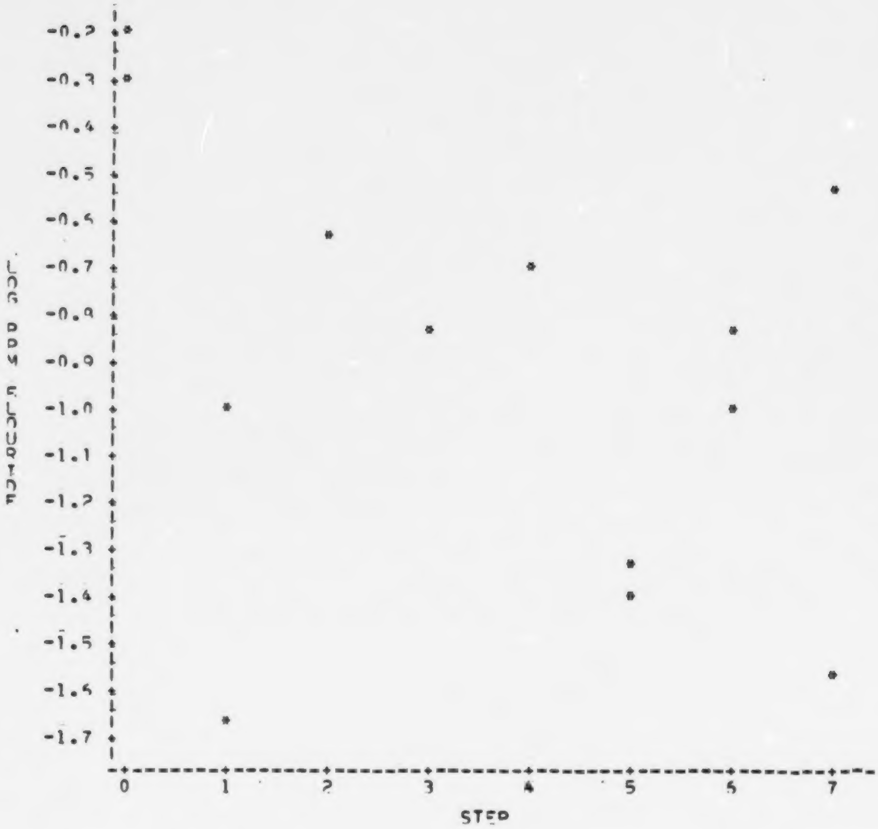

Figure G-40. Natural Logarithm of Fluoride Concentration vs. Shake-Test Extraction STEP for Exxon PFBC Waste.

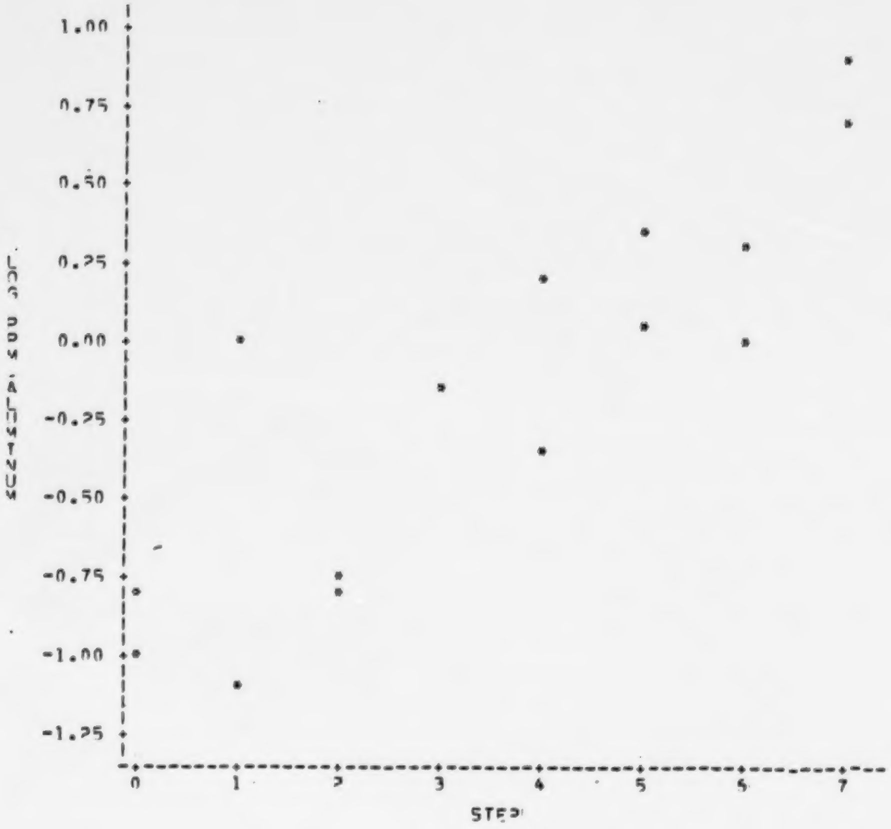

Figure G-41. **Natural Logarithm of Aluminum Concentration vs. Shake-Test Extraction STEP for Exxon PFBC Waste.**

Appendix G

Attachment 2

Table G-17

TABLE G-17. MODEL BUILDING RESULTS BASED ON SHAKE-TEST EXTRACTIONS OF PFBC WASTE: MAXIMUM R^2 MODELS WITH NO SPECIES LEADING VALUE (L) FORCED, BUT pH AND LEADING pH AVAILABLE

No. of Terms in Model	R^2	Variables in Model
REGRESSION MODELS FOR DEPENDENT VARIABLE SO_4		
1	0.895	LBA
1	0.989	LSO_4
1	0.995	PH
1	0.995	LPH
2	0.996	LPH LSR
2	0.997	LPH LCL
2	0.997	LPH LSI
2	0.998	PH LCL
3	0.999	PH LB LCL
3	0.999	PH LNA LCL
3	0.999	LPH LMG LCL
3	0.999	PH LMG LCL
REGRESSION MODELS FOR DEPENDENT VARIABLE CR		
1	0.398	LB
1	0.411	LCA
1	0.445	LBA
1	0.494	LSR
2	0.579	LAL LBA
2	0.651	PH LBA
2	0.656	LPH LBA
2	0.662	LSO_4 LBA
3	0.759	LCA LSO_4 LBA
3	0.760	LPH LNA LBA
3	0.765	LSO_4 LBA LZN
3	0.775	LNA LSO_4 LBA
4	0.863	LFE LNA LSO_4 LBA
4	0.872	PH LPH LNA LSR
4	0.918	PH LPH LSR LB
4	0.937	PH LPH LCA LSR
5	0.949	PH LPH LCA LBA LSR
5	0.951	PH LPH LCA LSR LCL
5	0.955	LCR PH LPH LCA LSR
5	0.955	PH LPH LCA LSR LF

(Continued)

Preceding page blank

TABLE G-17. (Continued)

No. of Terms in Model	R^2	Variables in Model
REGRESSION MODELS FOR DEPENDENT VARIABLE BA		
1	0.875	LPH
1	0.878	PH
1	0.919	LCA
1	0.923	LBA
2	0.963	LFE LF
2	0.969	LBA LCR
2	0.970	LPH LCR
2	0.970	PH LCR
3	0.988	PH LCA LCR
3	0.988	LBA PH LCR
3	0.988	LPH LCA LCR
3	0.989	LBA LPH LCR
REGRESSION MODELS FOR DEPENDENT VARIABLE NA		
1	0.716	LB
1	0.750	LFE
1	0.787	LNA
1	0.791	LSR
2	0.856	LBA LCR
2	0.863	LCA LCR
2	0.878	LNA LCR
2	0.931	LSR LCR
3	0.973	LBA LSR LCR
3	0.980	LPH LSR LCR
3	0.981	PH LSR LCR
3	0.983	LSO_4 LSR LCR

(Continued)

TABLE G-17. (Continued)

No. of Terms in Model	R^2	Variables in Model
REGRESSION MODELS FOR DEPENDENT VARIABLE FE		
1	0.719	LF
1	0.791	LCA
1	0.796	LSR
1	0.831	LBA
2	0.848	LCA LBA
2	0.851	LBA LZN
2	0.859	LNA LSR
2	0.866	LMG LBA
3	0.884	PH LAL LBA
3	0.892	LPH LAL LBA
3	0.893	LNA LSR LCL
3	0.895	LMG LBA LCL
4	0.920	PH LPH LMG LBA
4	0.934	PH LPH LMG LSR
4	0.938	PH LPH LSR LB
4	0.947	PH LPH LCA LSR
5	0.962	PH LPH LCA LSO_4 LSR
5	0.968	LFE LPH LNA LST LBA
5	0.970	LFE PH LNA LST LBA
5	0.973	LCA LNA LSI LSR LB
REGRESSION MODELS FOR DEPENDENT VARIABLE CA		
1	0.834	PH
1	0.865	LSR
1	0.888	LCA
1	0.895	LBA
2	0.944	PH LCR
2	0.944	LPH LCR
2	0.946	LFE LBA
2	0.953	LBA LCR
3	0.973	LST LSR LCR
3	0.976	PH LSR LCR
3	0.976	LPH LSR LCR
3	0.987	LCA LB LCR

(Continued)

TABLE G-17. (Continued)

No. of Terms in Model	R²	Variables in Model
REGRESSION MODELS FOR DEPENDENT VARIABLE ZN		
1	0.628	LBA
1	0.653	LCA
1	0.727	LNA
1	0.795	LSR
2	0.864	LCA LSR
2	0.876	LBA LF
2	0.877	LBA LSR
2	0.883	LSR LF
3	0.918	LBA LCL LF
3	0.920	LZN LNA LBA
3	0.920	LZN LCA LNA
3	0.926	LZN LNA LSR
4	0.937	PH LPH LSR LCL
4	0.938	PH LPH LSO_4 LSR
4	0.943	LZN LMG LNA LSR
4	0.944	PH LPH LSO_4 LBA
5	0.970	LAL LFE LSR LCR LF
5	0.972	LFE LSO_4 LBA LSR LCR
5	0.976	PH LFE LBA LSR LCR
5	0.978	LPH LFE LBA LSR LCR
REGRESSION MODELS FOR DEPENDENT VARIABLE SR		
1	0.832	LMG
1	0.837	LB
1	0.859	LBA
1	0.860	LCA
2	0.945	LSR LCL
2	0.957	LSR LCR
2	0.974	LCA LCR
2	0.983	LBA LCR
3	0.985	LAL LBA LCR
3	0.985	LSO_4 LBA LCR
3	0.986	LBA LCR LCL
3	0.989	LFE LBA LCR

(Continued)

TABLE G-17. (Continued)

No. of Terms in Model	R^2	Variables in Model
REGRESSION MODELS FOR DEPENDENT VARIABLE MG		
1	0.755	LB
1	0.765	LBA
1	0.796	LCA
1	0.893	LFE
2	0.919	LFE LBA
2	0.924	LCA LFE
2	0.926	LFE LB
2	0.926	LFE LF
3	0.932	LFE LSO_4 LB
3	0.933	LFE LSI LB
3	0.934	LFE LZN LB
3	0.942	LMG LFE LB
REGRESSION MODELS FOR DEPENDENT VARIABLE B		
1	0.715	LCA
1	0.753	LNA
1	0.792	LFE
1	0.816	LSR
2	0.842	LSR LF
2	0.849	LBA LF
2	0.872	LFE LSR
2	0.911	LSR LCR
3	0.945	LSR LCR LF
3	0.950	LBA LCR LF
3	0.953	LCA LSR LCR
3	0.968	LB LSR LCR

(Continued)

TABLE G-17. (Continued)

No. of Terms in Model	R^2	Variables in Model
REGRESSION MODELS FOR DEPENDENT VARIABLE F		
1	0.784	LBA
1	0.900	LSO_4
1	0.906	PH
1	0.910	LPH
2	0.925	PH LPH
2	0.934	LNA LSI
2	0.936	LF LPH
2	0.936	LF PH
3	0.952	LF PH LMG
3	0.953	LF LPH LMG
3	0.953	LF LPH LAL
3	0.953	LF PH LAL
REGRESSION MODELS FOR DEPENDENT VARIABLE CL		
1	0.460	LSR
1	0.464	LFE
1	0.471	LPH
1	0.471	PH
2	0.553	LSR LZN
2	0.560	PH LF
2	0.640	PH LSO_4
2	0.679	LPH LSO_4
3	0.810	LCL PH LSO_4
3	0.816	LCL LPH LSO_4
3	0.823	LPH LSO_4 LF
3	0.836	PH LSO_4 LF
4	0.879	LCL PH LSO_4 LB
4	0.884	LCL LPH LSO_4 LZN
4	0.886	LCL LPH LCA LSO_4
4	0.896	LCL PH LCA LSO_4
5	0.965	LCL PH LSO_4 LZN LCR
5	0.974	LCL LPH LNA LSO_4 LCR
5	0.977	LCA LFE LMG LNA LF
5	0.980	LCL PH LNA LSO_4 LCR

(Continued)

TABLE G-17. (Continued)

No. of Terms in Model	R-Square	Variables in Model
REGRESSION MODELS FOR DEPENDENT VARIABLE AL		
1	0.760	LPH
1	0.789	LSO_4
1	0.836	LAL
1	0.946	LSI
2	0.949	LAL LSI
2	0.951	LSI LF
2	0.952	LFE LSI
2	0.955	LSI LCR
3	0.971	LSI LBA LCR
3	0.972	LFE LSI LBA
3	0.974	LSI LCR LF
3	0.979	LMG LSI LF

NOTE: The prefix "L" indicates the value at the preceding laboratory leaching step. For example, suppose the dependent variable is SO_4, and the variables included in the model are LPH and LSR. In this model, then, the concentration of SO_4 at laboratory leaching extraction i is predicted as a linear function of the concentrations of pH and Sr in leaching extraction i-1.

Appendix G

Attachment 3

Table G-18

Preceding page blank

TABLE G-18. MODEL BUILDING RESULTS BASED ON SHAKE-TEST EXTRACTIONS OF PFBC WASTE: MAXIMUM R^2 MODELS WITH EACH SPECIES' LEADING VALUE (L) FORCED AND NO pH VALUES AVAILABLE

No. of Terms in Model	R^2	Variables in Model
REGRESSION MODELS FOR DEPENDENT VARIABLE SO_4		
1	0.989	LSO_4
Note: The above variables are included in all models to follow.		
2	0.993	LNA
2	0.994	LCA
2	0.994	LBA
2	0.995	LSR
3	0.995	LAL LSR
3	0.995	LBA LF
3	0.996	LMG LSR
3	0.996	LMG LCL
REGRESSION MODELS FOR DEPENDENT VARIABLE SI		
1	0.963	LSI
Note: The above variables are included in all models to follow.		
2	0.966	LZN
2	0.968	LMG
2	0.969	LFE
2	0.973	LCR
3	0.977	LCA LMG
3	0.977	LZN LB
3	0.978	LMG LF
3	0.983	LMG LB

(Continued)

Preceding page blank

TABLE G-18. (Continued)

No. of Terms in Model	R^2	Variables in Model
REGRESSION MODELS FOR DEPENDENT VARIABLE CR		
1	0.181	LCR
Note: The above variables are included in all models to follow.		
2	0.398	LB
2	0.412	LCA
2	0.446	LBA
2	0.494	LSR
3	0.577	LSO_4 LSR
3	0.578	LSI LBA
3	0.580	LAL LBA
3	0.667	LSO_4 LBA
4	0.762	LAL LNA LSR
4	0.766	LSO_4 LBA LZN
4	0.780	LNA LSO_4 LSR
4	0.782	LNA LSO_4 LBA
5	0.851	LAL LCA LFE LNA
5	0.853	LCA LNA LSR LB
5	0.899	LNA LSO_4 LSR LZN
5	0.928	LFE LNA LSO_4 LBA
REGRESSION MODELS FOR DEPENDENT VARIABLE BA		
1	0.923	LBA
Note: The above variables are included in all models to follow.		
2	0.944	LCL
2	0.946	LMG
2	0.963	LFE
2	0.969	LCR
3	0.978	LFE LCL
3	0.986	LSO_4 LCR
3	0.986	LAL LCR
3	0.986	LSI LCR

(Continued)

TABLE G-18. (Continued)

No. of Terms in Model	R^2	Variables in Model
REGRESSION MODELS FOR DEPENDENT VARIABLE NA		
1	0.787	LNA
Note: The above variables are included in all models to follow.		
2	0.824	LSR
2	0.826	LZN
2	0.832	LFE
2	0.878	LCR
3	0.904	LZN LCR
3	0.906	LZN LCL
3	0.909	LZN LF
3	0.931	LSR LCR
REGRESSION MODELS FOR DEPENDENT VARIABLE FE		
1	0.594	LFE
Note: The above variables are included in all models to follow.		
2	0.772	LF
2	0.792	LCA
2	0.797	LSR
2	0.832	LBA
3	0.854	LNA LBA
3	0.858	LBA LZN
3	0.872	LMG LBA
3	0.877	LNA LSR
4	0.902	LNA LSR LCL
4	0.903	LMG LBA LCL
4	0.904	LNA LSR LB
4	0.911	LNA LSO_4 LBA
5	0.933	LNA LSO_4 LBA LCR
5	0.939	LNA LSI LSO_4 LBA
5	0.942	LAL LNA LSR LZN
5	0.943	LNA LSO_4 LSR LZN

(Continued)

TABLE G-18. (Continued)

No. of Terms in Model	R^2	Variables in Model
REGRESSION MODELS FOR DEPENDENT VARIABLE CA		
1	0.888	LCA
Note: The above variables are included in all models to follow.		
2	0.899	LB
2	0.900	LCL
2	0.936	LFE
2	0.941	LCR
3	0.958	LAL LCR
3	0.959	LZN LCR
3	0.960	LSO_4 LCR
3	0.987	LB LCR
REGRESSION MODELS FOR DEPENDENT VARIABLE ZN		
1	0.581	LZN
Note: The above variables are included in all models to follow.		
2	0.643	LBA
2	0.654	LCA
2	0.808	LSR
2	0.808	LNA
3	0.892	LNA LF
3	0.920	LNA LBA
3	0.920	LCA LNA
3	0.926	LNA LSR
4	0.929	LFF LNA LSR
4	0.931	LMG LBA LSR
4	0.934	LNA LSR LCL
4	0.943	LMG LNA LSR
5	0.949	LMG LNA LSR LCR
5	0.950	LMG LNA LRA LSR
5	0.952	LFF LMG LNA LSR
5	0.954	LMG LNA LSR LB

(Continued)

TABLE G-18. (Continued)

No. of Terms in Model	R^2	Variables in Model
REGRESSION MODELS FOR DEPENDENT VARIABLE SR		
1	0.822	LSR
Note: The above variables are included in all models to follow.		
2	0.877	LFE
2	0.906	LMG
2	0.945	LCL
2	0.957	LCR
3	0.975	LCA LCR
3	0.982	LCR LCL
3	0.982	LCR LF
3	0.983	LBA LCR
REGRESSION MODELS FOR DEPENDENT VARIABLE MG		
1	0.643	LMG
Note: The above variables are included in all models to follow.		
2	0.771	LBA
2	0.776	LSR
2	0.796	LCA
2	0.900	LFE
3	0.919	LFE LBA
3	0.928	LCA LFE
3	0.929	LFE LF
3	0.942	LFE LB

(Continued)

TABLE G-18. (Continued)

No. of Terms in Model	R^2	Variables in Model
REGRESSION MODELS FOR DEPENDENT VARIABLES B		
1	0.629	LB
Note: The above variables are included in all models to follow.		
2	0.748	LCR
2	0.755	LNA
2	0.808	LFE
2	0.824	LSR
3	0.865	LSR LCL
3	0.875	LCA LCR
3	0.887	LFE LSR
3	0.968	LSR LCR
4	0.973	LAL LSR LCR
4	0.974	LNA LSR LCR
4	0.974	LBA LSR LCR
4	0.975	LFE LSR LCR
5	0.982	LCA LSI LBA LCR
5	0.983	LCA LNA LSI LCR
5	0.984	LCA LNA LSO$_4$ LCR
5	0.984	LFE LNA LSR LCR
REGRESSION MODELS FOR DEPENDENT VARIABLE F		
1	0.701	LF
Note: The above variables are included in all models to follow.		
2	0.797	LFE
2	0.807	LAL
2	0.823	LSI
2	0.916	LSO$_4$
3	0.940	LNA LSO$_4$
3	0.941	LSO$_4$ LCL
3	0.943	LCA LSI
3	0.950	LMG LSO$_4$

(Continued)

TABLE G-18. (Continued)

No. of Terms in Model	R^2	Variables in Model
REGRESSION MODELS FOR DEPENDENT VARIABLE CL		
1	0.141	LCL
Note: The above variables are included in all models to follow.		
2	0.450	LCA
2	0.452	LBA
2	0.461	LSR
2	0.467	LFE
3	0.533	LAL LSR
3	0.539	LNA LSR
3	0.560	LCA LZN
3	0.563	LSR LZN
4	0.672	LCA LFE LZN
4	0.675	LCA LZN LF
4	0.729	LCA LNA LF
4	0.762	LMG LSR LZN
5	0.831	LCA LNA LCR LF
5	0.843	LFE LMG LSR LZN
5	0.870	LCA LMG LNA LF
5	0.879	LCA LMG LZN LF
REGRESSION MODELS FOR DEPENDENT VARIABLE AL		
1	0.836	LAL
Note: The above variables are included in all models to follow.		
2	0.852	LFE
2	0.855	LF
2	0.855	LCR
2	0.949	LSI
3	0.953	LSI LBA
3	0.955	LSI LSO_4
3	0.956	LSI LF
3	0.956	LSI LCR

(Continued)

TABLE G-18. (Continued)

Dependent Variable	Variables Whose Leading Values Are In The Model													
	SO_4	Si	Cr	Ba	Na	Fe	Ca	Zn	Sr	Mg	B	F	Cl	Al
SO_4	X													
Si		X												
Cr	X		X	X	X	X								
Ba				X										
Na			X		X				X					
Fe	X			X	X	X								
Ca			X				X							
Zn					X			X	X					
Sr			X						X					
Mg						X				X	X			
B			X						X		X			
F	X											X		
Cl							X	X		X		X	X	
Al		X												X

Appendix G

Attachment 4

Table G-19

TABLE G-19. MODEL BUILDING RESULTS BASED ON SHAKE-TEST EXTRACTIONS OF PFBC WASTE: MAXIMUM R^2 MODELS WITH NO SPECIES' LEADING VALUE (L) FORCED INTO THE MODEL AND NO pH VALUES AVAILABLE

No. of Terms in Model	R^2	Variables in Model
REGRESSION MODELS FOR DEPENDENT VARIABLE SO_4		
1	0.863	LCA
1	0.867	LF
1	0.895	LBA
1	0.989	LSO_4
2	0.993	LSO_4 LNA
2	0.994	LSO_4 LCA
2	0.994	LSO_4 LBA
2	0.995	LSO_4 LSR
3	0.995	LSO_4 LAL LSR
3	0.995	LSO_4 LBA LF
3	0.996	LSO_4 LMG LSR
3	0.996	LSO_4 LMG LCL
REGRESSION MODELS FOR DEPENDENT VARIABLE SI		
1	0.556	LF
1	0.763	LSO_4
1	0.878	LAL
1	0.963	LSI
2	0.966	LSI LZN
2	0.968	LSI LMG
2	0.969	LSI LFE
2	0.973	LSI LCR
3	0.977	LSI LCA LMG
3	0.977	LSI LZN LB
3	0.978	LSI LMG LF
3	0.983	LSI LMG LB

(Continued)

Preceding page blank

TABLE G-19. (Continued)

No. of Terms in Model	R^2	Variables in Model
REGRESSION MODELS FOR DEPENDENT VARIABLE CR		
1	0.398	LB
1	0.411	LCA
1	0.445	LBA
1	0.494	LSR
2	0.574	LSI LBA
2	0.577	LSO_4 LSR
2	0.579	LAL LBA
2	0.662	LSO_4 LBA
3	0.752	LSO_4 LBA LB
3	0.759	LCA LSO_4 LBA
3	0.765	LSO_4 LBA LZN
3	0.775	LNA LSO_4 LBA
4	0.830	LAL LNA LSO_4 LBA
4	0.838	LAL LCA LSO_4 LBA
4	0.842	LCA LNA LSR LB
4	0.863	LFE LNA LSO_4 LBA
5	0.921	LAL LFE LNA LSR LZN
5	0.928	LCR LFE LNA LSO_4 LBA
5	0.936	LCA LNA LSI LSR LB
5	0.942	LFE LNA LSO_4 LSR LZN
REGRESSION MODELS FOR DEPENDENT VARIABLE BA		
1	0.838	LSO4
1	0.850	LSR
1	0.919	LCA
1	0.923	LBA
2	0.960	LCA LCR
2	0.963	LBA LFE
2	0.963	LFE LF
2	0.969	LBA LCR
3	0.986	LBA LSO_4 LCR
3	0.986	LCA LSO_4 LCR
3	0.986	LBA LAL LCR
3	0.986	LBA LSI LCR

(Continued)

TABLE G-19. (Continued)

No. of Terms in Model	R^2	Variables in Model
REGRESSION MODELS FOR DEPENDENT VARIABLE NA		
1	0.716	LB
1	0.750	LFE
1	0.787	LNA
1	0.791	LSR
2	0.856	LBA LCR
2	0.863	LCA LCR
2	0.878	LNA LCR
2	0.931	LSR LCR
3	0.970	LSR LCR LF
3	0.972	LCA LSR LCR
3	0.973	LBA LSR LCR
3	0.983	LSO_4 LSR LCR
REGRESSION MODELS FOR DEPENDENT VARIABLE FE		
1	0.719	LF
1	0.791	LCA
1	0.796	LSR
1	0.831	LBA
2	0.849	LCA LBA
2	0.851	LBA LZN
2	0.860	LNA LSR
2	0.866	LMG LBA
3	0.884	LNA LSR LB
3	0.884	LNA LSR LCR
3	0.893	LNA LSR LCL
3	0.895	LMG LBA LCL
4	0.906	LMG LSO_4 LBA LCL
4	0.911	LAL LMG LSO_4 LBA
4	0.911	LFE LNA LSO_4 LBA
4	0.913	LMG LSI LSO_4 LBA
5	0.939	LFE LNA LSI LSO_4 LBA
5	0.942	LFE LAL LNA LSR LZN
5	0.943	LFE LNA LSO_4 LSR LZN
5	0.973	LCA LNA LSI LSR LB

(Continued)

TABLE G-19. (Continued)

No. of Terms in Model	R^2	Variables in Model
REGRESSION MODELS FOR DEPENDENT VARIABLE CA		
1	0.832	LFE
1	0.865	LSR
1	0.888	LCA
1	0.895	LBA
2	0.936	LCA LFE
2	0.941	LCA LCR
2	0.946	LFE LBA
2	0.953	LBA LCR
3	0.971	LBA LB LCR
3	0.973	LSO_4 LSR LCR
3	0.973	LSI LSR LCR
3	0.987	LCA LB LCR
REGRESSION MODELS FOR DEPENDENT VARIABLE ZN		
1	0.628	LBA
1	0.653	LCA
1	0.727	LNA
1	0.795	LSR
2	0.864	LCA LSR
2	0.876	LBA LF
2	0.877	LBA LSR
2	0.883	LSR LF
3	0.918	LBA LCL LF
3	0.920	LZN LNA LBA
3	0.920	LZN LCA LNA
3	0.926	LZN LNA LSR
4	0.930	LSR LB LCLLF
4	0.931	LZN LMG LBA LSR
4	0.934	LZN LNA LSR LCL
4	0.943	LZN LMG LNA LSR
5	0.966	LLCA LSI LBARLCL LF
5	0.968	LAL LFE LBA LSR LCR
5	0.970	LAL LFE LSR LCR LF
5	0.972	LFE LSO_4 LBA LSR LCR

(Continued)

TABLE G-19. (Continued)

No. of Terms in Model	R^2	Variables in Model
REGRESSION MODELS FOR DEPENDENT VARIABLE SR		
1	0.832	LMG
1	0.837	LB
1	0.859	LBA
1	0.860	LCA
2	0.945	LSR LCL
2	0.957	LSR LCR
2	0.974	LCA LCR
2	0.983	LBA LCR
3	0.985	LAL LBA LCR
3	0.985	LSO_4 LBA LCR
3	0.986	LBA LCR LCL
3	0.989	LFE LBA LCR
REGRESSION MODELS FOR DEPENDENT VARIABLE MG		
1	0.755	LB
1	0.765	LBA
1	0.796	LCA
1	0.893	LFE
2	0.919	LFE LBA
2	0.924	LCA LFE
2	0.926	LFE LB
2	0.926	LFE LF
3	0.932	LFE LSO_4 LB
3	0.933	LFE LSI LB
3	0.934	LFE LZN LB
3	0.942	LMG LFE LB

(Continued)

TABLE G-19. (Continued)

No. of Terms in Model	R^2	Variables in Model
REGRESSION MODELS FOR DEPENDENT VARIABLE B		
1	0.715	LCA
1	0.753	LNA
1	0.792	LFE
1	0.816	LSR
2	0.842	LSR LF
2	0.849	LBA LF
2	0.872	LFE LSR
2	0.911	LSR LCR
3	0.945	LSR LCR LF
3	0.950	LBA LCR LF
3	0.953	LCA LSR LCR
3	0.968	LB LSR LCR
4	0.973	LB LAL LSR LCR
4	0.974	LB LNA LSR LCR
4	0.974	LB LBA LSR LCR
4	0.975	LB LFE LSR LCR
5	0.983	LB LCA LNA LSI LCR
5	0.983	LAL LFE LSR LCR LF
5	0.984	LB LCA LNA LSO$_4$ LCR
5	0.984	LB LFE LNA LSR LCR
REGRESSION MODELS FOR DEPENDENT VARIABLE F		
1	0.748	LSI
1	0.776	LCA
1	0.784	LBA
1	0.900	LSO$_4$
2	0.914	LCA LSI
2	0.916	LF LSO$_4$
2	0.923	LSI LSR
2	0.934	LNA LSI
3	0.940	LF LNA LSO$_4$
3	0.941	LF LSO$_4$ LCL
3	0.943	LF LCA LSI
3	0.950	LF LMG LSO$_4$

(Continued)

TABLE G-19. (Continued)

No. of Terms in Model	R^2	Variables in Model
REGRESSION MODELS FOR DEPENDENT VARIABLE CL		
1	0.436	LCA
1	0.441	LBA
1	0.460	LSR
1	0.464	LFE
2	0.533	LCA LB
2	0.538	LNA LSR
2	0.550	LCA LZN
2	0.553	LSR LZN
3	0.658	LCA LFE LZN
3	0.667	LCA LZN LF
3	0.683	LMG LSR LZN
3	0.695	LCA LNA LF
4	0.826	LMG LNA LBA LF
4	0.827	LCA LNA LCR LF
4	0.829	LCA LMG LZN LF
4	0.870	LCA LMG LNA LF
REGRESSION MODELS FOR DEPENDENT VARIABLE AL		
1	0.619	LF
1	0.789	LSO$_4$
1	0.836	LAL
1	0.946	LSI
2	0.949	LAL LSI
2	0.951	LSI LF
2	0.952	LFE LSI
2	0.955	LSI LCR
3	0.971	LSI LBA LCR
3	0.972	LFE LSI LBA
3	0.974	LSI LCR LF
3	0.979	LMG LSI LF

(Continued)

TABLE G-19. (Continued)

Dependent	Variables Whose Leading Values Are In The Model													
Variable	SO_4	Si	Cr	Ba	Na	Fe	Ca	Zn	Sr	Mg	B	F	Cl	Al
SO_4	X													
Si		X												
Cr	X				X	X		X	X					
Ba			X	X										
Na			X						X					
Fe	X			X	X	X								
Ca			X				X							
Zn					X			X	X					
Sr			X	X										
Mg						X	X							
B			X						X					
F	X													
Cl					X	X	X			X		X		
Al		X												

Appendix G

Attachment 5

Table G-22

TABLE G-22. MODEL BUILDING RESULTS BASED ON SHAKE-TEST EXTRACTIONS OF EXXON PFBC WASTE: SUMMARY OF ESTIMATED INITIAL SOLUBLE FRACTIONS y_o OBTAINED BY BACK-CALCULATION FROM SHAKE-TEST RESULTS

Variable	No.	Minimum Value	Maximum Value	Mean	Standard Deviation	Std. Error of Mean
SO_4	15	1.109	1.416	1.291	0.1001	0.0260
Si	15	0.000250	0.000646	0.00042	0.000114	0.0000295
Cr	15	−0.000183	0.000174	0.0000158	0.000121	0.0000312
Ba	15	0.000118	0.000192	0.000156	0.0000218	0.00000563
Na	15	−0.0683	0.0763	−0.00678	0.0387	0.00996
Fe	15	−0.00109	0.000352	−0.000305	0.000436	0.000113
Ca	15	1.0814	2.128	1.571	0.268	0.0693
Zn	15	−0.000250	0.000447	0.0000182	0.000169	0.0000436
Sr	15	0.00115	0.00259	0.00167	0.000466	0.000120
VOL = 10						
SO_4	2	1.223	1.252	1.237	0.0214	0.0151
Si	2	0.000498	0.000646	0.000572	0.000105	0.0000742
Cr	2	−0.000183	0.000171	−0.00000621	0.000250	0.000177
Ba	2	0.000159	0.000182	0.000170	0.0000162	0.0000114
Na	2	−0.0196	0.0763	0.0283	0.0678	0.0479
Fe	2	−0.000344	0.000242	−0.0000510	0.000414	0.000293
Ca	2	1.569	2.128	1.844	0.395	0.279
Zn	2	−0.000122	0.000447	0.000163	0.000403	0.000285
Sr	2	0.00171	0.00259	0.00215	0.000619	0.000437
VOL = 20						
SO_4	2	1.239	1.321	1.280	0.0577	0.0408
Si	2	0.000465	0.000586	0.000525	0.0000852	0.0000602
Cr	2	−0.00000280	0.000150	0.0000738	0.000108	0.0000766
Ba	2	0.000118	0.000166	0.000142	0.0000344	0.0000244
Na	2	−0.0238	0.0184	−0.00269	0.0299	0.0211
Fe	2	−0.000245	−0.0000734	−0.000159	0.000121	0.0000859
Ca	2	1.0814	1.797	1.439	0.506	0.358
Zn	2	−0.0000343	0.000114	0.0000398	0.000105	0.0000740
Sr	2	0.00118	0.00234	0.00176	0.000821	0.000581

(Continued)

Note: Values are in mg/g

Preceding page blank

TABLE G-22. (Continued)

Variable	No.	Minimum Value	Maximum Value	Mean	Standard Deviation	Std. Error of Mean
VOL = 30						
SO_4	2	1.318	1.339	1.329	0.0146	0.0103
Si	2	0.000407	0.000492	0.000450	0.0000600	0.0000424
Cr	2	−0.0000352	0.000174	0.0000693	0.000148	0.000104
Ba	2	0.000130	0.000156	0.000143	0.0000179	0.0000127
Na	2	0.0192	0.0213	0.0203	0.00149	0.00105
Fe	2	−0.000155	0.000222	0.0000334	0.000266	0.000188
Ca	2	1.345	1.812	1.579	0.330	0.233
Zn	2	0.00000685	0.000240	0.000123	0.000165	0.000116
Sr	2	0.00166	0.00240	0.00203	0.000526	0.000372
VOL = 40						
SO_4	1	1.378	1.378	1.378	—	—
Si	1	0.000498	0.000498	0.000498	—	—
Cr	1	0.000140	0.000140	0.000140	—	—
Ba	1	0.000132	0.000132	0.000132	—	—
Na	1	0.0363	0.0363	0.0363	—	—
Fe	1	0.000352	0.000352	0.000352	—	—
Ca	1	1.286	1.286	1.286	—	—
Zn	1	0.000126	0.000126	0.000126	—	—
Sr	1	0.00155	0.00155	0.00155	—	—
VOL = 50						
SO_4	2	1.109	1.416	1.262	0.217	0.153
Si	2	0.000250	0.000433	0.000342	0.000129	0.0000916
Cr	2	0.00000217	0.000136	0.0000692	0.0000949	0.0000671
Ba	2	0.000128	0.000163	0.000146	0.0000250	0.0000177
Na	2	−0.0225	0.0163	−0.00307	0.0274	0.0194
Fe	2	−0.000572	−0.0000363	−0.000304	0.000379	0.000268
Ca	2	1.288	1.554	1.421	0.188	0.133
Zn	2	−0.0000466	0.0000825	0.0000179	0.0000912	0.0000645
Sr	2	0.00136	0.00179	0.00158	0.000302	0.000214

(Continued)

Note: Values are in mg/g.

TABLE G-22. (Continued)

Variable	No.	Minimum Value	Maximum Value	Mean	Standard Deviation	Std. Error of Mean
VOL = 60						
SO_4	2	1.157	1.405	1.281	0.175	0.124
Si	2	0.000271	0.000399	0.000335	0.0000903	0.0000638
Cr	2	−0.0000800	−0.00000090	−0.0000404	0.0000559	0.0000395
Ba	2	0.000159	0.000160	0.000159	0.00000120	0.00000085
Na	2	−0.0376	−0.00786	−0.0227	0.0210	0.0149
Fe	2	−0.000848	−0.000168	−0.000508	0.000481	0.000340
Ca	2	1.452	1.677	1.565	0.159	0.112
Zn	2	−0.0000757	−0.00000792	−0.0000418	0.0000479	0.0000339
Sr	2	0.00129	0.00198	0.00164	0.000485	0.000343
VOL = 70						
SO_4	2	1.198	1.413	1.305	0.152	0.108
Si	2	0.000289	0.000386	0.000338	0.0000687	0.0000486
Cr	2	−0.0000776	0.0000935	0.00000797	0.000121	0.0000856
Ba	2	0.000142	0.000179	0.000161	0.0000259	0.0000184
Na	2	−0.0683	−0.0196	−0.0440	0.0344	0.0244
Fe	2	−0.000988	−0.000407	−0.000698	0.000411	0.000290
Ca	2	1.400	1.632	1.516	0.163	0.116
Zn	2	−0.000250	−0.0000221	−0.000136	0.000161	0.000114
Sr	2	0.00115	0.00137	0.00126	0.000158	0.000112
VOL = 80						
SO_4	2	1.203	1.394	1.298	0.136	0.0959
Si	2	0.000306	0.000381	0.000344	0.0000535	0.0000378
Cr	2	−0.000129	−0.000122	−0.000125	0.00000508	0.00000359
Ba	2	0.000173	0.000192	0.000182	0.0000136	0.00000963
Na	2	−0.0664	−0.0237	−0.0451	0.0302	0.0213
Fe	2	−0.00109	−0.000473	−0.000780	0.000434	0.000307
Ca	2	1.763	1.776	1.770	0.00932	0.00659
Zn	2	−0.000152	−0.0000321	−0.0000922	0.0000851	0.0000602
Sr	2	0.00121	0.00150	0.00136	0.000200	0.000141

Note: Values are in mg/g.

Appendix G

Attachment 6

Figures G-42 to G-50

Preceding page blank

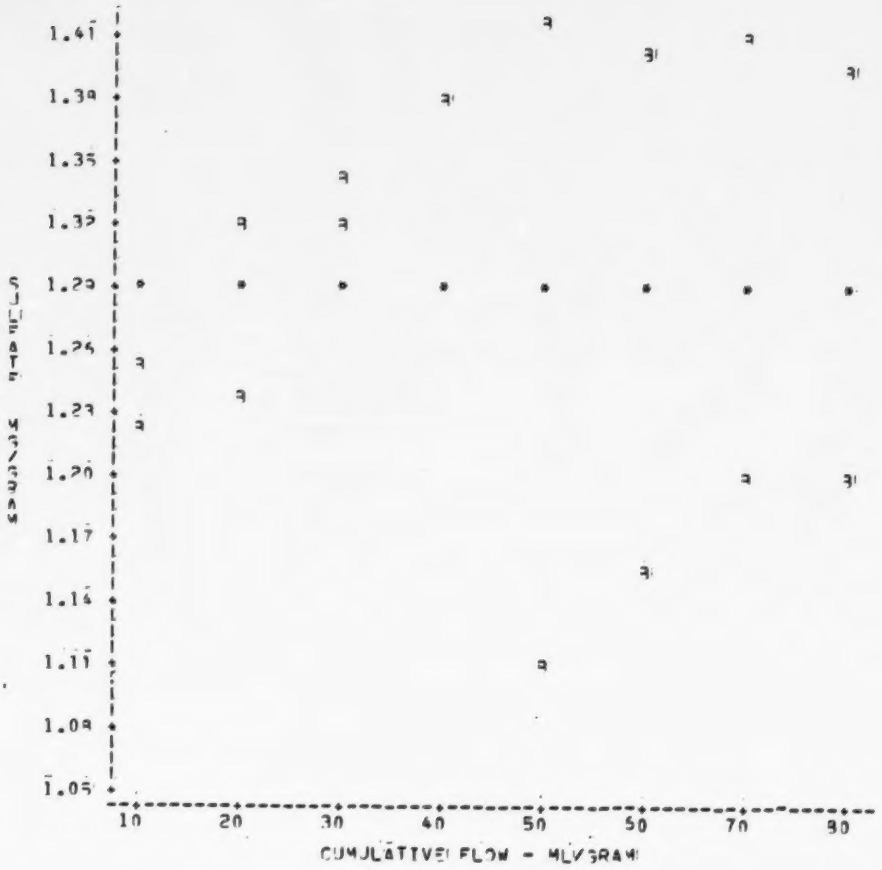

NOTE: Estimated initial soluble fraction ($\underline{y}_o$, shown by symbol B) was obtained by back-calculation from shake-test results. Mean values (*) are plotted.

Figure G-42. Model Building Results Based on Shake-Test Extractions of PFBC Waste: Initial Soluble Sulfate Fraction.

Preceding page blank

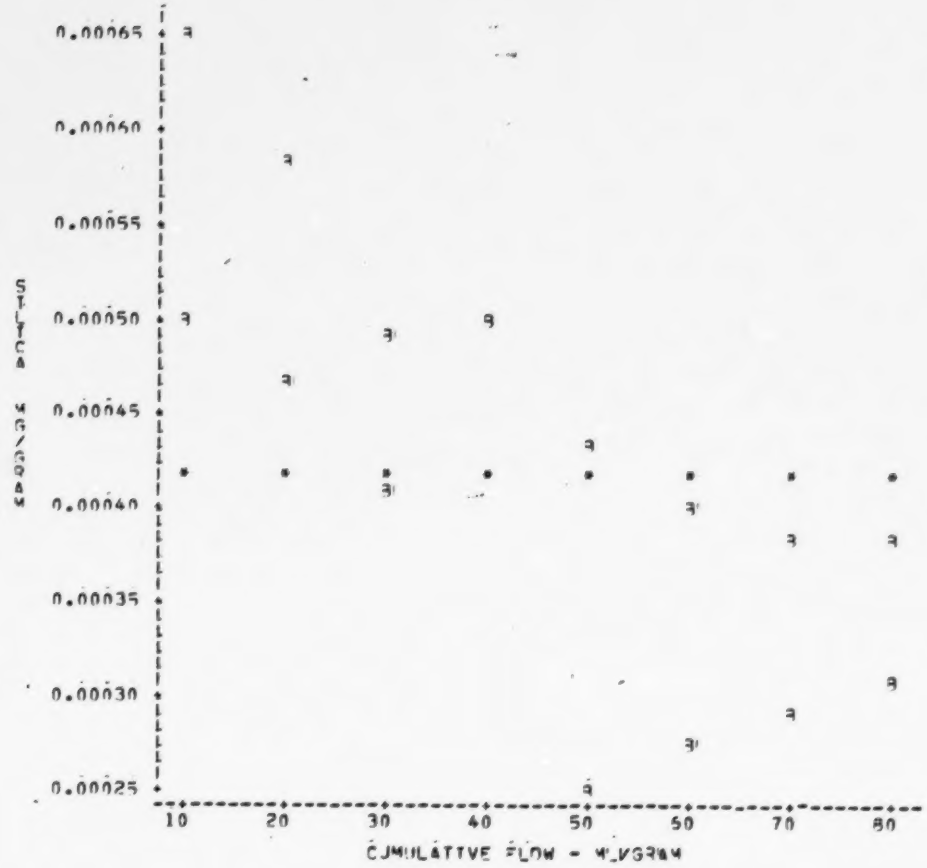

NOTE: Estimated initial soluble fraction (y_0, shown by symbol B) was obtained by back-calculation from shake-test results. Mean values (*) are plotted.

Figure G-43. Model Building Results Based on Shake-Test Extractions of PFBC Waste: Initial Soluble Silicon Fraction.

]

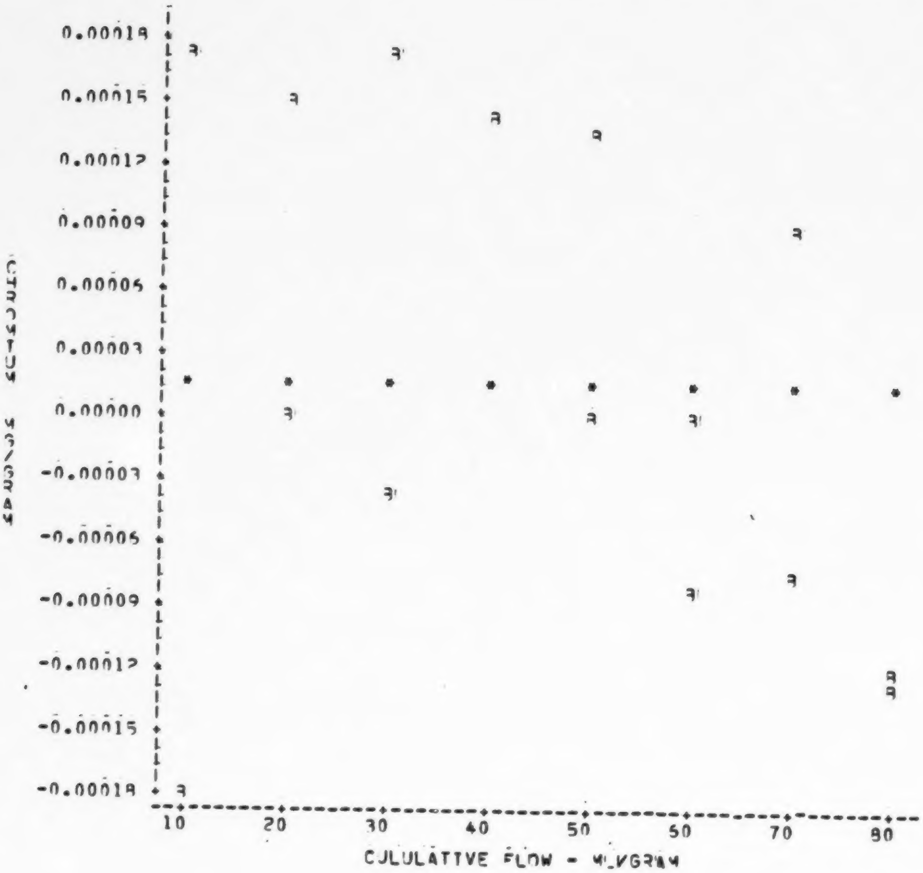

NOTE: Estimated initial soluble fraction (y_o, shown by symbol B) was obtained by back-calculation from shake-test results. Mean values (*) are plotted.

Figure G-44. Model Building Results Based on Shake-Test Extractions of PFBC Waste: Initial Soluble Chromium Fraction.

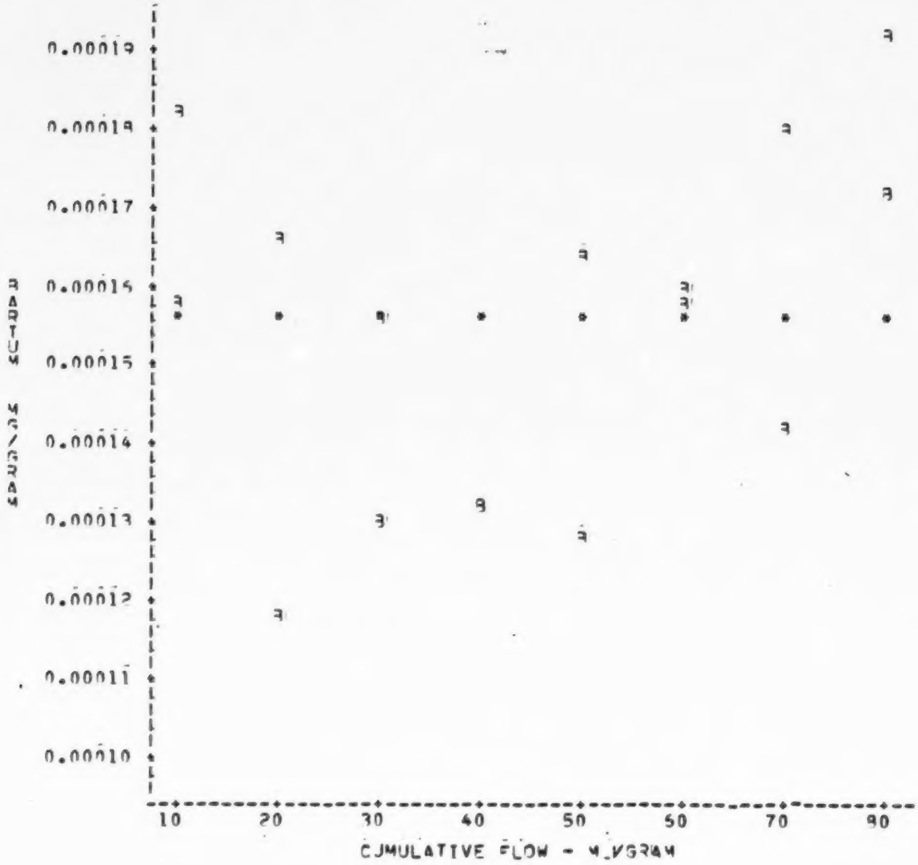

NOTE: Estimated initial soluble fraction ($\underline{y}_o$, shown by symbol B) was obtained by back-calculation from shake-test results. Mean values (*) are plotted.

Figure G-45. Model Building Results Based on Shake-Test Extractions of PFBC Waste: Initial Soluble Barium Fraction.

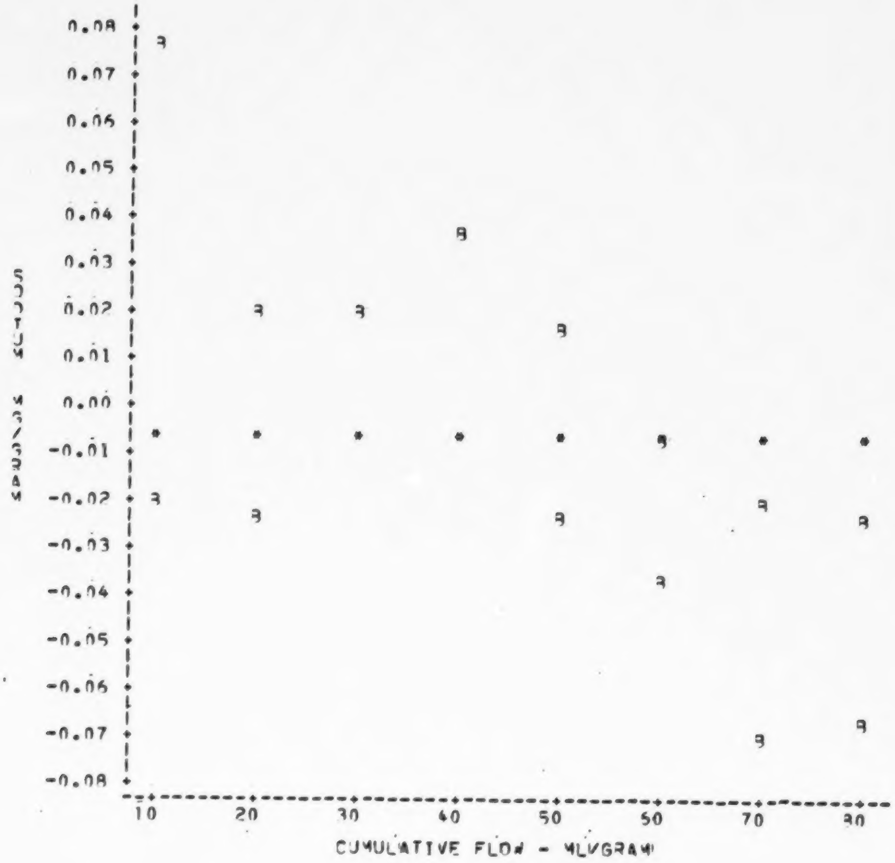

NOTE: Estimated initial soluble fraction ($\underline{y}_0$, shown by symbol B) was obtained by back-calculation from shake-test results. Mean values (*) are plotted.

Figure G-46. Model Building Results Based on Shake-Test Extractions of PFBC Waste: Initial Soluble Sodium Fraction.

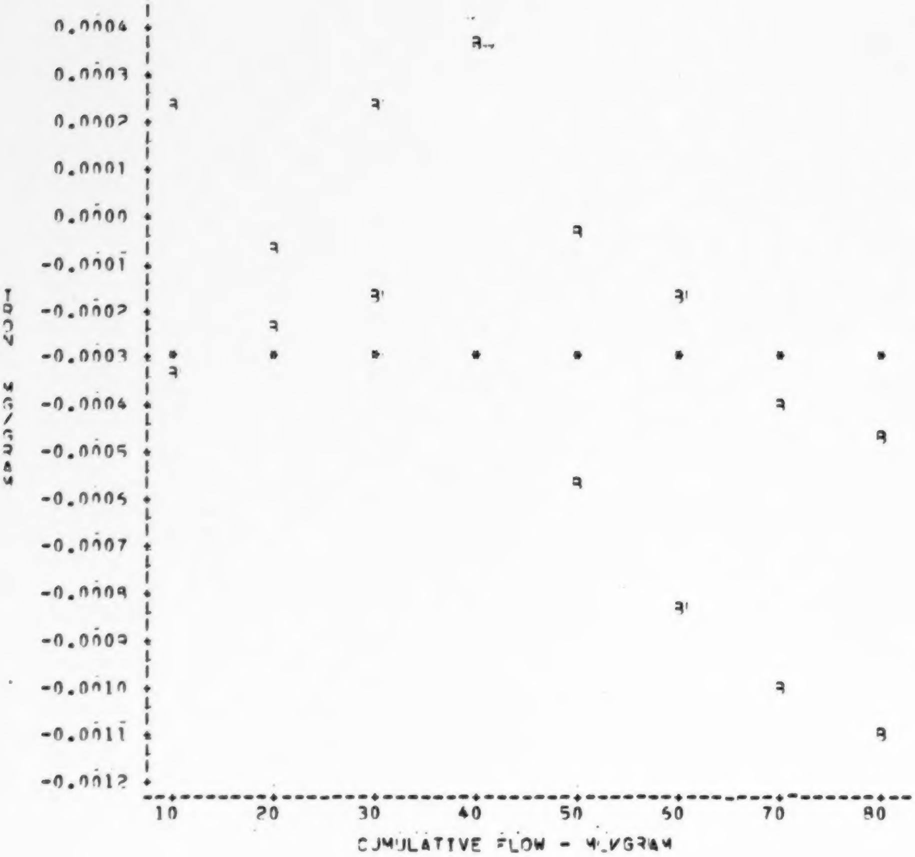

NOTE: Estimated initial soluble fraction ($\underline{y}_o$, shown by symbol B) was obtained by back-calculation from shake-test results. Mean values (*) are plotted.

Figure G-47. Model Building Results Based on Shake-Test Extractions of PFBC Waste: Initial Soluble Iron Fraction.

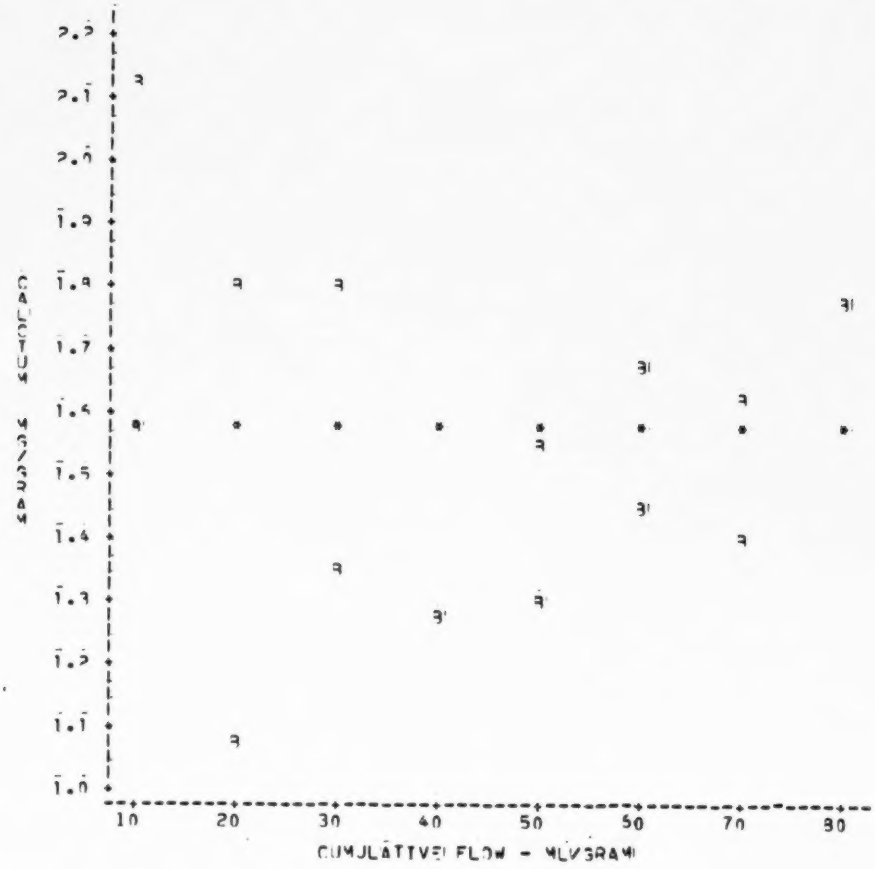

NOTE: Estimated initial soluble fraction ($\underline{y}_0$, shown by symbol B) was obtained by back-calculation from shake-test results. Mean values (*) are plotted.

Figure G-48. Model Building Results Based on Shake-Test Extractions of PFBC Waste: Initial Soluble Calcium Fraction.

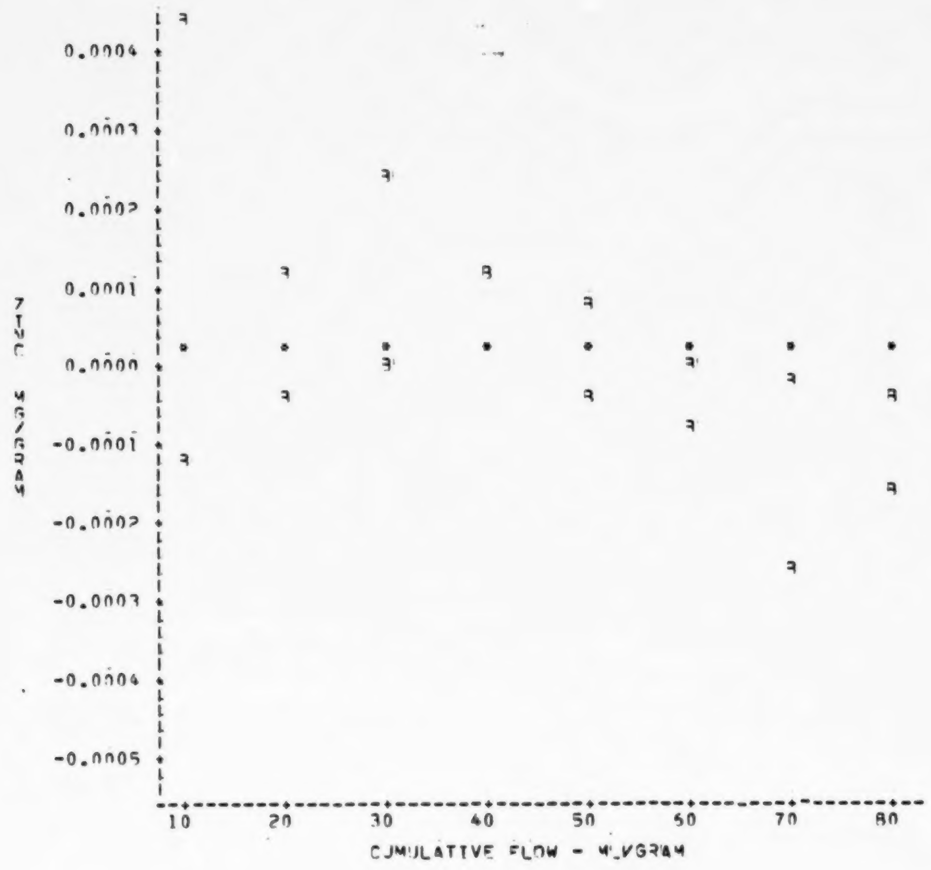

NOTE: Estimated initial soluble fraction ($\underline{y}_o$, shown by symbol B) was obtained by back-calculation from shake-test results. Mean values (*) are plotted.

Figure G-49. Model Building Results Based on Shake-Test Extractions of PFBC Waste: Initial Soluble Zinc Fraction.

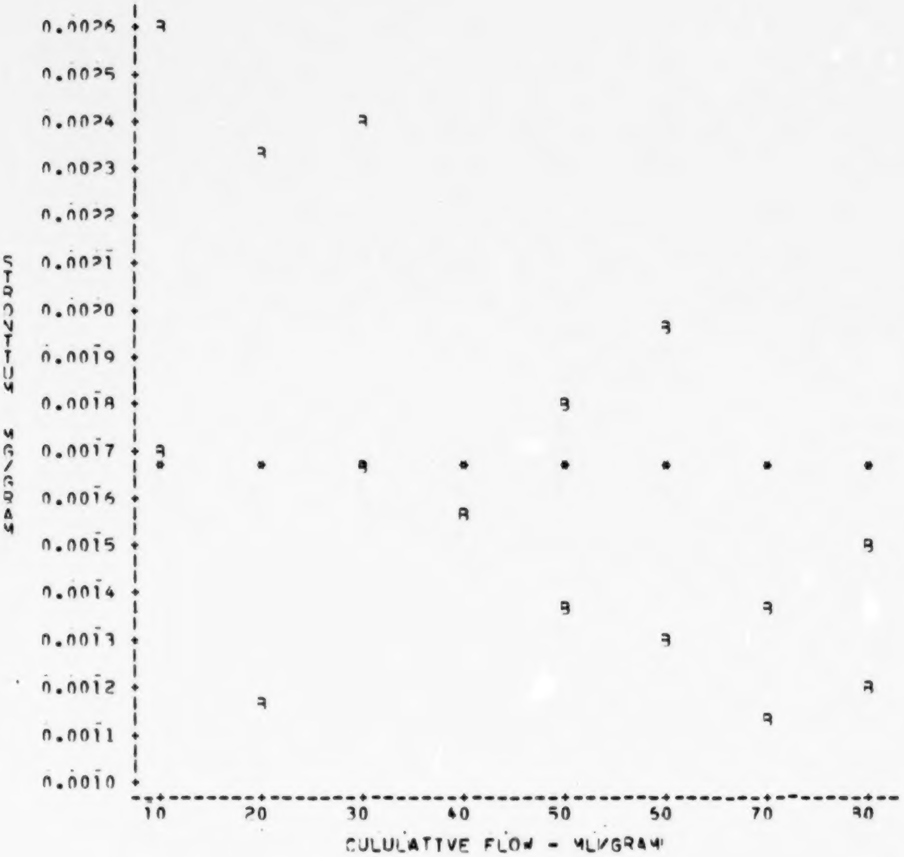

NOTE: Estimated initial soluble fraction ($\underline{y}_o$, shown by symbol B) was obtained by back-calculation from shake-test results. Mean values (*) are plotted.

Figure G-50. Model Building Results Based on Shake-Test Extractions of PFBC Waste: Initial Soluble Strontium Fraction.

Appendix G

Attachment 7

Figures G-51 to G-62

Preceding page blank

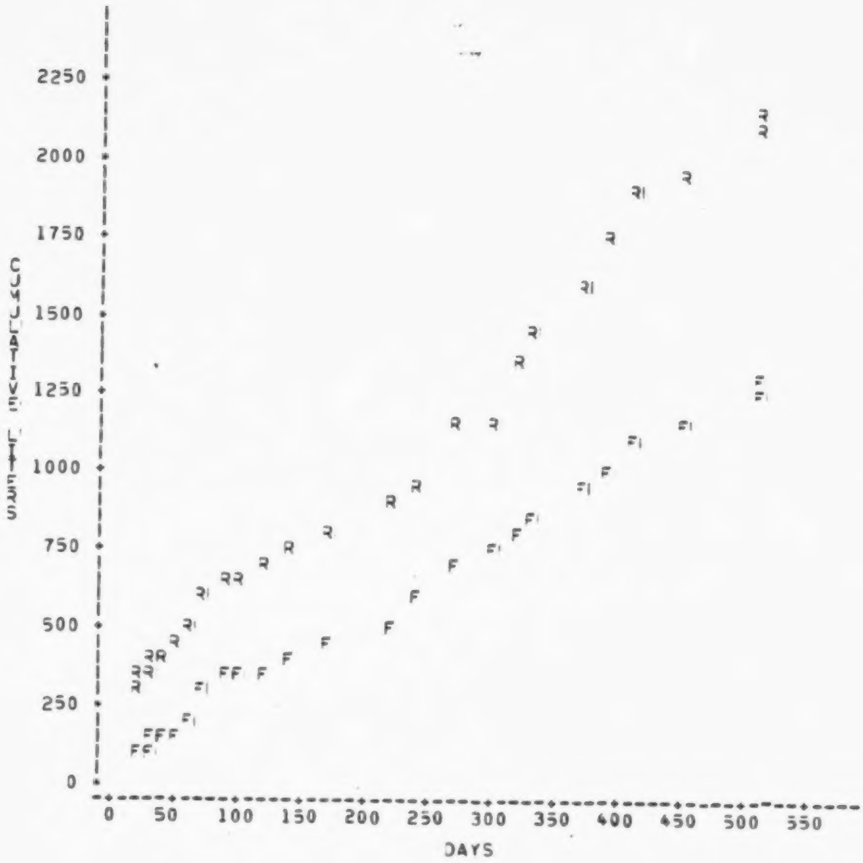

Figure G-51. Leading Cumulative Rainfall (R) and Lower Level Field Cell Flow (F): Field Cell 1.

Preceding page blank

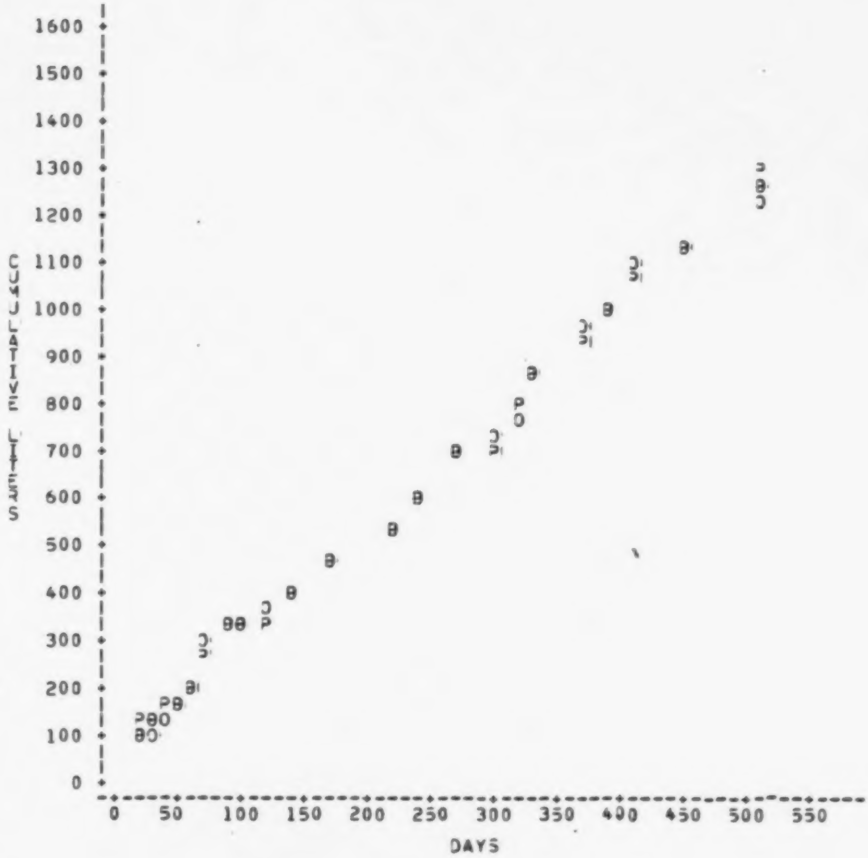

Figure G-52. Observed Flow (O) and Flow Predicted from a Rainfall-Flow Delay Model (P), with Rainfall Leading Flow by 12 Days: Field Cell 1.

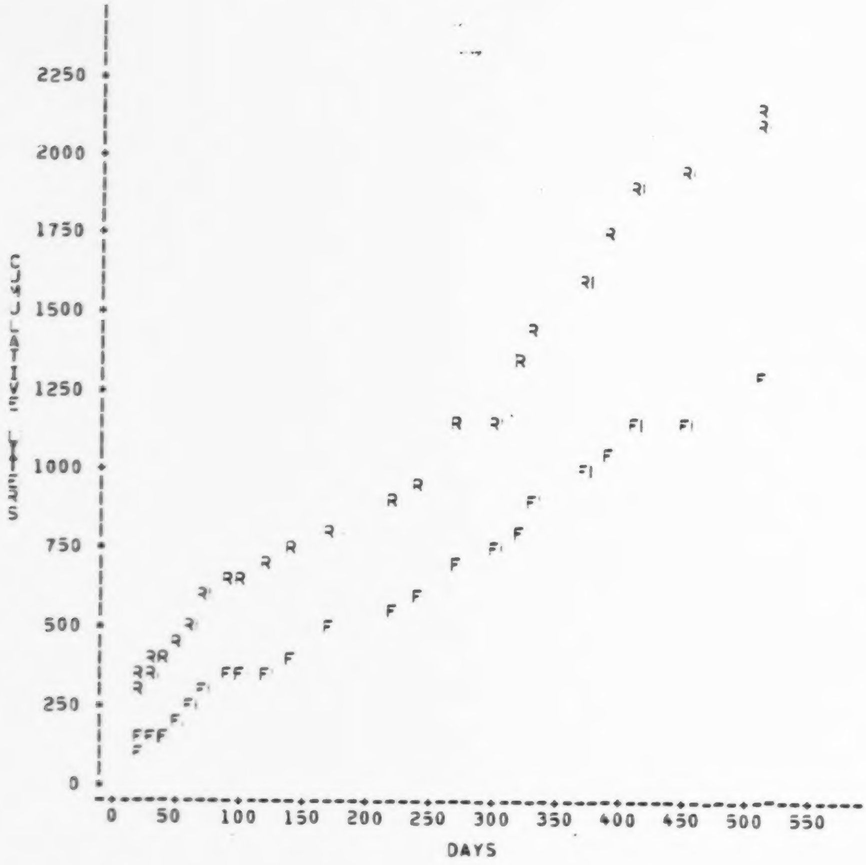

Figure G-53. Leading Cumulative Rainfall (R) and Lower Level Field Cell Flow (F): Field Cell 2

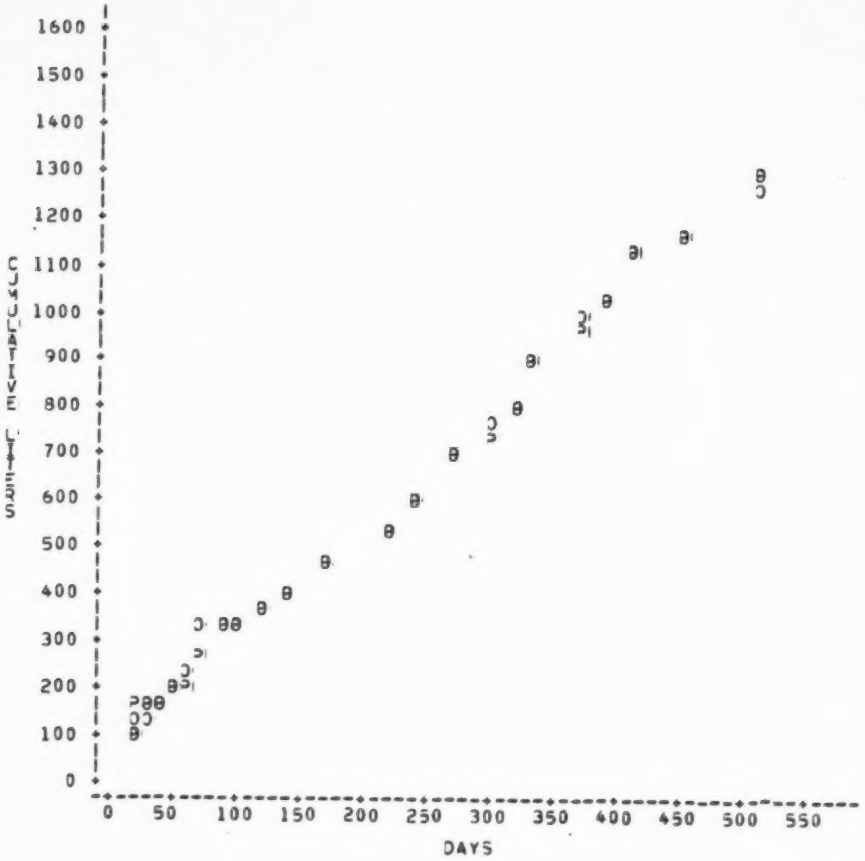

Figure G-54. Observed Flow (O) and Flow Predicted from a Rainfall-Flow Delay Model (P), with Rainfall Leading Flow by 12 Days: Field Cell 2.

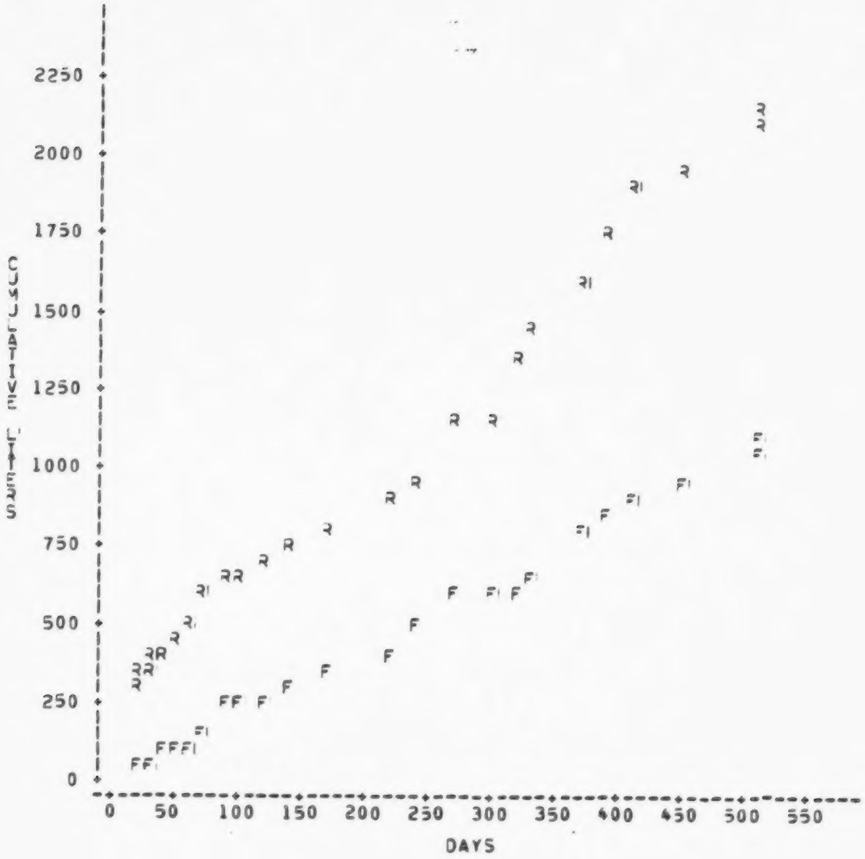

Figure G-55. Leading Cumulative Rainfall (R) and Lower Level Field Cell Flow (F): Field Cell 3.

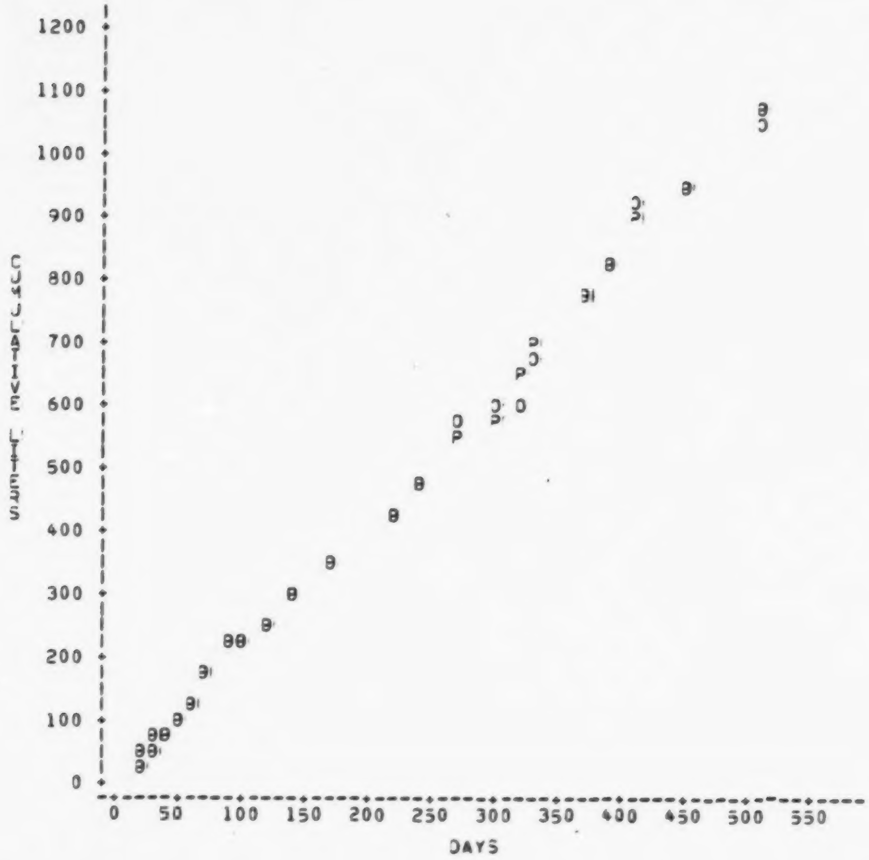

Figure G-56. Observed Flow (O) and Flow Predicted from a Rainfall-Flow Delay Model (P), with Rainfall Leading Flow by 12 Days: Field Cell 3.

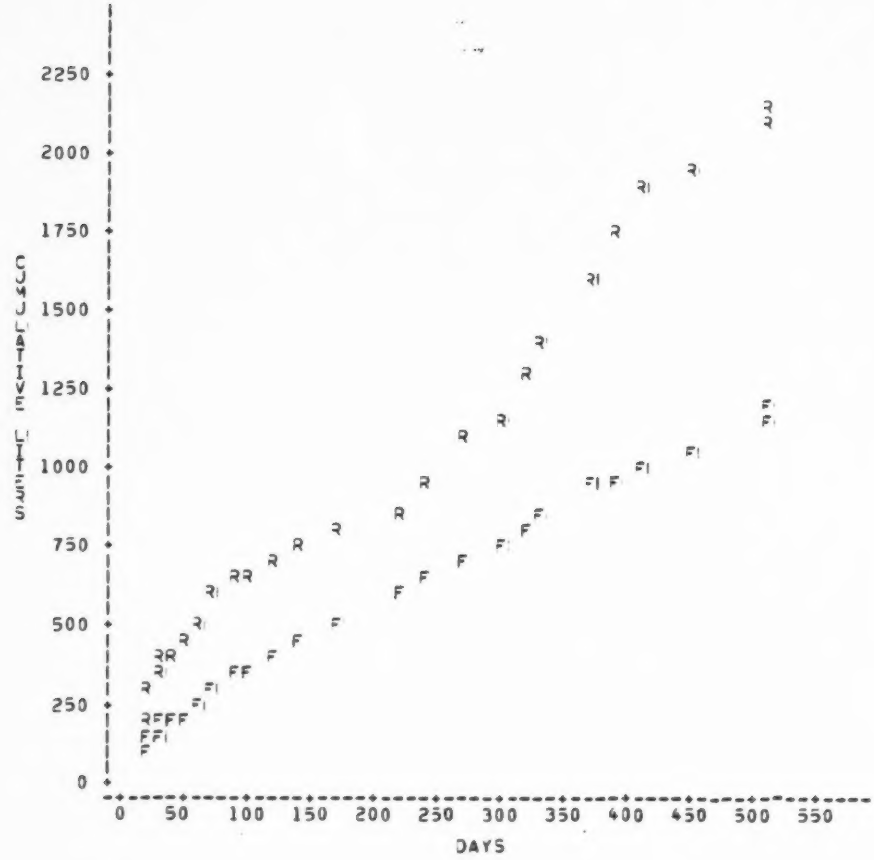

Figure G-57. Leading Cumulative Rainfall (R) and Lower Level Field Cell Flow (F): Field Cell 4.

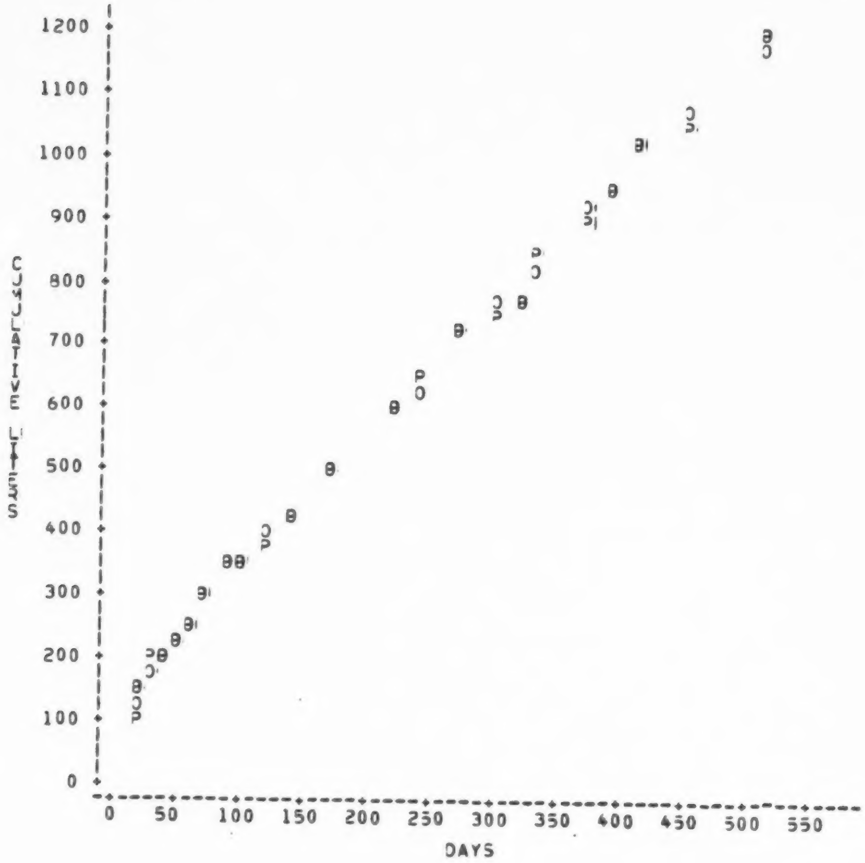

Figure G-58. Observed Flow (O) and Flow Predicted from a Rainfall-Flow Delay Model (P), with Rainfall Leading Flow by 12 Days: Field Cell 4.

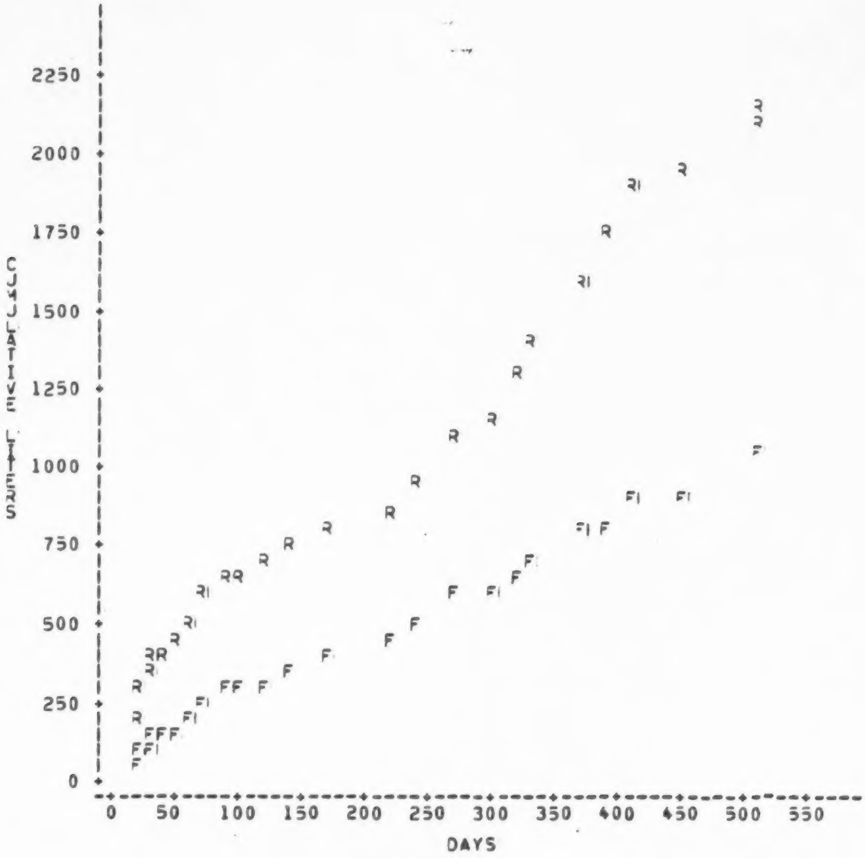

Figure G-59. Leading Cumulative Rainfall (R) and Lower Level Field Cell Flow (F): Field Cell 5.

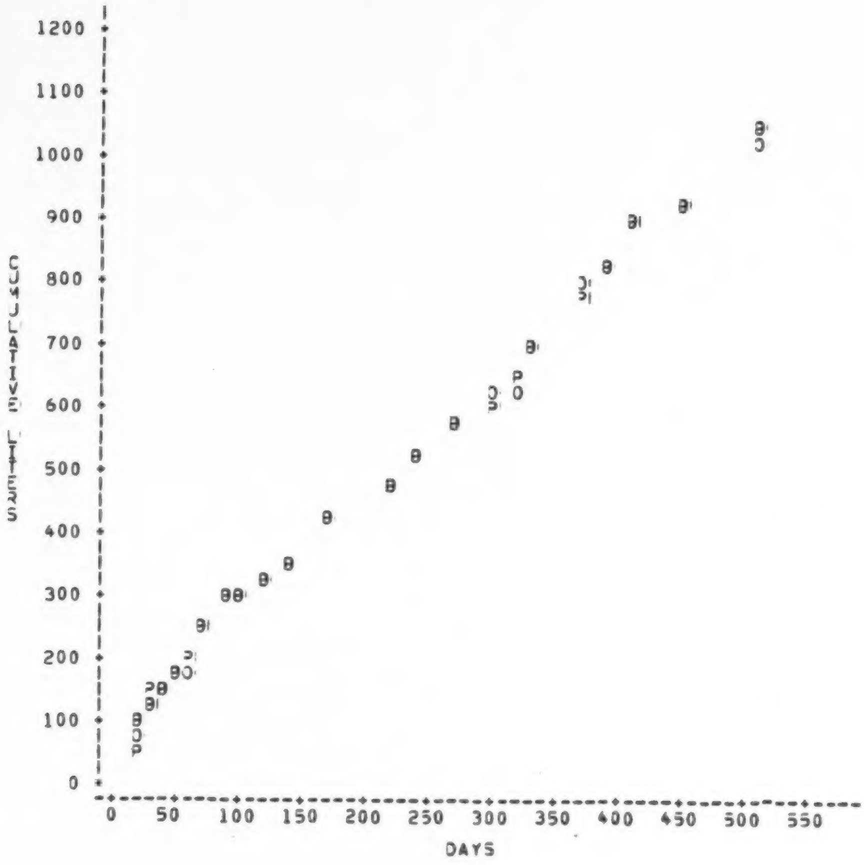

Figure G-60. Observed Flow (O) and Flow Predicted from a Rainfall-Flow Delay Model (P), with Rainfall Leading Flow by 12 Days: Field Cell 5.

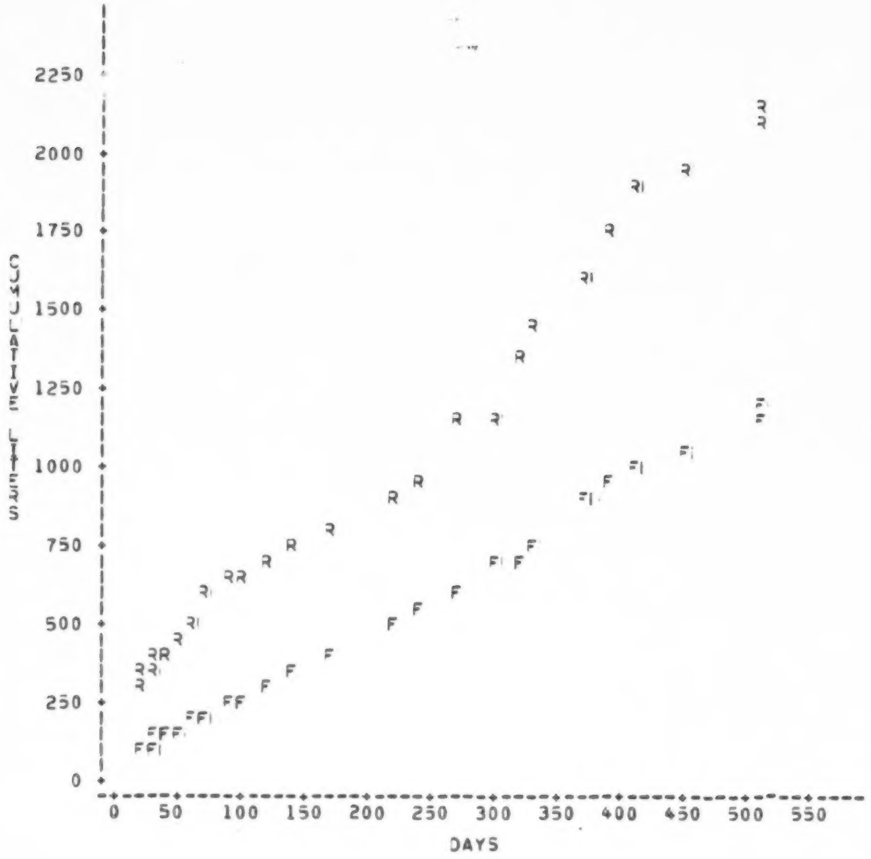

Figure G-61. Leading Cumulative Rainfall (R) and Lower Level Field Cell Flow (F): Field Cell 6.

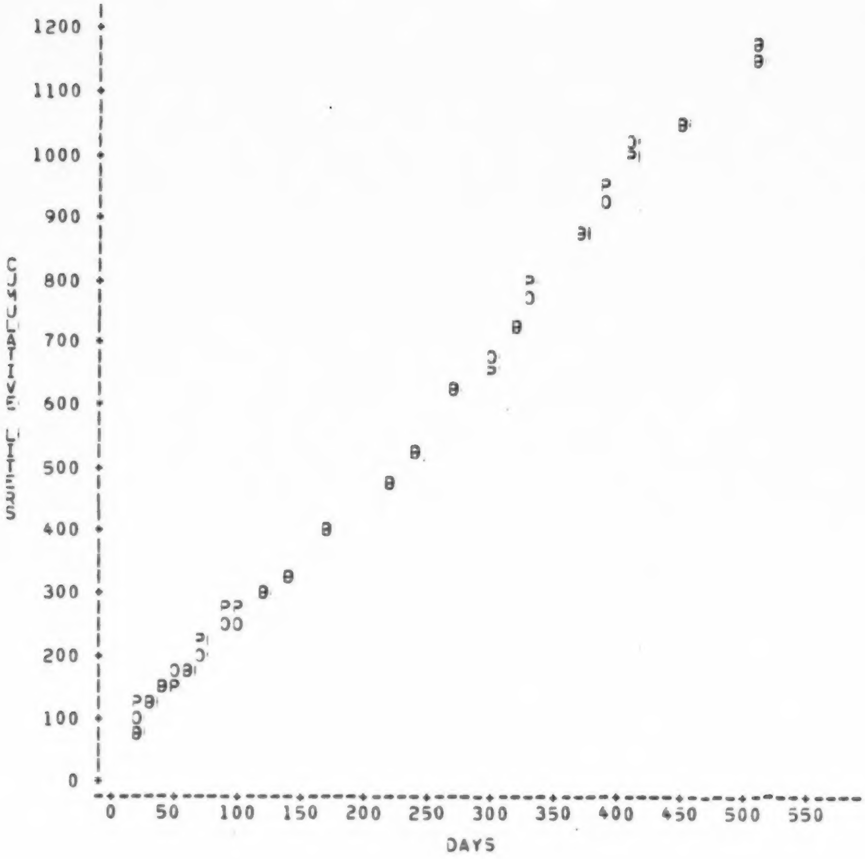

Figure G-62. Observed Flow (O) and Flow Predicted from a Rainfall-Flow Delay Model (P), with Rainfall Leading Flow by 12 Days: Field Cell 6.

Appendix G

Attachment 8

Figures G-72 to G-80

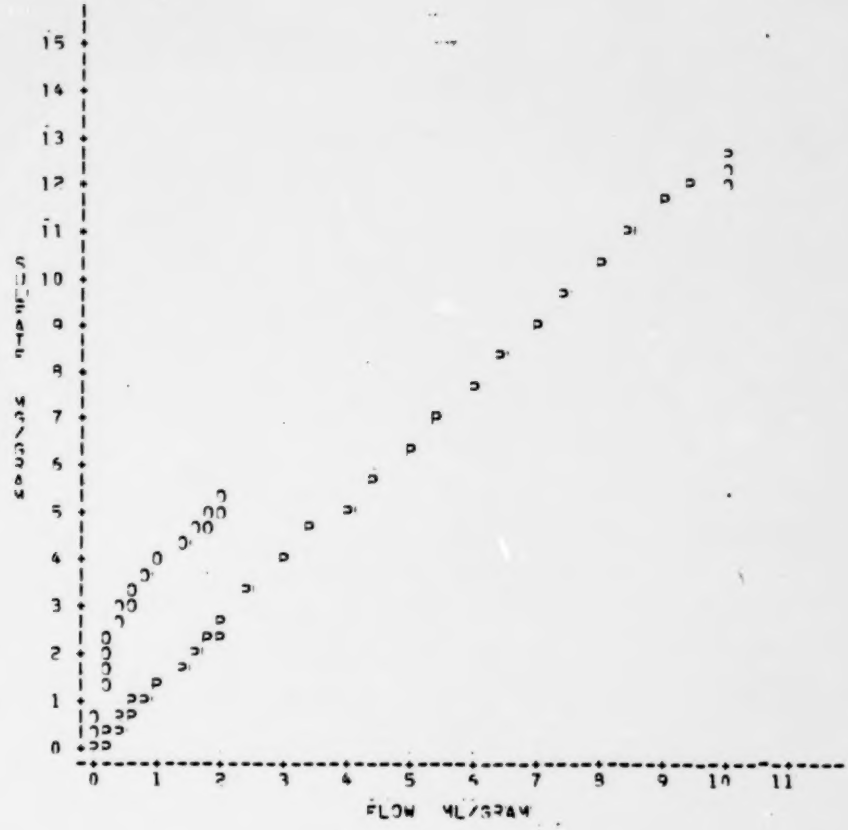

NOTE: The initial soluble fraction ($\underline{y}_0$) was estimated by a "mixed-rule" applied to back-calculated shake-test results. Extrapolation carried to the zero'th shake-test dilution (10 mL/gram).

Figure G-72. Model Confirmation Results for Sulfate Based on Shake-Test Extraction of PFBC Waste: Observed (O) and Predicted (P) Cumulative Field Cell No. 1 Extractions.

Preceding page blank

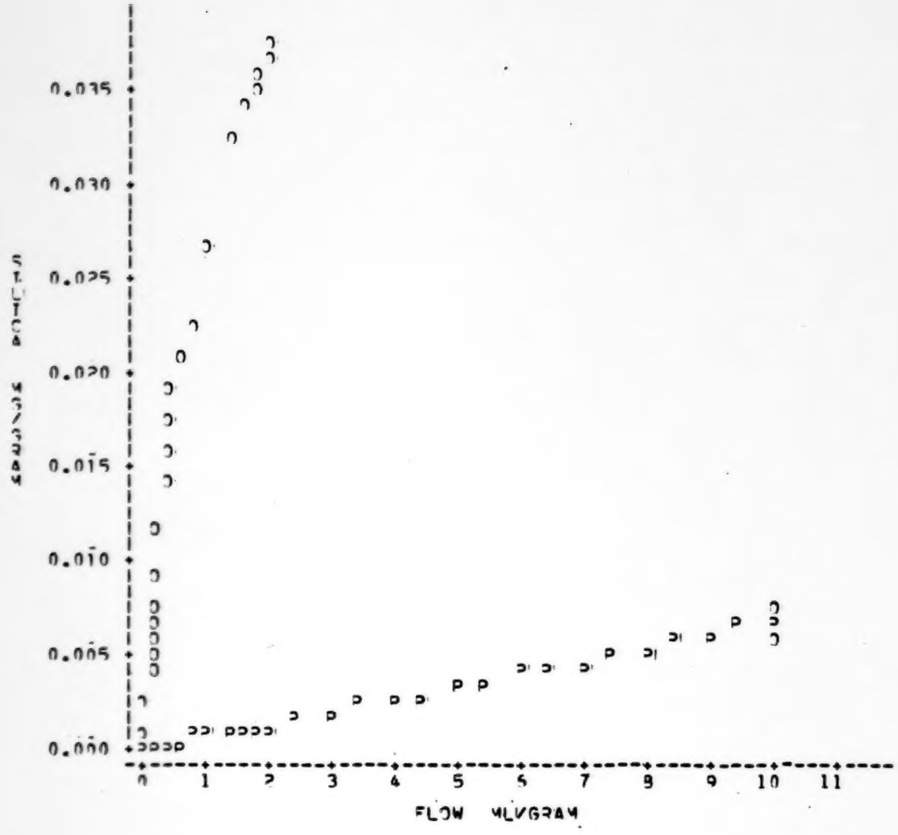

NOTE: The initial soluble fraction (y_0) was estimated by a "mixed-rule" applied to back-calculated shake-test results. Extrapolation carried to the zero'th shake-test dilution (10 mL/gram).

Figure G-73. Model Confirmation Results for Silicon Based on Shake-Test Extraction of PFBC Waste: Observed (O) and Predicted (P) Cumulative Field Cell No. 1 Extractions.

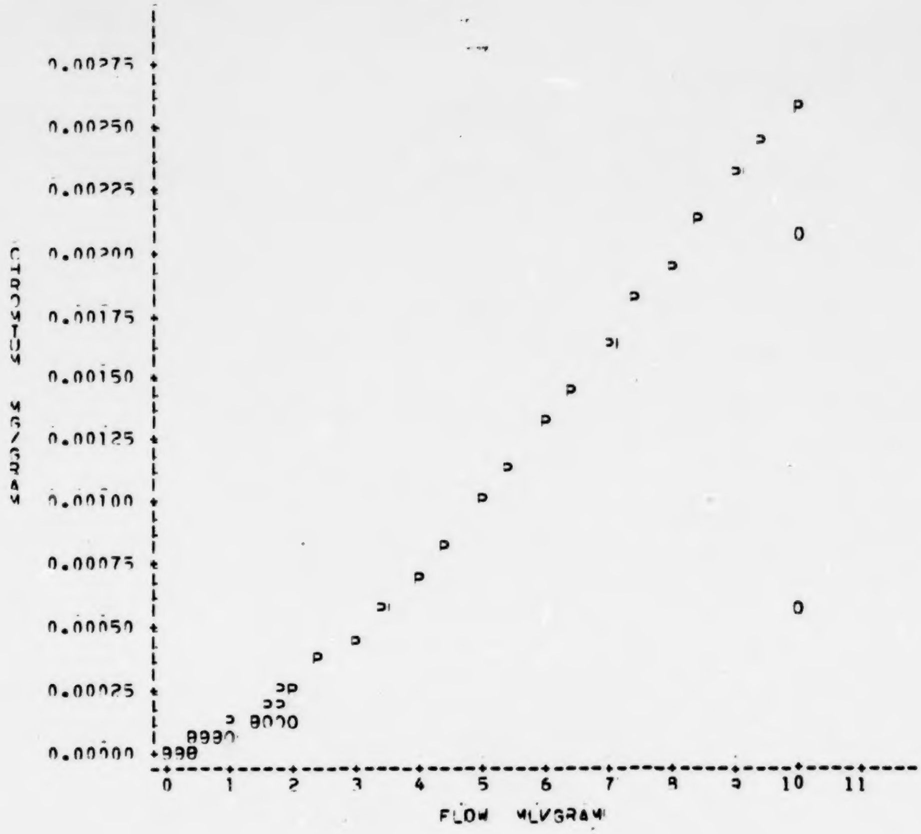

NOTE: The initial soluble fraction ($\underline{y}_o$) was estimated by a "mixed-rule" applied to back-calculated shake-test results. Extrapolation carried to the zero'th shake-test dilution (10 mL/gram).

Figure G-74. Model Confirmation Results for Chromium Based on Shake-Test Extraction of PFBC Waste: Observed (O) and Predicted (P) Cumulative Field Cell No. 1 Extractions.

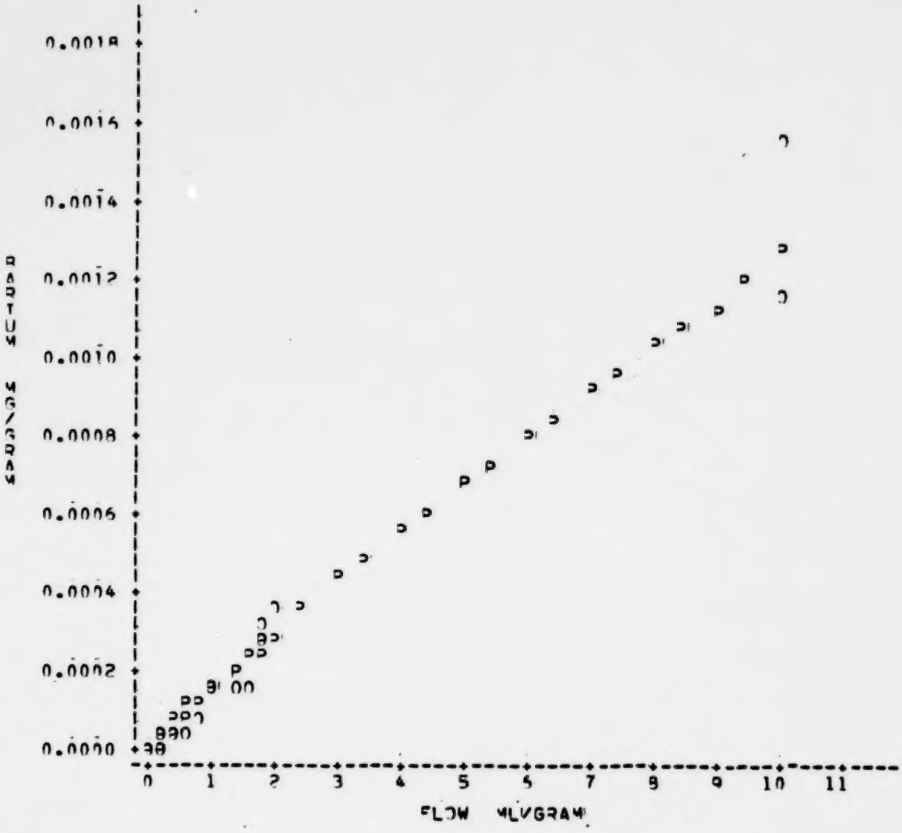

NOTE: The initial soluble fraction ($\underline{y}_0$) was estimated by a "mixed-rule" applied to back-calculated shake-test results. Extrapolation carried to the zero'th shake-test dilution (10 L/gram).

Figure G-75. Model Confirmation Results for Barium Based on Shake-Test Extraction of PFBC Waste: Observed (O) and Predicted (P) Cumulative Field Cell No. 1 Extractions.

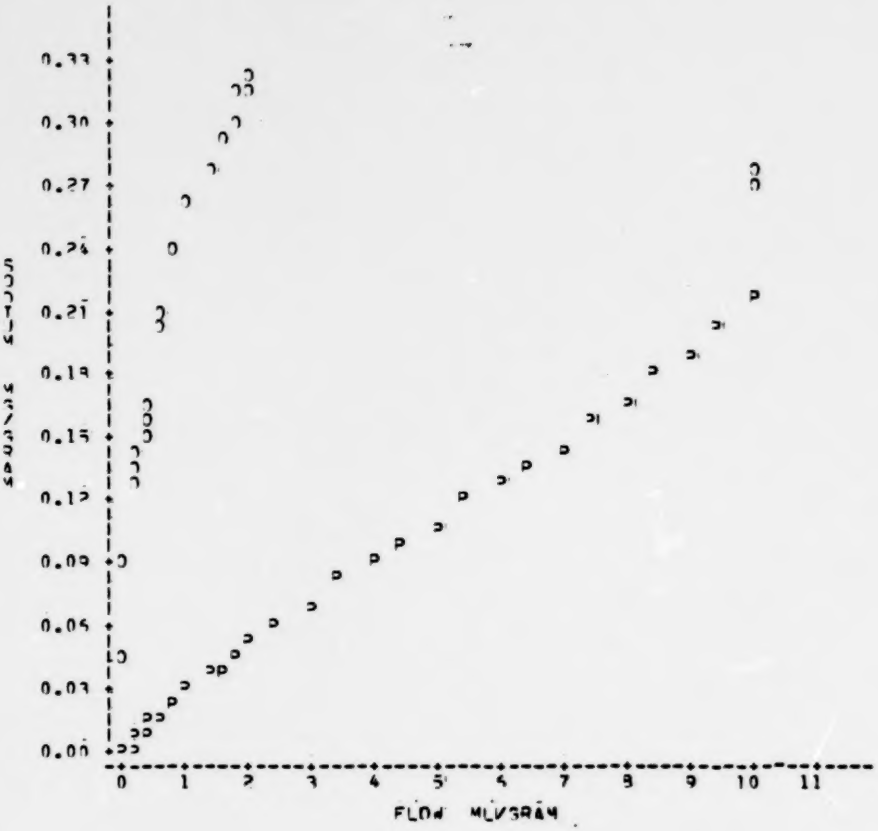

NOTE: The initial soluble fraction ($\underline{y}_o$) was estimated by a "mixed-rule" applied to back-calculated shake-test results. Extrapolation carried to the zero'th shake-test dilution (10 mL/gram).

Figure G-76. Model Confirmation Results for Sodium Based on Shake-Test Extraction of PFBC Waste: Observed (O) and Predicted (P) Cumulative Field Cell No. 1 Extractions.

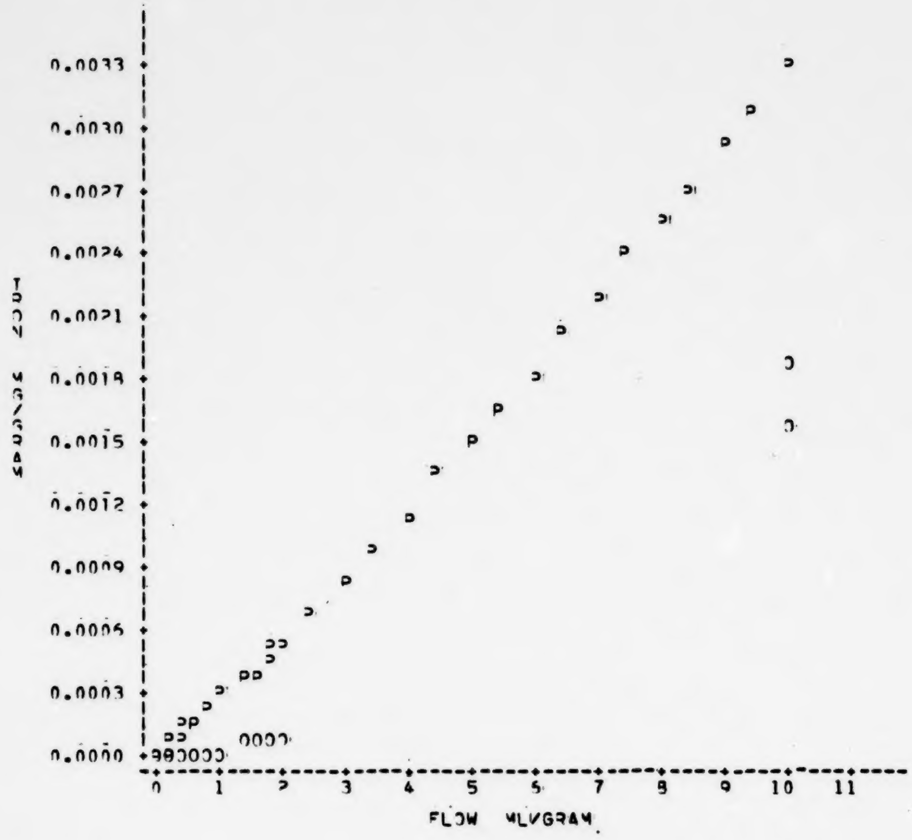

NOTE: The initial soluble fraction ($\underline{y}_o$) was estimated by a "mixed-rule" applied to back-calculated shake-test results. Extrapolation carried to the zero'th shake-test dilution (10 mL/gram).

Figure G-77. Model Confirmation Results for Iron Based on Shake-Test Extraction of PFBC Waste: Observed (O) and Predicted (P) Cumulative Field Cell No. 1 Extractions.

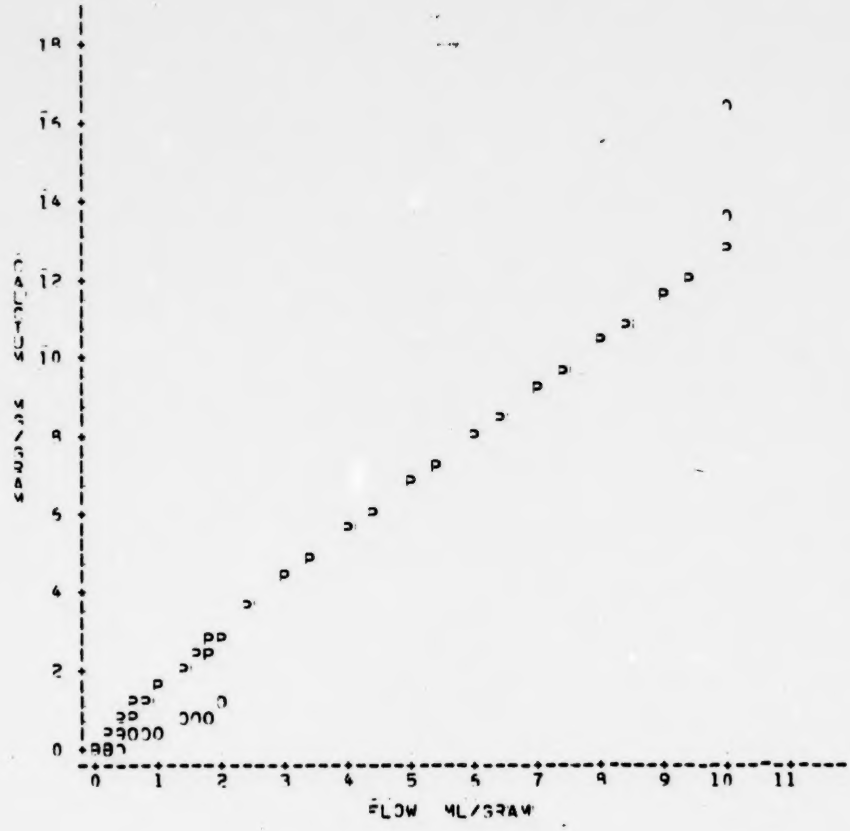

NOTE: The initial soluble fraction ($\underline{y}_0$) was estimated by a "mixed-rule" applied to back-calculated shake-test results. Extrapolation carried to the zero'th shake-test dilution (10 mL/gram).

Figure G-78. Model Confirmation Results for Calcium Based on Shake-Test Extraction of PFBC Waste: Observed (O) and Predicted (P) Cumulative Field Cell No. 1 Extractions.

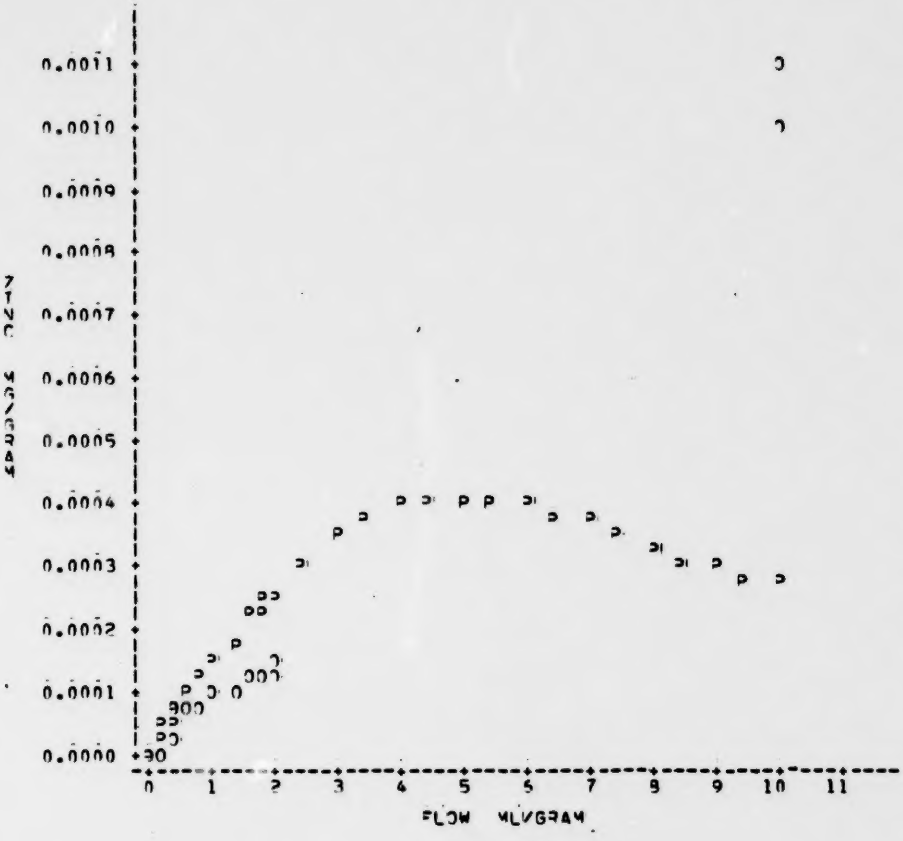

NOTE: The initial soluble fraction (y_o) was estimated by a "mixed-rule" applied to back-calculated shake-test results. Extrapolation carried to the zero'th shake-test dilution (10 mL/gram).

Figure G-79. Model Confirmation Results for Zinc Based on Shake-Test Extraction of PFBC Waste: Observed (O) and Predicted (P) Cumulative Field Cell No. 1 Extractions.

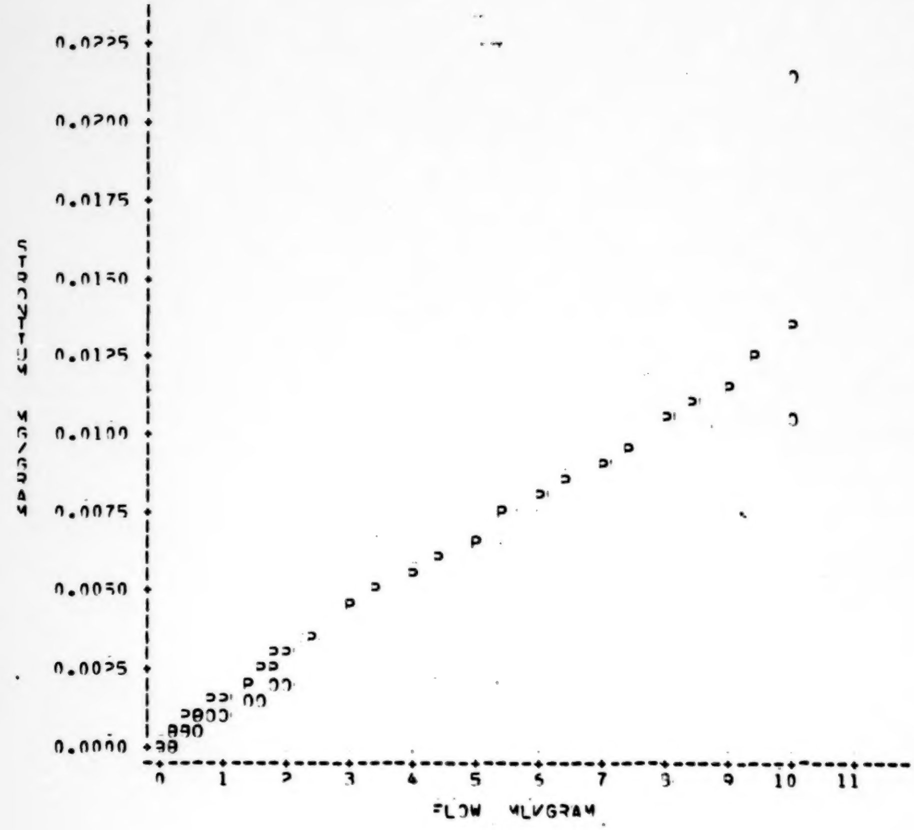

NOTE: The initial soluble fraction ($\underline{y}_0$) was estimated by a "mixed-rule" applied to back-calculated shake-test results. Extrapolation carried to the zero'th shake-test dilution (10 mL/gram).

Figure G-80. Model Confirmation Results for Strontium Based on Shake-Test Extraction of PFBC Waste: Observed (O) and Predicted (P) Cumulative Field Cell No. 1 Extractions.

Appendix G

Attachment 9

Figures G-81 to G-89

Preceding page blank

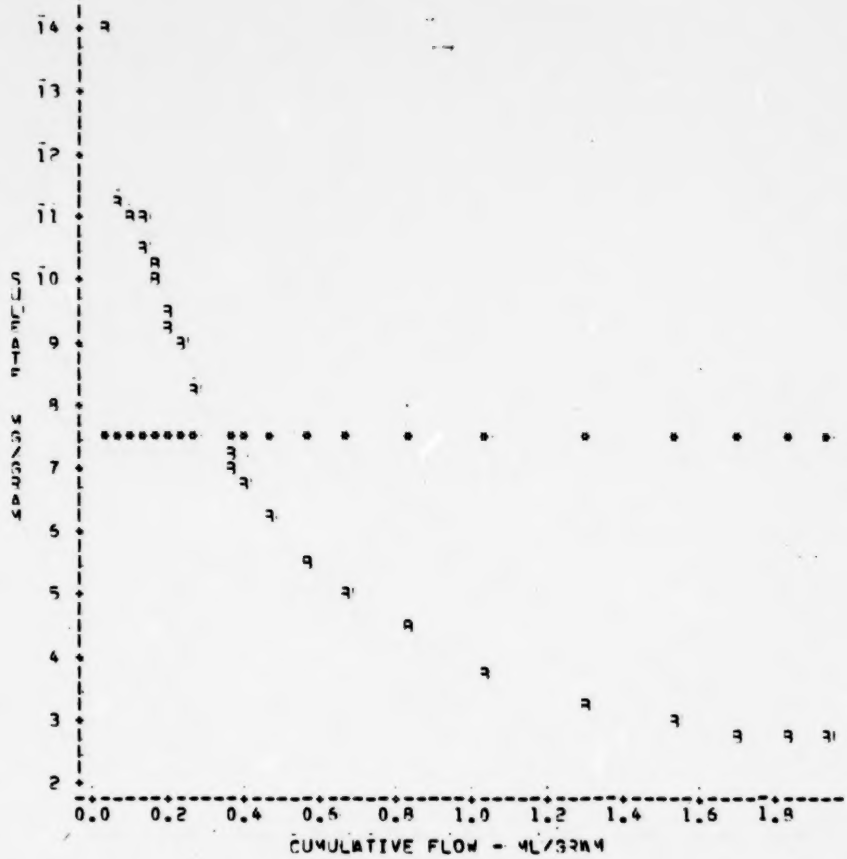

NOTE: Mean values (*) are indicated.

Figure G-81. Estimated Initial Soluble Fraction (y_0) of Sulfate in Field Cell 1 Obtained by Back-Calculation from Field Cell 1 Data.

Preceding page blank

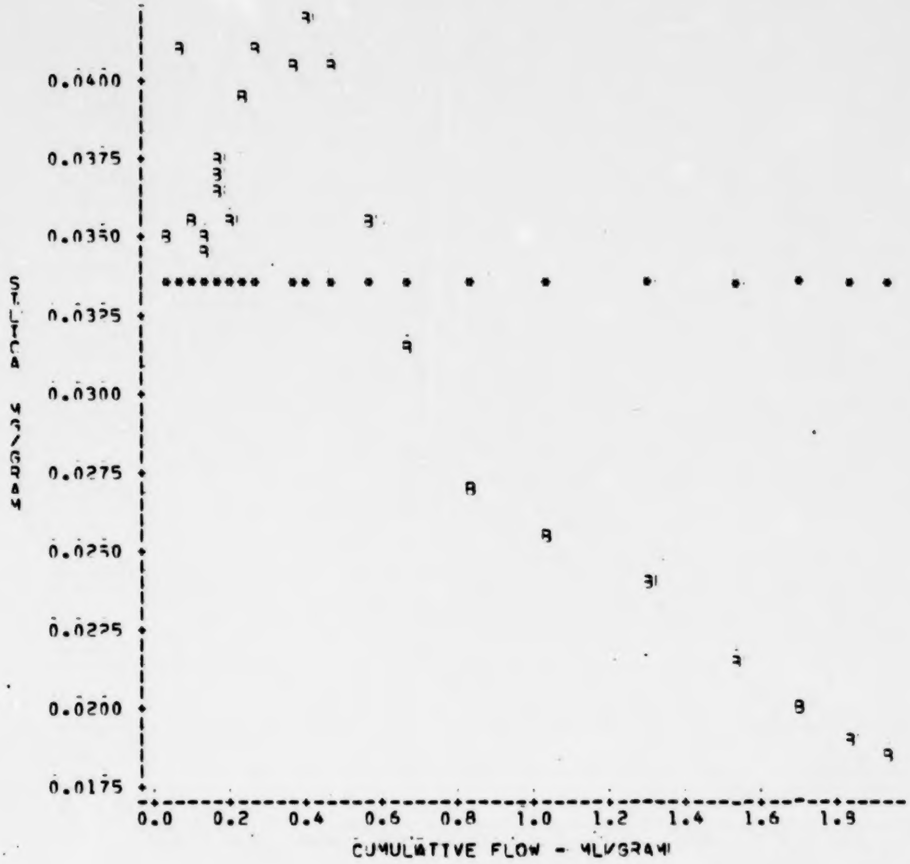

NOTE: **Mean values (*) are indicated.**

Figure G-82. **Estimated Initial Soluble Fraction (y_0) of Silicon in Field Cell 1 Obtained by Back-Calculation from Field Cell 1 Data.**

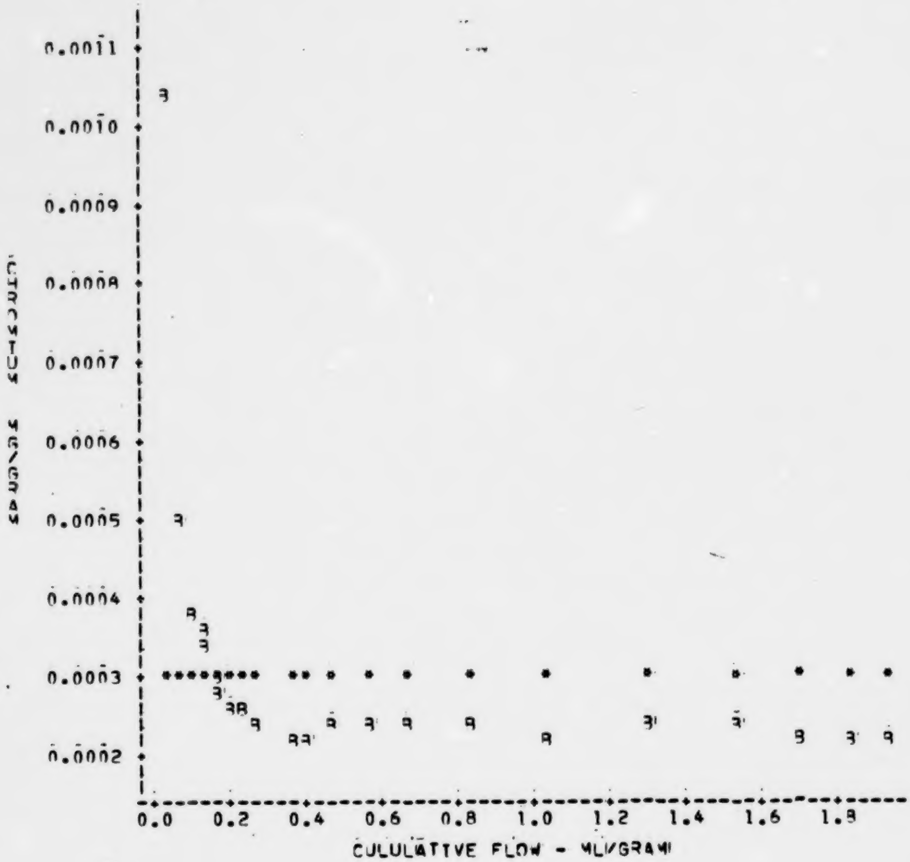

NOTE: Mean values (*) are indicated.

Figure G-83. Estimated Initial Soluble Fraction (y_0) of Chromium in Field Cell 1 Obtained by Back-Calculation from Field Cell 1 Data.

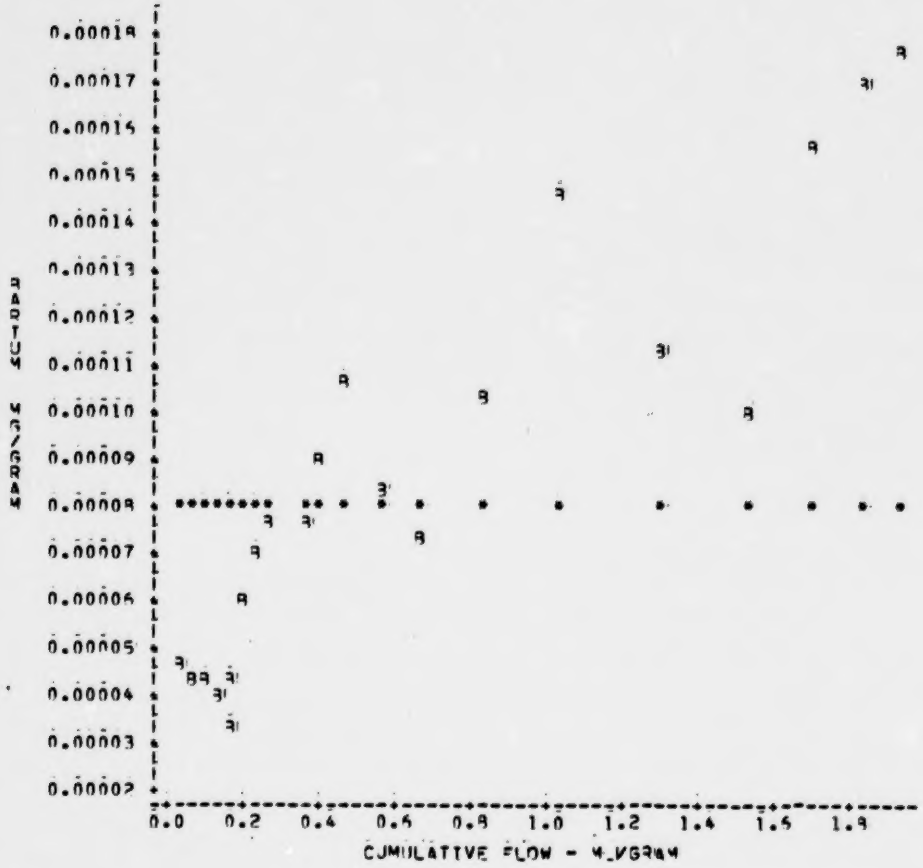

NOTE: Mean values (*) are indicated.

Figure G-84. Estimated Initial Soluble Fraction (y_0) of Barium in Field Cell 1 Obtained by Back-Calculation from Field Cell 1 Data.

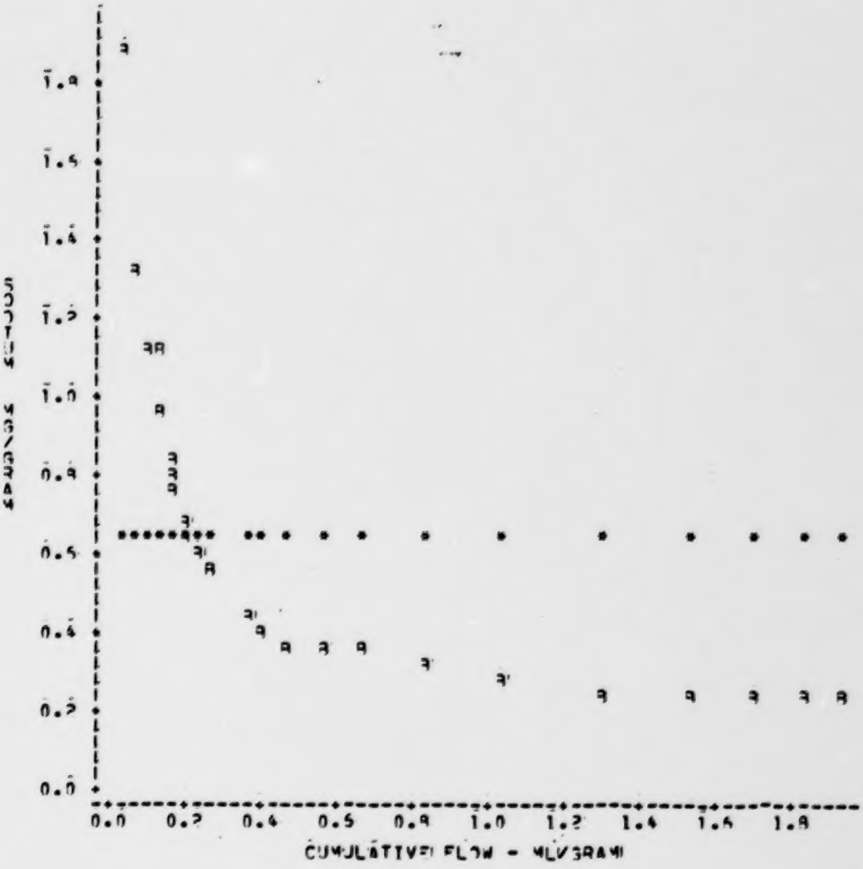

NOTE: Mean values (*) are indicated.

Figure G-85. Estimated Initial Soluble Fraction (y_0) of Sodium in Field Cell 1 Obtained by Back-Calculation from Field Cell 1 Data.

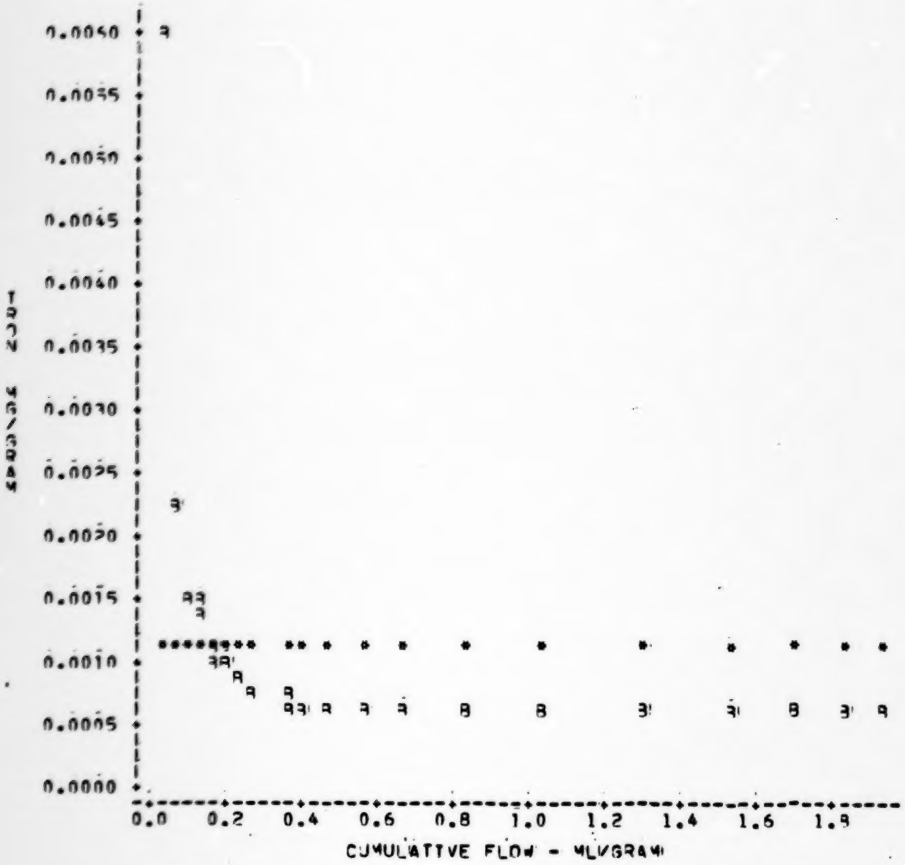

NOTE: Mean values (*) are indicated.

Figure G-86. Estimated Initial Soluble Fraction (y_0) of Iron in Field Cell 1 Obtained by Back-Calculation from Field Cell 1 Data.

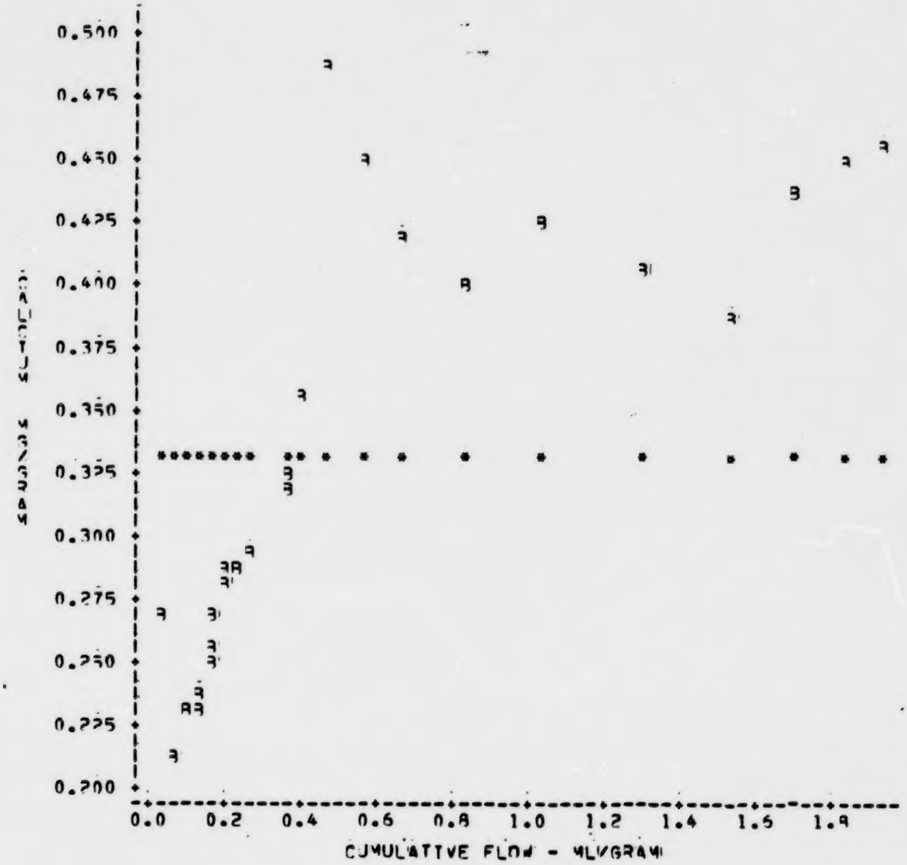

NOTE: Mean values (*) are indicated.

Figure G-87. Estimated Initial Soluble Fraction (y_0) of Calcium in Field Cell 1 Obtained by Back-Calculation from Field Cell 1 Data.

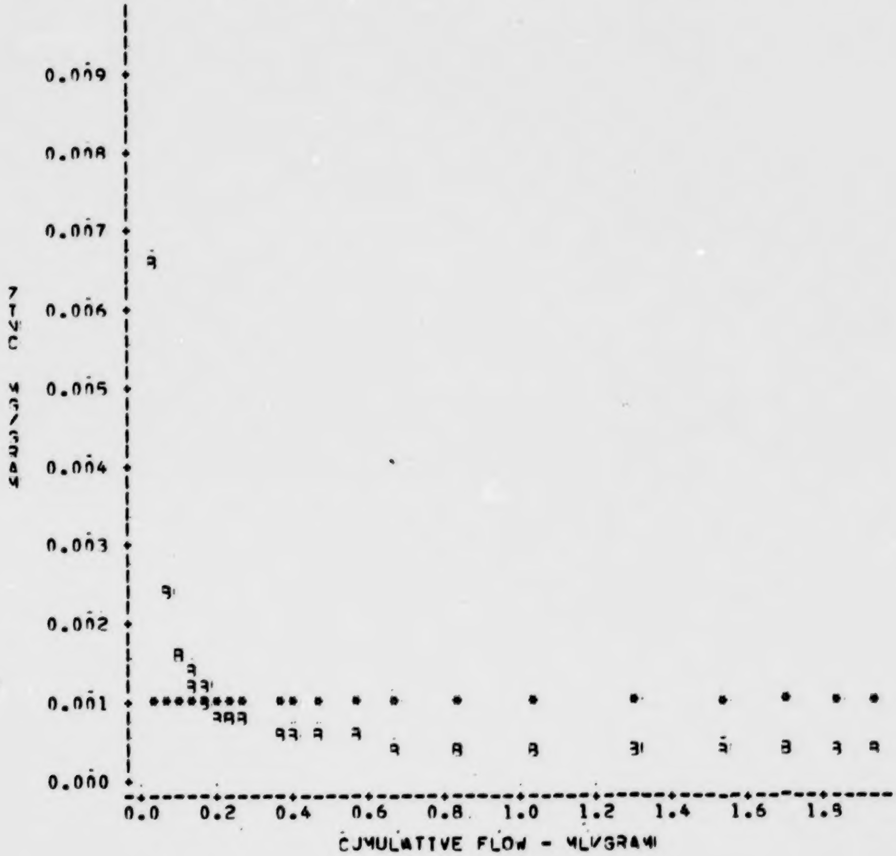

NOTE: Mean values (*) are indicated.

Figure G-88. Estimated Initial Soluble Fraction (y_0) of Zinc in Field Cell 1 Obtained by Back-Calculation from Field Cell 1 Data.

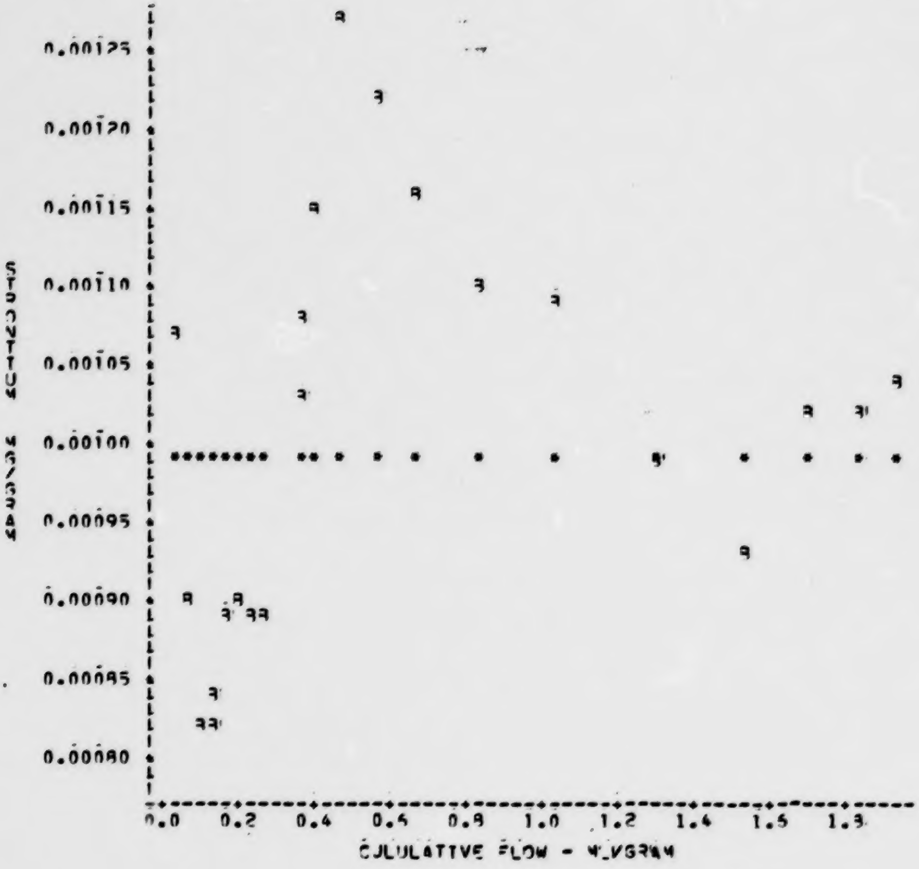

NOTE: Mean values (*) are indicated.

Figure G-89. Estimated Initial Soluble Fraction (y_0) of Strontium in Field Cell 1 Obtained by Back-Calculation from Field Cell 1 Data.

Appendix G

Attachment 10

Figures G-90 to G-98

Preceding page blank

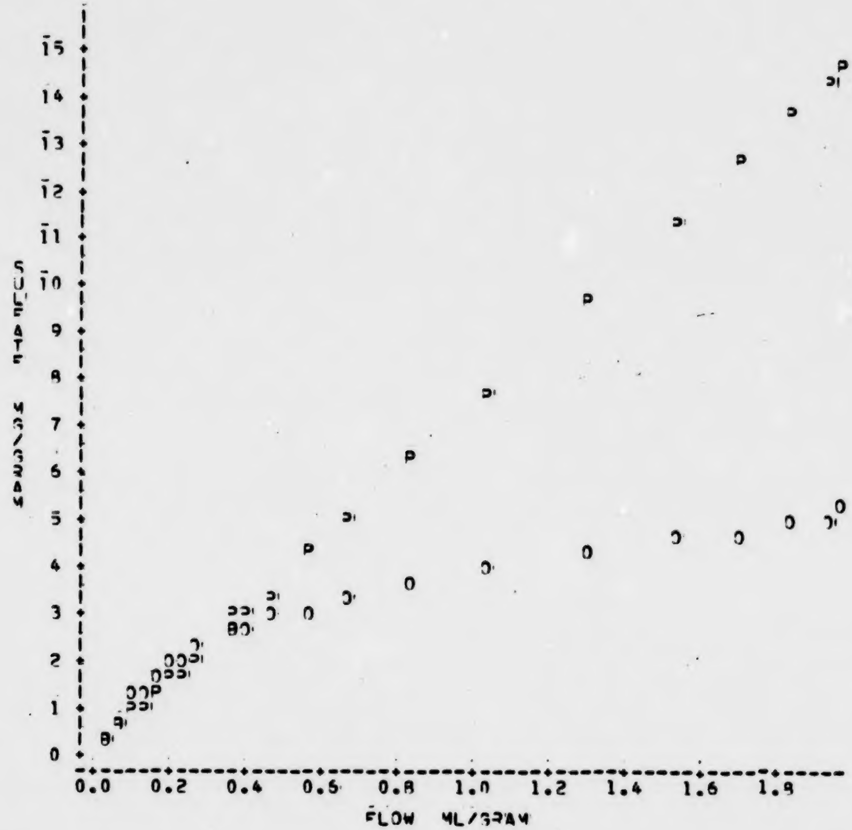

NOTE: The initial soluble fraction ($\underline{y}_o$) was estimated as the mean of back-calculated Field Cell No. 1 results. Flow is over the range experienced in the field.

Figure G-90. Observed (O) and Predicted (P) Cumulative Field Cell 1 Extractions for Sulfate.

Preceding page blank

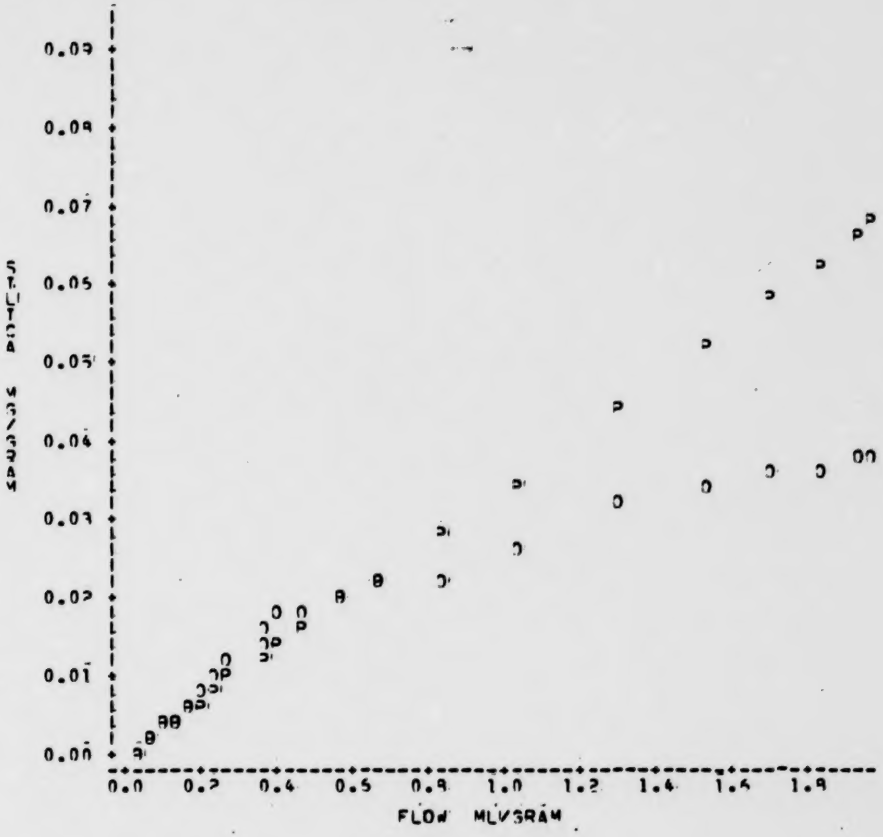

NOTE: The initial soluble fraction ($\underline{y}_o$) was estimated as the mean of back-calculated field cell no. 1 results. Flow is over the range experienced in the field.

Figure G-91. Observed (O) and Predicted (P) Cumulative Field Cell 1 Extractions for Silicon.

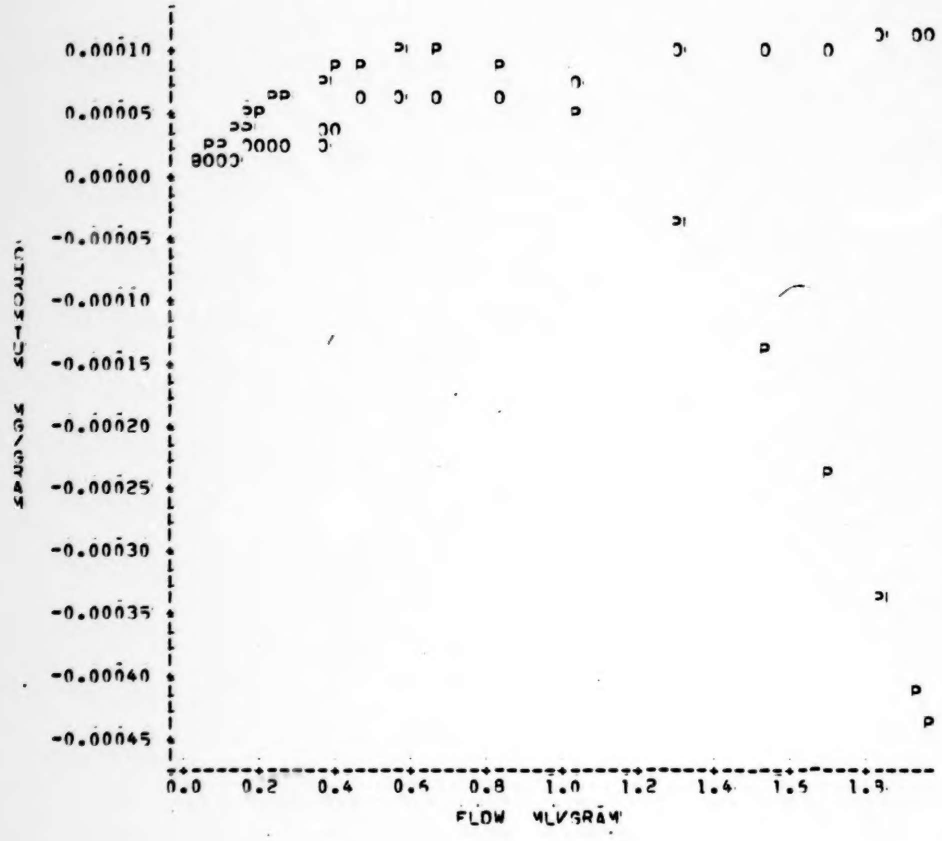

NOTE: The initial soluble fraction ($\underline{y}_0$) was estimated as the mean of back-calculated Field Cell No. 1 results. Flow is over the range experienced in the field.

Figure G-92. Observed (O) and Predicted (P) Cumulative Field Cell 1 Extractions for Chromium.

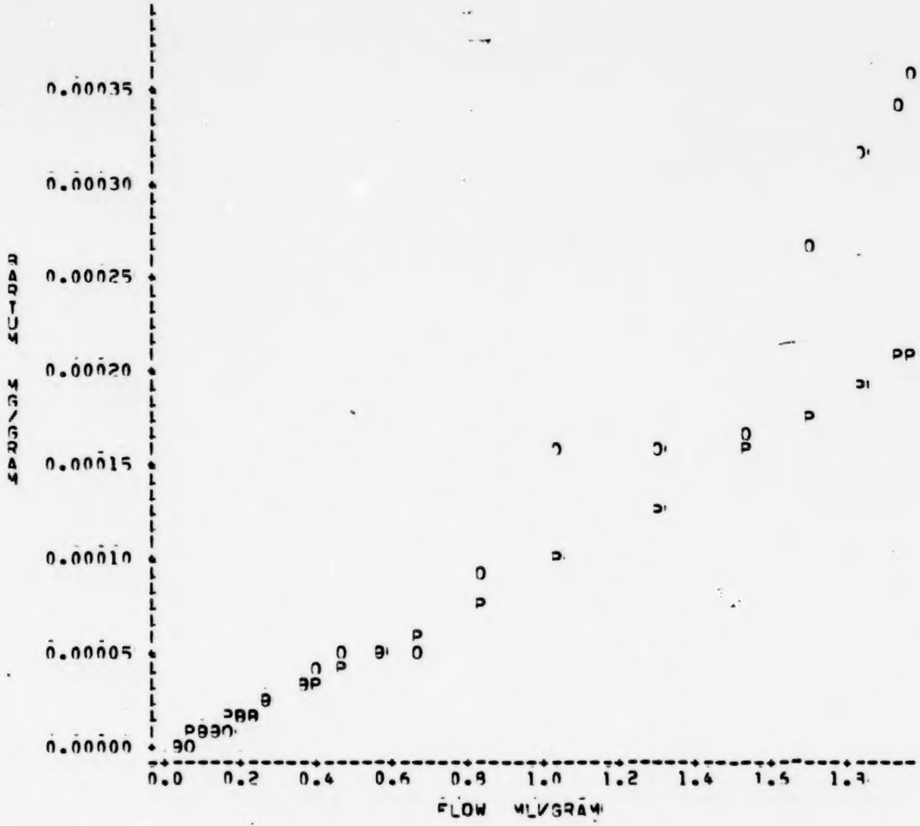

NOTE: The initial soluble fraction (y_o) was estimated as the mean of back-calculated Field Cell No. 1 results. Flow is over the range experienced in the field.

Figure G-93. Observed (O) and Predicted (P) Cumulative Field Cell 1 Extractions for Barium.

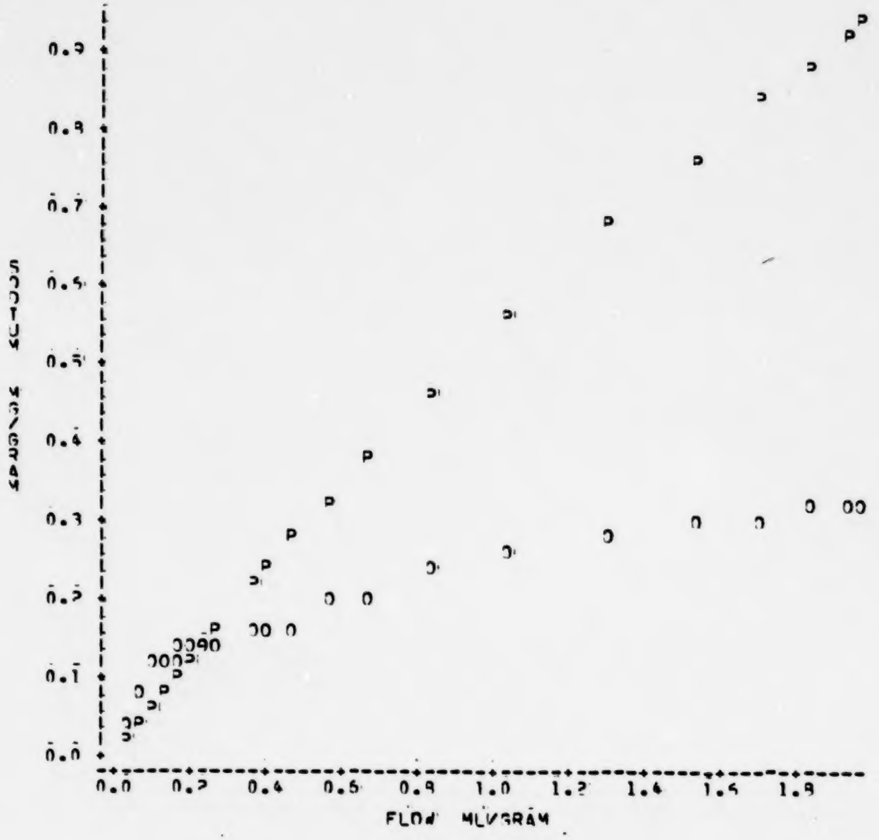

NOTE: The initial soluble fraction ($\underline{y}_0$) was estimated as the mean of back-calculated Field Cell No. 1 results. Flow is over the range experienced in the field.

Figure G-94. Observed (O) and Predicted (P) Cumulative Field Cell 1 Extractions for Sodium.

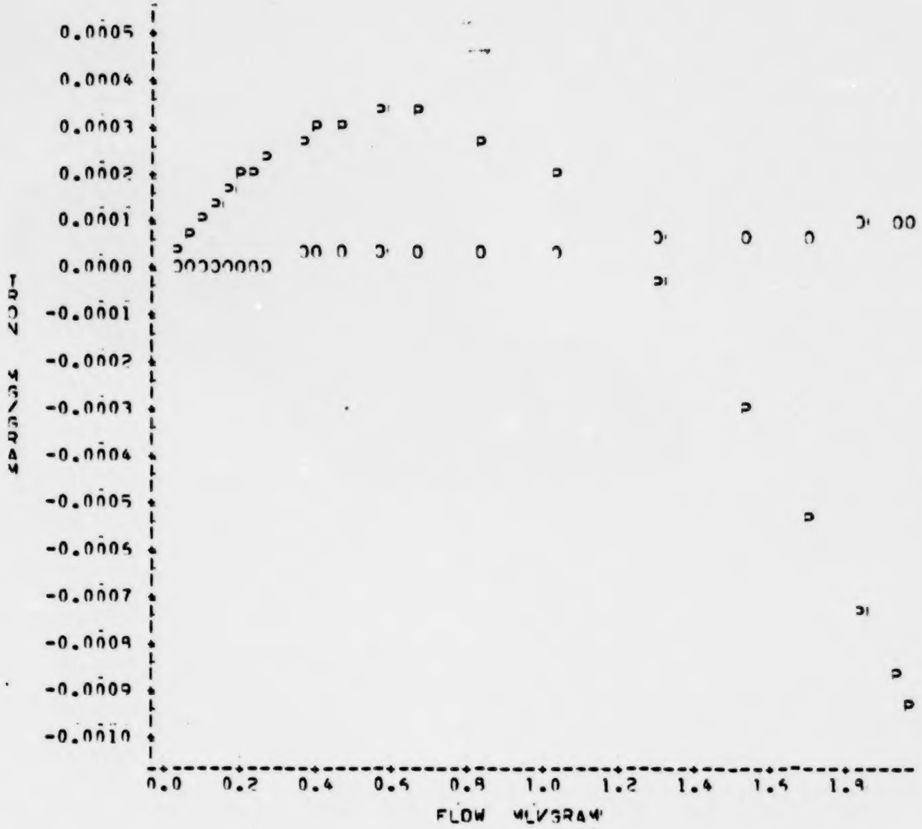

NOTE: The initial soluble fraction ($\underline{y}_0$) was estimated as the mean of back-calculated Field Cell No. 1 results. Flow is over the range experienced in the field.

Figure G-95. Observed (O) and Predicted (P) Cumulative Field Cell 1 Extractions for Iron.

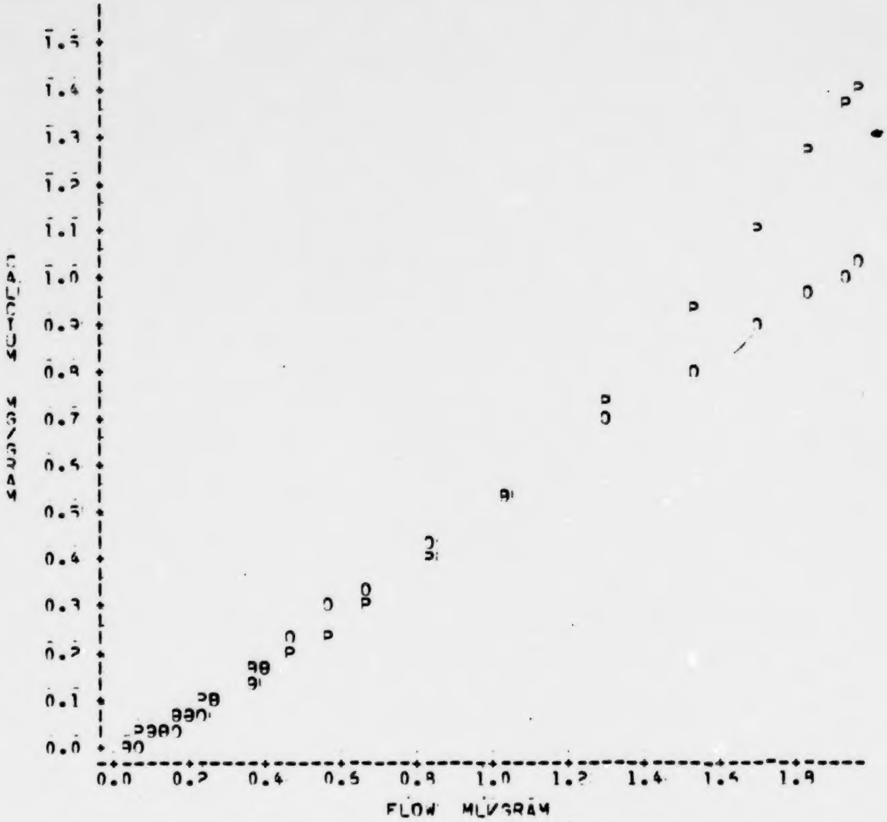

NOTE: The initial soluble fraction ($\underline{y}_o$) was estimated as the mean of back-calculated Field Cell No. 1 results. Flow is over the range experienced in the field.

Figure G-96. Observed (O) and Predicted (P) Cumulative Field Cell 1 Extractions for Calcium.

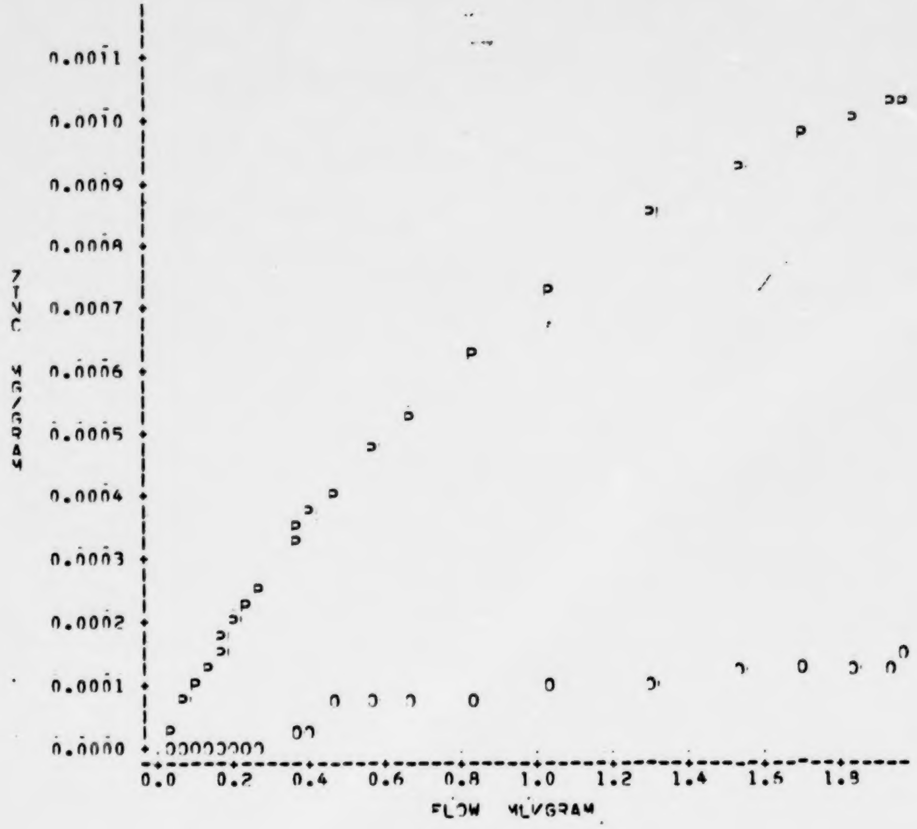

NOTE: The initial soluble fraction (y_0) was estimated as the mean of back-calculated Field Cell No. 1 results. Flow is over the range experienced in the field.

Figure G-97. Observed (O) and Predicted (P) Cumulative Field Cell 1 Extractions for Zinc.

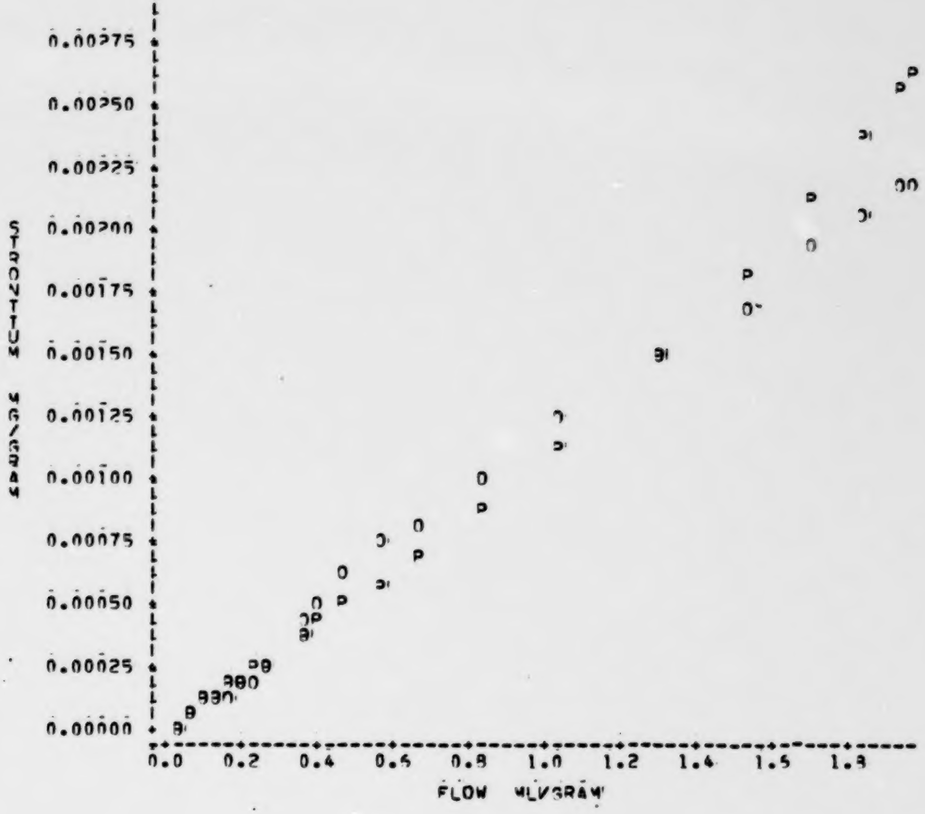

NOTE: The initial soluble fraction (y_o) was estimated as the mean of back-calculated Field Cell No. 1 results. Flow is over the range experienced in the field.

Figure G-98. Observed (O) and Predicted (P) Cumulative Field Cell 1 Extractions for Strontium.

Appendix G

Attachment 11

Figures G-99 to G-107

Preceding page blank

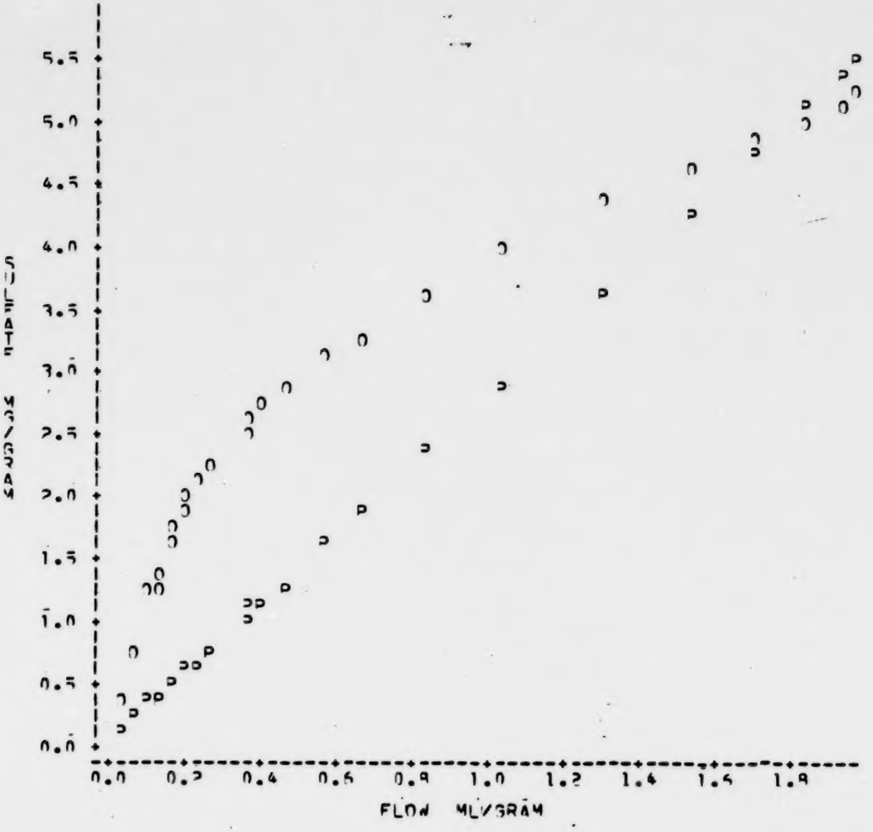

NOTE: The initial soluble fraction (y_o) was estimated by the asymptotic back-calculated Field Cell No. 1 results. Flow is over the range experienced in the field.

Figure G-99. Observed (O) and Predicted (P) Cumulative Field Cell 1 Extractions for Sulfate.

Preceding page blank

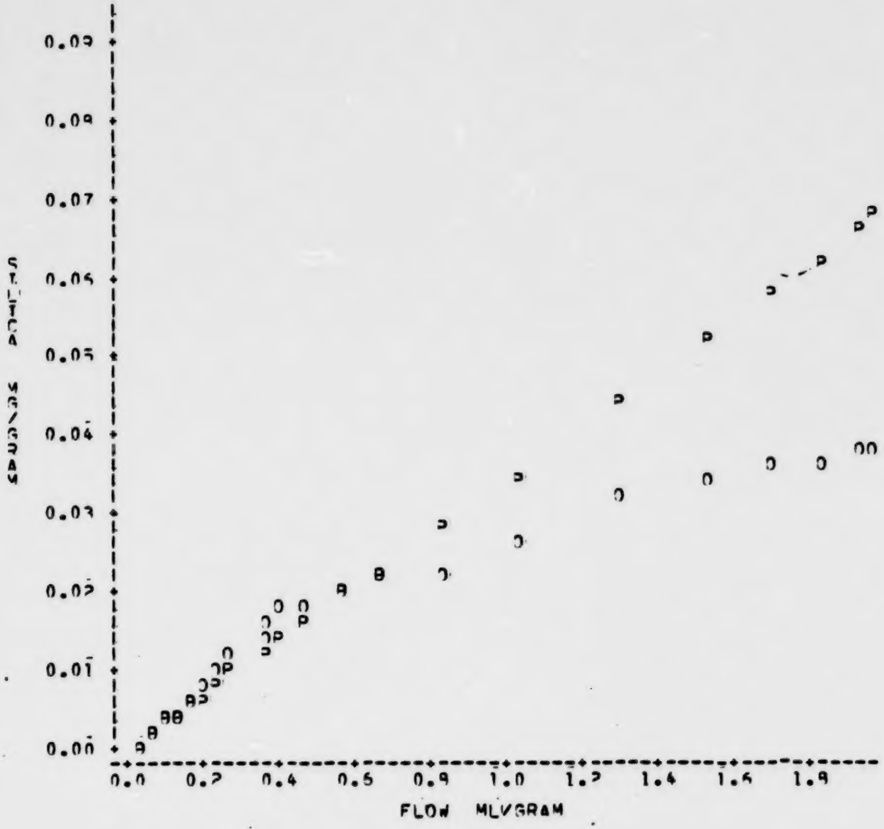

NOTE: The initial soluble fraction (y_O) was estimated by the mean back-calculated Field Cell No. 1 results. Flow is over the range experienced in the field.

Figure G-100. Observed (O) and Predicted (P) Cumulative Field Cell 1 Extractions for Silicon.

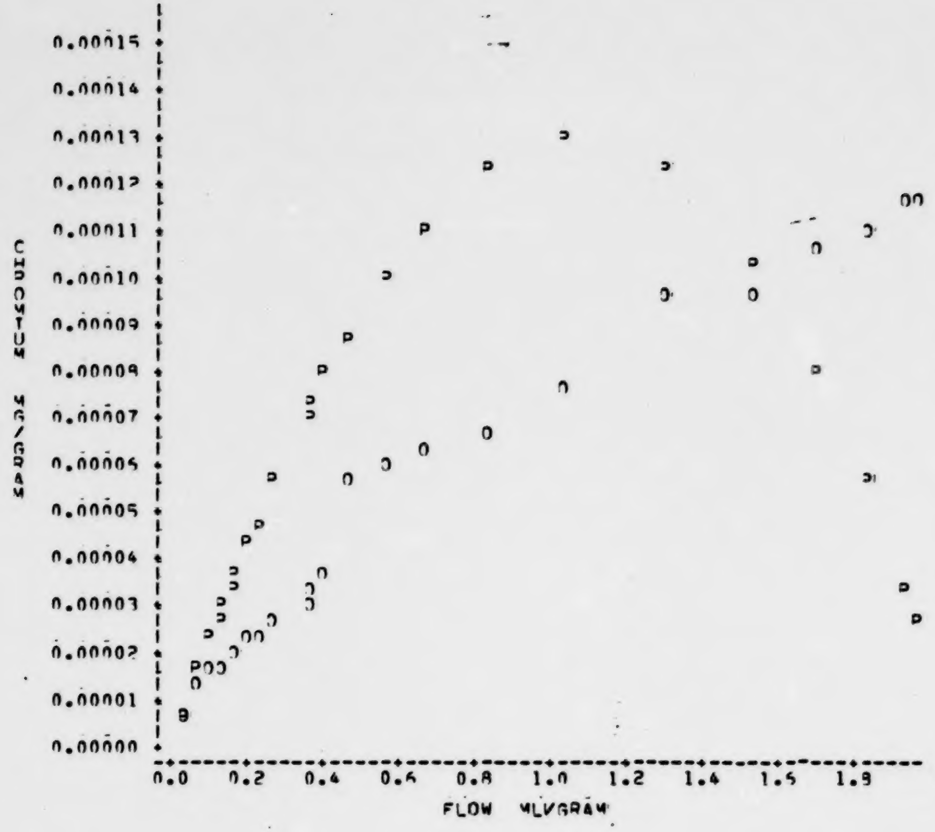

NOTE: The initial soluble fraction ($\underline{y}_0$) was estimated by the asymptotic back-calculated Field Cell No. 1 results. Flow is over the range experienced in the field.

Figure G-101. Observed (O) and Predicted (P) Cumulative Field Cell 1 Extractions for Chromium.

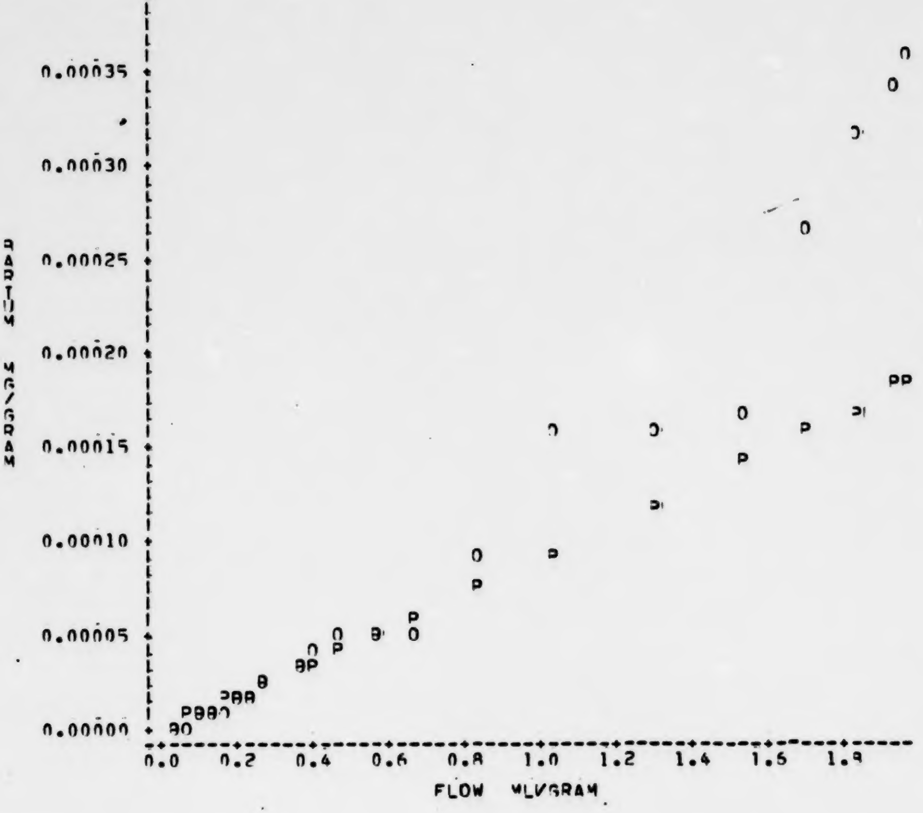

NOTE: The initial soluble fraction ($\underline{y}_o$) was estimated by the mean back-calculated Field Cell No. 1 results. Flow is over the range experienced in the field.

Figure G-102. Observed (O) and Predicted (P) Cumulative Field Cell 1 Extractions for Barium.

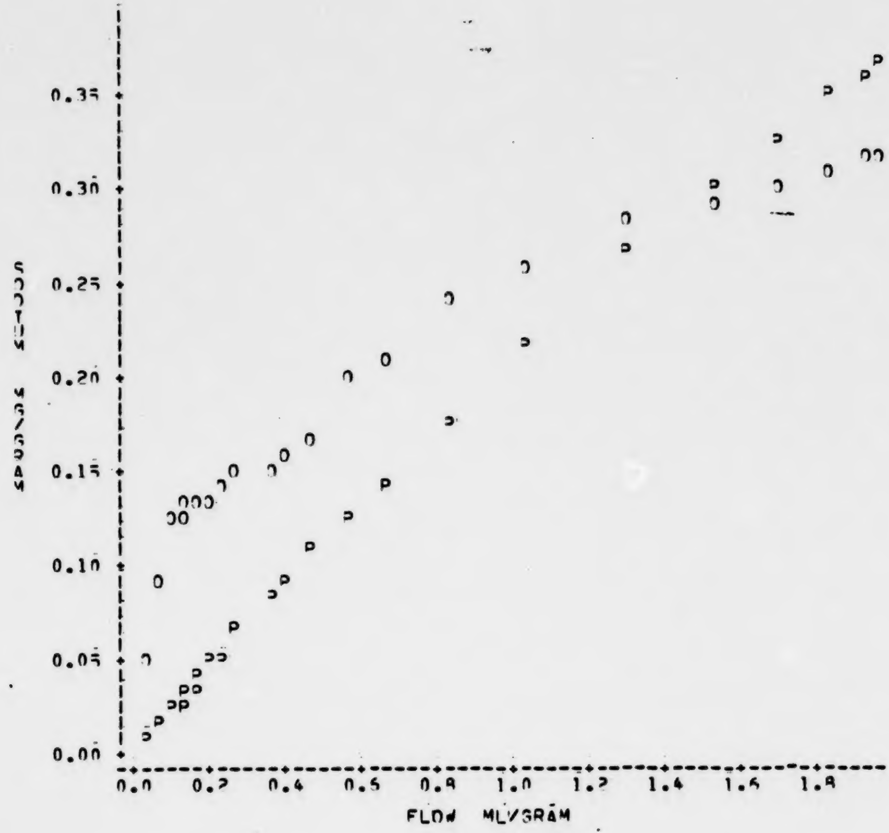

NOTE: The initial soluble fraction (y_o) was estimated by the asymptotic back-calculated Field Cell No. 1 results. Flow is over the range experienced in the field.

Figure G-103. Observed (O) and Predicted (P) Cumulative Field Cell 1 Extractions for Sodium.

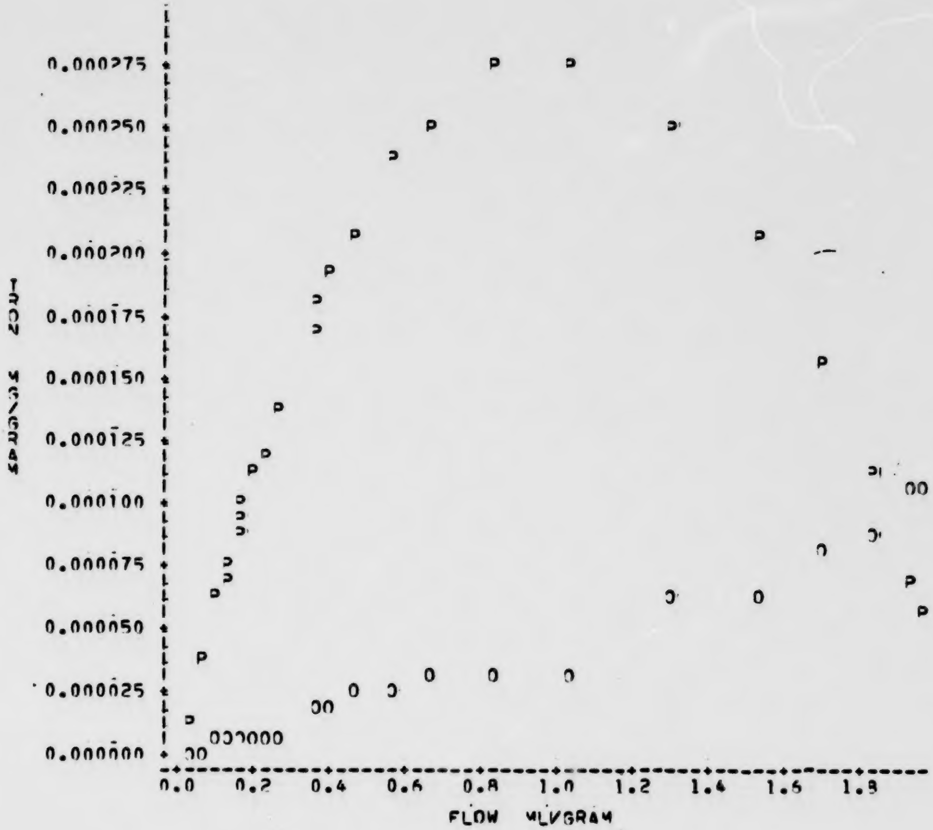

NOTE: The initial soluble fraction ($\underline{y}_o$) was estimated by the asymptotic back-calculated Field Cell No. 1 results. Flow is over the range experienced in the field.

Figure G-104. Observed (O) and Predicted (P) Cumulative Field Cell 1 Extractions for Iron.

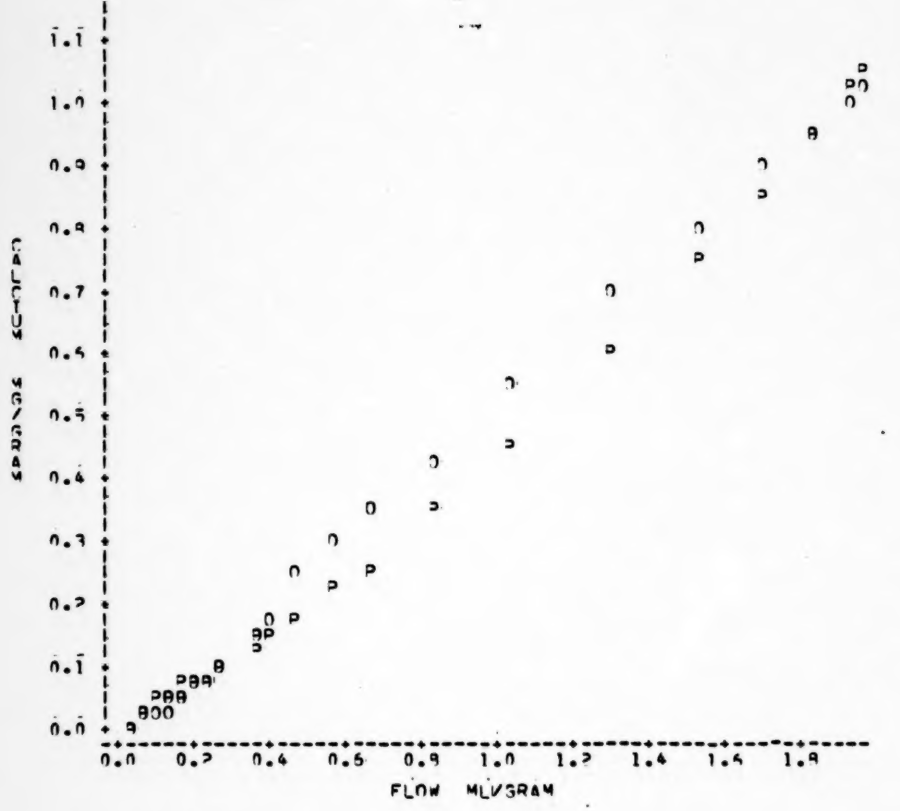

NOTE: The initial soluble fraction (y_o) was estimated by the mean back-calculated Field Cell No. 1 results. Flow is over the range experienced in the field.

Figure G-105. Observed (O) and Predicted (P) Cumulative Field Cell 1 Extractions for Calcium.

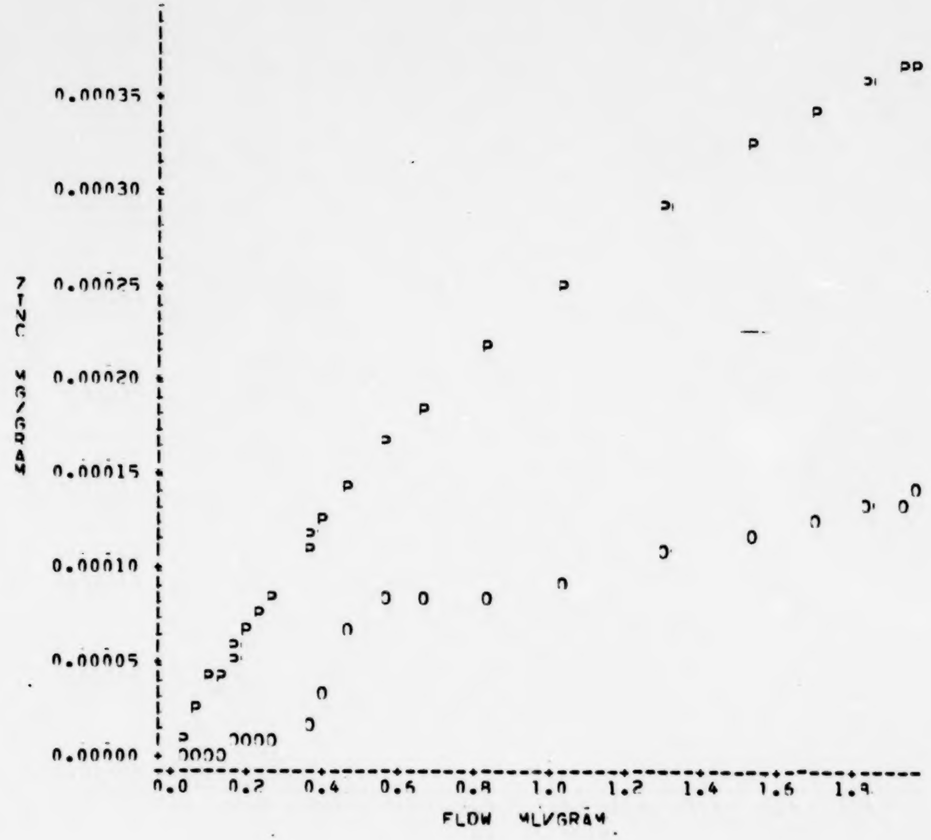

NOTE: The initial soluble fraction ($\underline{y}_o$) was estimated by the asymptotic back-calculated Field Cell No. 1 results. Flow is over the range experienced in the field.

Figure G-106. Observed (O) and Predicted (P) Cumulative Field Cell 1 Extractions for Zinc.

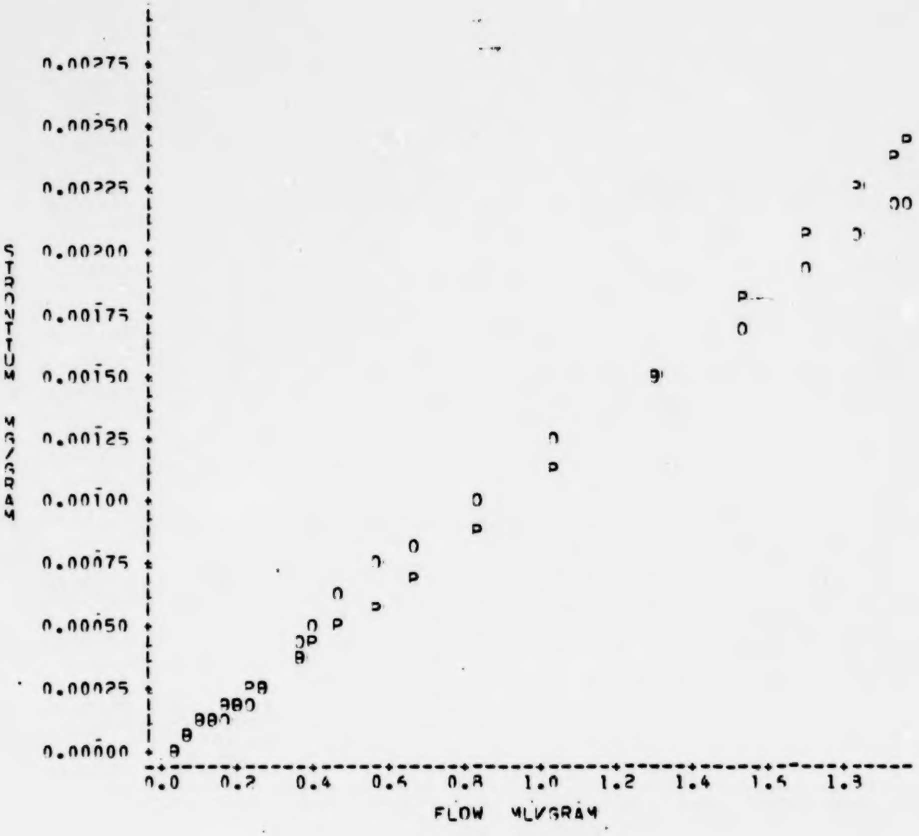

NOTE: The initial soluble fraction ($\underline{y}_o$) was estimated by the mean back-calculated Field Cell No. 1 results. Flow is over the range experienced in the field.

Figure G-107. Observed (O) and Predicted (P) Cumulative Field Cell 1 Extractions for Strontium.

Appendix G

Attachment 12

Figures G-108 to G-116

Preceding page blank

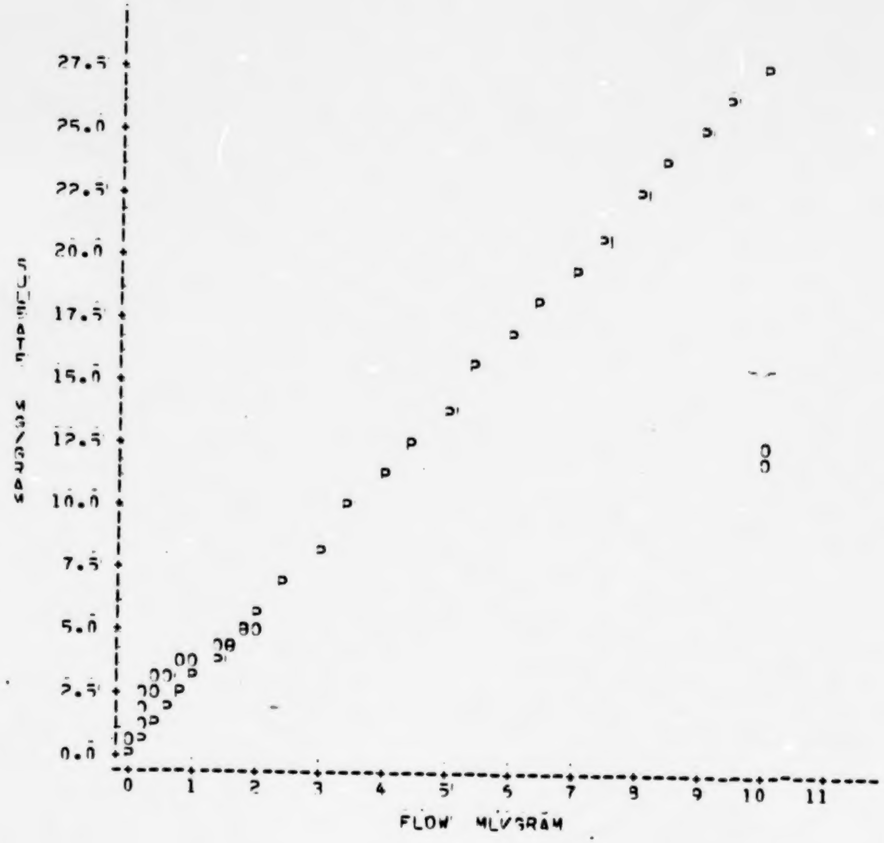

NOTE: The initial soluble fraction ($\underline{y}_o$) was estimated by the asymptotic back-calculated Field Cell No. 1 results. Extrapolation is carried to the zero'th shake-test dilution (10 mL/gram).

Figure G-108. Observed (O) and Predicted (P) Cumulative Field Cell 1 Extractions of Sulfate.

Preceding page blank

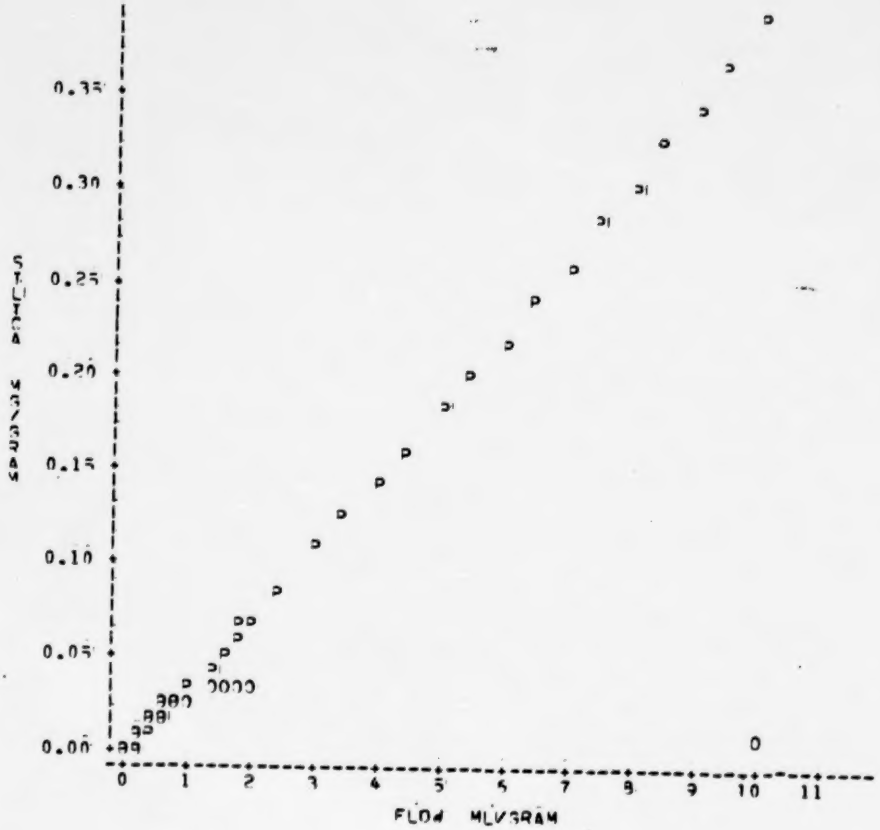

NOTE: The initial soluble fraction (y_0) was estimated by the mean back-calculated Field Cell No. 1 results. Extrapolation is carried to the zero'th shake-test diluation (10 mL/gram).

Figure G-109. Observed (O) and Predicted (P) Cumulative Field Cell 1 Extractions of Silicon.

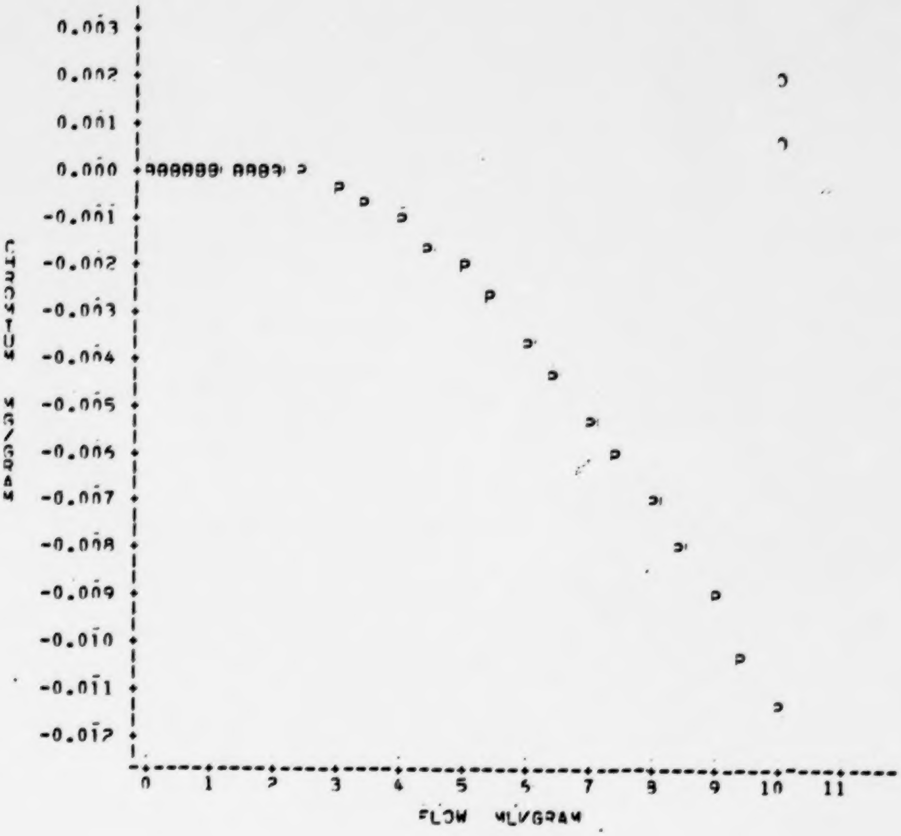

NOTE: The initial soluble fraction ($\underline{y}_o$) was estimated by the asymptotic back-calculated Field Cell No. 1 results. Extrapolation is carried to the zero'th shake-test dilution (10 mL/gram).

Figure G-110. Observed (O) and Predicted (P) Cumulative Field Cell 1 Extractions of Chromium.

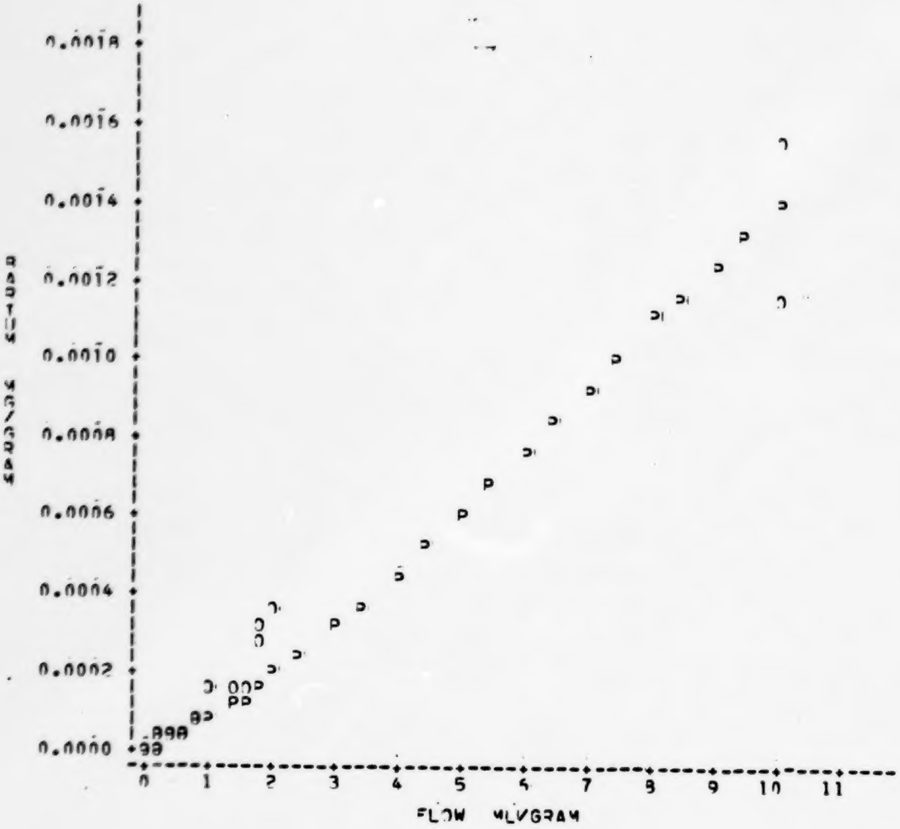

NOTE: The initial soluble fraction (y_o) was estimated by the mean back-calculated Field Cell No. 1 results. Extrapolation is carried to the zero'th shake-test dilution (10 mL/gram).

Figure G-111. Observed (O) and Predicted (P) Cumulative Field Cell 1 Extractions of Barium.

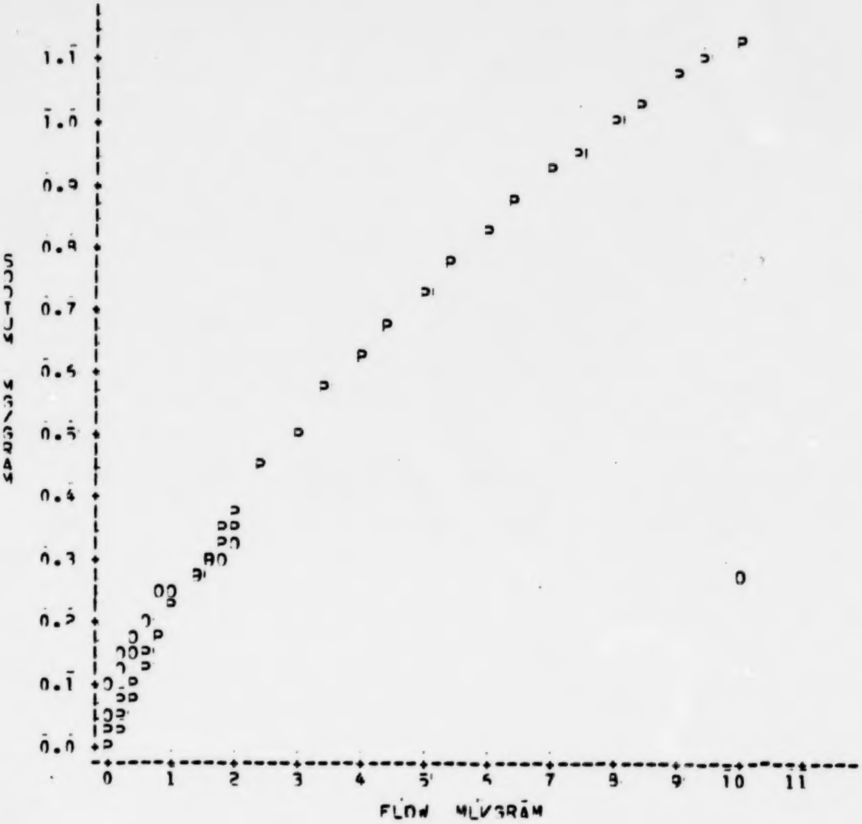

NOTE: The initial soluble fraction ($\underline{y}_0$) was estimated by the asymptotic back-calculated Field Cell No. 1 results. Extrapolation is carried to the zero'th shake-test dilution (10 mL/gram).

Figure G-112. Observed (O) and Predicted (P) Cumulative Field Cell 1 Extractions of Sodium.

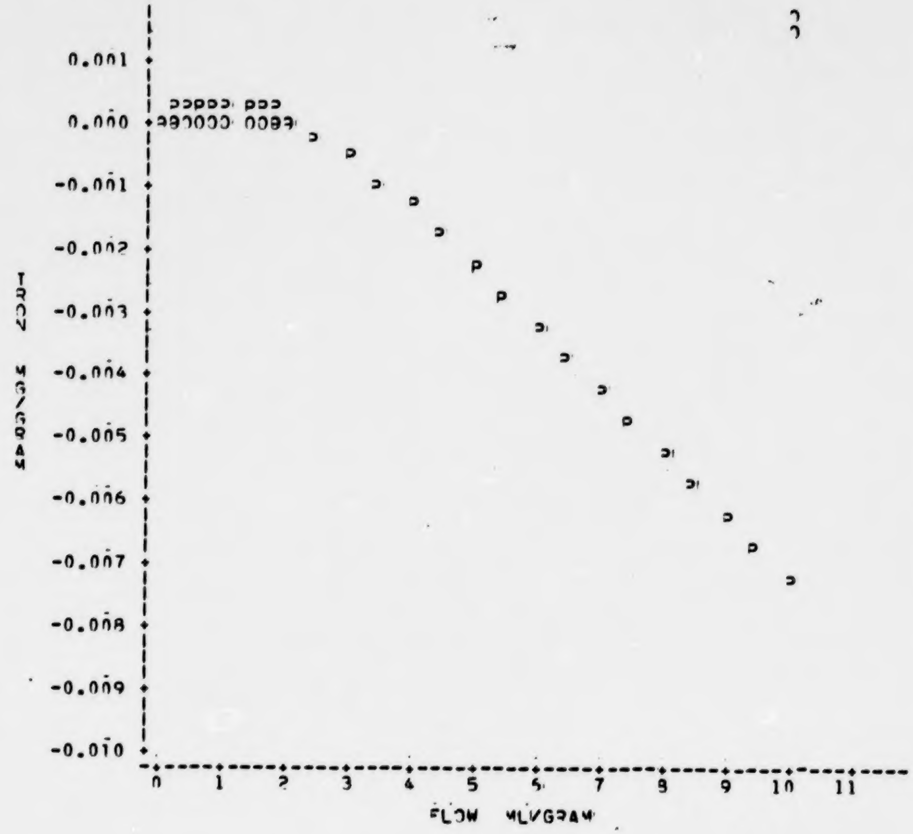

NOTE: The initial soluble fraction ($\underline{y}_o$) was estimated by the asymptotic back-calculated Field Cell No. 1 results. Extrapolation is carried to the zero'th shake-test dilution (10 mL/gram).

Figure G-113. Observed (O) and Predicted (P) Cumulative Field Cell 1 Extractions of Iron.

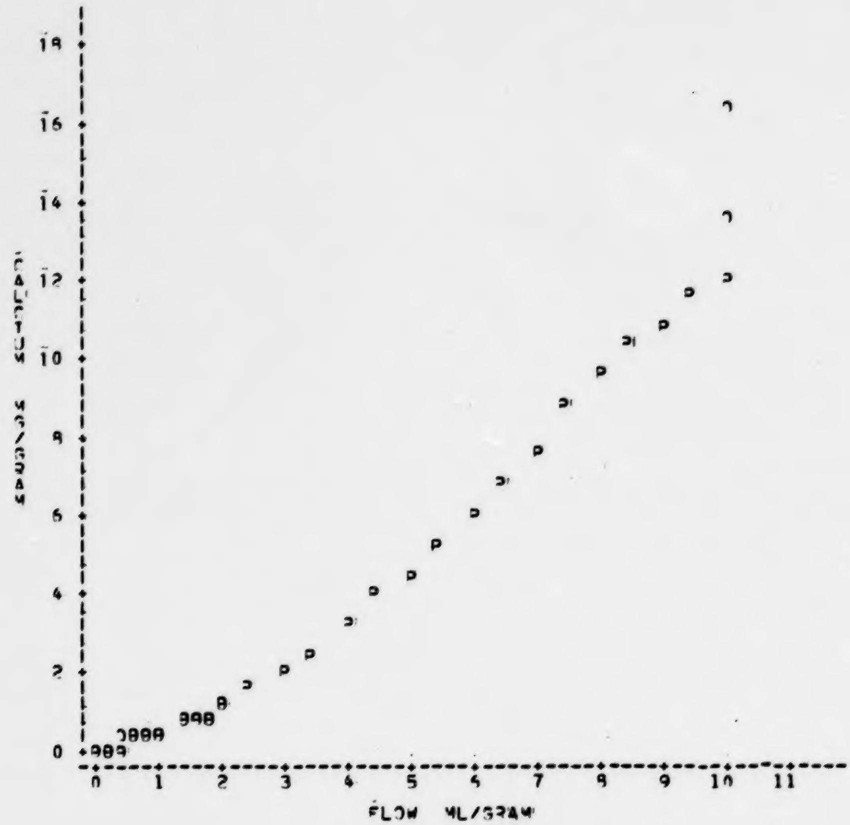

NOTE: **The initial soluble fraction ($\underline{y}_o$) was estimated by the mean back-calculated Field Cell No. 1 results. Extrapolation is carried to the zero'th shake-test dilution (10 mL/gram).**

Figure G-114. Observed (O) and Predicted (P) Cumulative Field Cell 1 Extractions of Calcium.

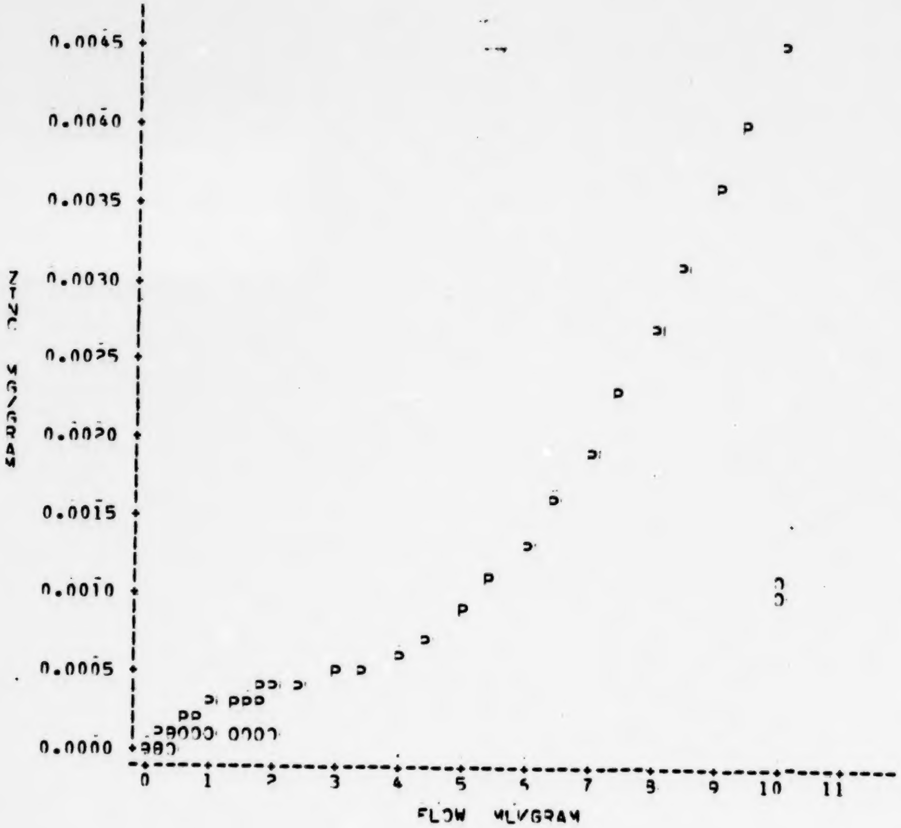

NOTE: The initial soluble fraction ($\underline{y}_0$) was estimated by the asymptotic back-calculated Field Cell No. 1 results. Extrapolation is carried to the zero'th shake-test dilution (10 mL/gram).

Figure G-115. Observed (O) and Predicted (P) Cumulative Field Cell 1 Extractions of Zinc.

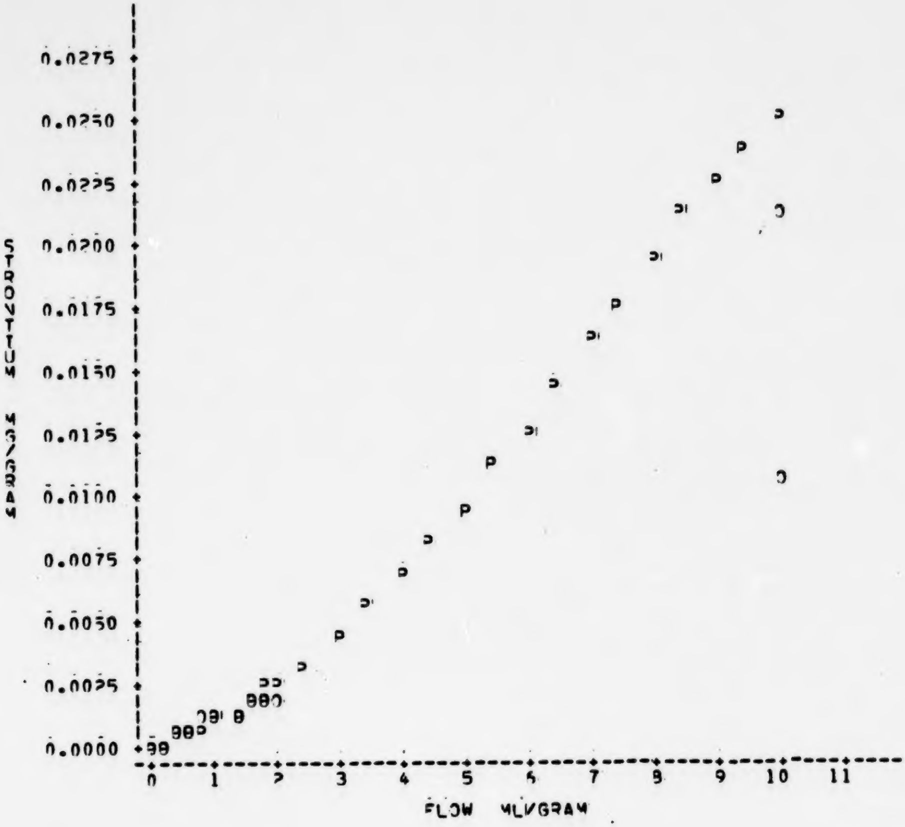

NOTE: The initial soluble fraction (y_o) was estimated by the mean back-calculated Field Cell No. 1 results. Extrapolation is carried to the zero'th shake-test dilution (10 mL/gram).

Figure G-116. Observed (O) and Predicted (P) Cumulative Field Cell 1 Extractions of Strontium.